Nonlinear Algebra in Quantum Chemistry

by

Svala Sverrisdóttir

A dissertation submitted in partial satisfaction of the

requirements for the degree of

Doctor of Philosophy

in

Mathematics

in the

Graduate Division

of the

University of California, Berkeley

Committee in charge:

Professor Bernd Sturmfels, Chair
Professor David Eisenbud
Professor Sylvie Corteel
Professor Lin Lin

Spring 2026

Nonlinear Algebra in Quantum Chemistry

Abstract

Nonlinear Algebra in Quantum Chemistry

by

Svala Sverrisdóttir

Doctor of Philosophy in Mathematics

University of California, Berkeley

Professor Bernd Sturmfels, Chair

The interplay between mathematics and physics has a long and rich history. Recently, ideas from algebraic geometry have played an increasingly important role in the study of physical phenomena, including those arising in particle physics, quantum mechanics, and cosmology. This exchange has led to major advances in both fields and continues to open new directions. In this thesis, I establish a novel connection between algebraic geometry and quantum chemistry. Through methods from nonlinear algebra, with particular emphasis on combinatorics, and representation theory, I develop geometric formulations of coupled cluster theory that lead to new structural, enumerative, and computational results.

First, we develop an algebraic-geometric framework for coupled cluster (CC) theory. At the heart of quantum chemistry is the problem of solving the electronic Schrödinger equation, which can be formulated as a finite but high-dimensional eigenvalue problem. To study this problem, we introduce the truncation varieties, a family of projective varieties parameterized by Laplace polynomials. These generalize the Grassmannian in its Plücker embedding. We then approximate this eigenvalue problem by a lower-dimensional nonlinear eigenvalue problem on the truncation varieties. This leads to a hierarchy of polynomial systems of equations, known as the unlinked coupled cluster equations. We define the coupled cluster degree, an invariant of the truncation varieties, as the generic number of solutions to these equations. By relating this degree to the total degree of a graph, we derive an explicit formula for the CC degree of the Grassmannian of lines. Using toric degenerations we also relate the CC degree of the Grassmannian with the volume of a polytope. Together with numerical algebraic methods, this algebraic framework enables us to completely solve main variants of the CC equations for the molecules LiH and H_4.

Next, we develop a second-quantized framework for coupled cluster theory, in which quantum states and observables are expressed in terms of polynomials in operators. To this end, we introduce the Fermi–Dirac algebra, the Clifford algebra generated by the creation and annihilation operators acting on the fermionic Fock space $\mathcal{F} \cong \wedge\mathbb{R}^n$. We describe a

Gröbner basis for this algebra and thereby obtain an alternative proof of Wick's theorem, a fundamental result in second quantization. We then realize the Hamiltonian as an element of the Fermi–Dirac algebra. Within this framework, we reformulate the truncation varieties and the coupled cluster equations in second quantization. By dropping the assumption of particle conservation, we obtain an extended family of truncation varieties, which includes many well-known varieties, such as flag varieties and the spinor variety.

Finally, we turn to spin, which is encoded by an SU(2)–action on the quantum states. We show that the dimension of the SU(2)–invariant subspace of the state space is given by the Narayana numbers, a refinement of the Catalan numbers. In quantum chemistry, this subspace is called the spin singlet sector and consists of states with total spin zero. We identify the spin singlet sector with a commutative ring defined by cubic relations. This identification, together with the RSK correspondence, yields an explicit bijection between the basis states of the spin singlet sector and the Dyck paths counted by the Narayana numbers. Because the Hamiltonian is SU(2)–invariant, we may restrict to the spin singlet sector and hence to the corresponding spin-adapted truncation varieties. We show that the Veronese square of the Grassmannian appears as a spin-adapted truncation variety. Compared with the spin-generalized formulation, the spin-adapted approach yields a substantial reduction in both dimension and degree, reducing the coupled cluster degree by orders of magnitude. We present scaling studies showing these asymptotic improvements. We exploit this reduction to compute the full solution landscapes of spin-adapted CC equations for LiH and water, showing that spin symmetry makes previously intractable systems accessible to algebraic methods.

To my family

I could not have done this without my dad.

Contents

List of Figures

List of Tables

Acknowledgments

First and foremost, I would like to say how grateful I am to my advisor, Bernd Sturmfels, for your mentorship, guidance, and support. Your influence has deeply shaped my academic journey, and I feel very fortunate to be part of your large academic family. I have always appreciated how much time and thought you put into your students, both in our work and in helping us navigate academic life. Your dedication to the advancement of mathematics and to mentoring students is a big inspiration to me.

I would also like to thank my collaborators, Viktoriia Borovik, Yassine El Maazouz, Fabian Faulstich, Abigail Price, Smita Rajan, and Ada Stelzer. It has been a pleasure to work and do mathematics with you. I would especially like to thank Fabian for our collaboration connecting nonlinear algebra with quantum chemistry. Building this bridge between fields took many discussions, much back and forth, and translation between scientific languages. I also spent a significant amount of time at the MPI in Leipzig during my PhD, and I am thankful for the people I came to know there.

I am deeply grateful for the friendships I made along the way during my PhD. My academic sister, Hannah, I am so glad we went through this journey together. Being in Leipzig and Berkeley together, along with our countless dinners over sushi or crispy duck, made this experience much more memorable. I also want to thank my other academic siblings, Lizzie and Smita, for navigating this experience with me. Nancy, our endless talks in the office about nothing and everything going on in our lives always made my day. Our Expression lunches on the Glade and our much-needed yoga classes were some of the best parts of my time here. I also want to thank the first friends I made in Berkeley, my roommates Katie, Nikki, and Dani, as well as our honorary roommate, Corina. I am also grateful for my friends in Iceland. Salka, Mist, and Thea, I am very glad that we have stayed close over the years, even while living in different parts of the world. Ingvar and Inga, it was such fun to begin my Berkeley journey with you.

I would also like to thank my family for their immense support over the years. My dad, Sverrir, was my first math teacher and has been my longest-standing one. You have gone through every class with me, and I hope you also got to learn some new math along the way. Even though the mathematics I work on now is very different from your own expertise, I still come to you with questions and for guidance. Your curiosity inspires me. You have given me more time and patience than I could ever have asked for. Mom, thank you for your love and encouragement throughout all of this. Seeing your love for what you do inspired me to pursue mathematics. Vífill, thank you for paving the way. In many ways, I seem to have followed in your footsteps, from the X-class in MR to making my way to California. Finally, thank you, Halli, for your love and support during the writing of this thesis, and for always believing in me. It has meant more to me than I can say.

Chapter 1

Introduction

In this thesis, we study problems in *quantum chemistry* using methods from *nonlinear algebra*, with a particular focus on highly structured polynomial equations. The electronic Schrödinger equation can be formulated as the eigenvalue problem for a matrix known as the Hamiltonian. The size of this matrix grows exponentially with the number of electrons, rendering direct approaches infeasible for large systems. Coupled cluster theory addresses this difficulty by introducing a smaller nonlinear model for the original linear-algebraic formulation. This model is governed by the coupled cluster equations, a system of polynomial equations. It is this polynomial nonlinear structure that brings the problem into the realm of nonlinear algebra.

In this introduction we provide background on the fields central to this thesis, namely those two highlighted in the title: nonlinear algebra and quantum chemistry. Section 1.1 is intended for readers with basic understanding of core mathematical fields, such as linear algebra, but with limited to no experience in algebraic geometry. Section 1.2, on the other hand, is aimed at mathematically trained readers with limited exposure to quantum chemistry beyond a high school level. In Section 1.3 we summarize the organization this thesis and in Section 1.4 we summarize our main contributions.

1.1 Nonlinear Algebra

Nonlinear algebra is a growing field that extends the ideas of linear algebra to nonlinear models, bringing together tools from many fields of mathematics. At its core lies algebraic geometry, with connections to many other areas, including commutative algebra, combinatorics, tensors and multilinear algebra, representation theory, convex and discrete geometry, and algebraic topology. As both symbolic and numerical computational methods continue to advance, computer algebra systems have become increasingly important tools in this area. In my research I frequently use `Macaulay2` [46] for symbolic computations and `Julia` packages such as `HomotopyContinuation.jl` [11] for numerical calculations. Because nonlinear models arise throughout science and mathematics, nonlinear algebra finds applications in many fields, including optimization, statistics, particle physics, cosmology, and, as demonstrated in

this thesis, quantum chemistry. We now provide a brief introduction to this field aimed at non-experts, focusing on algebraic geometry and the tools used in this thesis. Since nonlinear algebra covers a much broader range of topics than can be discussed here, we refer the reader to the book by Sturmfels and Michałek [72] for a more comprehensive introduction.

We begin our study with a polynomial ring $R = \mathbb{C}[\mathbf{x}] = \mathbb{C}[x_1, \ldots, x_k]$ in k variables over the complex numbers $\mathbb{C}$. It is important to work over an algebraically closed field for the results of this section to hold. Here we choose to work over $\mathbb{C}$ as it is the algebraic closure of $\mathbb{R}$. The ring R is generated as a vector space by the monomials $\mathbf{x}^{\mathbf{a}} = x_1^{a_1} x_2^{a_2} \cdots x_k^{a_k}$ where $\mathbf{a} \in \mathbb{Z}^k_{\geq 0}$. Each element in R is a polynomial f, uniquely written as a finite linear combination of these monomials, i.e.

$$f = \sum_{\mathbf{a} \in \mathbb{Z}^k_{\geq 0}} c_{\mathbf{a}} \mathbf{x}^{\mathbf{a}} = \sum_{\mathbf{a}} c_{\mathbf{a}} x_1^{a_1} \cdots x_k^{a_k}.$$

A central problem in algebraic geometry is to understand the zero sets of polynomials in R.

Example 1.1.1. Let $k = 3$. We consider the cubic polynomial

$$f = \det \begin{bmatrix} 1 & x & y \\ x & 1 & z \\ y & z & 1 \end{bmatrix} = 2xyz - x^2 - y^2 - z^2 + 1. \tag{1.1}$$

Its zero set $\{\mathbf{x} : f(\mathbf{x}) = 0\}$ is the cubic surface in Figure 1.1, there visualized in $\mathbb{R}^3$.

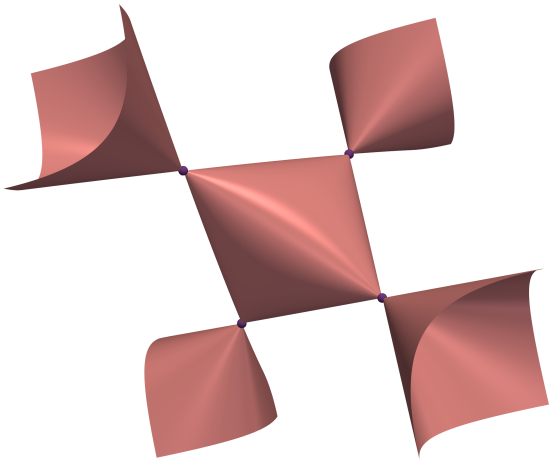

Figure 1.1: Affine Cayley cubic surface with the four singular points marked.

This is the set of all points where the 3×3 matrix in (1.1) has rank at most 2. The surface has 4 singular points, that is, points on the surface where the Jacobian ∇f also vanishes:

$$\frac{\partial f}{\partial x} = 2yz - 2x = 0, \quad \frac{\partial f}{\partial y} = 2xz - 2y = 0, \quad \frac{\partial f}{\partial z} = 2xy - 2z = 0.$$

The singular points are therefore $(1,1,1),(1,-1,-1),(-1,1,-1),(-1,-1,1)$. This is the common zero set of the polynomials f and ∇f. They are all real and are depicted in purple in Figure 1.1. These are exactly the points where the 3×3 matrix has rank at most 1.

Let $f_1, \ldots, f_s \in R$ be a collection of polynomials in k variables $\mathbf{x}$. We define the *affine variety* $V = V(f_1, \ldots, f_s)$ to be the common zero set of these polynomials. That is,

$$V = \{\mathbf{a} = (a_1, \ldots, a_k) \in \mathbb{C}^k \,:\, f_1(\mathbf{a}) = f_2(\mathbf{a}) = \cdots = f_s(\mathbf{a}) = 0\} \subseteq \mathbb{C}^k. \tag{1.2}$$

An affine variety is a geometric object in $\mathbb{C}^k$. An example of an affine variety is the Cayley cubic surface depicted in Figure 1.1; it is the *hypersurface* $V(f)$ where f is the polynomial in (1.1). A *hypersurface* is a variety defined by a single polynomial. A variety V is said to be *irreducible* if it cannot be written as the union of two proper subvarieties. This notion generalizes the concept of irreducibility for polynomials: if f is an irreducible polynomial, then the hypersurface $V(f)$ is an irreducible variety. On the other hand, if f is reducible, that is, if $f = gh$, then the hypersurface $V(f)$ is reducible, since $V(gh) = V(g) \cup V(h)$.

We now introduce a topology on $\mathbb{C}^k$, called the *Zariski topology*, which plays a central role in algebraic geometry. In this topology, the closed sets are precisely the affine varieties in $\mathbb{C}^k$. For a subset $S \subseteq \mathbb{C}^k$, the *Zariski closure* of S is then defined as the smallest variety containing S, and it is denoted by $\overline{S}$. Throughout this thesis we simply refer to $\overline{S}$ as the closure of S, since the topology is clear from the context.

Remark 1.1.2 (Rational varieties)**.** Some varieties can be defined by the image of a map. Explicitly, let ψ be a rational map

$$\psi : \mathbb{C}^m \dashrightarrow \mathbb{C}^k, \qquad \mathbf{t} \mapsto (h_1(\mathbf{t}), \ldots, h_k(\mathbf{t})), \tag{1.3}$$

where $h_1, \ldots, h_k$ are rational functions. That is, each h_i can be written as $h_i = \frac{f_i}{g_i}$ with $f_i, g_i \in R$ polynomials and $g_i \neq 0$. The map ψ is therefore defined only where all denominators are nonzero, which is what the dashed arrow is signifying. In particular, ψ is defined on the Zariski open subset $S = \mathbb{C}^m \setminus V(g_1 g_2 \cdots g_k)$, which is dense in $\mathbb{C}^m$. The image, $\mathrm{im}(\psi) = \psi(S)$, is not necessarily a variety, and hence we take the closure $\overline{\psi(S)}$. We say that the variety $V = \overline{\psi(S)}$ is parameterized by ψ. If the map ψ is injective on the dense subset S, then the induced map $\psi : \mathbb{C}^m \dashrightarrow V$ admits a rational inverse. In this case ψ is called *birational*, and V is said to be birationally equivalent to the affine space $\mathbb{C}^m$. Varieties with this property are called *rational varieties*.

Most varieties appearing in this thesis admit an injective polynomial parameterization and are therefore rational. Since polynomial maps are unbounded, such varieties are not compact in the Euclidean topology. Varieties of this type are particularly convenient to study, as they can be viewed as nonlinear deformations of linear space and their geometry can be described explicitly through these polynomial parameterizations.

Example 1.1.3. We now consider three varieties, a rational variety that admits a polynomial parameterization, a compact rational variety, and a non-rational variety. First we consider the twisted cubic, which is defined as the image of the polynomial map

$$\mathbb{C} \to \mathbb{C}^3, \qquad t \mapsto (t, t^2, t^3).$$

Hence it is rational. We can define it implicitly as the zero set of the three 2×2 minors of the following 2×3 matrix

$$\begin{bmatrix} x & y & z \\ 1 & x & y \end{bmatrix}.$$

Next, we consider the circle, defined by the polynomial $x^2 + y^2 - 1$. It is a rational variety; however, since the circle is compact, it does not admit a polynomial parameterization. It does admit the following rational parameterization

$$\mathbb{C} \dashrightarrow \mathbb{C}^2, \qquad t \mapsto \left(\frac{1 - t^2}{1 + t^2}, \frac{2t}{1 + t^2} \right).$$

Finally, we consider the variety defined by the polynomial $y^2 - x^3 + 3x - 1$. This is an example of an *elliptic curve*, and it is not rational, and hence does not admit any rational parameterization. We visualize these three curves in real space in Figure 1.2.

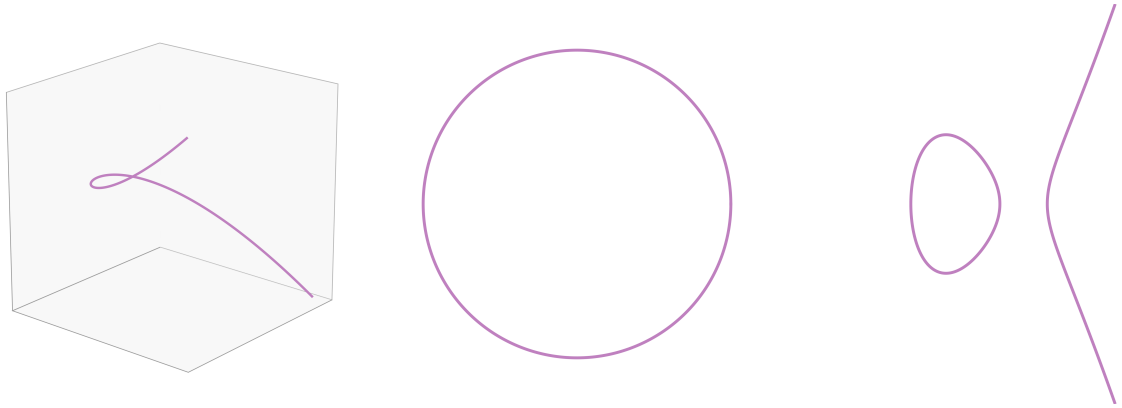

Twisted cubic Circle Elliptic curve

Figure 1.2: Three curves, visualized in $\mathbb{R}^3$ and $\mathbb{R}^2$.

We now introduce *ideals* in the polynomial ring R. Ideals are algebraic objects that capture the relations that define varieties. An *ideal* $I \subseteq R$ is a subset of R that is closed under addition and under multiplication by elements of R. That is, if $f, g \in I$, then $f + g \in I$, and if $f \in I$ and $h \in R$, then $hf \in I$. A collection $f_1, \ldots, f_s$ of polynomials in R is said to generate I if every polynomial in I can be written as a combination of them. That is,

$$I = \{ r_1 f_1 + \cdots + r_s f_s \, : \, r_1, \ldots, r_s \in R \} \subseteq R.$$

We then write $I = \langle f_1, \ldots, f_s \rangle$. By the Hilbert basis theorem [28, Theorem 1.2], the polynomial ring R is Noetherian, and therefore every ideal in R is generated by a finite set of polynomials. Note that generating sets are not unique, many different sets of polynomials can generate I.

An ideal $I \subseteq R$ is called *prime* if, whenever $fg \in I$, then either $f \in I$ or $g \in I$. An ideal $I \subseteq R$ is called *radical* if whenever $f^n \in I$ for some positive integer n, then $f \in I$. We may define the radical of I, denoted $\sqrt{I}$, as the smallest radical ideal containing I. Explicitly,

$$\sqrt{I} = \{ f \in R : f^n \in I \text{ for some } n \geq 1 \}.$$

If I is already radical then $I = \sqrt{I}$. Note that a prime ideal is radical. These classifications play an important role in the correspondence between varieties and ideals, which we now explain.

We illustrate the relationship between varieties and ideals, and justify our statement that ideals capture the relations that define varieties. Say a variety V is defined as the zero set of polynomials $f_1, \ldots, f_s$. Then every point on V is a zero point of any polynomial in the ideal $I = \langle f_1, \ldots, f_s \rangle$. Hence we may write

$$V = V(f_1, \ldots, f_s) = V(I) = \{ \mathbf{a} \in \mathbb{C}^k : f(\mathbf{a}) = 0 \text{ for all } f \in I \}.$$

We also want to define ideals in terms of varieties. Actually, the set of all polynomials in R vanishing on variety $V = V(f_1, \ldots, f_s)$ is an ideal. Hence we can define the ideal of V as:

$$\mathcal{I}(V) = \{ f \in R : f(\mathbf{a}) = 0 \text{ for all } \mathbf{a} \in V \} \supseteq \langle f_1, \ldots, f_s \rangle. \tag{1.4}$$

The ideal of V is not necessarily equal to the ideal generated by the polynomials defining V, that is, the inclusion in (1.4) may be strict. An example illustrating this is $V(x^2) = \{0\}$, while $I(\{0\}) = \langle x \rangle$. Consequently, there is no bijection between ideals and varieties. The precise relationship between these objects is described by Hilbert's Nullstellensatz, a foundational result that connects algebra and geometry through ideals and varieties.

Theorem 1.1.4 (Hilbert's Nullstellensatz)**.** *[72, Theorem 6.5] There is a one-to-one correspondence between varieties and radical ideals. In fact,*

$$\mathcal{I}(V(I)) = \sqrt{I}.$$

In particular, irreducible varieties are in one-to-one correspondence with prime ideals.

In this theorem, it is important to work over an algebraically closed field. There is, however, an analogue of Hilbert's Nullstellensatz over the real numbers, known as the real Nullstellensatz. We refer the interested reader to [72, Section 6.3], where the real case is discussed. In view of Hilbert's Nullstellensatz, we will switch between varieties V and their corresponding radical ideals. We now discuss some invariants of varieties and their ideals.

Algebraic Invariants

Varieties and ideals admit many invariants that help characterize their geometric and algebraic structure. Two fundamental examples are their *dimension* and *degree*. The dimension is a topological invariant and, in particular, is preserved under birational equivalence. The degree, on the other hand, depends on the chosen embedding of the variety rather than on the abstract variety itself. Nevertheless, it behaves well under algebraic deformations: in particular, the degree is preserved under *flat degenerations*. At the end of this section we introduce two important such deformations, namely Gröbner and toric degenerations.

Intuitively, the *dimension* of a variety measures how many degrees of freedom its points have. It can be thought of as the number of independent parameters needed to locally describe its points. For example, a curve has dimension one, a surface has dimension two, and affine space $\mathbb{C}^k$ has dimension k. More formally, the dimension of an affine variety $V \subseteq \mathbb{C}^k$, denoted $\dim(V)$, is defined as the maximal length d of a chain of distinct irreducible subvarieties

$$V_0 \subsetneq V_1 \subsetneq \cdots \subsetneq V_d \subseteq V.$$

For rational varieties, the notion of dimension becomes particularly simple, since they are birationally equivalent to affine space. If $\mathbb{C}^m \dashrightarrow V$ is a birational parameterization of V, then $\dim(V) = m$. In other words, the dimension equals the number of parameters required to describe the variety. Using the correspondence between varieties and radical ideals, we can define the dimension of an ideal I, denoted $\dim(I)$, to be the dimension of the variety $V(I)$. This agrees with the *Krull dimension* of the quotient ring R/I, see [28, Chapter 8]. Similarly, the *codimension* of $V \subseteq \mathbb{C}^k$, denoted $\operatorname{codim}(V)$, is defined as the difference $k - \dim(V)$.

The *degree* of a variety V generalizes the degree of a polynomial. Intuitively, it measures how much the variety deviates from being linear. More precisely, it counts how many times V intersects a linear space of complementary dimension. For a generic choice of such a linear space, the intersection with V consists of finitely many points, and this number is constant. We define the degree of V, denoted $\deg(V)$, to be this number. Linear spaces illustrate this: a linear space intersects another linear space of complementary dimension generically in a single point (except in the degenerate case when they are parallel). Hence linear spaces have degree one. The degree of an ideal I is defined as the degree of the variety $V(I)$.

Example 1.1.5. We revisit the Cayley cubic. It is a hypersurface $V(2xyz - x^2 - y^2 - z^2 + 1)$ in $\mathbb{C}^3$. It has dimension 2 and codimension 1. Since the degree of a variety generalizes the degree of a polynomial, its degree is 3. We illustrate its intersection with a generic line:

The three intersection points are marked in brown. Note that over the real numbers, as is illustrated in Figure 1.3, the number of intersection points may drop, even for a generic line, since some of the intersection points may be non-real. This highlights the importance of working over an algebraically closed field.

The following version of *Bézout's theorem* is a fundamental result describing how the degree behaves under intersections of varieties.

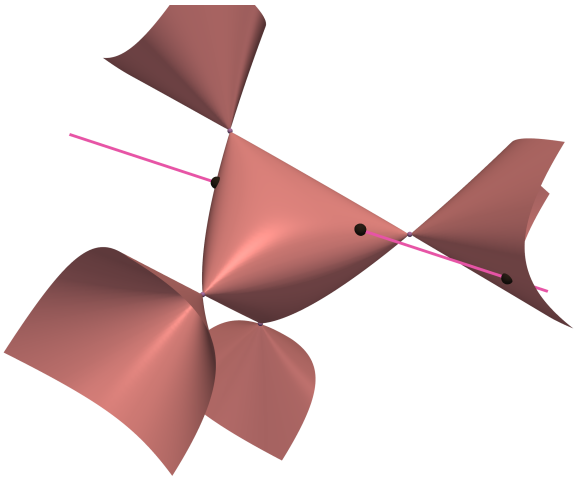

Figure 1.3: Cayley cubic intersected with a line.

Theorem 1.1.6 (Bézout's theorem)**.** *[29, Corollary 2.4] Let V and W be varieties in $\mathbb{C}^k$. Then the degree of their intersection is bounded by the product of their degrees, that is,*

$$\deg(V \cap W) \leq \deg(V)\deg(W).$$

This result can be used to obtain an upper bound on the degree of a variety $V = V(f_1, \ldots, f_s) \subseteq \mathbb{C}^k$. It is known as *Bézout's bound* and it is given by

$$\deg(V) \leq \deg(f_1) \cdots \deg(f_s).$$

Bézout's bound is the most general upper bound, depending only on the degrees of the defining polynomials. Since it does not take into account any further structure of the system, it often significantly overestimates the degree. Sharper bounds can be obtained by incorporating additional information about the polynomials. A widely used refinement is given by the *mixed volume* of their Newton polytopes. We refer to [22, Section 7.4-5] for an introduction into mixed volumes and how they bound degrees. See also [36] for their use in bounding the number of solutions to the coupled cluster equations, defined in Sections 1.2 and 2.3.

Projective Space

While affine space provides a convenient and natural setting for describing varieties, intersection behavior becomes more regular when points at infinity are included. For this reason, we now introduce projective space. To this end, we define the k–dimensional projective space over $\mathbb{C}$, denoted $\mathbb{P}^k$, as the set of all lines through the origin in $\mathbb{C}^{k+1}$. The line in $\mathbb{C}^{k+1}$ passing through the origin and a point $\mathbf{x} = (x_0, x_1, \ldots, x_k)$ is denoted by

$$[\mathbf{x}] = [x_0 : x_1 : \cdots : x_k] \in \mathbb{P}^k.$$

Note that $\mathbf{x}$ can itself not be the origin. Two points in $\mathbb{C}^{k+1}$ represent the same line if they differ only by a nonzero scalar multiple. Explicitly, $\mathbb{P}^k$ is the set of equivalence classes $[\mathbf{x}]$ with $\mathbf{x} \in \mathbb{C}^{k+1} \setminus \{0\}$, where two vectors $\mathbf{x}$ and $\mathbf{y}$ are equivalent if $\mathbf{x} = \lambda\mathbf{y}$ for some $\lambda \in \mathbb{C}^*$.

Let $f \in \mathbb{C}[x_0, \ldots, x_k]$ be a polynomial in $k+1$ variables. We say that f is *homogeneous* of degree d if it is a linear combination of degree d monomials. Notice that if $\mathbf{x}$ is a zero of a homogeneous polynomial f, then $\lambda\mathbf{x}$ is also a zero of f. Therefore f vanishes on all representatives of $[\mathbf{x}] \in \mathbb{P}^k$ if it vanishes on some representative. Now let $f_1, \ldots, f_s$ be a collection of homogeneous polynomials (not necessarily of the same degree). We define the *projective variety* $V = V(f_1, \ldots, f_s) \subseteq \mathbb{P}^k$ to be their common zero set in $\mathbb{P}^k$:

$$V = \{[\mathbf{a}] = [a_0 : \cdots : a_k] \in \mathbb{P}^k \,:\, f_1(\mathbf{a}) = \cdots = f_s(\mathbf{a}) = 0\} \subseteq \mathbb{P}^k.$$

Let $I \subseteq \mathbb{C}[x_0, \ldots, x_k]$ be an ideal generated by homogeneous polynomials $f_1, \ldots, f_s$ (again not necessarily of the same degree). We call I a *homogeneous ideal*. As in the affine case, we define

$$V(I) = V(\langle f_1, \ldots, f_s \rangle) = V(f_1, \ldots, f_s) \subseteq \mathbb{P}^k.$$

The Nullstellensatz holds in the projective setting as well. Hence, the ideal of a projective variety $V \subseteq \mathbb{P}^k$, denoted $\mathcal{I}(V) \subseteq \mathbb{C}[x_0, \ldots, x_k]$, is a homogeneous radical ideal.

We may projectivize affine varieties, that is, we associate a projective variety $\overline{V} \subseteq \mathbb{P}^k$ to an affine variety $V \subseteq \mathbb{C}^k$, called its *projective closure*. This is done via the corresponding ideals, through a process called *homogenization*. To this end, we first define the homogenization of a polynomial. Let $f \in \mathbb{C}[x_1, \ldots, x_k] = R$ be a polynomial of degree d. The *homogenization* of f is the polynomial $\overline{f} \in \mathbb{C}[x_0, x_1, \ldots, x_k]$ obtained by multiplying each monomial of f by a suitable power of the homogenizing variable x_0 so that every term has total degree d.

Example 1.1.7. We homogenize the cubic polynomial in (1.1) with homogenizing variable w as $\overline{f} = 2xyz - x^2w - y^2w - z^2w + w^3 \in \mathbb{C}[x, y, z, w]$.

We may now define the homogenization of the ideal I, denoted $\overline{I}$, as the homogeneous ideal generated by the homogenizations of all polynomials in I. That is

$$\overline{I} = \langle\, \overline{g} \,:\, g \in I \,\rangle \subseteq \mathbb{C}[x_0, x_1, \ldots, x_k].$$

The projective closure of V, denoted $\overline{V}$ is defined as the projective variety of the homogenization $\overline{\mathcal{I}(V)}$. Note that this definition only provides an infinite generating set. Finding a finite set of defining equations for the projective closure is not a trivial task. Say that the ideal $\mathcal{I}(V)$ is generated by polynomials $f_1, \ldots, f_s \in R$. Then we may define the ideal of $\overline{V}$ through saturation, see Definition 8 in [21, Section 4.4]. We get

$$\overline{\mathcal{I}(V)} = \mathcal{I}(\overline{V}) = \langle \overline{f}_1, \ldots, \overline{f}_s \rangle : \langle x_0 \rangle^\infty.$$

This is a description of the ideal, but it does not provide us with a finite generating set either. That can be done through Gröbner bases, defined later; see [72, Proposition 2.18].

Projectivization preserves most invariants of the affine variety V. In particular,

$$\dim(\overline{V}) = \dim(V), \qquad \deg(\overline{V}) = \deg(V).$$

This motivates the use of projectivization, since the degree is defined in terms of intersections, and intersections behave more regularly in projective space. For example, every pair of lines in $\mathbb{P}^2$ intersects, whereas parallel lines in $\mathbb{C}^2$ do not.

Remark 1.1.8. In the constructions appearing in this thesis, projective varieties typically arise from polynomial parameterizations in an *affine chart* of projective space. More precisely, most varieties considered here are given by polynomial parameterizations of the form

$$\psi : \mathbb{C}^m \to \mathbb{C}^{k+1}, \qquad t \mapsto (1, f_1(\mathbf{t}), \ldots, f_k(\mathbf{t})).$$

Composing this map with the natural embedding of affine space into projective space

$$\mathbb{C}^{k+1} \supsetneq \{x_0 = 1\} \hookrightarrow \mathbb{P}^k, \qquad (x_0, \ldots, x_k) \mapsto [x_0 : \cdots : x_k],$$

yields a morphism

$$\mathbb{C}^m \to \mathbb{P}^k, \qquad t \mapsto [1 : f_1(\mathbf{t}) : \cdots : f_k(\mathbf{t})].$$

The projective variety associated with this parameterization is defined as the Zariski closure of its image in $\mathbb{P}^k$. This variety is the projective closure of the affine variety V parameterized by ψ. Since the first coordinate of ψ is 1, the image of ψ lies in the affine subspace of $\mathbb{C}^{k+1}$ defined by $x_0 = 1$, which we naturally identify with $\mathbb{C}^k$. Hence we may view V as a variety in $\mathbb{C}^k$ and consider its projective closure in $\mathbb{P}^k$.

It is often convenient to further extend the parameterization to projective space by homogenizing the coordinate functions. Explicitly, suppose the polynomials $f_1, \ldots, f_k$ have degrees $d_1, \ldots, d_k$, and let $d = \max\{d_1, \ldots, d_k\}$ be the maximal degree. Introducing homogeneous coordinates $[s : t_1 : \cdots : t_m]$ on $\mathbb{P}^m$, we obtain the map

$$\mathbb{P}^m \dashrightarrow \mathbb{P}^k, \qquad [s : \mathbf{t}] \mapsto [s^d : s^{d-d_1} f_1(\mathbf{t}) : \cdots : s^{d-d_k} f_k(\mathbf{t})].$$

Since these homogeneous coordinates may vanish simultaneously for some points of $\mathbb{P}^m$, the map is not defined everywhere and is therefore a rational map. The closure of its image is the projective variety $\overline{V}$, so this map also provides a parameterization of $\overline{V}$. In this thesis, we will freely pass between these three equivalent parameterizations, interpreting them as affine or projective descriptions of the same underlying variety.

A key example of such parameterizations is a birational parameterization of the Grassmannian in its Plücker embedding, which will be a central object in this thesis.

The Grassmannian

We define the Grassmannian $\mathrm{Gr}(d,n)$ as the set of d-dimensional linear subspaces of $\mathbb{C}^n$. Projective space $\mathbb{P}^n$ can be viewed as the special case $\mathrm{Gr}(1,n+1)$. Any d-dimensional subspace of $\mathbb{C}^n$ arises as the row space of a full-rank $d \times n$ matrix M, and this choice is not unique. Two such matrices represent the same subspace if and only if they differ by left multiplication by an element of $\mathrm{GL}(d)$. Hence we may identify

$$\mathrm{Gr}(d,n) := \mathrm{Mat}_{d,n}^{\mathrm{rank}\, d} / \sim,$$

where $M \sim M'$ if and only if $M = gM'$ for some $g \in \mathrm{GL}(d)$.

We now describe an embedding of the Grassmannian into projective space, known as the Plücker embedding. This embedding realizes the Grassmannian as a projective variety, allowing it to be studied using the tools of algebraic geometry. Let M be a full-rank $d \times n$ matrix, and consider its $d \times d$ minors $p_I(M)$, indexed by d-element subsets $I \subseteq \{1,\dots,n\}$. If $g \in \mathrm{GL}(d)$ and $M' = gM$, then each minor $p_I(M')$ equals $p_I(M)$ times $\det(g)$. Hence the vector of maximal minors changes only by a common scalar factor. Since points in projective space are defined up to a common scalar multiple, the vectors of maximal minors of M and M' determine the same point in $\mathbb{P}^{\binom{n}{d}-1}$. Thus the resulting projective point depends only on the equivalence class of M. In particular, the maximal minors define a well-defined map

$$\mathrm{Gr}(d,n) \to \mathbb{P}^{\binom{n}{d}-1}, \qquad [M] \mapsto [\, p_I(M)\,]_{I \in \binom{[n]}{d}},$$

known as the *Plücker embedding*. Now we may identify the Grassmannian $\mathrm{Gr}(d,n)$ with the image of this map. We can therefore define the Grassmannian $\mathrm{Gr}(d,n)$ as the projective variety parameterized by the (non-injective) rational map

$$\mathbb{C}^{d\times n} \dashrightarrow \mathbb{P}^{\binom{n}{d}-1}, \qquad M \mapsto \psi = \text{all maximal minors of } M.$$

This map is undefined precisely when all maximal minors of M vanish, that is, when M does not have full rank. This map is not injective, since any two matrices representing the same subspace map to the same point in $\mathbb{P}^{\binom{n}{d}-1}$. The coordinates of the image are denoted by ψ_I, where $I \subseteq [n] = \{1,\dots,n\}$ with $|I| = d$, and they are called the *Plücker coordinates*.

Remark 1.1.9 (A birational parameterization of the Grassmannian)**.** For each element (subspace) in $\mathrm{Gr}(d,n)$ we may choose a representative matrix whose rows span it, of the form

$$[I_d\, X] \;=\; \begin{bmatrix} 1 & 0 & \cdots & 0 & x_{1,d+1} & \cdots & x_{1,n} \\ 0 & 1 & \cdots & 0 & x_{2,d+1} & \cdots & x_{2,n} \\ \vdots & \vdots & \ddots & \vdots & \vdots & \ddots & \vdots \\ 0 & 0 & \cdots & 1 & x_{d,d+1} & \cdots & x_{d,n} \end{bmatrix},$$

where X is a $d \times (n-d)$ matrix. The following injective map

$$\mathbb{C}^{d\times(n-d)} \to \mathbb{P}^{\binom{n}{d}-1}, \qquad X \mapsto \psi = \text{all maximal minors of } [I_d\, X], \tag{1.5}$$

defines a birational parameterization of $\mathrm{Gr}(d,n)$. Hence $\mathrm{Gr}(d,n)$ is rational and has dimension

$$\dim(\mathrm{Gr}(d,n)) = d(n-d).$$

Note that the first minor is $\det(I_d) = 1$, and hence this map maps the first coordinate $p_{[d]}$ to 1. Such maps are discussed in Remark 1.1.8.

As a variety, the Grassmannian $\mathrm{Gr}(d,n)$ is defined as the zero set of polynomials in the polynomial ring $\mathbb{C}[\psi] = \mathbb{C}[\,\psi_I \,:\, I \subseteq [n],\, |I| = d\,]$, whose variables are the Plücker coordinates on $\mathbb{P}^{\binom{n}{d}-1}$. To understand the defining equations of the Grassmannian, we study its ideal $\mathcal{I}(\mathrm{Gr}(d,n))$, which consists of all polynomial relations among maximal minors of matrices. This ideal is generated by quadratic polynomials called the *Plücker relations*. They are known explicitly, in fact the Plücker relations for $\mathrm{Gr}(d,n)$ can be obtained in `Macaulay2` [46] via the command `Grassmannian(d - 1, n - 1)`.

Example 1.1.10 (The Grassmannian of lines)**.** We consider the special case $d = 2$. Then $\mathrm{Gr}(2,n)$ is known as the Grassmannian of lines, since its points correspond to projective lines in $\mathbb{P}^{n-1}$. It can be viewed as the next step beyond projective space. The Plücker coordinates ψ_{ij}, where $i < j$, can be arranged as the entries of an $n \times n$ skew-symmetric matrix

$$\begin{bmatrix} 0 & \psi_{12} & \psi_{13} & \cdots & \psi_{1n} \\ -\psi_{12} & 0 & \psi_{23} & \cdots & \psi_{2n} \\ -\psi_{13} & -\psi_{23} & 0 & \cdots & \psi_{3n} \\ \vdots & \vdots & \vdots & \ddots & \vdots \\ -\psi_{1n} & -\psi_{2n} & -\psi_{3n} & \cdots & 0 \end{bmatrix}.$$

The Plücker relations of $\mathrm{Gr}(2,n)$ are precisely the 4×4 Pfaffians of this matrix. Explicitly, they are the following $\binom{n}{4}$ quadratic polynomials

$$\underline{\psi_{i\ell}\psi_{jk}} - \psi_{ik}\psi_{j\ell} + \psi_{ij}\psi_{k\ell}, \qquad 1 \le i < j < k < \ell \le n. \tag{1.6}$$

See Example 4.9 in [72] and the proof of Theorem 5.8 in [72] for the reasoning.

We conclude our discussion on the Grassmannian with an explicit formula for its degree. A derivation of this formula can be found in [72, Section 5.3]. The degree of $\mathrm{Gr}(d,n)$ equals the number of standard Young tableaux of rectangular shape $d \times (n-d)$. This number is

$$\deg(\mathrm{Gr}(d,n)) = \frac{(d(n-d))!}{\prod_{j=1}^{d} j(j+1)\cdots(j+n-d-1)}. \tag{1.7}$$

In the special case of the Grassmannian of lines, this simplifies to a Catalan number:

$$\deg(\mathrm{Gr}(2,n)) = \frac{1}{n-1}\binom{2n-4}{n-2} = C_{n-2}.$$

Gröbner and Khovanskii bases

Gröbner bases are fundamental tools in the study of algebraic varieties and ideals. Although they are not a central focus of this thesis, they appear naturally in several constructions and are therefore worth introducing. We discuss them together with the more recent notion of Khovanskii bases, see [5, 6, 59], as both play a role in the developments of this work. Ideals and algebras generally admit many different generating sets, and in fact infinitely many choices are possible. However, some generating sets are particularly well-behaved and reveal additional algebraic structure. Gröbner bases provide such distinguished generating sets for ideals, while Khovanskii bases play an analogous role for algebras.

First we fix an order on the variables of the polynomial ring $R = \mathbb{C}[x_1, \ldots, x_k]$ as

$$x_1 > x_2 > \cdots > x_k.$$

We then define a total order on the monomials in R, called a *monomial order*. Throughout this thesis we use the *degree reverse lexicographic order*. It is defined as follows: for monomials $x^{\mathbf{a}}$ and $x^{\mathbf{b}}$ we set $x^{\mathbf{a}} > x^{\mathbf{b}}$ if $|\mathbf{a}| > |\mathbf{b}|$, or if $|\mathbf{a}| = |\mathbf{b}|$ and the rightmost nonzero entry of $\mathbf{a} - \mathbf{b}$ is negative. Intuitively, monomials are first compared by total degree, and among monomials of the same degree those involving fewer smaller variables (towards the right) are considered larger. The largest monomial appearing in a polynomial $f \in R$ is called the *initial monomial* and it is denoted by $\mathrm{in}(f)$.

Example 1.1.11. The initial monomials of the Plücker relations for $\mathrm{Gr}(2, n)$ with respect to the degree reverse lexicographic order are underlined in (1.6). Here we assume the following order on the Plücker coordinates (the variables):

$$\psi_{12} < \psi_{13} < \cdots < \psi_{1n} < \psi_{23} < \cdots < \psi_{2n} < \cdots < \psi_{n-1,n}.$$

It corresponds to the lexicographic order on the index sets I, i.e. $J \leq I$ if at the first position ℓ where $i_\ell \neq j_\ell$ we have $j_\ell < i_\ell$.

We define the *initial ideal* of an ideal $I \subseteq R$ as the following ideal generated by initial monomials, $\mathrm{in}(I) = \langle\, \mathrm{in}(g) \,:\, g \in I \,\rangle$. Ideals generated by monomials are called *monomial ideals*. Such ideals are particularly well-behaved, as they admit rich combinatorial descriptions, see [73, Part I]. Note that the definition above describes $\mathrm{in}(I)$ using an infinite generating set. However, every ideal $I \subseteq R$ admits a finite subset $G \subseteq I$ which suffices in the definition:

$$\mathrm{in}(I) = \langle\, \mathrm{in}(g) \,:\, g \in G \,\rangle.$$

Such a set G is called a *Gröbner basis*. In particular, G generates the ideal I, that is, $I = \langle G \rangle$. Although the initial ideal $\mathrm{in}(I)$ is typically much simpler than I, it preserves important invariants; in particular, I and $\mathrm{in}(I)$ have the same dimension and degree. The deformation of the variety $V(I)$ to the variety $V(\mathrm{in}(I))$ is called a *Gröbner degeneration*. The power of Gröbner bases lies in the fact that they make the initial ideal effectively computable, allowing geometric and algebraic questions about I to be reduced to the combinatorics of monomials.

Example 1.1.12. The Plücker relations (1.6) for the Grassmannian of lines, $\mathrm{Gr}(2,n)$, form a Gröbner basis with respect to degree reverse lexicographic order. The degree of the squarefree monomial ideal

$$\mathrm{in}(\mathrm{Gr}(2,n)) = \langle \psi_{i\ell}\psi_{jk} : 1 \leq i < j < k < \ell \leq n \rangle$$

equals the number of maximal chains in a corresponding poset. This poset has the Plücker coordinates ψ_{ij} as elements, with $\psi_{ij} \leq \psi_{k\ell}$ whenever $i \leq k$ and $j \leq \ell$ (i.e. $\psi_{ij}\psi_{k\ell}$ is not a generator). This is precisely Young's lattice $P_{2,n-2}$, whose maximal chains are counted by the Catalan number C_{n-2}. Hence $\deg(\mathrm{Gr}(2,n)) = C_{n-2}$. See [73, Chapter 1] for an explanation of this correspondence.

We define the *standard monomials* of I as the monomials not in the initial ideal of I. That is, those monomials $\mathbf{x}^{\mathbf{a}}$ where $\mathbf{x}^{\mathbf{a}} \notin \mathrm{in}(I)$. The following result is fundamental, as it also establishes Gröbner bases as distinguished generating sets.

Theorem 1.1.13. *[72, Theorem 1.17] The standard monomials of I form a vector space basis for the quotient ring $\mathbb{C}[\mathbf{x}]/I$.*

Gröbner bases of explicit ideals can be computed using *Buchberger's algorithm*, see [21, Section 2.7]. Variants of this algorithm are implemented in many computer algebra systems, in particular `Macaulay2` [46]. However, computing a Gröbner basis can be computationally expensive: in the worst case the complexity is doubly exponential in the number of variables. In practice, it is therefore often necessary to choose monomial orders carefully, and in many situations the computation of a Gröbner basis becomes infeasible.

We now define *Khovanskii bases*, which serve as an analogue of Gröbner bases for subalgebras. To this end, let S be a subalgebra of a polynomial ring $\mathbb{C}[x_1,\ldots,x_m]$. That is, S is closed under addition and multiplication: if $f,g \in S$, then $f+g, fg \in S$. This differs from the case of ideals, which are additionally closed under multiplication by arbitrary elements. We say that polynomials $f_1,\ldots,f_s \in S$ generate S if every polynomial $g \in S$ can be expressed as a polynomial in the f_i, that is

$$g = \sum_{\mathbf{a} \in \mathbb{Z}^s_{\geq 0}} c_{\mathbf{a}} f_1^{a_1} \cdots f_s^{a_s},$$

where $c_{\mathbf{a}} \in \mathbb{C}$. In this case we write $S = \mathbb{C}[f_1,\ldots,f_s]$. As with ideals, we define the *initial algebra* of S as the algebra generated by the initial monomials of polynomials in S:

$$\mathrm{in}(S) = \mathbb{C}[\,\mathrm{in}(f) : f \in S\,].$$

Now assume $G \subseteq S$ is a finite subset such that

$$\mathrm{in}(S) = \mathbb{C}[\,\mathrm{in}(g) : g \in G\,].$$

Such a set G is called a *Khovanskii basis* of S. In particular, G generates the subalgebra S, that is $S = \mathbb{C}[G]$. Note that Hilbert's basis theorem does not hold for subalgebras, so they need not be finitely generated. Consequently, a finite Khovanskii basis need not exist.

We now explain how Khovanskii bases appear in the theory of varieties and why they are extremely useful. First we assume the variety $V \subseteq \mathbb{P}^k$ is parameterized by a polynomial map

$$\psi : \mathbb{C}^m \to \mathbb{P}^k, \qquad \mathbf{t} \mapsto \mathbf{x} = [1 : f_1(\mathbf{t}) : \cdots : f_k(\mathbf{t})]. \tag{1.8}$$

as in Remark 1.1.8. We emphasize that the map ψ need not be injective. We now consider the corresponding map on the polynomial functions on $\mathbb{P}^m$ and $\mathbb{P}^k$, given by substituting the parameterization into the coordinates:

$$\mathbb{C}[\mathbf{x}] \to \mathbb{C}[s, \mathbf{t}], \qquad x_0 \mapsto s, \ x_i \mapsto s \cdot f_i, \quad i = 1, \ldots, k. \tag{1.9}$$

Here we introduce a homogenizing variable s to obtain projective varieties. The homogeneous ideal $\mathcal{I}(V)$ is the kernel of this map. The image of this map is a subalgebra of $\mathbb{C}[s, \mathbf{t}]$ generated by s and the polynomials $s \cdot h_i$. Now assume these generators form a Khovanskii basis of $\mathbb{C}[s, \mathbf{t}]$ with respect to a chosen monomial order on $\mathbb{C}[s, \mathbf{t}]$. Then consider the following monomial map

$$\mathbb{C}[\mathbf{x}] \to \mathbb{C}[s, \mathbf{t}], \qquad x_0 \mapsto s, \ x_i \mapsto s \cdot \mathrm{in}(h_i), \quad i = 1, \ldots, k. \tag{1.10}$$

We call the variety parameterized by this map, i.e. the variety whose ideal is defined by the kernel of (1.10), a *toric degeneration* of V and we denote it by $\mathcal{T}_V$. Although the variety $\mathcal{T}_V$ is typically much simpler than V, it preserves many invariants, such as dimension and degree. Here it is important that the generators form a Khovanskii basis.

Varieties parameterized by monomial maps, such as $\mathcal{T}_V$, are called *toric varieties*. They are particularly well-behaved: their defining ideals are prime and generated by binomials. Moreover, many geometric invariants of toric varieties admit a combinatorial description, see [97, Chapter 4]. In particular, suppose a toric variety $T \subseteq \mathbb{P}^k$ is parameterized by

$$\mathbb{C}[\mathbf{x}] \to \mathbb{C}[\mathbf{t}], \qquad x_i \mapsto \mathbf{t}^{a_i}, \quad i = 0, 1, \ldots, k.$$

Then the dimension of T equals the dimension of the polytope defined as the convex hull of the exponent vectors. This polytope is denoted $P_T \subseteq \mathbb{R}^m$ and can be written as $P_T = \mathrm{conv}(a_0, a_1, \ldots, a_k)$. The degree of T is also determined by P_T, it is the *normalized volume* of P_T. That is, if $d = \dim T$, then $\deg(T) = d! \, \mathrm{Vol}(P_T)$, where $\mathrm{Vol}(P_T)$ is the Euclidean volume.

Example 1.1.14 (Veronese variety)**.** A basic example of a toric variety is the quadratic Veronese embedding of $\mathbb{P}^3$. This variety is parameterized by the map

$$\nu_2 : \mathbb{P}^3 \to \mathbb{P}^9, \quad [x_0 : x_1 : x_2 : x_3] \mapsto [x_0^2 : x_0x_1 : x_0x_2 : x_0x_3 : x_1^2 : x_1x_2 : x_1x_3 : x_2^2 : x_2x_3 : x_3^2].$$

The associated polytope is the convex hull of the exponent vectors of these monomials, which is the dilated simplex $2\Delta_3$. This polytope naturally lives in $\mathbb{R}^4$, but all exponent vectors satisfy the relation $a_0 + a_1 + a_2 + a_3 = 2$, so it lies in this affine hyperplane, which we may identify with $\mathbb{R}^3$. Under this identification the polytope can be visualized as in Figure 1.4.

In particular, $2\Delta_3$ is a 3-dimensional polytope, and hence the Veronese variety has dimension 3. Moreover, its degree equals the normalized volume of $2\Delta_3$. Since the volume of the standard 3 dimensional simplex Δ_3 is $\frac{1}{3!}$, and volume in $\mathbb{R}^3$ scales by the cube of the dilation factor, we obtain the degree $\deg(\nu_2(\mathbb{P}^3)) = 3!\mathrm{Vol}(2\Delta_3) = 2^3 \, 3!\mathrm{Vol}(\Delta_3) = 8$.

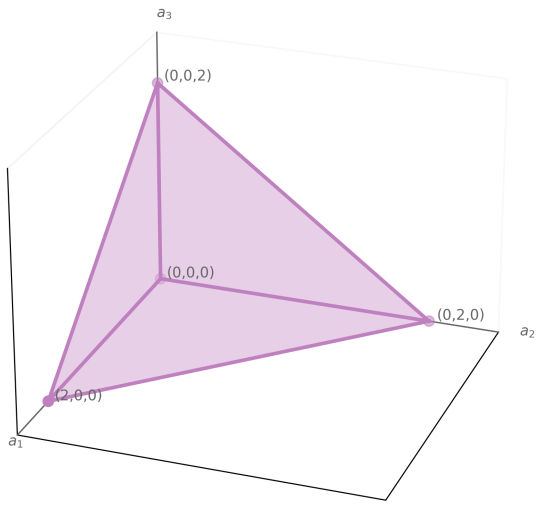

Figure 1.4: The dilated simplex $2\Delta_3$ in $\mathbb{R}^3$.

Remark 1.1.15 (Constructing a toric degeneration)**.** Previously we assumed that the polynomials parameterizing a projective variety $V \subseteq \mathbb{P}^k$ already form a Khovanskii basis. In practice, however, finding such parameterizations is not straightforward, and it may be necessary to embed V into a different projective space. Suppose that $V \subseteq \mathbb{P}^k$ is parameterized by the polynomial map (1.8). Then the image of the corresponding map on coordinate rings is the subalgebra $\mathbb{C}[s, sh_1, \ldots, sh_k] \subseteq \mathbb{C}[s, \mathbf{t}]$. Assume that this subalgebra admits a finite Khovanskii basis $G = \{s, sg_1, \ldots, sg_r\}$. The variety V can then be described via the map

$$\mathbb{C}[\mathbf{y}] \to \mathbb{C}[s, \mathbf{t}], \qquad y_0 \mapsto s,\ y_i \mapsto sg_i, \qquad i = 1, \ldots, r.$$

This realizes V as a projective variety embedded in $\mathbb{P}^r$, whose ideal is the kernel of this map. Taking initial monomials with respect to the chosen monomial order yields the corresponding initial map. Since the coordinates of that map are monomials, the corresponding variety is a toric variety, and thus this construction produces a toric degeneration of V in $\mathbb{P}^r$.

Algorithms for working with Khovanskii bases have been developed and implemented in computer algebra systems. In this context, Khovanskii bases are often referred to as *SAGBI bases* (Subalgebra Analogs to Gröbner Bases for Ideals). In particular, the algorithm `SagbiGbDetection` [7] determines all monomial orders for which a given generating set forms a Khovanskii basis. It has been implemented in both `Macaulay2` and `Julia`. Methods for computing Khovanskii bases are also available. For instance, they are implemented in the `Macaulay2` package `SubalgebraBases` [14].

We conclude this section with an example illustrating a Khovanskii basis for a birational parameterization of the Grassmannian of lines.

Example 1.1.16. Consider the Grassmannian of lines, $\mathrm{Gr}(2,n)$. The 2×2 minors in (1.5) parameterizing the $\mathrm{Gr}(2,n)$, form a Khovanskii basis with respect to a monomial order choosing the diagonal terms as leading terms. This is shown in [73, Section 14.3] and can be verified using `isSAGBI` in `SubalgebraBases.m2`. The corresponding polytope of the toric degeneration is called the Gel'fand-Tsetlin polytope, denoted $\mathrm{GT}(2,n)$. Its dimension is $2(n-2)$ and its normalized volume is the Catalan number C_{n-2}.

1.2 Quantum Chemistry

The material in this section provides a brief introduction to quantum chemistry aimed at mathematicians. No background in chemistry beyond what is taught in high school is assumed. This is largely based on Section 4 of [37]. Electronic structure theory is a powerful quantum mechanical framework for studying the behavior of electrons in molecules and crystalline materials [50]. At its core are the interactions between particles, in particular the electron–electron and electron–nucleus interactions, which determine the electronic structure of a system.

Throughout this thesis we consider electronic systems consisting of d electrons occupying n spin orbitals. A running example is the lithium hydride molecule (LiH), which has $d=4$ electrons. Depending on whether a frozen-core approximation is used, the number of spin orbitals ranges from $n=8=2d$ to $n=12$. A central problem in electronic structure theory is to determine the stable states of this electronic system, and their corresponding energies [50]. This problem is encoded by the *electronic Schrödinger equation*

$$\mathscr{H}\,\Psi(\mathbf{x}_1,\mathbf{x}_2,\ldots,\mathbf{x}_d) \;=\; E\,\Psi(\mathbf{x}_1,\mathbf{x}_2,\ldots,\mathbf{x}_d). \tag{1.11}$$

This equation contains two unknowns: the *wave function* $\Psi(\mathbf{x}_1,\mathbf{x}_2,\ldots,\mathbf{x}_d)$ and the *energy* E.

The wave function Ψ is a sufficiently differentiable real-valued function. Its arguments are points $\mathbf{x}_i=(\mathbf{r}_i,s_i)$, where $\mathbf{r}_i=(r_i^{(1)},r_i^{(2)},r_i^{(3)})\in\mathbb{R}^3$ denotes the position of the ith electron and s_i encodes its spin, taking values $\uparrow$ or $\downarrow$. Hence $\mathbf{x}_i\in\mathbb{R}^3\times\{\uparrow,\downarrow\}=X$. The wave function Ψ describes the *quantum state* of the electrons in the molecule. Its squared magnitude $|\Psi|^2$ gives the probability density of finding the electrons at the specified positions and spins. Thus the wave function determines the joint probability distribution of all electrons in the system. By *Pauli's exclusion principle* [82], the wave function must be antisymmetric in its d arguments, that is exchanging two electrons changes the sign of Ψ. Consequently we may view

$$\Psi : X^d\to\mathbb{R}, \qquad \Psi\in\wedge^d L^2(X)\subsetneq L^2(X^d).$$

Here we write $\wedge^d L^2(X)$ for the subspace of skew-symmetric functions in $L^2(X^d)$. That is,

$$\wedge^d L^2(X)=\left\{\Psi\in L^2(X^d) : \Psi(\mathbf{x}_{\sigma(1)},\ldots,\mathbf{x}_{\sigma(d)})=\mathrm{sign}(\sigma)\Psi(\mathbf{x}_1,\ldots,\mathbf{x}_d) \text{ for all } \sigma\in S_d\right\}.$$

The second unknown is the energy E corresponding to Ψ. The lowest energy solution of (1.11) is called the *ground state* and it corresponds to the most stable electronic configuration

of the system. Solutions with higher energy are called *excited states*. These states can be observed when energy is supplied to the system, for example through heat, electricity, or light.

Equation (1.11) encodes the eigenvalue problem for the Hamiltonian $\mathscr{H}$. It is a second-order self-adjoint differential operator describing the behavior of an electronic system with d interacting electrons in the vicinity of d_{nuc} stationary nuclei. Its formula is

$$\mathscr{H} \;=\; -\frac{1}{2}\sum_{i=1}^{d}\Delta_{\mathbf{r}_i} \;-\; \sum_{i=1}^{d}\sum_{j=1}^{d_{\text{nuc}}}\frac{Z_j}{|\mathbf{r}_i-\mathbf{R}_j|} \;+\; \sum_{i=1}^{d}\sum_{j=i+1}^{d}\frac{1}{|\mathbf{r}_i-\mathbf{r}_j|}. \tag{1.12}$$

The symbol $\Delta_{\mathbf{r}_i}$ in the leftmost sum denotes the Laplacian $\sum_{j=1}^{3}(\partial/\partial r_i^{(j)})^2$. All other summands in (1.12) act on Ψ by multiplication. They contain constants which we now explain. The atoms in the system and their nuclei are indexed by $j = 1, 2, \ldots, d_{\text{nuc}}$. The constant Z_j is the nuclear charge of the jth atom. This is the atomic number listed in the periodic table, i.e. Z_j is a positive integer. The position of the jth nucleus is the point $\mathbf{R}_j \in \mathbb{R}^3$, which is also constant. We mostly consider charge-neutral molecules, in which case $d = \sum_{j=1}^{d_{\text{nuc}}} Z_j$.

Example 1.2.1 (Lithium hydride)**.** This molecule has the formula LiH. It involves $d_{\text{nuc}}=2$ atoms, namely lithium Li and hydrogen H. Their atomic numbers are $Z_1 = 3$ and $Z_2 = 1$, respectively. Hence the number of electrons is $d = Z_1 + Z_2 = 4$.

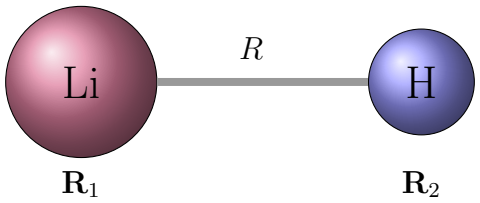

The two nuclei are fixed at locations $\mathbf{R}_1$ and $\mathbf{R}_2$, whereas the four electrons have variable locations $\mathbf{r}_1, \mathbf{r}_2, \mathbf{r}_3, \mathbf{r}_4$. The bond distance between the two atoms is $R = |\mathbf{R}_1 - \mathbf{R}_2|$.

Discretization

The electronic Schrödinger equation is posed on the infinite-dimensional space $\wedge^d L^2(X) \times \mathbb{R}$. Consequently, it cannot be solved exactly for realistic electronic systems. To make the problem computationally tractable, we approximate the state space $\wedge^d L^2(X)$ by a finite-dimensional vector space. This discretization transforms (1.11) into a finite-dimensional algebraic system of equations, namely to an eigenvalue equation for a matrix. There are many ways to select a suitable basis, and hence a discretization of $\wedge^d L^2(X)$. See [63] and [103, Section 2.2] for an overview. We apply the method called *linear combination of atomic orbitals* (LCAO). This is used widely in quantum chemistry. The LCAO method starts with *atomic orbitals*. They are real-valued functions $\chi : \mathbb{R}^3 \to \mathbb{R}$, defined as the eigenfunctions of the Schrödinger equation of a single electron moving in the potential of a nucleus. Here the spin is omitted.

Remark 1.2.2. The hydrogen-like (one-electron) Schrödinger equation can be written as

$$\left(-\frac{1}{2}\Delta - \frac{Z}{|\mathbf{r}|}\right)\Psi(\mathbf{r}) = E\Psi(\mathbf{r}).$$

The equation has spherical symmetry. We may therefore introduce spherical coordinates $\mathbf{r} = (r, \theta, \phi)$ and separate the wave function as $\Psi(r, \theta, \phi) = R(r)Y(\theta, \phi)$. Substituting this ansatz into the Schrödinger equation leads to two independent equations.

The angular part satisfies the differential equation

$$L^2 Y(\theta, \phi) = \ell(\ell + 1)Y(\theta, \phi),$$

where L^2 is the total angular momentum operator. The solutions of this equation are the spherical harmonics $Y_\ell^k(\theta, \phi)$, indexed by a nonnegative integer $\ell = 0, 1, 2, \dots$ and an integer $k = -\ell, \dots, \ell$, see [51, Section 6.4]. These describe the angular momentum of the electron.

The radial part is an ordinary differential equation depending on ℓ. Physical wave functions must be square integrable, since the quantity $|\Psi(\mathbf{r})|^2$ represents a probability density and therefore satisfies $\int_{\mathbb{R}^3} |\Psi(\mathbf{r})|^2 \, d\mathbf{r} = 1$. Imposing this condition yields a discrete set of solutions with energies $E_n = -\frac{Z^2}{2n^2}$, where $n = 1, 2, \dots$ is a positive integer, see [51, Section 6.5].

The *atomic orbitals* are therefore indexed by three *quantum numbers*: the principal quantum number $n = 1, 2, \dots$, the angular momentum quantum number $\ell = 0, 1, \dots, n-1$, and the magnetic quantum number $k = -\ell, \dots, \ell$. Atomic orbitals are commonly denoted by combining the principal quantum number n with a letter indicating the angular momentum quantum number ℓ ($\ell = 0, 1, 2, \dots$ corresponds to $s, p, d, \dots$). For example, the orbital labeled $2p$ has $n = 2$ and $\ell = 1$. The magnetic quantum number k determines the orientation of the orbital, for example when $\ell = 1$ then $k = -1, 0, 1$ corresponds to the p orbitals p_x, p_y, p_z. Readers can refer to [51, Chapters 5, 6 and 8] for a comprehensive explanation and motivation.

For our electronic system of interest, we select a basis set $\{\chi_1, \chi_2, \dots, \chi_m\}$ of atomic orbitals. The orbitals used in computations are usually not exact atomic orbitals, but approximations constructed from functions such as Gaussians. Notably, approximated atomic orbital basis sets for different atoms are well documented and available through online data resources such as `www.basissetexchange.org`. The number m of atomic orbitals is greater than or equal to the number d of electrons, i.e. $d \leq m$. Note that the equality $d = m$ can hold.

Example 1.2.3 ($d = m = 4$)**.** We revisit the lithium hydride (LiH) molecule. We select $m = 4$ atomic orbitals. We choose the three orbitals 1s, 2s, $2p_z$ for lithium and 1s for hydrogen. A graphical representation of these four atomic orbitals is shown in Figure 1.5. The pictures are iso-surfaces for $\chi_1, \dots, \chi_4$. An *iso-surface* has the form $\{\mathbf{r} \in \mathbb{R}^3 : \chi_i(\mathbf{r}) = c\}$, for a constant c that can be positive or negative.

We now need to account for the *electronic spin*, a crucial degree of freedom in electronic structure theory that distinguishes physical states. In the non-relativistic Born–Oppenheimer model considered here [103, Section 2.1.2], spin does not appear explicitly in the electronic

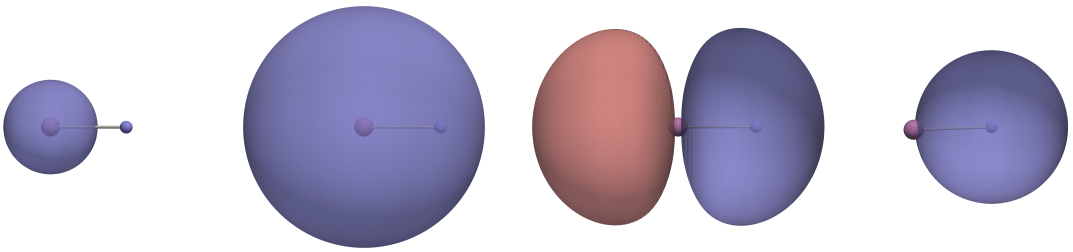

Figure 1.5: Iso-surfaces of four atomic orbitals (Li: 1s, 2s, $2p_z$; H: 1s) of lithium hydride. The iso-surfaces correspond to the value ± 0.025, with blue for $c = +0.025$ and red for $c = -0.025$.

Hamiltonian (1.12). Hence we may introduce a product basis. That is, for each atomic orbital χ_i we introduce two spin orbitals [103, Section 2.2.1]:

$$\phi_{i,\uparrow}(\mathbf{r}, s) = \chi_i(\mathbf{r})\delta_{s\uparrow}, \quad \phi_{i,\downarrow}(\mathbf{r}, s) = \chi_i(\mathbf{r})\delta_{s\downarrow}.$$

We will also use the shorthand indexing $\phi_{2i-1} = \phi_{i,\uparrow}$ and $\phi_{2i} = \phi_{i,\downarrow}$. We therefore have $2m$ spin orbitals, and we set $n = 2m$, the number of spin-orbitals.

The spin orbitals form a basis of an n–dimensional real vector space. This space is called the *one-particle space*, and it is denoted by $\mathcal{H} \cong \mathbb{R}^n$. By the definition of the basis vectors $\{\phi_i\}$ we also write $\mathcal{H} \cong \mathbb{R}^m \otimes \mathcal{H}_{\text{spin}}$, where $\mathcal{H}_{\text{spin}} \cong \mathbb{R}^2$ is the two-dimensional *spin space* and $\mathbb{R}^m$ is the space spanned by the spatial orbitals. We discuss the spin degree of freedom in more detail later in this section. In practice, the atomic spin orbitals are usually not chosen as a basis for the one-particle space. Instead, we perform a change of basis to $\{\xi_1, \ldots, \xi_n\}$ using an invertible $n \times n$ matrix C. The resulting basis orbitals ξ_i are called the *molecular spin orbitals*, and C is the *MO coefficient matrix*. It is obtained from *Hartree–Fock theory*; see, for example, [51, Chapter10] or [64, Chapter2.1] for a detailed account. In brief, the molecular orbitals are the eigenvectors of the Fock operator F, an operator determined by the electronic system and acting on single orbitals. Here we assume that F is an $n \times n$ matrix.

Example 1.2.4 ($d = 4, m = 4$)**.** For our specific example, lithium hydride, we compute the MO coefficient matrix C using PySCF [99, 100]. In this example, the Hartree–Fock computation is carried out at the level of the $m = 4$ atomic spatial orbitals, and spin is added only afterward. Thus the change of basis is performed on the 4 spatial orbitals, rather than directly on the $n = 8$ spin orbitals. As a result, C is a 4×4 matrix:

$$C = \begin{bmatrix} -0.99112752 & -0.17382072 & -0.20878285 & 0.08016223 \\ -0.0320641 & 0.44684406 & 0.80124872 & -0.74021563 \\ 0.00710779 & 0.34924425 & -0.61278358 & -1.00784027 \\ -0.00676776 & 0.54437143 & -0.13420716 & 1.23313556 \end{bmatrix}.$$

The molecular spatial orbitals obtained from this change of basis are depicted in Figure 1.6.

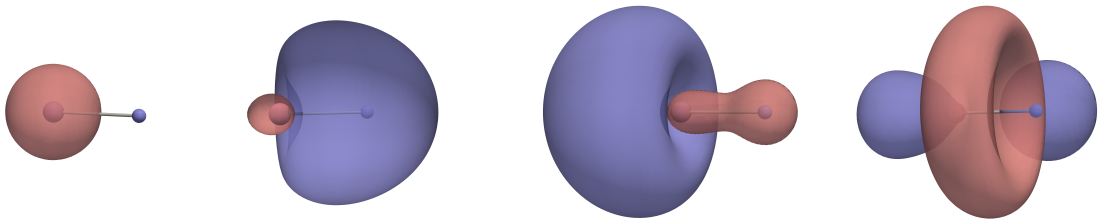

Figure 1.6: Iso-surfaces for ± 0.04 of four molecular orbitals of lithium hydride.

The $n = 8$ molecular spin orbitals $\xi_1, \dots, \xi_8$ are then constructed from the molecular spatial orbitals by associating, to each spatial orbital indexed by i, two spin orbitals ξ_{2i-1} and ξ_{2i}, obtained by multiplying that spatial orbital by $\delta_{s\uparrow}$ and $\delta_{s\downarrow}$, respectively.

This construction differs from the one above only in the order of the steps: here one first applies Hartree–Fock to the spatial orbitals and only afterward introduces spin, whereas above one first forms the spin product basis and then applies Hartree–Fock. Both approaches are common; the present one is used when one wishes to preserve spin symmetry.

We now construct the *d–electron state space*, which discretizes $\wedge^d L^2(X)$, by skew symmetrization; see [62, Section 2.6.7]. This space is the dth exterior power $\mathcal{H}_d := \wedge^d \mathcal{H} \cong \wedge^d \mathbb{R}^n$. A basis of $\mathcal{H}_d$ is given by the normalized wedge products

$$\Psi_J(\mathbf{x}) = \frac{1}{\sqrt{d!}} (\xi_{j_1} \wedge \cdots \wedge \xi_{j_d})(\mathbf{x}) = \frac{1}{\sqrt{d!}} \det((\xi_j(\mathbf{x}_i)_{j \in J, i \in [d]})).$$

Here $J = \{j_1 < \cdots < j_d\}$ ranges over the subsets $J \subseteq [n]$ of size d, and $\mathbf{x} = (\mathbf{x}_1, \dots, \mathbf{x}_d) \in X^d$. Wavefunctions of the form $\psi_1 \wedge \cdots \wedge \psi_d$ with $\psi_i \in \mathcal{H}$ are called *Slater determinants* in quantum chemistry. In particular, the basis vectors Ψ_J are the Slater determinants obtained from the orbital basis $\{\xi_1, \dots, \xi_n\}$, see [51, Section 1.1]. The d–electron space $\mathcal{H}_d$ has dimension $\binom{n}{d}$ and it serves as a finite-dimensional approximation to the function space $\wedge^d L^2(X)$ of d–electron wave functions. Consequently, the electronic Schrödinger equation restricted to $\mathcal{H}_d$ becomes an eigenvalue equation for a symmetric matrix. That is

$$H\psi = E\psi, \qquad \psi \in \mathcal{H}_d. \tag{1.13}$$

Here H is the $\binom{n}{d} \times \binom{n}{d}$ symmetric matrix representing the Hamiltonian operator $\mathscr{H}$ in the basis $\{\Psi_J\}$ of $\mathcal{H}_d$. Its entries are determined by expanding $\mathscr{H}\Psi_J$ in this basis. This formulation of the electronic Schrödinger equation is known as *first quantization*.

Remark 1.2.5 (Expanding functions in the basis $\{\Psi_J\}$)**.** We want to represent the Hamiltonian operator $\mathscr{H}$ on the finite-dimensional subspace $\mathcal{H}_d \subset \wedge^d L^2(X)$ spanned by the basis $\{\Psi_J\}$. To this end we equip $L^2(X)$ with the inner product

$$\langle \phi_i, \phi_j \rangle_{L^2(X)} := \int \phi_i(\mathbf{x}) \phi_j(\mathbf{x}) \, d\mathbf{x}.$$

The atomic orbitals need not be orthonormal with respect to this inner product. By contrast, the molecular orbitals ξ_i are chosen to form an orthogonal basis of $\mathcal{H}$ with respect to it. This induces the canonical inner product on the exterior power $\wedge^d L^2(X)$, under which the Slater determinants $\{\Psi_J\}$ form an orthogonal basis of $\mathcal{H}_d$. The entries of the symmetric $\binom{n}{d} \times \binom{n}{d}$ Hamiltonian matrix H are then

$$H_{I,J} = \langle \Psi_I, \mathscr{H}\Psi_J \rangle_{\wedge^d L^2(X)}.$$

Hence H represents the projection of $\mathscr{H}$ onto the finite-dimensional subspace $\operatorname{span}\{\Psi_J\}$.

Example 1.2.6 (Lithium hydride)**.** In our running example we consider $d = 4$ electrons and $n = 2d = 8$ spin orbitals. The Hamiltonian matrix H for LiH is therefore a symmetric 70×70 matrix, since $\binom{8}{4} = 70$. Using PySCF [99], we evaluate the following one- and two-electron integrals for all indices $p, q, r, s \in [8]$:

$$h_{p,q} = -\int \xi_p(\mathbf{x}) \left(\frac{\Delta_{\mathbf{r}}}{2} + \sum_j \frac{Z_j}{|\mathbf{r} - \mathbf{R}_j|} \right) \xi_q(\mathbf{x})\, d\mathbf{x}, \;\; v_{p,q,r,s} = \int \frac{\xi_p(\mathbf{x})\xi_q(\mathbf{x})\xi_r(\mathbf{x}')\xi_s(\mathbf{x}')}{|\mathbf{r} - \mathbf{r}'|}\, d\mathbf{x}\, d\mathbf{x}'. \tag{1.14}$$

These integrals are computed with respect to the molecular orbital basis $\{\xi_1(\mathbf{x}), \ldots, \xi_8(\mathbf{x})\}$ obtained in Example 1.2.4. Since each molecular orbital depends on a single variable, the integrals arising in the matrix elements $H_{I,J} = \langle \Phi_I, \mathscr{H}\Phi_J \rangle$ factorize into combinations of the one-electron integrals $h_{p,q}$ and the two-electron integrals $v_{p,q,r,s}$. This yields the following expression for the Hamiltonian entries:

$$H_{I,J} = \sum_{\substack{\rho \in S_I \\ \pi \in S_J}} \operatorname{sgn}(\rho) \operatorname{sgn}(\pi) \sum_{\ell=1}^{4} \Bigg(h_{\rho(i_\ell),\pi(j_\ell)} \prod_{\ell \neq k = 1}^{4} \delta_{\rho(i_k),\pi(j_k)} + \sum_{j > \ell}^{4} v_{\rho(i_\ell),\pi(j_\ell),\rho(i_j),\pi(j_j)} \prod_{\ell \neq j \neq k = 1}^{4} \delta_{\rho(i_k),\pi(j_k)} \Bigg).$$

From now on, our main objective is to solve the eigenvalue problem for the *Hamiltonian matrix* H, that is, to solve (1.13). We interpret this as an eigenvalue problem over an abstract vector space via the identification $\mathcal{H}_d \cong \wedge^d \mathbb{R}^n$. Using the standard basis $\{e_1, \ldots, e_n\}$ of $\mathbb{R}^n$, the space $\wedge^d \mathbb{R}^n$ has the canonical wedge basis e_J, where $J \in \binom{[n]}{d}$. Vectors $\psi \in \wedge^d \mathbb{R}^n$ are called *quantum states*, and their coordinates ψ_J in the basis $\{e_J\}$ are called *Plücker coordinates*, referring to the Grassmannian. The wave function $\Psi(\mathbf{x})$ corresponding to the quantum state $\psi \in \wedge^d \mathbb{R}^n$ is obtained by taking the linear combination of the basis states $\{\Psi_J(\mathbf{x})\}_J$ with coefficients given by the coordinates of ψ.

Remark 1.2.7 (Complexification)**.** Later, when applying algebraic-geometric methods to this problem, it becomes necessary to work over an algebraically closed field. In that setting, we extend the real numbers to their algebraic closure $\mathbb{C}$ and consider the state space $\wedge^d \mathbb{C}^n$. This extension is made for algebraic purposes rather than to study genuinely complex quantum states, and accordingly we model the Hamiltonian as a complex symmetric matrix. In particular, we do not impose the Hermitian condition on H, although that would be natural in a genuinely complex quantum-mechanical setting. The reason is that Hermitianity involves

complex conjugation and is therefore not an algebraic property. Symmetry, by contrast, is algebraic and fits naturally into our framework. This is sufficient for our purposes, since we are ultimately interested in real solutions, while the complex ones arise as part of the algebraic closure. We will also later extend this construction to projective space, $\mathbb{P}(\mathcal{H}_d) \cong \mathbb{P}^{\binom{n}{d}-1}$.

Coupled Cluster Theory

Eigenvalue problems are a central theme in mathematics and among the most widely studied computational problems. While conceptually elementary, they can become infeasible for large matrices. Since the dimension of the Hamiltonian matrix H grows exponentially with the system size, efficient and tractable numerical schemes are essential for approximating the behavior of complex atoms and molecules [64]. One class of widely used high-accuracy approximation methods is based on *coupled cluster (CC) theory* [51, Section 13], which forms a central theme of this thesis. It is considered the gold standard for accurately approximating ground-state energies of weakly correlated systems near equilibrium. Coupled cluster theory in first quantization, viewed from the perspective of nonlinear algebra, will be the main focus of Part I in this thesis. We now give a brief introduction from a more quantum chemical perspective. A more detailed and algebraic treatment can be found in Chapter 2.

We begin with the reference state $e_{[d]} = e_1 \wedge \cdots \wedge e_d$. This is also known as the *Hartree–Fock state*, as it corresponds to the optimal Slater determinant Ψ obtained from Hartree–Fock theory (see the discussion on molecular orbitals above). The eigenstates of the Hamiltonian are typically correlated (entangled) and are therefore not Slater determinants (i.e. represented by rank 1 elements in $\wedge^d\mathbb{R}^n$). To describe such states, we first introduce *excitation operators*. For each $I \subseteq [d]$ and $B \subseteq [n]\backslash[d]$ where $|I| = |B|$ we define the excitation operator

$$\chi_{I,B} : \mathcal{H}_d \to \mathcal{H}_d, \quad e_J \mapsto \begin{cases} \pm e_{(J\backslash I)\cup B} & \text{if } I \subseteq J \text{ and } B \cap J = \varnothing \\ 0 & \text{otherwise} \end{cases}$$

In particular it maps the reference state $e_{[d]}$ to a signed basis vector $e_{([d]\backslash I)\cup B}$. We call $k = |I|$ the level of the operator. The basis vector $e_J = \chi_{I,B} e_{[d]}$ is then also said to have level k. The *cluster operator* T is defined as a general linear combination of these excitation operators. It decomposes as a graded operator

$$T = T_1 + \cdots + T_d, \qquad T_k = \sum_{|I|=|B|=k} t_{I,B}\chi_{I,B}, \tag{1.15}$$

where T_k is a general linear combination of all level-k excitation operators. The coefficients $t_{I,B}$ are unknowns and are called *cluster amplitudes*. The corresponding cluster matrix is a nilpotent $\binom{n}{d} \times \binom{n}{d}$ matrix, also denoted T. Indeed $T^{d+1} = 0$.

We are able to describe higher-rank (entangled) states by the following ansatz. In coupled cluster theory one assumes that quantum states can be parameterized as

$$\psi = \exp(T)\, e_{[d]}. \tag{1.16}$$

The new unknowns are the cluster amplitudes $t_{I,B}$. Since $T^{d+1} = 0$, the exponential $\exp(T)$ is a finite polynomial in T. Substituting the parameterization (1.16) into (1.13) yields

$$H \exp(T) e_{[d]} = E \exp(T) e_{[d]}, \qquad \text{i.e.} \qquad \exp(-T) H \exp(T) e_{[d]} = E e_{[d]}. \tag{1.17}$$

These are known as the *coupled cluster equations*. Different approximations are obtained by truncating T to certain excitation levels. The resulting equations are then projected onto the subspace spanned by basis vectors of those levels. The most common approximations are CCS (singles), CCD (doubles), and CCSD (singles and doubles), corresponding to the truncations $T := T_1$, $T := T_2$, and $T := T_1 + T_2$, respectively. In this thesis we study abstract truncations, that is, we consider arbitrary truncation sets $\sigma \subseteq [d]$. In this notation, CCS corresponds to $\sigma = \{1\}$, CCD corresponds to $\sigma = \{2\}$, and CCSD corresponds to $\sigma = \{1, 2\}$.

More precisely, (1.17) are called the *linked coupled cluster equations*, and they are the formulation most commonly used in practice. In this thesis, however, we focus on the algebraically simpler *unlinked coupled cluster equations*. We refer to [51, Section 13.2.3] for the definition of both formulations and a comparison between them. Both formulations are also introduced in Section 2.3, and in Theorem 2.3.10 we show that they are equivalent in all cases of chemical interest.

Second Quantization

Mathematically, the formulation above is very neat. However, for large molecules — for instance with $d = 50$ electrons in at least $n = 100$ spin-orbitals — the state space $\mathcal{H}_d$ becomes enormous: it has dimension $\binom{100}{50} \approx 10^{29}$. In such cases, even writing the Hamiltonian as a matrix becomes infeasible. A key observation is that the physical electronic Hamiltonian is highly structured. This motivates the use of *second quantization*. In this framework, instead of representing many-electron operators on $\wedge^d \mathcal{H}$ (such as the Hamiltonian) by explicit matrices, we express them as polynomials in an operator algebra known as the Fermi–Dirac algebra. We give a brief introduction to this formalism here. Its systematic algebraic development forms the focus of Part II of this thesis.

To this end, we introduce the *fermionic Fock space* $\mathcal{F}$ as the exterior algebra $\wedge\mathcal{H} \cong \wedge\mathbb{R}^n$. In this way, the state space is extended from the dth exterior power $\mathcal{H}_d \cong \wedge^d \mathbb{R}^n$ to the full exterior algebra, which is naturally equipped with the product $\wedge$. On $\mathcal{F}$ we then define the *creation and annihilation operators* as exterior and interior products:

$$a_p^\dagger : \mathcal{F} \to \mathcal{F}, \quad \psi \mapsto e_p \wedge \psi = \sum_{J \subseteq [n]} \psi_J e_p \wedge e_J$$
$$a_p : \mathcal{F} \to \mathcal{F}, \quad \psi \mapsto e_p \lrcorner \psi = \sum_{J \subseteq [n]} \psi_J e_p \lrcorner e_J.$$

The symbol $\lrcorner$ denotes the dual operation of the wedge product $\wedge$, called the hook product,

see [44, Section 3.6] for a definition. Explicitly we have

$$e_p \wedge e_I = \begin{cases} (-1)^h e_{I\cup\{p\}} & \text{if } p \notin I \\ 0 & \text{otherwise,} \end{cases} \qquad e_p \lrcorner e_I = \begin{cases} (-1)^h e_{I\setminus\{p\}} & \text{if } p \in I \\ 0 & \text{otherwise.} \end{cases} \tag{1.18}$$

Here the signs are determined by $h = |\{i \in I \,:\, i < p\}|$. As the name suggests these operators correspond to creating and annihilating particles at the orbital numbered p, for $p = 1, \ldots, n$. They fulfill the following anticommutation relations (often denoted CAR, see [32, Section 2])

$$a_p^\dagger a_q^\dagger + a_q^\dagger a_p^\dagger = 0, \quad a_p a_q + a_q a_p = 0, \quad a_p^\dagger a_q + a_q a_p^\dagger = \delta_{p,q}.$$

Hence, the operators encode the skew-symmetry properties of fermionic states.

The Hamiltonian operator $\mathscr{H}$, defined in (1.12), consists of a term acting on a single electron, called the *one-body part*, and a term acting on pairs of electrons, called the *two-body part*. We can therefore express the electronic Hamiltonian in second-quantized form as the following sum of a one-body term and a two-body term

$$H = \sum_{p,q=1}^{n} h_{p,q}\, a_p^\dagger a_q + \frac{1}{2} \sum_{p,q,r,s=1}^{n} v_{p,q,r,s}\, a_p^\dagger a_r^\dagger a_s a_q. \tag{1.19}$$

Here the coefficients $h_{p,q}$ and $v_{p,q,r,s}$ are given by the integrals (1.14). Since the creation and annihilation operators are endomorphisms of the Fock space $\mathcal{F}$, the second-quantized Hamiltonian defines an endomorphism of $\mathcal{F}$. Moreover, each monomial in (1.19) contains the same number of creation and annihilation operators. Therefore the Hamiltonian preserves particle number and restricts to an endomorphism of $\mathcal{H}_d$. This provides a compact and equivalent representation of the Hamiltonian matrix H in terms of a symmetric $n \times n$ matrix h and an $n \times n \times n \times n$ tensor v, with symmetry properties which are described in Section 6.2.

Second quantization is particularly well suited for methods such as coupled cluster theory. In this framework, the excitation operators are monomials in the creation and annihilation operators, and we may write the cluster operator T as the polynomial

$$T = \sum_{\substack{I\subseteq[d],\, B\subseteq[n]\setminus[d] \\ |I|=|B|>0}} t_{I,B}\, a_{b_k}^\dagger \cdots a_{b_1}^\dagger a_{i_1} \cdots a_{i_k}.$$

Furthermore, by working over the full exterior algebra $\mathcal{F} \cong \wedge\mathbb{R}^n$, we can extend our study from systems with a fixed number of electrons (fixed-N) to processes involving ionization and electron attachment. There we obtain approximation schemes such as *Fock space coupled cluster* (FSCC) [30, 58, 65] and *equations of motion coupled cluster* (EOM-CC) [93].

Spin

In the formulation so far, spin has appeared only implicitly through the definition of spin orbitals. Physically, spin represents an additional internal degree of freedom of the electron.

Electrons possess an intrinsic angular momentum called *spin* [89]. Since electrons are fermions, the spin quantum number is $s = \frac{1}{2}$, giving rise to two possible spin states, "spin up" ($\uparrow$) and "spin down" ($\downarrow$). Taking spin into account reveals additional symmetries and leads to important simplifications in the structure of the state space and the resulting equations. We briefly introduce these ideas here. Their full development, especially from an algebraic point of view, is the subject of Part III of this thesis.

The intrinsic angular momentum of an electron (i.e. its spin) is described by the action of the *special unitary group* $\mathrm{SU}(2)$ on the two-dimensional spin space $\mathcal{H}_{\text{spin}}$. To this end, we introduce the following *spin operators*

$$S_+ = \begin{bmatrix} 0 & 1 \\ 0 & 0 \end{bmatrix}, \qquad S_- = \begin{bmatrix} 0 & 0 \\ 1 & 0 \end{bmatrix}, \qquad S_z = \frac{1}{2}\begin{bmatrix} 1 & 0 \\ 0 & -1 \end{bmatrix}.$$

The operators S_+ and S_- are known as the *raising and lowering operators* [51, Section 2.2.2]. These matrices form a basis of the complex Lie algebra $\mathfrak{sl}_2(\mathbb{C})$, which is the complexification of the Lie algebra $\mathfrak{su}(2)$ of $\mathrm{SU}(2)$. They define a Lie algebra action of $\mathfrak{sl}_2(\mathbb{C})$ on the spin space $\mathcal{H}_{\text{spin}}$ via left multiplication with respect to the basis $e_\uparrow = e_1$ and $e_\downarrow = -e_2$ of $\mathcal{H}_{\text{spin}}$, see [104, Section 3.2]. This Lie algebra representation integrates to a representation of $\mathrm{SU}(2)$ on $\mathcal{H}_{\text{spin}}$, and hence induces an action of $\mathrm{SU}(2)$ on $\mathcal{H}_{\text{spin}}$. We also introduce the *total spin operator*

$$S^2 := S_z^2 + \tfrac{1}{2}\big(S_+S_- + S_-S_+\big).$$

This is the *Casimir operator* of $\mathfrak{sl}_2(\mathbb{C})$. Hence it acts as a scalar on each irreducible representation of $\mathfrak{sl}_2(\mathbb{C})$, see for example [43, Chapter 11].

This action on the spin space extends naturally to the one-particle space $\mathcal{H} \cong \mathbb{R}^m \otimes \mathcal{H}_{\text{spin}}$ and therefore induces an action on the d–electron space $\mathcal{H}_d \cong \wedge^d\mathcal{H}$. Consequently, $\mathcal{H}_d$ is an $\mathrm{SU}(2)$–representation. We may therefore decompose $\mathcal{H}_d$ into isotypic components

$$\mathcal{H}_d \cong \bigoplus_s V_s^{\oplus c_s},$$

where V_s denotes the irreducible $\mathrm{SU}(2)$–representation corresponding to total spin s. The irreducible representations of $\mathrm{SU}(2)$ are indexed by half-integers $s = 0, \frac{1}{2}, 1, \frac{3}{2}, \ldots$, called the total spin. On the s–isotypic component $V_s^{\oplus c_s}$, the total spin operator S^2 acts by multiplication by $s(s+1)$. In quantum chemistry these isotypic components are referred to as the spin singlet, doublet, triplet, quartet, and higher spin sectors, respectively. For example, the spin triplet sector corresponds to total spin $s = 1$.

Spin does not appear explicitly in the electronic Hamiltonian (1.12). Consequently, the Hamiltonian commutes with the spin operators and is therefore *spin-symmetric*. As a result, it preserves the isotypic decomposition of $\mathcal{H}_d$. We may therefore restrict our computations to a fixed spin sector. In practice one usually restricts to the spin singlet sector, that is, the $\mathrm{SU}(2)$–invariant subspace $\mathcal{H}_d^{\mathrm{SU}(2)}$. This is the space of quantum states annihilated by the total spin operator S^2. Such states are said to have total spin zero. This observation leads to

spin-adapted coupled cluster theory (RCC), in which the coupled cluster equations are solved within the SU(2)–invariant subspace $\mathcal{H}_d^{\mathrm{SU}(2)}$. Such formulations are discussed in Section 9.2. As in the spin-generalized setting (GCC), the most common truncation schemes are singles (RCCS), doubles (RCCD), and singles and doubles (RCCSD).

We conclude this section with a table summarizing the coupled cluster approximation schemes discussed above. It also illustrates the correspondence between the naming conventions used in quantum chemistry and the truncation sets used in this thesis.

Method	**State Space**	**Dimension**	**Truncation set**	**CC notation**
CC / GCC	$\mathcal{H}_d \cong \wedge^d \mathbb{R}^n$	$\binom{n}{d}$	$\{1\}$ $\{2\}$ $\{1,2\}$	CCS CCD CCSD
FSCC / EOM-CC	$\mathcal{F} \cong \wedge \mathbb{R}^n$	2^n	$\{(1,0),(1,1)\}$ $\{(2,1),(2,2)\}$ $\{(1,0),(2,1),(1,1),(2,2)\}$	FSCCS FSCCD FSCCSD
RCC	$\mathcal{H}_d^{\mathrm{SU}(2)}$	$N(m{+}1,k{+}1)$	$\{1\}$ $\{2\}$ $\{1,2\}$	RCCS RCCD RCCSD

Table 1.1: CC variants, their state spaces, and math/chemistry notation.

We now clarify some of the entries in this table. In the RCC case, the number of electrons must be even, as will be explained in Section 8.2. We therefore write $d = 2k$, where k denotes the number of electron pairs. Similarly, m denotes the number of spatial orbitals, so $n = 2m$. The dimension $N(m+1, d+1)$ of the spin-invariant state space $\mathcal{H}_d^{\mathrm{SU}(2)}$ is given by the *Narayana number*, a fact also established in Section 8.2. We do not list the EOM-CC variants in detail, as they do not correspond directly to truncation sets, see Theorem 7.2.9. The FSCC method includes both ionization and electron attachment variants. In the table, we display only the truncation sets corresponding to ionization; those for electron attachment are obtained by exchanging the entries in each pair.

1.3 Overview

In Part I, we study the most straightforward formulation of the coupled cluster equations, known as *first quantization*. In Chapter 2, we introduce the algebraic structures arising in this setting. We begin with the *exponential map*, a polynomial bijection that parametrizes quantum states. Restricting this map to suitable domains gives rise to a family of projective varieties, called *truncation varieties*. These are indexed by subsets $\sigma \subseteq [d]$, which specify

the allowed excitation levels. Each truncation variety encodes the feasible quantum states for a given coupled cluster variant. The most common variants are CCS, CCD, and CCSD, corresponding to $\sigma = \{1\}, \{2\}, \{1, 2\}$. We show that the Grassmannian arises as the CCS truncation variety. This shows that truncation varieties can be viewed as generalizations of the Grassmannian. We then formulate the *coupled cluster equations* as a nonlinear eigenvalue problem on these varieties. This leads to the *coupled cluster degree*, defined as the number of solutions to a generic instance. It serves as a complexity measure for solving the equations. This chapter is based on [37], joint work with Fabian M. Faulstich and Bernd Sturmfels.

In Chapter 3, we study the CCS truncation variety, which is the Grassmannian in its Plücker embedding. We show that its CC degree equals the total degree of the graph of a birational parameterization. For the Grassmannian of lines, we construct both a Gröbner basis and a Khovanskii basis for this graph. This allows us to derive an explicit formula for the CC degree, based on the combinatorial properties of squarefree monomial ideals. For the Grassmannian in general, we express the CC degree in terms of the volume of a polytope. This chapter is based on the joint paper [8] with Viktoriia Borovik and Bernd Sturmfels.

In Chapter 4, we extend results from Chapter 3, which focuses on the Grassmannian, to truncation varieties in general. We express the exponential parameterization in terms of Laplace polynomials, giving a more algebraic description of truncation varieties. We also introduce an alternative parameterization via Möbius inversion. We then show that the CC degree of a truncation variety coincides with the total degree of the graph of this parameterization. This allows us to study the CC degree using Gröbner and Khovanskii bases.

In Chapter 5 we study the numerical aspects of the CC equations. We introduce numerical methods for solving systems of polynomial equations, namely `parameter homotopy` and `monodromy`. We then describe the procedure for computing all solutions of physical CC equations. We analyze how the CC degree scales with different truncations and system sizes, and compare our bounds with exact values as well as previously known bounds. We then study the molecules lithium hydride (LiH) and H_4. For LiH, we solve the CCS and CCSD equations at a bond distance close to equilibrium (energy-minimizing geometry). The resulting CC energies approximate not only the ground state but also excited eigenvalues. By comparing the corresponding eigenvectors, we find that only a subset provides accurate approximations of the true quantum states. Finally, we examine the dissociation processes of LiH and H_4 in several symmetries. We compute all CCD solutions for varying bond distances and compare them with the exact dissociation. This chapter is based on the paper [102], joint work with Fabian M. Faulstich, and on Section 6 of [37].

In Part II we focus on the *second quantized* formalism, where quantum states and observables are encoded algebraically by operators. In Chapter 6 we introduce the underlying algebraic structures. We begin with the *Fermi–Dirac algebra*, a Clifford algebra generated by *creation and annihilation operators* acting on the *fermionic Fock space* $\mathcal{F} \cong \wedge\mathbb{R}^n$. We construct a Gröbner basis for the Fermi–Dirac algebra and use it to prove Wick's theorem. We also show that the Fermi–Dirac algebra is isomorphic to the algebra of endomorphisms of $\mathcal{F}$. This explains why observables can be expressed in terms of creation and annihilation operators. Finally, we describe the Hamiltonian as an element of the Fermi–Dirac algebra.

In particular, we express its one-body component as an additive compound matrix, whose eigenvectors lie on the Grassmannian. This chapter is based on my solo paper [101].

In Chapter 7 we construct the coupled cluster equations in the second quantized formalism. Since we work over the full exterior algebra, i.e. the Fock space $\mathcal{F} \cong \wedge\mathbb{R}^n$, particle number conservation need not be imposed. This allows us to incorporate processes such as ionization and electron attachment. As a consequence, the class of truncation varieties extends to projective varieties in $\mathbb{P}^{2^n-1}$. We relate these truncations to established approximation schemes in quantum chemistry, including Fock space coupled cluster (FSCC) and equation-of-motion coupled cluster (EOM-CC). From a geometric perspective, this framework also reveals familiar varieties such as the flag varieties and spinor varieties. We study these truncation varieties in detail. We provide birational parameterizations, defining equations, and dimension formulas. Moreover, we show that for special truncation varieties, including the flag and spinor varieties, the CC degree coincides with the total degree of the graph of these parameterizations. This chapter is also based on my solo paper [101].

In Part III we focus on *spin*, the internal angular momentum of electrons. It is described by an action of the special unitary group SU(2) on the spin space generated by $e_\uparrow$ and $e_\downarrow$. In Chapter 8 we study the induced representation of SU(2) on the particle space $\mathcal{H}_d$. To simplify the analysis, we pass to the Lie algebra $\mathfrak{sl}_2(\mathbb{C})$ via derivation and complexification. We describe the irreducible decomposition of $\mathcal{H}_d$ and show that the dimension of the invariant subspace $\mathcal{H}_d^{\mathrm{SU}(2)}$ is given by the Narayana numbers, a refinement of the Catalan numbers. We then introduce the *excitation ring*, an Artinian commutative ring defined by cubic relations. The main result identifies this ring with $\mathcal{H}_d^{\mathrm{SU}(2)}$. Through this identification, we obtain a bijection between the basis elements of $\mathcal{H}_d^{\mathrm{SU}(2)}$ and Dyck paths counted by the Narayana numbers via the RSK correspondence. This chapter is based on the paper [87], joint work with Abigail Price and Ada Stelzer, and on the paper [38], joint work with Fabian M. Faulstich.

In Chapter 9 we study the spin-adaptation of the coupled cluster equations. Since the Hamiltonian does not act on the spin space, it preserves the $\mathfrak{sl}_2(\mathbb{C})$ decomposition of the state space $\mathcal{H}_d$. We may therefore restrict to the spin-invariant subspace $\mathcal{H}_d^{\mathrm{SU}(2)}$, known in quantum chemistry as the *spin singlet sector*. We define the *spin-adapted* truncation varieties as the restriction of the truncation varieties to this sector. A key result is that Veronese squares of Grassmannians arise in this way. In the special case of the quadratic Veronese variety, we derive an explicit formula for the CC degree, which coincides with its ED degree. We then formulate the spin-adapted coupled cluster equations and their CC degree. We compare this degree with its spin-generalized counterpart, revealing a reduction by orders of magnitude. This reduction enables numerical studies of larger systems. In particular, we compute the full solution spectrum for the RCCD equations of LiH (using all orbitals) and water (H_2O). This chapter is based on joint work with Fabian M. Faulstich [38].

1.4 Contributions

In this section, we summarize the main contributions of the thesis; see Table 1.2 for an overview by chapter. These contributions include structural results on truncation varieties, such as identifications with classical varieties and descriptions of their parameterizations and CC degrees. They also include computational advances, such as improved upper bounds on complexity and complete solutions of previously unsolved CC equations for systems such as water. These computational advances are made possible by the algebraic framework developed in the thesis together with numerical algebraic methods.

Among the results summarized in Table 1.2, the principal contributions of the thesis are the explicit formula for the CC degree of the Grassmannian of lines (Theorem 3.1.2), a combinatorial description of a basis for the spin-invariant state space via plane partitions (Corollary 8.5.4), and the computation of the RCCD solution spectrum for H_2O (Figure 9.4).

Table 1.2: Main contributions of the thesis by chapter.

Chapter	**Main result(s)**	**Description**
Chapter 2	Theorem 2.2.5	We prove that the CCS truncation variety is the Grassmannian, thereby showing that the truncation varieties naturally generalize it.
	Theorem 2.3.2	We derive new upper bounds for the CC degree. These bounds are significantly lower than previously known bounds and capture the scaling behavior more accurately; see Examples 5.2.3 and 5.2.2.
Chapter 3	Theorem 3.1.2, Conjecture 3.4.2	We derive an explicit formula for the CC degree of the Grassmannian of lines in terms of the Catalan numbers. Using [39], we also deduce that the CC degree of $\mathrm{Gr}(d, n)$ equals the normalized volume of the CFFLV polytope.
Chapter 4	Theorem 4.3.8	We construct explicit parameterizations of every truncation variety via graph maps, yielding a simpler algebraic description.
	Corollary 4.3.10	We prove that the CC degree of a truncation variety coincides with the total degree of the graph of this parameterization. This gives an algebraic interpretation of the CC degree, an important measure of complexity.
Chapter 5	Figure 5.8	We compute the full CCSD energy spectrum for LiH alongside the exact energy spectrum. This provides one of the first complete solutions of the CC equations for a molecular system of this size.

Chapter	Main result(s)	Description
Chapter 7	Theorem 7.3.3, Theorem 7.3.7	We show that flag and spinor varieties arise as FSCC truncation varieties.
	Theorem 7.4.1	We classify the truncation varieties whose CC degree equals the total degree of the graph of their exponential parameterization.
Chapter 8	Corollary 8.5.4	We give an explicit combinatorial description of the basis states of the spin-invariant state space via a bijection with plane partitions.
Chapter 9	Theorem 9.1.4	We prove that the RCCS truncation variety is the Veronese square of the Grassmannian.
	Figure 9.4	We compute the RCCD energy spectrum for H_2O. To our knowledge, this is the largest electronic system for which a full CC solution spectrum has been computed, enabled by our algebraic methods together with the reduction in complexity from spin adaptation; see Figure 9.1.

Part I

Coupled Cluster Theory

Chapter 2

Algebraic Quantum Chemistry

In this chapter we introduce the algebraic objects arising in coupled cluster theory. We define the truncation varieties, a family of projective varieties indexed by truncations. We show that the Grassmannian appears as a truncation variety and therefore view the truncation varieties as generalizations of the Grassmannian. We then define the coupled cluster equations as truncated eigenvalue equations over the truncation varieties. These give rise to a hierarchy of approximation schemes for the electronic Schrödinger equation, known as CCS, CCD, CCSD, and so on. These polynomial systems generically have finitely many solutions, and we call the generic root count the coupled cluster degree. This degree is an invariant of the truncation variety and it serves as a complexity measure for fully solving the CC equations. It is analogous to other complexity measures in nonlinear algebra, such as the ED degree, polar degree, and ML degree [10, 72]. This chapter is based on the paper *Algebraic Varieties in Quantum Chemistry* [37], which is joint work with Fabian M. Faulstich and Bernd Sturmfels.

2.1 Exponential Parametrization

We work in the vector space $\mathcal{H}_d = \wedge^d \mathbb{R}^n$. It is a discretized Hilbert space of wave functions, see Section 1.2 for the construction. Here n denotes the number of spin-orbitals and d the number of particles in an electronic system. The standard basis vectors of $\mathcal{H}_d$ are $e_I = e_{i_1} \wedge e_{i_2} \wedge \cdots \wedge e_{i_d}$. In this notation, $I = (i_1 < i_2 < \ldots < i_d) \in \binom{[n]}{d}$ is a subset of $[n]$ of cardinality d whose elements are always written in (increasing) order. Here $d \leq n$ are positive integers. The *reference state* is the first basis vector $e_{[d]}$ for $[d] = \{1, 2, \ldots, d\}$. Vectors in $\mathcal{H}_d$ are called *quantum states* and they are written uniquely as linear combinations of the basis vectors:

$$\psi \;=\; \sum_{I \in \binom{[n]}{d}} \psi_I \, e_I .$$

Motivated by nonlinear algebra [72, Chapter 5], we call ψ_I the *Plücker coordinates*. Sometimes it is preferable to write the Plücker coordinates as $c_{\alpha,\beta}$, where α is a subset of $[d]$ and β is a subset of $[n]\backslash[d] = \{d+1, \ldots, n\}$ of the same cardinality $|\alpha| = |\beta|$. The $c_{\alpha,\beta}$ are known as

configuration interaction coefficients in quantum chemistry. The identification between these two systems of coordinates on the space of quantum states $\mathcal{H}_d = \wedge^d \mathbb{R}^n$ is as follows:

$$c_{\alpha,\beta} \;=\; \psi_I \qquad \text{where} \quad I = ([d]\backslash\alpha) \cup \beta. \tag{2.1}$$

We think of the ψ_I as the $d \times d$ minors of a $d \times n$ matrix, and we think of the $c_{\alpha,\beta}$ as the minors of all sizes in a $d \times (n-d)$ matrix. These two sets have the same cardinality

$$\binom{n}{d} \;=\; \sum_{k=0}^{\min(d,n-d)} \binom{d}{k}\binom{n-d}{k}.$$

The title of this section refers to a birational map, defined shortly, between two copies of $\mathbb{R}^{\binom{n}{d}}$. It restricts to a polynomial map with polynomial inverse on the affine hyperplane

$$\mathcal{H}'_d \;=\; \{\psi \in \mathcal{H}_d \,:\, \psi_{[d]} = 1\} \;\simeq\; \mathbb{R}^{\binom{n}{d}-1}.$$

Later on, when we come to algebraic varieties, we shall pass from the vector space $\mathcal{H}_d$ to the projective space $\mathbb{P}^{\binom{n}{d}-1} = \mathbb{P}(\mathcal{H}_d)$. This is the projective closure of the affine space $\mathcal{H}'_d$. Thus the above coordinates ψ_I and $c_{\alpha,\beta}$ also serve as homogeneous coordinates on $\mathbb{P}^{\binom{n}{d}-1}$. See Section 1.1 and [21, Chapter 8] for the basics on projective algebraic geometry with a view toward computation. In particular, note Remark 1.1.8.

To define the exponential parameterization, we introduce our second vector space $\mathcal{V}_d$. It is isomorphic to $\mathcal{H}_d$, with coordinates indexed by $\binom{[n]}{d}$. The elements of $\mathcal{V}_d$ are called *cluster amplitudes* and we denote them by $x = (x_I)_{I \in \binom{[n]}{d}}$. The cluster amplitudes x also have alternate coordinates that are indexed by minors of a $d \times (n-d)$-matrix. As in (2.1), we set

$$t_{\alpha,\beta} \;=\; x_I \qquad \text{where} \quad I = ([d]\backslash\alpha) \cup \beta. \tag{2.2}$$

The *level* of a coordinate ψ_I or x_I is defined as the cardinality of $I\backslash[d]$. Equivalently, the level of $c_{\alpha,\beta}$ or $t_{\alpha,\beta}$ equals $|\alpha| = |\beta|$. For example, for $d = 3$ and $n = 6$, each of the spaces $\mathcal{H}_d$ and $\mathcal{V}_d$ has 20 coordinates: one of level 0, nine of level 1, nine of level 2, and one of level 3:

$$\begin{aligned}
&\psi_{123} = c_\emptyset, \psi_{124} = c_{3,4}, \psi_{125} = c_{3,5}, \ldots, \psi_{136} = c_{2,6}, \psi_{145} = c_{23,45}, \ldots, \psi_{356} = c_{12,56}, \psi_{456} = c_{123,456}, \\
&x_{123} = t_\emptyset,\; x_{124} = t_{3,4}, x_{125} = t_{3,5}, \ldots,\; x_{136} = t_{2,6},\; x_{145} = t_{23,45}, \ldots, x_{356} = t_{12,56},\; x_{456} = t_{123,456}.
\end{aligned}$$

The term level refers to the excitation level of the electrons in a chemical system.

Our workhorse is the nonlinear coordinate transformation between quantum states and cluster amplitudes. The basic ingredient is a lower-triangular matrix $T(x)$ of square format $\binom{n}{d} \times \binom{n}{d}$, described using *excitation operators*, see [35, 36]. See also Section 1.2 for a short introduction. Explicitly, the cluster operator $\chi_{\alpha,\beta}$, for $\alpha \subseteq [d]$, $\beta \subseteq [n]\backslash[d]$ where $|\alpha| = |\beta|$, is defined as the following endomorphism:

$$\chi_{\alpha,\beta} : \mathcal{H}_d \to \mathcal{H}_d, \quad z \mapsto (e_\alpha \lrcorner z) \wedge e_\beta.$$

The interior product $\lrcorner$ is the operator dual to the exterior product, see the explicit definition in (1.18). Informally, $e_\alpha \lrcorner z$ removes e_α from all terms of z, with certain sign conventions for compatibility. Its corresponding matrix $X_{\alpha,\beta}$ is lower triangular of size $\binom{n}{d} \times \binom{n}{d}$. The cluster operator is then defined as the following linear combination of the excitation operators

$$T(x) = \sum_{J \in \binom{[n]}{d}, J \neq [d]} x_J X_{[d]\setminus J, J\setminus[d]}. \tag{2.3}$$

In conclusion, $T(x)$ is a well-defined lower-triangular matrix of size $\binom{n}{d} \times \binom{n}{d}$ that depends linearly on the cluster amplitudes x. This matrix represents the *cluster operator* in [35, 36].

Example 2.1.1 ($d = 2, n = 5$)**.** The lower-triangular 10×10 matrix defined above equals

$$T(x) = \begin{bmatrix} 0 & 0 & 0 & 0 & 0 & 0 & 0 & 0 & 0 & 0 \\ x_{13} & 0 & 0 & 0 & 0 & 0 & 0 & 0 & 0 & 0 \\ x_{14} & 0 & 0 & 0 & 0 & 0 & 0 & 0 & 0 & 0 \\ x_{15} & 0 & 0 & 0 & 0 & 0 & 0 & 0 & 0 & 0 \\ -x_{23} & 0 & 0 & 0 & 0 & 0 & 0 & 0 & 0 & 0 \\ -x_{24} & 0 & 0 & 0 & 0 & 0 & 0 & 0 & 0 & 0 \\ -x_{25} & 0 & 0 & 0 & 0 & 0 & 0 & 0 & 0 & 0 \\ x_{34} & -x_{24} & x_{23} & 0 & -x_{14} & x_{13} & 0 & 0 & 0 & 0 \\ x_{35} & -x_{25} & 0 & x_{23} & -x_{15} & 0 & x_{13} & 0 & 0 & 0 \\ x_{45} & 0 & -x_{25} & x_{24} & 0 & -x_{15} & x_{14} & 0 & 0 & 0 \end{bmatrix}.$$

The level zero variable x_{12} does not appear. Three variables x_{34}, x_{35}, x_{45} have level two.

The lower-triangular matrix $T(x)$ is nilpotent of order d. This is shown in [36, Section 3.2] and also follows from equation (2.3). Hence, the matrix exponential is the finite sum

$$\exp(T(x)) \;=\; \sum_{k=0}^{d} \frac{1}{k!} T(x)^k. \tag{2.4}$$

In particular, the entries of the matrix $\exp(T(x))$ are polynomials in x of degree at most d.

Example 2.1.2 ($d = 2, n = 5$)**.** The exponential of the matrix in Example 2.1.1 equals

$$\exp(T(x)) = \begin{bmatrix} 1 & 0 & 0 & 0 & 0 & 0 & 0 & 0 & 0 & 0 \\ x_{13} & 1 & 0 & 0 & 0 & 0 & 0 & 0 & 0 & 0 \\ x_{14} & 0 & 1 & 0 & 0 & 0 & 0 & 0 & 0 & 0 \\ x_{15} & 0 & 0 & 1 & 0 & 0 & 0 & 0 & 0 & 0 \\ -x_{23} & 0 & 0 & 0 & 1 & 0 & 0 & 0 & 0 & 0 \\ -x_{24} & 0 & 0 & 0 & 0 & 1 & 0 & 0 & 0 & 0 \\ -x_{25} & 0 & 0 & 0 & 0 & 0 & 1 & 0 & 0 & 0 \\ x_{14}x_{23}-x_{13}x_{24}+x_{34} & -x_{24} & x_{23} & 0 & -x_{14} & x_{13} & 0 & 1 & 0 & 0 \\ x_{15}x_{23}-x_{13}x_{25}+x_{35} & -x_{25} & 0 & x_{23} & -x_{15} & 0 & x_{13} & 0 & 1 & 0 \\ x_{15}x_{24}-x_{14}x_{25}+x_{45} & 0 & -x_{25} & x_{24} & 0 & -x_{15} & x_{14} & 0 & 0 & 1 \end{bmatrix}. \tag{2.5}$$

The following observation will be important later on: If we set the level two parameters to zero, i.e. $x_{34} = x_{35} = x_{45} = 0$, then the first column consists of all 10 maximal minors of

$$\begin{bmatrix} 1 & 0 & x_{23} & x_{24} & x_{25} \\ 0 & 1 & x_{13} & x_{14} & x_{15} \end{bmatrix} \quad = \quad \begin{bmatrix} 1 & 0 & t_{1,3} & t_{1,4} & t_{1,5} \\ 0 & 1 & t_{2,3} & t_{2,4} & t_{2,5} \end{bmatrix}.$$

Thus the Grassmannian $\mathrm{Gr}(2,5) \subseteq \mathbb{P}^9$ makes an appearance in the first column of $\exp(T(x))$.

Returning to general d and n, the *exponential parameterization* is the map

$$\mathcal{V}_d \,\to\, \mathcal{H}_d,\, x \,\mapsto\, \psi\,, \qquad \text{where} \quad \psi \,=\, \exp(T(x))\, e_{[d]}. \tag{2.6}$$

Here $e_{[d]}$ is the reference state in $\mathcal{H}_d \simeq \mathbb{R}^{\binom{n}{d}}$, i.e. the first standard basis vector. The transformation (2.6) gives a formula for the quantum states ψ in terms of the cluster amplitudes x. To be precise, each of the $\binom{n}{d}$ coordinates ψ_I is a polynomial $\psi_I(x)$ in the $\binom{n}{d}$ unknowns x_J. In the definition (2.6), we had assumed that $x_{[d]} = 1$ and $\psi_{[d]} = 1$. Geometrically, this means that we work in the affine spaces $\mathcal{V}'_d$ and $\mathcal{H}'_d$, both of which are identified with $\mathbb{R}^{\binom{n}{d}-1}$. Later on, we shall extend (2.6) to a birational automorphism of the projective space $\mathbb{P}^{\binom{n}{d}-1}$. The reference coordinates $x_{[d]} = t_{\emptyset,\emptyset}$ and $\psi_{[d]} = c_{\emptyset,\emptyset}$ will then serve as homogenizing variables.

The formula $\psi = \exp(T(x))e_{[d]}$ simply says that ψ equals the leftmost column vector of the matrix $\exp(T(x))$. For instance, in Example 2.1.2, the formula for the Plücker coordinates of the quantum state $\psi = (\psi_{12}, \psi_{13}, \ldots, \psi_{45})$ in terms of cluster amplitudes is given by the first column of (2.5). Here is a slightly larger example, where the matrices have size 20×20:

Example 2.1.3 ($d = 3, n = 6$)**.** The 20 coordinates in the formula (2.6) are as follows:

$$\begin{array}{llll}
\psi_{123} = x_{123} = 1 & \psi_{135} = -x_{135} & \psi_{145} = x_{145} - x_{124}x_{135} + x_{125}x_{134} & \psi_{256} = -x_{256} + x_{125}x_{236} - x_{126}x_{235} \\
\psi_{124} = x_{124} & \psi_{136} = -x_{136} & \psi_{146} = x_{146} - x_{124}x_{136} + x_{126}x_{134} & \psi_{345} = x_{345} - x_{134}x_{235} + x_{135}x_{234} \\
\psi_{125} = x_{125} & \psi_{234} = x_{234} & \psi_{156} = x_{156} - x_{125}x_{136} + x_{126}x_{135} & \psi_{346} = x_{346} - x_{134}x_{236} + x_{136}x_{234} \\
\psi_{126} = x_{126} & \psi_{235} = x_{235} & \psi_{245} = -x_{245} + x_{124}x_{235} - x_{125}x_{234} & \psi_{356} = x_{356} - x_{135}x_{236} + x_{136}x_{235} \\
\psi_{134} = -x_{134} & \psi_{236} = x_{236} & \psi_{246} = -x_{246} + x_{124}x_{236} - x_{126}x_{234} &
\end{array}$$

Finally, at level three we find that ψ_{456} is equal to

$$\begin{aligned} x_{456} \,+\, & x_{124}x_{356} - x_{125}x_{346} + x_{126}x_{345} - x_{134}x_{256} + x_{135}x_{246} - x_{136}x_{245} + x_{145}x_{236} - x_{146}x_{235} + x_{156}x_{234} \\ & - x_{124}x_{135}x_{236} + x_{124}x_{136}x_{235} + x_{125}x_{134}x_{236} - x_{125}x_{136}x_{234} - x_{126}x_{134}x_{235} + x_{126}x_{135}x_{234}. \end{aligned}$$

In both examples, we can easily solve the equation $\psi = \exp(T(x))\, e_{[d]}$ for x. This is done inductively by level. For levels zero and one, we simply have $x_I = \pm\psi_I$. At each larger level, we use the formulas for lower level coordinates x_I in terms of the ψ_J, and we substitute these into the equation. For instance, in Example 2.1.3, this yields the inversion formulas

$$\begin{aligned}
& x_{124} = \psi_{124},\ \ldots\ , \psi_{236} = x_{236} \\
& x_{145} = \psi_{145} - \psi_{124}\psi_{135} + \psi_{125}\psi_{134},\ \ldots\ , \psi_{356} = x_{356} - x_{135}x_{236} + x_{136}x_{235} \\
& x_{456} = \psi_{456} - \psi_{124}\psi_{356} + \psi_{125}\psi_{346} - \psi_{126}\psi_{345} + \psi_{134}\psi_{256} - \psi_{135}\psi_{246} + \psi_{136}\psi_{245} - \psi_{145}\psi_{236} + \psi_{146}\psi_{235} \\
& \quad - \psi_{156}\psi_{234} + 2(\psi_{124}\psi_{135}\psi_{236} - \psi_{124}\psi_{136}\psi_{235} - \psi_{125}\psi_{134}\psi_{236} + \psi_{125}\psi_{136}\psi_{234} + \psi_{126}\psi_{134}\psi_{235} - \psi_{126}\psi_{135}\psi_{234}).
\end{aligned}$$

We next show that such inversion formulas can always be found.

Proposition 2.1.4. *The map (2.6) from x-coordinates to ψ-coordinates has a polynomial inverse. Namely, x_I is equal to $\pm\psi_I$ plus a polynomial in ψ-coordinates of strictly lower level.*

Proof. We proceed by induction on the level. At level zero, we have $x_{[d]} = \psi_{[d]} = 1$. For level one, we already saw that $x_I = \pm\psi_I$. If the index I has level r then the formula in (2.6) writes ψ_I as $\pm x_I$ plus a polynomial in variables x_J of level $< r$. Each of these lower level x_J can now be replaced with a polynomial in ψ, by the induction hypothesis. This yields the promised representation for x_I as $\pm\psi_I$ plus a polynomial in lower level ψ-coordinates. □

Let $x_I(\psi)$ denote the polynomial that expresses the cluster amplitudes in terms of the Plücker coordinates. Conversely, $\psi_I(x)$ is a polynomial in cluster amplitudes. As is apparent from the proof of Proposition 2.1.4, the degree of each polynomial is the level of I and the variable x_I occurs linearly in $\psi_I(x)$. Similarly, the variable ψ_I occurs linearly in $x_I(\psi)$.

The monomials occurring in $\psi_I(x)$ are in natural bijection with those occurring in $x_I(\psi)$, and we shall give an explicit formula for these monomials and their coefficients. For this, it helps to note that, for each degree d, there is really only one ψ-polynomial and x-polynomial. Here we refer to the symmetric group actions that permute the indices in $[d]$ and in $[n]\backslash[d]$. For fixed d and fixed level $|I\backslash[d]|$, all $\psi_I(x)$ are in the same orbit, and ditto for $x_I(\psi)$. Each coordinate in the exponential parameterization is a replicate of a certain *master polynomial*.

It would be desirable to better understand our equations from the perspective of representation theory. In this setting, the master polynomials should be highest weight vectors.

The master polynomials of degree d are $\psi_I(x)$ and $x_I(\psi)$ where $n = 2d$ and $I = [2d]\backslash[d]$. All coordinates in (2.6) and its inverse are obtained from these two by changing indices. For instance, all quadratic entries in the matrix (2.5) are replicates of $\psi_{34}(x) = x_{14}x_{23} - x_{13}x_{24} + x_{34}$.

By inverting the map (2.6), we find the following master polynomials of degree $d \leq 5$:

$$\begin{array}{rcll}
x_{34}(\psi) & = & \psi_{34} - \psi_{13}\psi_{24} + \psi_{14}\psi_{23} & 3 \text{ terms} \\
x_{456}(\psi) & = & \psi_{456} - \psi_{124}\psi_{356} + \cdots - 2\psi_{126}\psi_{135}\psi_{234} & 16 \text{ terms} \\
x_{5678}(\psi) & = & \psi_{5678} - \psi_{1235}\psi_{4678} + \cdots - 2\psi_{1278}\psi_{1346}\psi_{2345} + \cdots - 6\psi_{1238}\psi_{1247}\psi_{1346}\psi_{2345} & 131 \text{ terms} \\
x_{67890}(\psi) & = & \psi_{67890} - \psi_{12346}\psi_{57890} + \cdots - 2\psi_{12890}\psi_{13457}\psi_{23456} + \cdots & \\
 & & \quad + 6\psi_{12390}\psi_{12458}\psi_{13457}\psi_{23456} + \cdots + 24\psi_{12349}\psi_{12358}\psi_{12457}\psi_{13456}\psi_{23450} & 1496 \text{ terms}
\end{array}$$

The first Plücker coordinate $\psi_{[d]}$ plays a special role. It does not occur in our polynomials. Let $\bar{x}_I(\psi)$ denote the homogenization of $x_I(\psi)$ with respect to $\psi_{[d]}$. This is a homogeneous polynomial of degree $|I\backslash[d]|$. Its hypersurface $V(\bar{x}_I) \subseteq \mathbb{P}^{\binom{n}{d}-1}$ will be important in Section 2.2.

We close this section by giving explicit combinatorial formulas for the master polynomials. Formulas for all other coordinates in (2.6) and their inverse are obtained by adjusting the indices. The number of monomials is found in *The On-Line Encyclopedia of Integer Sequences*, which is published electronically at `http://oeis.org`. Namely, it is the sequence

$$\#\mathcal{U}_d \;=\; 3, 16, 131, 1\,496, 22\,482, 426\,833, 9\,934\,563 \quad \text{for } d = 2, 3, 4, 5, 6, 7, 8. \qquad \text{(A005046)}$$

This is the number of uniform block permutations. Let $[\bar{d}] = [2d]\backslash[d]$. We recall (e.g. from [79]) that a *uniform block permutation* is a partition π of the set $[d] \cup [\bar{d}] = [2d]$, here denoted

$$\pi \;=\; \{\pi_1, \pi_2, \ldots, \pi_k\} \;=\; \{\alpha_1 \cup \beta_1, \alpha_2 \cup \beta_2, \ldots, \alpha_k \cup \beta_k\},$$

which satisfies $\alpha_i \subseteq [d]$, $\beta_i \subseteq [\overline{d}]$ and $|\alpha_i| = |\beta_i|$ for all $i \in [k]$. We denote by $\mathcal{U}_d$ the set of all uniform block permutations of $[2d]$. For details on the algebraic and combinatorial structures of $\mathcal{U}_d$ we refer to [79, Section 2.3] and the references therein.

The connection to coupled cluster theory arises from identifying $\mathcal{U}_d$ with the set of monomials that appear in the above polynomials $\psi_I(x)$ and $x_I(\psi)$. To see this, we pass to the coordinates in (2.1) and (2.2). The polynomial $\psi_I(x)$ is now written as $c_{\alpha,\beta}(t)$, and $x_I(\psi)$ is now written as $t_{\alpha,\beta}(c)$. With this notation, the master polynomials of degree d are $c_{[d],[\overline{d}]}(t)$ and $t_{[d],[\overline{d}]}(c)$, and we write the monomial corresponding to a given uniform block permutation as

$$t_\pi \,:=\, t_{\alpha_1,\beta_1} t_{\alpha_2,\beta_2} \cdots t_{\alpha_k,\beta_k} \quad \text{and} \quad c_\pi \,:=\, c_{\alpha_1,\beta_1} c_{\alpha_2,\beta_2} \cdots c_{\alpha_k,\beta_k}.$$

The master polynomials are $\mathbb{Z}$-linear combinations of these monomials for $k = 1, 2, \ldots, d$.

Theorem 2.1.5. *The coordinates in the exponential parameterization are*

$$c_{[d],[\overline{d}]}(t) \,=\, \sum_{\pi \in \mathcal{U}_d} \operatorname{sign}(\pi)\, t_\pi \quad \textit{and} \quad t_{[d],[\overline{d}]}(c) \,=\, \sum_{\pi \in \mathcal{U}_d} \operatorname{sign}(\pi)(-1)^{\nu+k-1}(k-1)!\, c_\pi.$$

In these formulas, the sign of an element $\pi \in \mathcal{U}_d$ is the product of the signs of the permutations

$$[d] \mapsto (\alpha_1, \alpha_2, \ldots, \alpha_k) \quad \textit{and} \quad [\overline{d}] \mapsto (\beta_1, \beta_2, \ldots, \beta_k), \tag{2.7}$$

where each α_i and β_i is an increasing sequence. We also have $\nu = \frac{d(d-1)}{2} - \sum_{r=1}^{k} \frac{|\alpha_r|(|\alpha_r|-1)}{2}$.

Proof. Let $\pi \in \mathcal{U}_d$. We consider the monomial t_π in the master polynomial $c_{[d],[\overline{d}]}(t)$. Its term is the product of matrix entries of $T(x)$ whose respective rows and columns are

$$([d] \backslash A_r) \cup B_r \quad \text{and} \quad ([d] \backslash A_{r-1}) \cup B_{r-1},$$

where $A_r = \cup_{i=1}^{r} \alpha_i$ and $B_r = \cup_{i=1}^{r} \beta_i$. One checks from the definition of $T(x)$ that the sign of such an entry comes from the number of inversions of (B_{r-1}, β_r) and $(\alpha_r, [d] \backslash A_r)$ and from the sign $(-1)^{|\alpha_r|(d-|\alpha_r|)}$. We take the product of the signs of these entries for all $r \leq k$. Since

$$\sum_{r=1}^{k} |\alpha_r|(d - |\alpha_r|) \,=\, \sum_{r=1}^{k} |\alpha_r|(d-1) - \sum_{r=1}^{k} |\alpha_r|(|\alpha_r| - 1) \,=\, d(d-1) - \sum_{r=1}^{k} |\alpha_r|(|\alpha_r| - 1)$$

is an even integer, the sign of π equals the product of the signs of the permutations in (2.7).

The set $\mathcal{U}_d$ of uniform block permutations has a natural partial order, induced by the partial orders on the set partitions of $[d]$ and $[\overline{d}]$. The Möbius function of the poset $\mathcal{U}_d$ is given by $\mu(\pi) = (-1)^{k-1}(k-1)!$. For any uniform block partition $\rho \in \mathcal{U}_d$ we can write

$$(-1)^\nu \operatorname{sign}(\rho)\, c_\rho(t) \,=\, \sum_{\pi \leq \rho} \operatorname{sign}(\pi)\, t_\pi.$$

Using Möbius inversion, we obtain the asserted formula for $t_{[d],[\overline{d}]}$ in terms of the c_π. □

2.2 Truncation Varieties

In this section, we study the algebraic varieties arising in coupled cluster theory. They are found by truncating the exponential parameterization (2.6) to a certain coordinate subspace. We consider the image of this truncation in $\mathcal{H}_d$. Its closure in $\mathbb{P}^{\binom{n}{d}-1}$ is our variety.

More precisely, let σ be a non-empty proper subset of $[d] = \{1, 2, \ldots, d\}$, and define

$$\mathcal{V}_\sigma \;=\; \text{span}\,\big\{\, e_J \,:\, J \in \tbinom{[n]}{d} \text{ and } |J\backslash[d]| \in \sigma \cup \{0\}\big\}. \tag{2.8}$$

This is a linear subspace of the vector space $\mathcal{V}_d$ spanned by all basis vectors e_J of level in σ. The subspace $\mathcal{V}_\sigma$ is the variety of the ideal

$$P_\sigma \;=\; \big\langle\, x_I \;:\; I \in \tbinom{[n]}{d} \text{ and } |I\backslash[d]| \in [d]\backslash\sigma \,\big\rangle. \tag{2.9}$$

The restriction of the exponential parameterization to the subspace $\mathcal{V}_\sigma$ is injective. It maps $\mathcal{V}_\sigma$ into the full space of quantum states $\mathcal{H}_d$, and it maps further to the projective space $\mathbb{P}(\mathcal{H}_d) = \mathbb{P}^{\binom{n}{d}-1}$. We define the *truncation variety* V_σ as the closure of the image of $\mathcal{V}_\sigma$ under this map to $\mathbb{P}^{\binom{n}{d}-1}$. Since the exponential parameterization is invertible, the dimension of the projective variety V_σ is one less than the dimension of its linear space of parameters $\mathcal{V}_\sigma$.

The varieties V_σ correspond to the various models in CC theory. For instance, in the notation of [36, Section 1.2], the index set $\sigma = \{1, 2\}$ corresponds to CCSD, the index set $\sigma = \{1, 2, 3\}$ corresponds to CCSDT, etc. But here we allow arbitrary truncation sets. For instance, taking $\sigma = \{2, 3\}$ means that doubles and triples are included but singles are not.

Example 2.2.1 ($d = 2, n = 5$)**.** There are only two proper subsets of $[d]$, namely $\sigma = \{1\}$ and $\sigma = \{2\}$. The two varieties V_σ live in $\mathbb{P}^9$. They are defined by truncating the exponential parameterization, which is given by the leftmost column in (2.5). For $\sigma = \{2\}$ we set $x_{13} = x_{14} = x_{15} = x_{23} = x_{24} = x_{25} = 0$. Hence $V_{\{2\}}$ is the subspace $\mathbb{P}^3$ with coordinates $(\psi_{12} : \psi_{34} : \psi_{35} : \psi_{45})$. For $\sigma = \{1\}$ we set $x_{34} = x_{35} = x_{45} = 0$, and we obtain the Grassmannian $\text{Gr}(2, 5)$. See Example 2.1.2 and Theorem 2.2.5. We revisit the ideal of $\text{Gr}(2, 5)$ in Example 2.2.3.

Our next result characterizes the homogeneous prime ideals of the truncation varieties. It shows how to derive these ideals from the master polynomials that are given in Theorem 2.1.5.

Theorem 2.2.2. *The homogeneous prime ideal of the truncation variety V_σ is the saturation*

$$\mathcal{I}(V_\sigma) \;=\; \big\langle\, \bar{x}_I(\psi) \,:\, |I\backslash[d]| \in [d]\backslash\sigma \,\big\rangle \,:\, \langle\, \psi_{[d]} \,\rangle^\infty. \tag{2.10}$$

In particular, the restriction of V_σ to the affine chart $\mathbb{C}^{\binom{n}{d}-1} = \{\psi_{[d]} = 1\}$ of projective space $\mathbb{P}^{\binom{n}{d}-1}$ is the complete intersection defined by the equations $x_I(\psi) = 0$ where $|I\backslash[d]| \in [d]\backslash\sigma$.

The provided explicit description of the ideal of the truncation variety allows the computation of $\deg(V_\sigma)$ – and hence the bound in Theorem 2.3.2 – via the degree of the ideal. See Section 1.1 for a discussion on the projectivization of ideals via saturation. Its role in the context of projective geometry is explained in [21, Section 8.5]. These references and the following example are meant to help our readers in understanding Theorem 2.2.2.

Example 2.2.3 (d=2, n=5, σ=$\{1\}$)**.** The truncation variety $V_{\{1\}} = \mathrm{Gr}(2,5)$ has codimension 3 in $\mathbb{P}^9$. Its restriction to the affine chart $\mathbb{C}^9 = \mathbb{P}^9 \backslash V(\psi_{12})$ is the zero set of three polynomials:

$$\begin{aligned} x_{34}(\psi) &= \psi_{34} - \psi_{13}\psi_{24} + \psi_{14}\psi_{23}, \\ x_{35}(\psi) &= \psi_{35} - \psi_{13}\psi_{25} + \psi_{15}\psi_{23}, \\ x_{45}(\psi) &= \psi_{45} - \psi_{14}\psi_{25} + \psi_{15}\psi_{24}. \end{aligned}$$

By multiplying each first term with ψ_{12}, we obtain the quadratic forms $\bar{x}_{34}(\psi), \bar{x}_{35}(\psi), \bar{x}_{45}(\psi)$. These do not cut out $V_{\{1\}}$. Indeed, the ideal on the left below is radical but it is not prime:

$$\langle \bar{x}_{34}(\psi), \bar{x}_{35}(\psi), \bar{x}_{45}(\psi) \rangle = \mathcal{I}(\mathrm{Gr}(2,5)) \cap \langle \psi_{12}, \psi_{13}\psi_{24} - \psi_{14}\psi_{23}, \psi_{13}\psi_{25} - \psi_{15}\psi_{23}, \psi_{14}\psi_{25} - \psi_{15}\psi_{24} \rangle.$$

This is a complete intersection, of codimension 3 and degree $2^3 = 8 = 5 + 3$. The saturation with respect to ψ_{12} removes the second associated prime and yields the desired prime ideal.

Proof of Theorem 2.2.2. We write $\mathbb{C}[\psi]$ and $\mathbb{C}[x]$ for the rings of polynomial functions on $\mathcal{H}'_d$ and $\mathcal{V}'_d$ respectively. These are polynomial rings in $\binom{n}{d} - 1$ variables, where $\psi_{[d]} = x_{[d]} = 1$. The exponential parameterization defines an isomorphism $\iota : \mathbb{C}[\psi] \to \mathbb{C}[x]$ between these polynomial rings. Note that $\iota^{-1}(x_I) = x_I(\psi)$ is the polynomial constructed in Proposition 2.1.4.

The linear subspace $\mathcal{V}_\sigma$ in (2.8) corresponds to the ideal P_σ in (2.9). We write $\gamma_\sigma : \mathbb{C}[x] \to \mathbb{C}[x]/P_\sigma$ for the associated quotient map. By definition, the prime ideal of $V_\sigma \cap \mathbb{C}^{\binom{n}{d}-1}$ is the kernel of $\gamma_\sigma \circ \iota$. This equals $\iota^{-1}(P_\sigma)$, and it is a prime ideal because P_σ is prime. Hence,

$$\iota^{-1}(P_\sigma) \;=\; \big\langle x_I(\psi) \,:\, |I \backslash [d]| \in [d] \backslash \sigma \big\rangle.$$

This is the inhomogeneous prime ideal defining the irreducible affine variety $V_\sigma \cap \mathbb{C}^{\binom{n}{d}-1}$. We pass to the prime ideal of the projective closure $V_\sigma \subseteq \mathbb{P}^{\binom{n}{d}-1}$ by the saturation in (2.10). □

Example 2.2.4 (d=3, n=6)**.** There are six distinct truncation varieties V_σ in $\mathbb{P}^{19}$. We compute their prime ideals by the formula in (2.10). Each item is indexed by the corresponding set σ:

$\{2\}$ The linear space $V_{\{2\}} \simeq \mathbb{P}^9$ is the zero set of the ten coordinates ψ_I of level 1 or 3.

$\{3\}$ Here we obtain the line $V_{\{3\}} \simeq \mathbb{P}^1$ that is spanned by the two points e_{123} and e_{456}.

$\{2,3\}$ The linear space $V_{\{2,3\}} \simeq \mathbb{P}^{10}$ is the zero set of the nine coordinates ψ_I of level 1.

$\{1,2\}$ This is the cubic hypersurface $V_{\{1,2\}}$ which is given by the master polynomial $\bar{x}_{456}(\psi)$.

$\{1,3\}$ The ideal $\mathcal{I}(V_{\{1,3\}})$ is generated by 25 quadrics, and $\dim(V_{\{1,3\}}) = 10$, $\deg(V_{\{1,3\}}) = 41$.

$\{1\}$ This is the Grassmannian $V_{\{1\}} = \mathrm{Gr}(3,6)$, of dimension 9 and degree 42. Its ideal is generated by 35 quadrics. In (2.10) we start with nine quadrics and the cubic $\bar{x}_{456}(\psi)$.

These computations were carried out with the computer algebra system `Macaulay2` [46].

We have already seen Grassmannians a few times for $\sigma = \{1\}$. This is a general result:

Theorem 2.2.5. *The truncation variety $V_{\{1\}}$ equals the Grassmannian $\mathrm{Gr}(d,n)$ in its Plücker embedding in $\mathbb{P}^{\binom{n}{d}-1}$. The truncation varieties V_σ are thus generalizations of Grassmannians.*

Proof. The excitation operators $\chi_{\alpha,\beta}$ span a linear subspace $\mathcal{L}$ of $\mathrm{Hom}(\mathcal{H}_d, \mathcal{H}_d)$ of dimension $\binom{n}{d}$. Elements in this subspace are represented by cluster matrices $T(t)$. We now consider the truncation to $\sigma = \{1\}$. Let $\mathcal{L}_\sigma$ denote the subspace of $\mathcal{L}$ spanned by $\{\chi_{i,j} : i \in [d],\, j \in [n]\backslash[d]\}$. Operators in $\mathcal{L}_\sigma$ are derivations, i.e. for $\tau \in \mathcal{L}_\sigma$ we have

$$\tau(x \wedge y) \;=\; \tau(x) \wedge y \,+\, x \wedge \tau(y). \tag{2.11}$$

Let T_k denote the matrix for the linear map $\tau \in \mathcal{L}_\sigma$ restricted to $\wedge^k \mathbb{R}^n$. From (2.11) we infer

$$T_{k+1} \;=\; T_k \wedge \mathrm{Id}_n \,+\, \mathrm{Id}_{\binom{n}{k}} \wedge T_1. \tag{2.12}$$

We further note that T_k has nilpotency k, that is $T_k^{k+1} = 0$. Since the summands on the right hand side of (2.12) commute, we conclude that $\exp(T_{k+1}) = \exp(T_k) \wedge \exp(T_1)$. The analogous property for Kronecker sums appears in [53, Theorem 10.9]. By induction on k,

$$\exp(T(t)) \;=\; \wedge^d \exp(T_1(t)). \tag{2.13}$$

Formula (2.13) shows that the first column of the matrix $\exp(T(t))$ consists of the $d \times d$ minors of the first d columns of the $n \times n$ matrix $\exp(T_1(t)) = \mathrm{Id}_n + T_1(t)$. These columns are

$$\begin{bmatrix} 1 & 0 & \cdots & 0 & t_{1,d+1} & t_{1,d+2} & \cdots & t_{1,n} \\ 0 & 1 & \cdots & 0 & t_{2,d+1} & t_{2,d+2} & \cdots & t_{2,n} \\ 0 & 0 & \ddots & 0 & \vdots & \vdots & \ddots & \vdots \\ 0 & 0 & \cdots & 1 & t_{d,d+1} & t_{d,d+2} & \cdots & t_{d,n} \end{bmatrix}^T .$$

This holds because the operator $\tau \in \mathcal{L}_\sigma$ acts on the basis vectors e_i of $\mathbb{R}^n = \wedge^1 \mathbb{R}^n$ as follows:

$$\tau e_i \;=\; \sum_{j=d+1}^{n} t_{i,j} \chi_{i,j} e_i \;=\; \sum_{j=d+1}^{n} t_{i,j} e_j \quad \text{for } i \le d \quad \text{and} \quad \tau e_i \,=\, 0 \quad \text{for } i > d.$$

We conclude that the first column of $\exp(T(t))$ gives the Plücker coordinates for $\mathrm{Gr}(d,n)$. □

Remark 2.2.6. All Grassmannians are obtained from the polynomials $\bar{x}_I(\psi)$ with $|I\backslash[d]| \in \{2,3,\ldots,d\}$, by the saturation in (2.10). Starting with these polynomials for other level sets, we obtain all truncation varieties. This is the sense in which the V_σ generalize $\mathrm{Gr}(d,n)$.

There is a natural isomorphism between the vector spaces $\wedge^d\mathbb{R}^n$ and $\wedge^{n-d}\mathbb{R}^n$, and hence between corresponding projective spaces. This swaps the Grassmannians $\mathrm{Gr}(d,n)$ and $\mathrm{Gr}(n-d,n)$. The duality extends to all truncation varieties. This is the content of the next result, which is our algebraic interpretation of *particle-hole symmetry* in electronic structure theory.

Proposition 2.2.7. *Fix a subset σ of $[d]$ and let $n \geq 2d$. There is a linear isomorphism between two copies of $\mathbb{P}^{\binom{n}{d}-1}$ which switches the truncation varieties V_σ for (d,n) and $(n-d,n)$.*

Proof. The Plücker coordinates on the two spaces are ψ_I with $|I| = d$ and $\psi_{I'}$ with $|I'| = n-d$. Similarly, the coordinates in (2.1) are $c_{\alpha,\beta}$ with $\alpha \subseteq [d]$ and $\beta \subseteq [n]\backslash[d]$ for the first copy of $\mathbb{P}^{\binom{n}{d}-1}$, and $c_{\alpha',\beta'}$ with $\alpha' \subseteq [n-d]$ and $\beta' \subseteq [n]\backslash[n-d]$ for the second copy of $\mathbb{P}^{\binom{n}{d}-1}$. The natural isomorphism in the statement of the proposition is given by relabelling as follows:

$$I \mapsto I' = \{n{+}1{-}i : i \notin I\},\ \alpha \mapsto \alpha' = \{n{+}1{-}j : j \in \beta\},\ \ \beta \mapsto \beta' = \{n{+}1{-}k : k \in \alpha\}.$$

One checks that our construction of the matrix $T(x)$ and the exponential parameterization in Section 2.1 are invariant under this relabeling. It hence induces the desired isomorphism. □

In light of this proposition, we shall assume $n \geq 2d$ in everything that follows. In Example 2.2.4 we saw a first census of truncation varieties. We next present two further cases.

Example 2.2.8 $(d = 3, n = 7)$**.** The six varieties correspond to the six columns in Table 2.1. The last row lists the CC degrees, to be introduced in Section 2.3. The fourth row gives the number of minimal generators in degrees $1, 2, 3$ of the ideal $\mathcal{I}(V_\sigma)$. All varieties live in $\mathbb{P}^{34}$. The first column is the Grassmannian $\mathrm{Gr}(3,7)$. Among the other five, three are linear spaces.

σ	$\{1\}$	$\{2\}$	$\{3\}$	$\{1,2\}$	$\{1,3\}$	$\{2,3\}$
dim	12	18	4	30	16	22
degree	462	1	1	43	405	1
mingens	$[0, 140]$	$[16]$	$[30]$	$[0, 0, 7]$	$[0, 76, 10]$	$[12]$
CCdeg	2 883	19	5	1 195	3 425	287

Table 2.1: The truncation varieties for $d = 3$ and $n = 7$.

Example 2.2.9 $(d = 4, n = 8)$**.** The 14 varieties live in $\mathbb{P}^{69}$. Five of them are linear spaces: $V_{\{3\}} \simeq \mathbb{P}^{16}$, $V_{\{4\}} \simeq \mathbb{P}^1$, $V_{\{2,4\}} \simeq \mathbb{P}^{37}$, $V_{\{3,4\}} \simeq \mathbb{P}^{17}$, $V_{\{2,3,4\}} \simeq \mathbb{P}^{53}$. The other nine are listed here.

σ	$\{1\}$	$\{2\}$	$\{1,2\}$	$\{1,3\}$	$\{1,4\}$	$\{2,3\}$	$\{1,2,3\}$	$\{1,2,4\}$	$\{1,3,4\}$
dim	16	36	52	32	17	52	68	53	33
mingens	$[0, 721]$	$[32, 1]$	$[0,0,63]$	$[0, 237, 200]$	$[0, 668]$	$[16, 1]$	$[0,0,0,1]$	$[0, 46, 120]$	$[0,236,200]$
degree	24 024	2	442 066	24 024	24 203	2	4	221 033	12 012
CCdeg	154 441	73	$\approx$ 16 952 996	465 915	177 503	105	273	??	245 239

Table 2.2: The nonlinear truncation varieties for $d = 4$ and $n = 8$.

Our methodology for computing these degrees and CC degrees will be explained in Section 5.2.

We saw in our examples that the truncation variety V_σ is a linear space for various subsets σ of $[d]$. The final theorem in this section identifies those subsets for which this happens.

Theorem 2.2.10. *The truncation variety V_σ is a linear subspace of $\mathbb{P}^{\binom{n}{d}-1}$ if and only if the index set σ is closed under addition, i.e. if $i, j \in \sigma$ with $i + j \in [d]$ then $i + j \in \sigma$.*

Proof. We identify V_σ with its restriction to the affine chart $\mathcal{H}'_d = \mathbb{R}^{\binom{n}{d}-1}$. First assume that σ is closed under addition. We have $1 \notin \sigma$ because σ is a proper subset of $[d]$. Hence $\psi_I = 0$ for all I of level 1. Consider $k \geq 2$ with $k \in [d]\backslash\sigma$. For all K with $|K\backslash[d]| = k$ we have

$$x_K(\psi) \;=\; \pm\psi_K \,+\, \sum_j a_j\, \psi_{I_1^{(j)}} \psi_{I_2^{(j)}} \cdots \psi_{I_{r_j}^{(j)}} \;=\; 0. \tag{2.14}$$

Here $a_j \in \mathbb{Z}\backslash\{0\}$ and $\sum_{s=1}^{r_j} |I_s^{(j)}\backslash[d]| = k$ for each j, i.e. the levels of the variables in each monomial sum up to k. Since $k \in [d]\backslash\sigma$ and σ is closed under addition, each monomial contains some ψ_I of level $i < k$ and $i \in [d]\backslash\sigma$. By induction, $\psi_I = 0$. This now implies $\psi_K = 0$. The restriction $V_\sigma \cap \mathcal{H}'_d$ is thus linear and therefore its projective closure V_σ as well.

Next suppose that σ is not closed under addition. Fix the smallest $k \in [d]\backslash\sigma$ such that $k = i + j$ for some $i, j \in \sigma$. By the same argument as above, $\psi_I = \pm x_I(\psi) = 0$ for all ψ_I of level $i < k$ where $i \in [d]\backslash\sigma$. Consider any level k equation (2.14) that holds on the variety V_σ. Fix any degree-compatible monomial order. The initial monomial of $x_K(\psi)$ has degree > 1:

$$\mathrm{in}(x_K(\psi)) \;=\; \psi_{I_1^{(j)}} \psi_{I_2^{(j)}} \cdots \psi_{I_{r_j}^{(j)}} \qquad \text{where } r_j \geq 2.$$

Since k is minimal, no monomial appearing in $x_I(\psi) \in P_\sigma = \mathcal{I}(V_\sigma)$ divides the above initial monomial $\mathrm{in}(x_K(\psi))$. Hence $\mathrm{in}(x_K(\psi))$ is a minimal generator for the initial ideal of P_σ. This cannot be an initial ideal for a linear variety, and therefore V_σ itself is not linear. □

2.3 The Coupled Cluster Equations

We now present the coupled cluster (CC) equations. These approximate the eigenvalue problem (1.13). The ambient space will be one of the truncation varieties V_σ. The equations are determined by a Hamiltonian matrix H as defined in Remark 1.2.5. A first systematic study, with a focus on Newton polytopes, was undertaken in [36]. In what follows we derive the CC equations from the perspective of algebraic geometry, leading to an alternative description. In Theorem 2.3.10 we examine to what extent our formulation is equivalent to the one seen in [35, 36] and (1.17).

Let σ be a non-empty proper subset of $[d]$. The set of indices with level in σ is denoted

$$\widetilde{\sigma} \;=\; \big\{ I \in \tbinom{[n]}{d} \,:\, |I\backslash[d]| \in \sigma \big\}.$$

We already saw that the dimension of the truncation variety V_σ equals the cardinality $|\widetilde{\sigma}|$. For the Grassmannian $V_{\{1\}} = \mathrm{Gr}(d,n)$, the set $\widetilde{\{1\}}$ consists of all d-tuples that differ from $[d]$ in exactly one index, so we have $|\widetilde{\{1\}}| = d(n-d) = \dim(\mathrm{Gr}(d,n))$. For $\psi \in \mathcal{H}_d$, we denote by ψ_σ the projection of the vector ψ to the coordinates ψ_I where $I \in \widetilde{\sigma}$ and the homogeneous coordinate $\psi_{[d]}$. We define the *unlinked coupled cluster equations* to be

$$(H\psi)_\sigma \;=\; \lambda\,\psi_\sigma, \qquad \psi \in V_\sigma. \tag{2.15}$$

This translates into a system of quadratic equations on the projective variety V_σ. The linear dependence condition in (2.15) can be expressed by the 2×2 minors of the $(|\widetilde{\sigma}|+1)\times 2$ matrix $\big[(H\psi)_\sigma\,,\psi_\sigma\big]$. The number $|\widetilde{\sigma}|$ of constraints imposed by this equation equals the dimension of V_σ, so the CC equations should have a finite number of solutions for generic H. This is indeed the case. We call this number the *CC degree* of the variety V_σ, denoted by $\mathrm{CCdeg}(V_\sigma)$.

Example 2.3.1 ($d=2, \sigma=\{1\}$)**.** Consider the CC equations on the Grassmannian $\mathrm{Gr}(2,n)$. There are $\binom{n}{2}$ Plücker coordinates ψ_{ij} of ψ. The truncated column vector ψ_σ has $2n-3$ entries, namely all coordinates ψ_{ij} where $\{i,j\}\cap\{1,2\}\neq\emptyset$. These coordinates form a transcendence basis for the coordinate ring of $\mathrm{Gr}(2,n)$. The Hamiltonian H is a matrix of format $\binom{n}{2}\times\binom{n}{2}$ so $H\psi$ and $(H\psi)_\sigma$ are column vectors of length $\binom{n}{2}$ and $2n-3$ respectively. The CC equations (2.15) impose $2n-4$ conditions on the $(2n-4)$-dimensional variety $\mathrm{Gr}(2,n)$. See Theorem 3.1.2 for the number of solutions.

The CC degree is the number of solutions to the CC equations. Some non-trivial values of $\mathrm{CCdeg}(V_\sigma)$ were shown in the tables of Examples 2.2.8 and 2.2.9. We have the following general upper bound for the CC degree in terms of the degree of the truncation variety V_σ.

Theorem 2.3.2. *For any Hamiltonian H, the number of isolated solutions to (2.15) satisfies*

$$\mathrm{CCdeg}(V_\sigma) \quad\leq\quad \big(\dim(V_\sigma)+1\big)\,\deg(V_\sigma). \tag{2.16}$$

Proof. We set $N = |\widetilde{\sigma}| = \dim(V_\sigma)$. For generic Hamiltonians H, the variety in $\mathbb{P}^{\binom{n}{d}-1}$ defined by the 2×2 minors of the $(N+1)\times 2$ matrix $\big[(H\psi)_\sigma\,,\psi_\sigma\big]$ has codimension N and degree $N+1$. Geometrically, this variety is a cone over a generic section of the Segre variety $\mathbb{P}^1\times\mathbb{P}^N\subseteq\mathbb{P}^{2N+1}$. The first factor on the right-hand side in (2.16) is $N+1=\deg(\mathbb{P}^1\times\mathbb{P}^N)$. The intersection with V_σ has expected dimension zero, but it can have higher-dimensional components. We are interested in the number of isolated solutions. By Bézout's Theorem, this number is at most the product of the degrees of the two varieties, seen on the right in (2.16). That bound on the number of isolated solutions also holds for special matrices H. □

We note that the equality holds in (2.16) for the linear cases described in Theorem 2.2.10.

Corollary 2.3.3. *Suppose that V_σ is a linear space. Then $\mathrm{CCdeg}(V_\sigma)=\dim(V_\sigma)+1$, we have $(H\psi)_\sigma = H_{\sigma,\sigma}\psi_\sigma$, and (2.15) is the eigenvalue problem for the symmetric matrix $H_{\sigma,\sigma}$. In particular, all complex solutions to the CC equations (2.15) are real.*

Proof. The vector ψ is zero in all coordinates outside $\widetilde{\sigma} \cup \{[d]\}$, and it is arbitrary otherwise, since $V_\sigma = \mathbb{P}^{|\widetilde{\sigma}|}$. This implies $(H\psi)_\sigma = H_{\sigma,\sigma}\psi_\sigma$, and the other assertions follow from this. □

We expect (2.16) to be strict whenever $\deg(V_\sigma) \geq 2$. This holds whenever $\mathrm{CCdeg}(V_\sigma)$ is known. There is a geometric explanation: the intersection of V_σ with the variety of 2×2 minors of $\big[(H\psi)_\sigma\,, \psi_\sigma\big]$ is not transverse on the hyperplane $V(\psi_{[d]})$. Finding the true CC degree is a problem in intersection theory, just like computing the degree of V_σ itself. The two numbers are important for quantum chemistry because they govern the complexity of solving the CC equations. In particular, $\mathrm{CCdeg}(V_\sigma)$ is the number of paths to be tracked when solving numerically with `HomotopyContinuation.jl`. This is discussed in Section 5.2.

Example 2.3.4 ($d = 2, \sigma = \{1\}$)**.** We continue Example 2.3.1. The degree of the Grassmannian $\mathrm{Gr}(2,n)$ is the Catalan number $\frac{1}{n-1}\binom{2n-4}{n-2}$. We see this in [72, equation (5.5) and Theorem 5.13]. The degree of the variety of 2×2 minors is $2n-3$. Hence the upper bound in (2.16) equals $\frac{2n-3}{n-1}\binom{2n-4}{n-2} = \binom{2n-3}{n-1}$. This binomial coefficient is $10, 35, 126, 462, 1\,716, 6\,435$ for $n = 4, 5, 6, 7, 8, 9$. Using computational methods, we found that the true CC degrees are $9, 27, 83, 263, 857, 2\,859$ for $n = 4, 5, 6, 7, 8, 9$. In Theorem 3.1.2 we provide an explicit formula.

The inequality (2.16) is strict for $\mathrm{Gr}(2,n)$ because the CC equations admit extraneous solutions that lie on the hyperplane $\{\psi_{12} = 0\}$. These form a higher-dimensional component which can be removed by saturation as in (2.10). We discuss this in detail for a small instance.

Example 2.3.5 ($d = 2, n = 5$)**.** The CC equations are written via rank constraints as follows:

$$\operatorname{rank}\begin{bmatrix} 0 & \psi_{12} & \psi_{13} & \psi_{14} & \psi_{15} \\ -\psi_{12} & 0 & \psi_{23} & \psi_{24} & \psi_{25} \\ -\psi_{13} & -\psi_{23} & 0 & \psi_{34} & \psi_{35} \\ -\psi_{14} & -\psi_{24} & -\psi_{34} & 0 & \psi_{45} \\ -\psi_{15} & -\psi_{25} & -\psi_{35} & -\psi_{45} & 0 \end{bmatrix} \leq 2 \quad \text{and} \quad \operatorname{rank}\begin{bmatrix} (H\psi)_{12} & \psi_{12} \\ (H\psi)_{13} & \psi_{13} \\ (H\psi)_{14} & \psi_{14} \\ (H\psi)_{15} & \psi_{15} \\ (H\psi)_{23} & \psi_{23} \\ (H\psi)_{24} & \psi_{24} \\ (H\psi)_{25} & \psi_{25} \end{bmatrix} \leq 1.$$

Indeed, the Grassmannian $V_{\{1\}} = \mathrm{Gr}(2,5)$ is cut out in $\mathbb{P}^9$ by the 4×4 Pfaffians of a skew-symmetric 5×5 matrix (see Example 1.1.10). Let $\mathcal{I}$ be the ideal generated by these 5 Pfaffians plus the $\binom{7}{2} = 21$ maximal minors of the 7×2 matrix on the right. Its degree gives the upper bound $35 = 5 \cdot 7$ in Theorem 2.3.2. The ideal $\mathcal{I}$ is radical, and it is the intersection of the desired ideal of codimension 9 and a linear ideal of codimension 7, namely $\langle \psi_{12}, \psi_{13}, \psi_{14}, \psi_{15}, \psi_{23}, \psi_{24}, \psi_{25} \rangle$. This extraneous component is responsible for the difference 8 between the upper bound and the true CC degree, which is 27, as in Theorem 3.1.2.

Example 2.3.6 ($d = 3, n = 6$)**.** We consider the six truncation varieties V_σ in Example 2.2.4. We describe them along with listing bounds for their CC degree in Table 2.3.

In three cases, the variety V_σ is a linear space in $\mathbb{P}^{19}$, and the CC degree is $\dim(V_\sigma) + 1$. In the other three cases, the CC degree is a bit below the bound given by Theorem 2.3.2. See Examples 2.2.8 and 2.2.9 for more comparisons between our upper bound and the CC degree.

σ	$\{1\}$	$\{2\}$	$\{3\}$	$\{1,2\}$	$\{1,3\}$	$\{2,3\}$
dim	9	9	1	18	10	10
degree	42	1	1	3	41	1
bound	420	10	2	57	451	11
CCdeg	250	10	2	55	420	11

Table 2.3: The truncation varieties for $d = 3$, $n = 6$, with our upper bound for the CC degrees.

Of special interest is the case when the truncation variety V_σ is a hypersurface. This is the hypersurface defined by the master polynomial $t_{[d],[\bar{d}]}(c) = x_{[2d]\setminus[d]}(\psi)$. This polynomial was shown explicitly in Theorem 2.1.5. Our next result gives the CC degree for this hypersurface.

Proposition 2.3.7. *If $n = 2d$ and $\sigma = \{1, 2, \ldots, d-1\}$, then the bound (2.16) is off by $d-1$:*

$$\mathrm{CCdeg}_{d,2d}(V_\sigma) \;=\; \big(\dim(V_\sigma)+1\big)\,\deg(V_\sigma) \;-\; (d-1) \;=\; d\binom{2d}{d} - 2d + 1. \tag{2.17}$$

Proof. We wish to count all scalars $\lambda \in \mathbb{C}$ such that the truncated eigenvalue equation $\big[(H - \lambda\,\mathrm{Id})\psi\big]_\sigma = 0$ has a solution ψ in V_σ. For this, we delete the last row of the matrix $H - \lambda\,\mathrm{Id}$ to get a matrix with one more column than rows. Using Cramer's Rule, we write the entries of ψ as signed maximal minors of that matrix. The last entry of ψ is a polynomial in λ of degree $\binom{2d}{d} - 1$, which is the size of these minors. All other entries of $\psi = \psi(\lambda)$ are polynomials of degree $\binom{2d}{d} - 2$, because λ does not occur in the last column of our matrix.

We substitute the vector $\psi = \psi(\lambda)$ into the equation $f = x_{[2d]\setminus[d]}(\psi)$ that defines V_σ. We know that f has degree d and it is linear in the last variable $\psi_{[2d]\setminus[d]}$. This implies that $f(\psi(\lambda))$ is a polynomial in one variable λ of degree $\big(\binom{2d}{d} - 2\big)(d-1) + \big(\binom{2d}{d} - 1\big)$. Since H is generic, the polynomial is squarefree, and its number of complex zeros is given in (2.17). □

We next express the CC equations in terms of the cluster amplitudes x_I. Let x_σ denote the restriction of the vector x to the coordinates in $\widetilde{\sigma}$. To be precise, x_σ is the vector of length $\binom{n}{d}$ which is obtained from x by setting $x_{[d]} = 1$ and $x_J = 0$ for all $J \notin \widetilde{\sigma}$. We identify $\mathbb{C}^{|\widetilde{\sigma}|}$ with the space of such vectors. The truncation variety V_σ has the parametric representation

$$\mathbb{C}^{|\widetilde{\sigma}|} \;\to\; \mathbb{P}^{\binom{n}{d}-1},\; z \;\mapsto\; \exp(T(x_\sigma))e_{[d]}.$$

We substitute this parameterization into (2.15). The CC equations are therefore equivalent to the following square system of $|\widetilde{\sigma}| + 1$ equations in $|\widetilde{\sigma}| + 1$ unknowns:

$$\big[\,(H - \lambda\,\mathrm{Id})\,\exp(T(x_\sigma))e_{[d]}\,\big]_\sigma \;=\; 0 \qquad \text{for some } \lambda \in \mathbb{C}. \tag{2.18}$$

We now compare the system (2.18) with the traditional formulation of the CC equations, called the linked CC equations, which were used in [36] and in earlier works. It is based on the observation

$$\exp(T(x))^{-1} \;=\; \exp(T(-x)). \tag{2.19}$$

Before truncation, one left-multiplies (2.18) by the matrix inverse (2.19). In this new system of equations, λ appears only in the top equation, and there it appears linearly. Hence, we can eliminate the first equation and write the linked CC equations as a square system of $|\widetilde{\sigma}|$ equations in $|\widetilde{\sigma}|$ unknowns:

$$\big[\exp(T(-x_\sigma))\, H\, \exp(T(x_\sigma))\, e_{[d]}\,\big]_\sigma \;=\; 0. \tag{2.20}$$

Remark 2.3.8. The square system in (2.20) is equivalent to the linked CC equations presented in [36, equation (4.2)]. The Newton polytopes of these equations are studied in [36, Section 4.1], and [36, Section 4.2] offers a reformulation as quadratic equations in more variables.

It turns out that – sometimes – the traditional formulation (2.20) yields a polynomial system that is fundamentally different from the system we derived in (2.18). The reason for this discrepancy is that the left multiplication with (2.19) need not commute with truncation.

Example 2.3.9. Let $d = 3, n = 6$ and $\sigma = \{2, 3\}$. The variety V_σ is a linear space $\mathbb{P}^{10}$, and (2.18) is an ordinary eigenvalue problem for the 11×11 matrix $H_{\sigma,\sigma}$. It has 11 solutions, all real. On the other hand, the system (2.20) has 20 complex solutions. Experimentally, the number of real solutions ranges between 6 and 14. The two systems are genuinely different.

The following result says that the discrepancy we discovered is actually not so bad. It characterizes all CC variants where the unlinked and linked CC equations agree.

Theorem 2.3.10. *The system (2.18) is equivalent to the system (2.20) if and only if the set σ has the form $m[k] = \{m, 2m, \ldots, km\}$ for some positive integers m, k with $km \leq d$.*

Proof. We consider a matrix A whose rows and columns are indexed by $\binom{[n]}{d}$. The identity

$$[\,AB\,]_\sigma \;=\; [\,A\,]_{\sigma,\sigma}[\,B\,]_\sigma$$

holds for a general matrix B if and only if $[\,A\,]_{\sigma,\sigma^c} = 0$, where $\sigma^c = [d]\backslash\sigma$. Suppose this is true for $\exp(T(x_\sigma))$. Then the same block is zero in the inverse matrix $\exp(-T(x_\sigma))$, and

$$\begin{aligned}[\,(H - \lambda\,\mathrm{Id})\exp(T(x_\sigma))e_{[d]}\,]_\sigma \;&=\; [\exp(-T(x_\sigma))\,]_{\sigma,\sigma}[\,(H - \lambda\,\mathrm{Id})\exp(T(x_\sigma))e_{[d]}\,]_\sigma \\ &=\; [\exp(-T(x_\sigma))H\exp(T(x_\sigma))e_{[d]} - \lambda e_{[d]}\,]_\sigma.\end{aligned}$$

This means that (2.18) is equivalent to (2.20). Conversely, if this holds then $[\exp T(x_\sigma)]_{\sigma,\sigma^c}$ is zero because the Hamiltonian H can be an arbitrary symmetric $\binom{n}{d} \times \binom{n}{d}$ matrix.

We shall now prove that $[\exp T(x_\sigma)]_{\sigma,\sigma^c}$ is zero if and only if σ has the form $m[k]$. The (I, J) entry in $\exp(T(x_\sigma))$ is non-zero if and only if we can map from state e_J to state e_I via a composition of excitation operators $X_{\alpha,\beta}$. This is possible if and only if $J\backslash[d] \subseteq I\backslash[d]$ and

$$|\,I\backslash[d]\,| \;-\; |\,J\backslash[d]\,| \;=\; \sum_{k\in\sigma} p_k k \quad \text{for some } p_k \in \mathbb{N}.$$

Given any $1 \leq j < i \leq d$, we can always find $I, J \subseteq [n]$ of levels i and j respectively such that $J\backslash[d] \subseteq I\backslash[d]$. Hence the block $[\exp(T(x_\sigma))]_{\sigma,\sigma^c}$ is non-zero if and only if

$$\exists\, j \in [d]\backslash\sigma,\ \ \exists\, i \in \sigma\ :\ i > j\ \text{ and }\ j = i - \sum_{k\in\sigma} p_k k \quad \text{for some } p_k \in \mathbb{N}. \tag{2.21}$$

Let m and M be the minimal and maximal elements of σ. If $M - p_m m \in [d]\backslash\sigma$ for some $p_m \in \mathbb{N}_+$ then (2.21) holds and $[\exp(T(x_\sigma))]_{\sigma,\sigma^c}$ is non-zero. Suppose now that $M - p_m m \in \sigma$ for all positive integers $p_m < M/m$. Then $M = km$ by the choice of m, and we have $m[k] \subseteq \sigma$. Next suppose $m[k] = \sigma$. No $j \in [d]\backslash\sigma$ with $j < M$ is a multiple of m, and thus (2.21) fails. Finally suppose $m[k] \subsetneq \sigma$. We take the smallest element $i \in \sigma$ that is not a multiple of m. Then $i - m \in [d]\backslash\sigma$ and (2.21) holds for $p_m = 1$. Therefore $[\exp(T(x_\sigma))]_{\sigma,\sigma^c}$ is non-zero. □

Theorem 2.3.10 shows that the traditional formulation (2.20) coincides with our formulation (2.15) in all cases that have appeared in the computational chemistry literature [35, 36, 61] including CCS, CCD, CCSD, CCSDT, see Table 1.1. Scenarios where the two formulations differ, like $\sigma = \{2, 3\}$, are less relevant for coupled cluster theory. For electronic structure Hamiltonians, the formulation (2.20) contains equations of at most degree 4, because of the special structure of these Hamiltonians. See [51, Section 13.2.5] for a proof. For us, (2.15) is more elegant than (2.20), and its algebraic degree is lower. This is why we refer to (2.15) as **the** CC equations.

For special Hamiltonians H, the number of isolated solutions to the CC equations can be much lower than the CC degree. This happens in applications, as seen in Chapter 5. It would be interesting to understand this phenomenon for H on special loci in the space of symmetric matrices. The next example suggests such a study for low rank matrices.

Example 2.3.11 ($d = 2, n = 4, \sigma = \{1\}$)**.** The CC degree is 9 for the Plücker quadric $\mathrm{Gr}(2, 4)$. Let H be a general symmetric 6×6 matrix of rank r. For $r = 1, 2, 3, 4, 5$, the number of solutions to (2.18) is $1, 3, 5, 7, 9$, seen by Cramer's Rule as in the proof of Proposition 2.3.7.

We conclude with a brief summary of the main contributions of this chapter and describe the next steps. We have now developed the coupled cluster equations from an algebraic-geometric perspective. To this end, we introduced the truncation varieties, a class of varieties parameterized by restrictions of the exponential map. Moreover, we showed that the Grassmannian arises as an example of such a variety. We also defined the CC degree, an invariant of truncation varieties that counts the generic number of solutions to the CC equations over the variety in question. The next two chapters study this invariant in more detail. We begin with the Grassmannian. In particular, we relate its CC degree to the total degree of the graph of its exponential parameterization, thereby obtaining a more algebraic description of this invariant.

Chapter 3

CC Degree of the Grassmannian

In this chapter we focus on the CCS truncation variety, the Grassmannian $\mathrm{Gr}(d,n)$ in its Plücker embedding. We show that its CC degree coincides with the total degree of the graph of a birational parameterization. We provide an explicit formula for the CC degree of the Grassmannian of lines in terms of Catalan numbers, see Theorem 3.1.2. This result rests on the geometry of the graph of the birational parameterization. We present a squarefree Gröbner basis for this graph and develop connections to toric degenerations from representation theory. Finally, we identify the CC degree of Grassmannians with the volume of a polytope known as the CFFLV polytope. This chapter is based on the paper *Coupled Cluster Degree of the Grassmannian* [8], which is joint work with Viktoriia Borovik and Bernd Sturmfels.

3.1 The Graph of the Grassmannian

In this section we focus on the CCS (Coupled Cluster Single) model, allowing only single level electronic excitations, so $\sigma = \{1\}$. By Theorem 2.2.5 the corresponding truncation variety is the Grassmannian in its Plücker embedding in $\mathbb{P}^{\binom{n}{d}-1}$, i.e. $V_{\{1\}} \cong \mathrm{Gr}(d,n)$. The coupled cluster equations for the CCS model then take the form

$$(H\psi)_* \;=\; \lambda\,\psi_* \quad \text{for} \quad \psi \in \mathrm{Gr}(d,n). \tag{3.1}$$

Here, ψ is the column vector of Plücker coordinates ψ_I indexed by $I = (i_1 < i_2 < \ldots < i_d) \in \binom{[n]}{d}$ and $(\cdot)_*$ denotes the projection to the $d(n-d)+1$ coordinates which satisfy $i_{d-1} \leq d$. It is equivalent to the projection $(\cdot)_{\{1\}}$, defined in the beginning of Section 2.3. Our system (3.1) is a truncation of the eigenvalue problem for the symmetric $\binom{n}{d} \times \binom{n}{d}$ Hamiltonian matrix H.

The Grassmannian is the closure in $\mathbb{P}^{\binom{n}{d}-1}$ of the image of the parameterization map

$$\gamma : T = [t_{i,j}] \;\mapsto\; \text{all } \tbinom{n}{d} \text{ maximal minors of } [\,\mathrm{I}_d\; T\,] \;=\; \begin{bmatrix} 1 & 0 & \cdots & 0 & t_{1,d+1} & t_{1,d+2} & \cdots & t_{1,n} \\ 0 & 1 & \cdots & 0 & t_{2,d+1} & t_{2,d+2} & \cdots & t_{2,n} \\ \vdots & \vdots & \ddots & \vdots & \vdots & \vdots & \ddots & \vdots \\ 0 & 0 & \cdots & 1 & t_{d,d+1} & t_{d,d+2} & \cdots & t_{d,n} \end{bmatrix}.$$

This maps the $d \times (n-d)$ matrix T to all its minors, see also Remark 1.1.9. We view this as a rational map:

$$\gamma \,:\, \mathbb{P}^{d(n-d)} \dashrightarrow \mathrm{Gr}(d,n) \,\subseteq\, \mathbb{P}^{\binom{n}{d}-1}.$$

In fact, we define the map γ on an affine subset $\mathbb{C}^{d(n-d)}$ and extend it to the whole $\mathbb{P}^{d(n-d)}$ by multiplying the matrix I_d by an additional variable s. See Remark 1.1.8. The closure of the graph of the map γ is a subvariety $\mathcal{G}(d,n)$ of dimension $d(n-d)$ in the product space $\mathbb{P}^{d(n-d)} \times \mathbb{P}^{\binom{n}{d}-1}$. Its class, $[\mathcal{G}(d,n)]$, in the cohomology ring

$$H^*(\mathbb{P}^{d(n-d)} \times \mathbb{P}^{\binom{n}{d}-1}, \mathbb{Z}) \cong \mathbb{Z}[u,v] / \left\langle u^{d(n-d)+1}, v^{\binom{n}{d}} \right\rangle$$

is represented by a binary form of degree $\mathrm{codim}(\mathcal{G}(d,n)) = \binom{n}{d} - 1$. The coefficients of the monomials are known as *bidegrees*. Explicitly, the graph $\mathcal{G}(d,n)$ admits a natural $\mathbb{Z}^2$-grading with respect to its grading in $\mathbb{P}^{d(n-d)}$ and $\mathbb{P}^{\binom{n}{d}-1}$. The ith bidegree is then defined as

$$\delta_i(\mathcal{G}(d,n)) = \delta_i = \#(\mathcal{G}(d,n) \cap (L \times L'))$$

where $L \subseteq \mathbb{P}^{d(n-d)}$ and $L' \subseteq \mathbb{P}^{\binom{n}{d}-1}$ are general linear subspaces of dimension i and $\binom{n}{d}-1-i$, respectively. We can also define the ith bidegree as the degree of the image of the restriction $\gamma(L) \subseteq \mathbb{P}^{\binom{n}{d}-1}$ to a general linear space $L \subseteq \mathbb{P}^{d(n-d)}$ of dimension i. We notice that $\delta_i = 0$ for $i < 0$ and $i > d(n-d)$. Additionally we see that $\delta_0 = 1$ and $\delta_{d(n-d)} = \deg(\mathrm{Gr}(d,n))$. The coefficient of the monomial $u^i v^{\binom{n}{d}-1-i}$ in the class $[\mathcal{G}(d,n)]$ is then the bidegree $\delta_{d(n-d)-i}(\mathcal{G}(d,n))$.

The *total degree* of $\mathcal{G}(d,n)$ is defined to be the sum of its bidegrees. The total degree can also be defined in terms of the projectivization of the cone of $\mathcal{G}(d,n)$ in affine space $\mathbb{A}^{d(n-d)+1} \times \mathbb{A}^{\binom{n}{d}} \cong \mathbb{A}^{\binom{n}{d}+d(n-d)+1}$. The affine cone has dimension $d(n-d)+2$ and the associated projective variety in $\mathbb{P}^{\binom{n}{d}+d(n-d)}$ has dimension $d(n-d)+1$. The total degree of $\mathcal{G}(d,n)$ is then defined as the degree of this projective variety. The two definitions are equivalent, see e.g. [105].

Theorem 3.1.1. *The CC degree of the Grassmannian* $\mathrm{Gr}(d,n) \subseteq \mathbb{P}^{\binom{n}{d}-1}$ *is the total degree of the graph* $\mathcal{G}(d,n)$.

This result will be proved in Section 3.2. Our approach is to argue that the following bilinear equations on $\mathbb{P}^{d(n-d)} \times \mathbb{P}^{\binom{n}{d}-1}$ are equivalent to the CC equations (3.1):

$$(H\psi)_* \,=\, \lambda\,\xi \quad \text{for} \quad (\xi,\psi) \in \mathcal{G}(d,n). \tag{3.2}$$

The coordinates $\xi_{i_1 i_2 \cdots i_d}$ on $\mathbb{P}^{d(n-d)}$ are indexed by $1 \le i_1 < i_2 < \cdots < i_d \le n$ with $i_{d-1} \le d$. They correspond to the variables $t_{i,j}$ such that $i = [d] \backslash \{i_1, \ldots, i_{d-1}\}$ and $j = i_d$. The coordinate $\xi_{[d]}$ corresponds to the additional variable s. The solutions to the equation (3.2) are counted by the total degree of the graph $\mathcal{G}(d,n)$. In the case of the Grassmannian of lines we have an explicit formula for the total degree of the graph.

Theorem 3.1.2. *The CC degree of the Grassmannian* $\mathrm{Gr}(2,n)$ *is*

$$\mathrm{CCdeg}(\mathrm{Gr}(2,n)) \;=\; 2C_{n-1}-1 \;=\; \frac{2}{n}\binom{2n-2}{n-1} \;-\; 1.$$

This result will be proved in Section 3.3 using a Gröbner basis. Additionally we describe a Khovanskii basis that gives a toric degeneration of the graph. Both flavors of bases are well-studied for Grassmannians, see Examples 1.1.12 and 1.1.16 for the case of the Grassmannian of lines. Here we lift them from $\mathrm{Gr}(2,n)$ to the graph $\mathcal{G}(2,n)$. In Section 3.4 the same approach is developed for $d \geq 3$. It is essential to make judicious choices of monomial orders, building on recent advances on toric degenerations in [19, 31, 59, 68, 69].

Example 3.1.3 ($d=2, n=6$)**.** The prime ideal of the Grassmannian $\mathrm{Gr}(2,6) \subseteq \mathbb{P}^{14}$ is generated by the 15 Plücker quadrics $\psi_{il}\psi_{jk} - \psi_{ik}\psi_{jl} + \psi_{ij}\psi_{kl}$ for $1 \leq i < j < k < l \leq 6$. For the graph $\mathcal{G}(2,6) \subseteq \mathbb{P}^8 \times \mathbb{P}^{14}$, we augment the Plücker ideal by the 2×2 minors of the 2×9 matrix

$$\begin{bmatrix} \psi_{12} & \psi_{13} & \psi_{14} & \psi_{15} & \psi_{16} & \psi_{23} & \psi_{24} & \psi_{25} & \psi_{26} \\ \xi_{12} & \xi_{13} & \xi_{14} & \xi_{15} & \xi_{16} & \xi_{23} & \xi_{24} & \xi_{25} & \xi_{26} \end{bmatrix}. \tag{3.3}$$

The bihomogeneous prime ideal of $\mathcal{G}(2,6)$ is obtained by saturating with respect to ψ_{12}. This ideal is minimally generated by the 15 Plücker quadrics of bidegree $(0,2)$, and 50 quadrics of bidegree $(1,1)$. In addition to the 36 maximal minors of (3.3), there are 14 polarized Plücker relations, like $\psi_{14}\xi_{23} - \psi_{13}\xi_{24} + \psi_{34}\xi_{12}$. The entries of the 2×4 matrix T in the definition of γ serve as local coordinates. In these coordinates, the matrix (3.3) is seen to have rank one:

$$\begin{bmatrix} u \\ v \end{bmatrix} \cdot \begin{bmatrix} 1 & t_{2,3} & t_{2,4} & t_{2,5} & t_{2,6} & -t_{1,3} & -t_{1,4} & -t_{1,5} & -t_{1,6} \end{bmatrix}.$$

By applying the command `multidegree` in `Macaulay2` to our bihomogeneous ideal, we find that the class of the graph $\mathcal{G}(2,6)$ in the cohomology ring $H^*(\mathbb{P}^8 \times \mathbb{P}^{14}) = \mathbb{Z}[u,v]/\langle u^9, v^{15}\rangle$ is

$$[\mathcal{G}(2,6)] = u^8v^6 + 2u^7v^7 + 4u^6v^8 + 8u^5v^9 + 12u^4v^{10} + 14u^3v^{11} + 14u^2v^{12} + 14uv^{13} + 14v^{14}.$$

The total degree of the graph $\mathcal{G}(2,6)$ is the sum of the coefficients. This sum equals 83, so it agrees with the CC degree of $\mathrm{Gr}(2,6)$ as computed in Example 2.3.4. The proof of Theorem 3.1.2 in Section 3.3 rests on the fact that the 65 ideal generators of $\mathcal{G}(2,6)$ form a Gröbner basis. A combinatorial study of its squarefree leading monomials reveals the Catalan number $42 = \deg(\mathrm{Gr}(2,7))$, which is the key ingredient for $\deg(\mathcal{G}(2,6)) = 2 \cdot 42 - 1$.

Using the combinatorial and computational techniques to be developed in Section 3.4, it is now possible to compute some new CC degrees that go beyond those reported in Chapter 2.

Example 3.1.4. Here are three new values for the census of CC degrees of Grassmannians:

$$\deg(\mathcal{G}(3,9)) = 574\,507, \;\; \deg(\mathcal{G}(3,10)) = 9\,239\,646 \;\; \text{and} \;\; \deg(\mathcal{G}(4,9)) = 10\,907\,231.$$

These CC degrees are at most around 10^7, which means that all complex solutions of the corresponding CC equations can be found numerically with `HomotopyContinuation.jl` [11].

3.2 Intersecting the Graph

The objective of this section is to prove Theorem 3.1.1. We need the following general lemma. Let V be any irreducible subvariety of dimension k in $\mathbb{P}^m \times \mathbb{P}^s$. Fix the homogeneous coordinates $\mathbf{x} = [x_0 : \cdots : x_m]$ and $\mathbf{y} = [y_0 : \cdots : y_s]$ on the two factors. For $i = 0, 1, \ldots, k$ we consider generic linear forms $\ell_i(\mathbf{x})$ and $m_i(\mathbf{y})$, defining hyperplanes in $\mathbb{P}^m$ and $\mathbb{P}^s$, respectively.

Lemma 3.2.1. *The total degree of the variety V equals the number of points $(\mathbf{x}, \mathbf{y})$ on V such that the vectors $(\ell_0(\mathbf{x}), \ell_1(\mathbf{x}), \ldots, \ell_k(\mathbf{x}))$ and $(m_0(\mathbf{y}), m_1(\mathbf{y}), \ldots, m_k(\mathbf{y}))$ are linearly dependent.*

Proof. The bidegrees of V are the coefficients of the binary form representing the cohomology class $[V] \in H^*(\mathbb{P}^m \times \mathbb{P}^s) = \mathbb{Z}[u, v]/\langle u^{m+1}, v^{s+1} \rangle$. As before, the total degree of V is the sum of its bidegrees. We consider the $2 \times (k+1)$ matrix whose rows are the two vectors introduced above. Its 2×2 minors are the bilinear forms $\ell_i(\mathbf{x}) \cdot m_j(\mathbf{y}) - \ell_j(\mathbf{x}) \cdot m_i(\mathbf{y})$ for $0 \leq i < j \leq k$. We need to count their zeros on V. To this end, we introduce a small real parameter $\varepsilon > 0$, and we replace $\ell_i(\mathbf{x})$ by $\varepsilon^i \cdot \ell_i(\mathbf{x})$ for all i. Then our equations become

$$\ell_i(\mathbf{x}) \cdot m_j(\mathbf{y}) \;=\; \varepsilon^{j-i} \cdot \ell_j(\mathbf{x}) \cdot m_i(\mathbf{y}) \qquad \text{for} \;\; 0 \leq i < j \leq k.$$

When ε approaches zero, we obtain the equations $\ell_i(\mathbf{x}) \cdot m_j(\mathbf{y}) = 0$ for $0 \leq i < j \leq k$. This system decomposes into $k+1$ systems of k linear equations which are indexed by $i = 0, 1, \ldots, k$. Each of them amounts to intersecting V with a product of subspaces in $\mathbb{P}^m \times \mathbb{P}^s$:

$$\ell_0(\mathbf{x}) = \cdots = \ell_{i-1}(\mathbf{x}) \;=\; m_{i+1}(\mathbf{y}) = \cdots = m_k(\mathbf{y}) \;=\; 0 \quad \text{for } i = 0, 1, \ldots, k. \tag{3.4}$$

This is a system of k linear equations. Since the linear forms ℓ_i and m_j are generic, the system (3.4) has finitely many solutions $(\mathbf{x}, \mathbf{y})$ on the k-dimensional variety V, and each solution is nondegenerate. By the Implicit Function Theorem, each solution extends from $\varepsilon = 0$ to a small positive value $\varepsilon_0 > 0$, and these are all solutions of the original system for ε_0. The number of solutions to (3.4) is a bidegree of V, namely it is the coefficient of $u^{m-i} v^{s-k+i}$ in the binary form $[V]$. By summing over all i, we obtain the total degree of V, as desired. □

Proof of Theorem 3.1.1. We shall apply Lemma 3.2.1 to the variety $V := \mathcal{G}(d, n)$, which is the graph of the parameterization γ of the Grassmannian $\mathrm{Gr}(d, n)$. This V lives in $\mathbb{P}^{d(n-d)} \times \mathbb{P}^{\binom{n}{d}-1}$ and it has dimension $d(n-d)$. We denoted the coordinates by $\xi = \mathbf{x}$ and $\psi = \mathbf{y}$, in order to be consistent with [36] and Chapter 2. After eliminating λ from (3.1), the CC equations on the Grassmannian $\mathrm{Gr}(d, n)$ are the 2×2 minors of the two-column matrix $\big[(H\psi)_*\,,\, \psi_*\big]$. Up to change of sign of the coordinates, the projection ψ_* is equal to the vector ξ on the graph $\mathcal{G}(d, n)$. We can thus write the CC equations on $\mathcal{G}(d, n)$ as the 2×2 minors of $\big[(H\psi)_*\,,\, S\xi\big]$, where the diagonal matrix S has entries ± 1.

Hence the system of CC equations is precisely as in Lemma 3.2.1, where $\ell_i(\xi) = \pm \xi_i$ and $m_j(\psi)$ denotes the linear form given by the jth row in the Hamiltonian H. The coordinate functions $\ell_i(\xi) = \pm \xi_i$ are not generic, but we can replace them with generic linear forms by a linear change of coordinates on $\mathbb{P}^{d(n-d)}$, given by an invertible matrix M of size $d(n-d)+1$.

This coordinate change can be compensated by multiplying the Hamiltonian H on the left by the block matrix $M^{-1} \oplus I_{\binom{n}{d}-d(n-d)-1}$, which is square of size $\binom{n}{d}$. Since the Hamiltonian matrix H is generic, the resulting linear forms exhibit the generic behavior that is needed for Lemma 3.2.1 to be applicable. We conclude that the number of complex solutions to the CC equations (3.1) is equal to the total degree of the variety $\mathcal{G}(d,n)$. □

Remark 3.2.2. The definition of the CC degree in Section 2.3 counts the number of solutions to the CC equations with multiplicities. It still needs to be shown that there exists a Hamiltonian H for which all solutions are nondegenerate. Ideally, we want them to be all real. If we relax the requirement that the square matrix H should be symmetric, then this would follow from the squarefree Gröbner basis promised in Conjecture 3.4.2. Namely, representing the monomial order by a weight vector, the Gröbner degeneration corresponds to scaling the unknowns:

$$\psi \to D_1(\varepsilon) \cdot \psi \quad \text{and} \quad \xi \to D_2(\varepsilon) \cdot \xi.$$

Here D_1 and D_2 are diagonal matrices whose entries are different powers of the parameter ε. Our polynomial system on $\mathcal{G}(d,n)$ is now given by the 2×2 minors of $\big[(HD_1(\varepsilon)\psi)_*\,,\, D_2(\varepsilon)\xi\big]$.

For $\varepsilon = 0$, we are solving linear equations on an arrangement of reduced linear subspaces, because the initial monomial ideal is radical. Here, all solutions are real and nondegenerate. By the Implicit Function Theorem, each solution extends to a small $\varepsilon_0 > 0$. We now define

$$D_3(\varepsilon_0) := D_2(\varepsilon_0)^{-1} \oplus I_{\binom{n}{d}-d(n-d)-1} \quad \text{and} \quad H(\varepsilon_0) := D_3(\varepsilon_0) \cdot H \cdot D_1(\varepsilon_0).$$

With these matrices, our polynomial system is given by the 2×2 minors of $\big[(H(\varepsilon_0)\psi)_*\,,\, \xi\big]$. Thus, using $H(\varepsilon_0)$ for the Hamiltonian, all solutions to the CC equations are real and nondegenerate. At present we do not know how to replace $H(\varepsilon_0)$ by a symmetric matrix.

3.3 Catalan Numbers

The degree of the Grassmannian $\mathrm{Gr}(2,n)$ is the Catalan number $C_{n-2} = \frac{1}{n-1}\binom{2n-4}{n-2}$, see Example 1.1.12. Theorem 3.1.2 states that the graph $\mathcal{G}(2,n)$ has degree $2C_{n-1}-1$. In this section we shall prove this. For the proof it is convenient to permute the columns in the parameterization of $\mathrm{Gr}(2,n)$. Namely, we redefine γ to be the map that evaluates the 2×2 minors of

$$\begin{bmatrix} 1 & t_{1,2} & t_{1,3} & \cdots & t_{1,n-1} & 0 \\ 0 & t_{2,2} & t_{2,3} & \cdots & t_{2,n-1} & 1 \end{bmatrix}. \tag{3.5}$$

As before, $\mathcal{G}(2,n)$ is the closure of the graph of γ. This is a subvariety of dimension $2n-4$ in $\mathbb{P}^{2n-4} \times \mathbb{P}^{\binom{n}{2}-1}$. The prime ideal of $\mathcal{G}(2,n)$ is the kernel of the ring homomorphism:

$$\begin{aligned} \mathbb{C}[\xi,\psi] &\to \mathbb{C}[u,v,\mathbf{t}], & \xi_{1n} &\mapsto u, & \xi_{1i} &\mapsto ut_{2i}, & \xi_{jn} &\mapsto ut_{1j}, \\ \psi_{ij} &\mapsto v(t_{1i}t_{2j} - t_{1j}t_{2i}), & \psi_{1n} &\mapsto v, & \psi_{1i} &\mapsto vt_{2i}, & \psi_{jn} &\mapsto vt_{1j}, \end{aligned} \quad 1 < i < j < n. \tag{3.6}$$

The polynomial ring $\mathbb{C}[\xi,\psi]$ has $2n-3+\binom{n}{2}$ variables. We order these variables as follows:

$$\begin{aligned}\xi_{12} < \psi_{12} < \xi_{13} < \psi_{13} < \cdots < \xi_{1n} < \psi_{1n} < \psi_{23} < \psi_{24} < \cdots < \psi_{2,n-1} < \xi_{2n} < \psi_{2n} \\ < \psi_{34} < \psi_{35} < \cdots < \psi_{n-2,n-1} < \xi_{n-2,n} < \psi_{n-2,n} < \xi_{n-1,n} < \psi_{n-1,n}.\end{aligned} \tag{3.7}$$

In words, we order the variables ψ_{ij} by sorting their index pairs lexicographically, and we then insert each variable ξ_{1i} or ξ_{jn} right before the ψ-variable with the same index pair. We fix the reverse lexicographic monomial order on $\mathbb{C}[\xi,\psi]$ that is induced by this variable order.

Lemma 3.3.1. *The following $(n-1)(n-2)(n^2+5n+12)/24$ quadrics minimally generate the ideal of $\mathcal{G}(2,n)$. They form the reduced Gröbner basis for the monomial order described above:*

$$\begin{array}{rlll}
\binom{n}{4} & \text{trinomials} & \underline{\psi_{il}\psi_{jk}} - \psi_{ik}\psi_{jl} + \psi_{ij}\psi_{kl} & \text{for } 1 \le i<j<k<l \le n, \\
\binom{n-1}{2} & \text{binomials} & \underline{\psi_{in}\xi_{jn}} - \psi_{jn}\xi_{in} & \text{for } 1 \le i < j < n, \\
(n-2)^2 & \text{binomials} & \underline{\psi_{1j}\xi_{kn}} - \psi_{kn}\xi_{1j} & \text{for } 1 < j\,,\, k\, < n, \\
\binom{n-1}{2} & \text{binomials} & \underline{\psi_{1k}\xi_{1l}} - \psi_{1l}\xi_{1k} & \text{for } 1 < k < l \le n, \\
\binom{n-2}{3} & \text{trinomials} & \underline{\xi_{1l}\psi_{jk}} - \xi_{1k}\psi_{jl} + \xi_{1j}\psi_{kl} & \text{for } 1 < j < k < l < n, \\
\binom{n-1}{3} & \text{trinomials} & \underline{\xi_{in}\psi_{jk}} - \xi_{jn}\psi_{ik} + \xi_{kn}\psi_{ij} & \text{for } 1 \le i < j < k < n.
\end{array}$$

Proof. We first check that the six classes of quadrics vanish on $\mathcal{G}(2,n)$. The $\binom{n}{4}$ trinomials in ψ are the Plücker relations which generate the ideal of $\mathrm{Gr}(2,n)$. Next come three groups of binomials, for a total of $\binom{n-1}{2}+(n-2)^2+\binom{n-1}{2}=\binom{2n-3}{2}$. These are the 2×2 minors of the matrix whose two rows are the ψ variables and the matching ξ variables. This matrix is displayed in (3.3) for $n=6$. It has rank one on the graph $\mathcal{G}(2,n)$, as we can see from (3.6). The last two groups are $\binom{n-2}{3}+\binom{n-1}{3}=\binom{n}{4}-\binom{n-2}{4}$ trinomials that are bilinear in ξ and ψ. These are obtained from the Plücker relations by applying the 2×2 minors of the previous matrix. They are also mapped to zero under the ring map (3.6) that describes $\mathcal{G}(2,n)$.

We next check that the underlined monomials are the leading monomials with respect to the reverse lexicographic monomial order that is induced by the variable order (3.7). Let M be the ideal generated by these monomials. Since the monomials are squarefree, M is a radical ideal. We have argued that $M \subseteq \mathrm{in}(\mathcal{G}(2,n))$, and we now need to show that equality holds.

Consider any monomial in the initial ideal of $\mathcal{G}(2,n)$. It is the leading monomial $\mathrm{in}(f)$ of some bihomogeneous polynomial $f(\xi,\psi)$ that vanishes on $\mathcal{G}(2,n)$. We write $f=\sum c_{\mathbf{a},\mathbf{b}}\xi^{\mathbf{a}}\psi^{\mathbf{b}}$, so our polynomial has bidegree $(|\mathbf{a}|,|\mathbf{b}|)\in\mathbb{Z}^2_{\ge 0}$. Note that $|\mathbf{b}|>0$ because the images of the ξ-variables under the ring map (3.6) are algebraically independent.

First assume $|\mathbf{a}|=0$. Then $f=\sum c_{\mathbf{b}}\psi^{\mathbf{b}}$ lies in the ideal of the Grassmannian $\mathrm{Gr}(2,n)$. The quadrics $\underline{\psi_{il}\psi_{jk}}-\psi_{ik}\psi_{jl}+\psi_{ij}\psi_{kl}$ are known to form a Gröbner basis for this ideal with respect to our monomial order. See e.g. [72, Theorem 5.8] or [73, Theorem 14.6]. Therefore, the leading monomial $\mathrm{in}(f)$ is a multiple of $\psi_{il}\psi_{jk}$ for some $1\le i<j<k<l\le n$.

Next suppose $|\mathbf{a}|>0$. We consider the polynomial $\sum c_{\mathbf{a},\mathbf{b}}\psi^{\mathbf{a}+\mathbf{b}}$ that is obtained from f by replacing each ξ_{ij} with the corresponding ψ_{ij}. We see from (3.6) that this polynomial

vanishes on $\mathcal{G}(2,n)$ and hence on $\mathrm{Gr}(2,n)$. We write the leading monomial of f as follows:

$$\mathrm{in}(f) \;=\; \xi_{\sigma^{(1)}}^{a_1} \cdots \xi_{\sigma^{(h)}}^{a_h} \cdot \psi_{\tau^{(1)}}^{b_1} \cdots \psi_{\tau^{(r)}}^{b_r}.$$

Here $\sigma^{(i)}$ and $\tau^{(j)}$ are index pairs. A key property of our monomial order is that it respects the substitution $\xi \mapsto \psi$. Using this, we now examine the leading monomial of $\sum c_{\mathbf{a},\mathbf{b}} \psi^{\mathbf{a}+\mathbf{b}}$.

First assume that the leading monomial of $\sum c_{\mathbf{a},\mathbf{b}} \psi^{\mathbf{a}+\mathbf{b}}$ differs from the monomial

$$\psi_{\sigma^{(1)}}^{a_1} \cdots \psi_{\sigma^{(h)}}^{a_h} \cdot \psi_{\tau^{(1)}}^{b_1} \cdots \psi_{\tau^{(r)}}^{b_r}.$$

Then f contains another monomial m which cancels $\mathrm{in}(f)$ after the substitution $\xi \mapsto \psi$. Let ρ be the smallest index pair in the list $\sigma^{(1)}, \ldots, \sigma^{(h)}, \tau^{(1)}, \ldots, \tau^{(r)}$. From the cancellation and the definition of the reverse lexicographic order, we see that $\rho = \tau^{(j)}$ for some j. Hence $\mathrm{in}(f)$ contains ψ_ρ and m contains ξ_ρ. In particular, $\rho \cap \{1,n\} \neq \varnothing$. This implies that $\mathrm{in}(f)$ is divisible by one of the underlined leading monomials of the binomials in our list.

Next we suppose that $\psi_{\sigma^{(1)}}^{a_1} \cdots \psi_{\sigma^{(h)}}^{a_h} \cdot \psi_{\tau^{(1)}}^{b_1} \cdots \psi_{\tau^{(r)}}^{b_r}$ is the leading monomial of $\sum c_{\mathbf{a},\mathbf{b}} \psi^{\mathbf{a}+\mathbf{b}}$, which is in the ideal of $\mathrm{Gr}(2,n)$. This leading monomial is divisible by $\psi_{il}\psi_{jk}$ for some indices $1 \leq i < j < k < l \leq n$. Since $\{j,k\} \cap \{1,n\} = \varnothing$, the corresponding factor of $\mathrm{in}(f)$ is either $\psi_{il}\psi_{jk}$ or $\xi_{il}\psi_{jk}$. Both of these occur among the underlined monomials in our list. We conclude that $\mathrm{in}(f)$ is in the ideal generated by the underlined leading monomials.

We have proved that our list of quadratic binomials and trinomials is a Gröbner basis for $\mathcal{G}(2,n)$. To see that it is a reduced Gröbner basis, one checks that no trailing term occurs among the leading monomials. Since all polynomials have the same degree two, it follows that they minimally generate the ideal. This completes the proof of Lemma 3.3.1. □

Let M be the ideal generated by the underlined monomials in Lemma 3.3.1. We have shown that M is the initial ideal of the graph $\mathcal{G}(2,n)$ with respect to the monomial order we defined. This means that the degree of $\mathcal{G}(2,n)$ is equal to the degree of M. We shall prove Theorem 3.1.2 by showing that M has degree $2C_{n-1} - 1$. This will be done by constructing a combinatorial model for the simplicial complex that is represented by the squarefree monomial ideal M. Example 1.1.12 constructs such a model of $\mathrm{Gr}(2,n)$.

We begin with Young's poset on $\binom{[n]}{2}$. The elements in this poset are the variables ψ_{ij} with $1 \leq i < j \leq n$, and the order relation $\preceq$ is defined by setting $\psi_{ij} \preceq \psi_{kl}$ if and only if $i \leq k$ and $j \leq l$. Recall from Example 1.1.12 that the incomparable pairs are precisely the leading monomials $\psi_{il}\psi_{jk}$ for the Grassmannian $\mathrm{Gr}(2,n)$. The simplices in the associated simplicial complex are the chains in the poset. The degree is the number of maximal chains, which is the Catalan number C_{n-2}.

We define the *outer chain* in Young's poset to be the following maximal chain:

$$\psi_{12} \preceq \psi_{13} \preceq \cdots \preceq \psi_{1,n-1} \preceq \psi_{1n} \preceq \psi_{2n} \preceq \psi_{3n} \preceq \cdots \preceq \psi_{n-1,n}.$$

The chain from ψ_{12} up to ψ_{1n} is called the *lower outer chain*, and the chain from ψ_{1n} up to $\psi_{n-1,n}$ is the *upper outer chain*. We now take another copy of Young's poset, indexed by

variables ξ_{ij}, using artificial variables when $\{i,j\} \cap \{1,n\} = \varnothing$. We link the ξ-poset together with the ψ-poset by the outer chains. To be precise, we define a poset $\mathrm{P}_{2,n}$ on $n(n-1)$ elements by taking the union of the two Young's posets together with the additional cover relations $\xi_{ij} \to \psi_{ij}$ whenever $\{i,j\} \cap \{1,n\} \neq \varnothing$.

Example 3.3.2 ($n = 4$)**.** The poset $\mathrm{P}_{2,4}$ has 12 elements. Its Hasse diagram is shown in Figure 3.1. The number of maximal chains of $\mathrm{P}_{2,4}$ is $9 = 2 \cdot 5 - 1$, which is the CC degree of $\mathrm{Gr}(2,4)$.

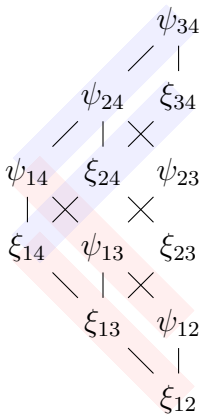

Figure 3.1: Diagram of $\mathrm{P}_{2,4}$ highlighting the two outer chains: the lower outer chains are pink, and the upper outer chains are purple. The outer chain in the ξ-poset consists of variables in our polynomial ring $\mathbb{C}[\xi, \psi]$. The label ξ_{23} is not a coordinate on $\mathcal{G}(2,4)$.

Lemma 3.3.3. *The number of maximal chains in the poset* $\mathrm{P}_{2,n}$ *is* $2 \cdot C_{n-1} - 1 = \frac{2}{n}\binom{2n-2}{n-1} - 1$.

Proof. Every maximal chain in $\mathrm{P}_{2,n}$ transitions precisely once from the ξ-poset to the ψ-poset. It therefore contains a unique cover relation $\xi_{ij} \to \psi_{ij}$ where $\{i,j\} \cap \{1,n\} \neq \varnothing$. We distinguish the two cases when the chain contains $\xi_{in} \to \psi_{in}$ and when it contains $\xi_{1j} \to \psi_{1j}$.

First consider maximal chains that move up to ψ on the upper outer chain. These are the chains containing a cover relation $\xi_{in} \to \psi_{in}$. Such chains are in bijection with maximal chains in Young's poset $\binom{[n+1]}{2}$, so their number is C_{n-1}. This bijection is seen by replacing the labels ψ_{in} with $\xi_{i,n+1}$ for $i = 1, 2, \ldots, n-1$, and by adding a new top element $\xi_{n,n+1}$.

Next we consider maximal chains in $\mathrm{P}_{2,n}$ that transition from ξ to ψ on the lower outer chain. Such maximal chains contain a unique cover relation $\xi_{1j} \to \psi_{1j}$. These maximal chains correspond to maximal chains in the first case by reversing the order of the poset and switching ψ and ξ variables. Hence there are also C_{n-1} maximal chains in the second class.

There is precisely one maximal chain that is covered by both cases. This is the chain which uses the transition $\xi_{1n} \to \psi_{1n}$. This is the concatenation of the lower outer ξ-chain and the upper outer ψ-chain. This chain is counted twice, so we subtract one in our total count. We conclude that the number of maximal chains in the poset $\mathrm{P}_{2,n}$ equals $2C_{n-1} - 1$. □

Proof of Theorem 3.1.2. We now change the labels of the poset $\mathrm{P}_{2,n}$ by replacing ξ_{ij} with ψ_{ij} whenever $\{i,j\}\cap\{1,n\} = \varnothing$. Since such pairs ξ_{ij} and ψ_{ij} are incomparable, each maximal chain in $\mathrm{P}_{2,n}$ with the new labeling consists of $2n-2$ distinct variables in our coordinate ring $\mathbb{C}[\xi,\psi]$. These maximal chains are the facets in a pure simplicial complex of dimension $2n-3$ on $2n-3+\binom{n}{2}$ vertices. By Lemma 3.3.3, the number of facets is equal to $2C_{n-1}-1$.

Consider now the ideal M that is generated by the underlined monomials in Lemma 3.3.1. These squarefree quadratic monomials are precisely the incomparable pairs in $\mathrm{P}_{2,n}$ that have distinct labels after the relabeling. Hence M is the Stanley-Reisner ideal of our pure simplicial complex. The degree of M is the number of facets, which is $2C_{n-1}-1$. This is therefore the degree of $\mathcal{G}(2,n)$, which equals the CC degree of $\mathrm{Gr}(2,n)$ by Theorem 3.1.1. □

We have proved Theorem 3.1.2 by means of a Gröbner degeneration. This replaces the irreducible variety $\mathcal{G}(2,n)$ by a union of $2C_{n-1}-1$ coordinate subspaces in $\mathbb{P}^{2n-4}\times\mathbb{P}^{\binom{n}{2}-1}$. In what follows, we describe a toric degeneration that underlies our Gröbner degeneration. Recall from Section 1.1 that toric degenerations [9, 19, 31] are described algebraically by Khovanskii bases [59], which are defined at the end of Section 1.1.

We fix a monomial order on the polynomial ring $\mathbb{C}[u,v,\mathbf{t}]$ which selects the diagonal monomial $t_{1,i}t_{2,j}$ to be the leading monomial for each of the 2×2 minors of (3.5). Let $\mathcal{T}(2,n)$ denote the toric variety in $\mathbb{P}^{2n-4}\times\mathbb{P}^{\binom{n}{2}-1}$ obtained by passing to these leading monomials in (3.6). Equivalently, the toric ideal of $\mathcal{T}(2,n)$ is the kernel of ring homomorphism

$$\begin{array}{rcl} \mathbb{C}[\xi,\psi] & \to & \mathbb{C}[u,v,\mathbf{t}], \quad \xi_{1n}\mapsto u, \quad \xi_{1i}\mapsto u\cdot t_{2i}, \quad \xi_{jn}\mapsto u\cdot t_{1j}, \\ \psi_{ij} & \mapsto & v\cdot t_{1i}t_{2j}, \quad \psi_{1n}\mapsto v, \quad \psi_{1i}\mapsto v\cdot t_{2i}, \quad \psi_{jn}\mapsto v\cdot t_{1j}, \end{array} \qquad \text{for } 1<i<j<n. \quad (3.8)$$

Proposition 3.3.4. *The minors in (3.6) form a Khovanskii basis with respect to the diagonal monomial order. Hence the toric variety $\mathcal{T}(2,n)$ is a toric degeneration of the graph $\mathcal{G}(2,n)$.*

Proof. The 2×2 minors of (3.5) form a Khovanskii basis of the Grassmannian $\mathrm{Gr}(2,n)$; see Example 1.1.16. The toric degeneration is given by the Gel'fand-Tsetlin polytope $\mathrm{GT}(2,n)$. Our variety $\mathcal{T}(2,n)$ is the graph of the associated monomial parameterization.

By the same argument as in Lemma 3.3.1, the kernel of (3.8) has the following Gröbner basis

$$\begin{array}{rlll} \binom{n}{4} & \text{binomials} & \underline{\psi_{il}\psi_{jk}}-\psi_{ik}\psi_{jl} & \text{for } 1\le i<j<k<l\le n, \\ \binom{n-1}{2} & \text{binomials} & \underline{\psi_{in}\xi_{jn}}-\psi_{jn}\xi_{in} & \text{for } 1\le i<j<n, \\ (n-2)^2 & \text{binomials} & \underline{\psi_{1j}\xi_{kn}}-\psi_{kn}\xi_{1j} & \text{for } 1<j,k<n, \\ \binom{n-1}{2} & \text{binomials} & \underline{\psi_{1k}\xi_{1l}}-\psi_{1l}\xi_{1k} & \text{for } 1<k<l\le n, \\ \binom{n-2}{3} & \text{binomials} & \underline{\xi_{1l}\psi_{jk}}-\xi_{1k}\psi_{jl} & \text{for } 1<j<k<l<n, \\ \binom{n-1}{3} & \text{binomials} & \underline{\xi_{in}\psi_{jk}}-\xi_{jn}\psi_{ik} & \text{for } 1\le i<j<k<n. \end{array}$$

Each of these binomials lifts to a relation on $\mathcal{G}(2,n)$, by adding one trailing term to those in the first, fifth and sixth group. This yields the Khovanskii basis property. □

The Gel'fand-Tsetlin polytope $\mathrm{GT}(2,n)$ is the convex hull of the exponent vectors of the $\binom{n}{2}$ images of ψ_{ij} in (3.8). This is the *Newton-Okounkov body* [9] for the toric degeneration of the Grassmannian $\mathrm{Gr}(2,n)$ with respect to the diagonal monomial order. We define the *Cayley–Gel'fand–Tsetlin polytope* $\mathrm{CGT}(2,n)$ to be the Newton-Okounkov body of the toric degeneration $\mathcal{T}(2,n)$. We here identify this toric variety with the projectivization of its cone in $\mathbb{A}^{2n-3} \times \mathbb{A}^{\binom{n}{2}}$. Thus $\mathrm{CGT}(2,n)$ is the $(2n-3)$-dimensional polytope whose vertices are the exponent vectors of the $2n-3+\binom{n}{2}$ monomials in (3.8). Here is a geometric construction:

$$\mathrm{CGT}(2,n) \;=\; \mathrm{conv}\big(\mathrm{GT}(2,n)\times\{0\} \,\cup\, \Delta_{2n-4}\times\{1\}\big) \;\subseteq\; \mathbb{R}^{\binom{n}{2}} \times \mathbb{R}. \tag{3.9}$$

In words, $\mathrm{CGT}(2,n)$ is the *Cayley sum* of $\mathrm{GT}(2,n)$ with the simplex Δ_{2n-4} that is formed by the $2n-3$ coordinate points in $\mathbb{R}^{\binom{n}{2}}$ which are indexed by pairs i,j with $\{i,j\} \cap \{1,n\} \neq \varnothing$.

Corollary 3.3.5. *The polytope* $\mathrm{CGT}(2,n)$ *has normalized volume* $2C_{n-1}-1$.

Proof. We use results from [97, Chapter 8]. We saw that the binomial generators of the toric ideal of $\mathcal{T}(2,n)$ form a Gröbner basis with squarefree leading monomials. Its initial ideal defines a regular unimodular triangulation of the Cayley-Gel'fand-Tsetlin polytope $\mathrm{CGT}(2,n)$ into $2C_{n-1}-1$ simplices. These simplices are the maximal chains in the poset $\mathrm{P}_{2,n}$. □

We conclude this section with a census of small Cayley-Gel'fand-Tsetlin polytopes.

Example 3.3.6. For each polytope $\mathrm{CGT}(2,n)$ we list the f-vector and Ehrhart polynomial. For instance, $\mathrm{CGT}(2,6)$ is a 9-dimensional polytope with 24 vertices and 15 facets:

$$\begin{aligned}
n=4\text{: }& \dim = 5,\ (11,32,42,28,9),\ \tfrac{1}{5!}(t+1)(t+2)(t+3)(\mathbf{9}t^2+26t+20),\\
n=5\text{: }& \dim = 7,\ (17,77,166,200,141,57,12),\\
&\qquad \tfrac{1}{7!}(t+1)(t+2)(t+3)(t+4)(\mathbf{27}t^3+164t^2+313t+210),\\
n=6\text{: }& \dim = 9,\ (24,152,467,836,941,685,321,93,15),\\
&\qquad \tfrac{1}{9!}(t+1)(t+2)(t+3)(t+4)(t+5)(\mathbf{83}t^4+861t^3+3172t^2+4956t+3024).
\end{aligned}$$

3.4 Khovanskii Bases for the Graph

This section concerns the extension of Proposition 3.3.4 from $d=2$ to $d \geq 3$. The CC degree of $\mathrm{Gr}(d,n)$ should be the normalized volume of a polytope from a nice toric degeneration of the graph $\mathcal{G}(d,n)$. It turns out that the general case is considerably more difficult than the $d=2$ case which was treated in Section 3.3. From now on we assume $d \geq 3$. The construction that follows is related to the Cayley-Gel'fand-Tsetlin polytope via [1, Section 4.1].

There are many known toric degenerations of the Grassmannian $\mathrm{Gr}(d,n)$. Our aim is to describe one particular degeneration of $\mathrm{Gr}(d,n)$ which can be lifted to the graph $\mathcal{G}(d,n)$. This will give rise to the desired toric degeneration $\mathcal{T}(d,n)$ and its associated polytope.

We now index the coordinates ψ_σ and ξ_σ using the convention in [69, Example 2.11]. Each element in $\binom{[n]}{d}$ is represented by its unique *PBW tuple* $\sigma = (\sigma_1,\ldots,\sigma_d)$. Such tuple fulfills:

- the entries σ_i are distinct elements of $\{1, 2, \ldots, n\}$,
- $\sigma_i \leq d$ implies $\sigma_i = i$,
- and $d < \sigma_j < \sigma_k$ implies $j < k$.

We fix a monomial order on $\mathbb{C}[u, v, \mathbf{t}]$ which selects diagonal leading terms for PBW tuples:

$$\text{in}(\psi_\sigma) \;=\; t_{1\sigma_1} t_{2\sigma_2} \cdots t_{d\sigma_d}. \tag{3.10}$$

It is known from [31, 68, 69] that the $d \times d$ minors of the $d \times n$ matrix (t_{ij}) form a Khovanskii basis for the Grassmannian $\text{Gr}(d, n)$ with respect to this monomial order. Here, we can either take all dn matrix entries t_{ij} to be unknowns, or we can use the birational parameterization γ introduced in Section 3.1, where t_{ij} is a variable if $j \geq d+1$, and $t_{ij} \in \{0, 1\}$ if $j \leq d$. The resulting toric degeneration has the *Hibi-Li ideal* [52, 68] of a distributive lattice on $\binom{[n]}{d}$ which is known as the *PBW poset*. The PBW poset for $d = 3$ and $n = 6$ is shown in Figure 3.2.

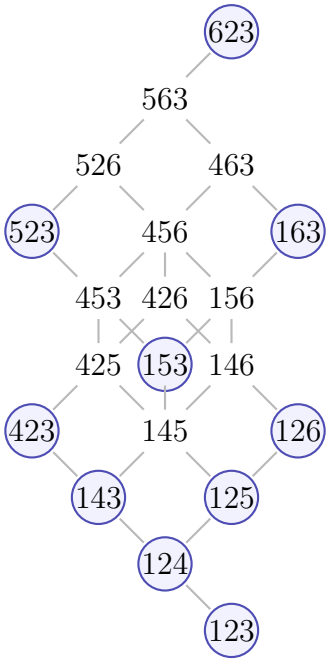

Figure 3.2: The PBW poset for $d = 3, n = 6$. The 20 PBW tuples σ index the coordinates ψ_σ. The 10 PBW tuples that also index coordinates ξ_σ are marked in blue. The incomparable pairs in the poset generate our initial monomial ideal of $\text{Gr}(3, 6)$.

The Hibi-Li ideal describes the PBW degeneration of $\text{Gr}(d, n)$. In representation theory (cf. [1, 31]), this is known as the *Feigin–Fourier–Littelmann–Vinberg (FFLV) degeneration*, and we write $\text{FFLV}(d, n)$ for the associated polytope of dimension $d(n-d)$ with $\binom{n}{d}$ vertices. Thus, $\text{FFLV}(d, n)$ is the convex hull of the exponent vectors of the $\binom{n}{d}$ monomials in (3.10).

Analogous to (3.9), we now define the *Cayley–Feigin–Fourier–Littelmann–Vinberg polytope* $\mathrm{CFFLV}(d,n)$. This is a polytope of dimension $d(n-d)+1$ with $\binom{n}{d}+d(n-d)+1$ vertices. Geometrically, we construct $\mathrm{CFFLV}(d,n)$ as the Cayley sum in $\mathbb{R}^{\binom{n}{d}} \times \mathbb{R}$ of the polytope $\mathrm{FFLV}(d,n)$ with the simplex $\Delta_{d(n-d)}$ that is formed by the $d(n-d)+1$ coordinate points which are indexed by PBW tuples σ with at most one entry σ_j larger than d. It is established by [39] that $\mathrm{CFFLV}(d,n)$ represents a toric degeneration $\mathcal{T}(d,n)$ of the projectivization of the affine cone in $\mathbb{A}^{d(n-d)+1} \times \mathbb{A}^{\binom{n}{d}}$ over the graph $\mathcal{G}(d,n)$. Thus $\mathcal{T}(d,n)$ is a toric variety in $\mathbb{P}^{d(n-d)+\binom{n}{d}}$, and its degree equals the CC degree of $\mathrm{Gr}(d,n)$. Furthermore, the polytope $\mathrm{CFFLV}(d,n)$ has a regular unimodular triangulation. The number of simplices is the CC degree of $\mathrm{Gr}(d,n)$. Such a triangulation can be described using a squarefree Gröbner basis, which is the content of Conjecture 3.4.2 part (2). We illustrate all concepts and results for $d=3, n=6$ with a computation in `Macaulay2` [46].

Example 3.4.1 ($d=3, n=6$)**.** The code uses `p` and `q` for the Greek letters ψ and ξ:

```
R = QQ[v,u,t14,t15,t16,t24,t25,t26,t34,t35,t36,
       p623,q623,p563,p463,p526,p163,q163,p456,p523,q523,
       p156,p426,p453,p146,p153,q153,p425,p126,q126,p145,
       p423,q423,p125,q125,p143,q143,p124,q124,p123,q123, MonomialOrder=>Eliminate 11];
I = ideal(p123-v, q123-u,
          p145-v*(t24*t35-t25*t34), p146-v*(t24*t36-t26*t34), p156-v*(t25*t36-t26*t35),
          p425-v*(t14*t35-t15*t34), p426-v*(t14*t36-t16*t34), p453-v*(t14*t25-t15*t24),
          p463-v*(t14*t26-t16*t24), p526-v*(t15*t36-t16*t35), p563-v*(t15*t26-t16*t25),
          p456-v*(t14*t25*t36-t14*t26*t35-t15*t24*t36+t15*t26*t34+t16*t24*t35-t16*t25*t34),
          p124-v*t34, p125-v*t35, p126-v*t36, p143-v*t24, p153-v*t25, p163-v*t26,
          p423-v*t14, p523-v*t15, p623-v*t16, q124-u*t34, q125-u*t35, q126-u*t36,
          q143-u*t24, q153-u*t25, q163-u*t26, q423-u*t14, q523-u*t15, q623-u*t16);
G = ideal selectInSubring(1,gens gb I); toString mingens G
codim G, degree G, betti mingens G
M = ideal leadTerm ideal selectInSubring(1,gens gb I);
codim M, degree M, betti mingens M
```

The output `G` is the homogeneous prime ideal of $\mathcal{G}(3,6)$. It is minimally generated by 106 quadrics. The command `degree G` shows that $\mathcal{G}(3,6)$ has degree 250. This coincides with the CC degree of $\mathrm{Gr}(3,6)$, by Example 2.3.6. The output `M` is the initial ideal for the reverse lexicographic monomial order given by a linear extension of the PBW poset in Figure 3.2.

We compute the toric degeneration $\mathcal{T}(3,6)$ with the same code after replacing each parenthesized minor by its leading monomial, e.g. replace `(t24*t35-t25*t34)` by `t24*t35`. The output is a toric ideal of degree 250, minimally generated by 106 quadrics and one cubic. The Khovanskii basis property holds because each of these binomials lifts to polynomial in `G`. This toric ideal represents the 10-dimensional polytope $\mathrm{CFFLV}(3,6)$. Its f-vector equals

$$f_{\mathrm{CFFLV}(3,6)} \;=\; (30, 236, 901, 2017, 2873, 2695, 1672, 670, 163, 21).$$

The command `hilbertPolynomial G` computes the Ehrhart polynomial of this polytope. The graph $\mathcal{G}(3,6)$ and its toric degeneration $\mathcal{T}(3,6)$ have the same initial monomial ideal, here

denoted by `M`. This is generated by 132 squarefree polynomials: 106 quadrics, 21 cubics, and 5 quartics. We view `M` as the Stanley-Reisner ideal of a pure simplicial complex of dimension 10 with 250 maximal simplices. This is our unimodular triangulation of CFFLV$(3, 6)$.

We conjecture the following result, which should hold for arbitrary d and n.

Conjecture 3.4.2. We fix the monomial orders on $\mathbb{C}[\xi, \psi]$ and $\mathbb{C}[u, v, \mathbf{t}]$ described above.

1. The FFLV Khovanskii basis of the Grassmannian $\mathrm{Gr}(d, n)$ lifts to the graph $\mathcal{G}(d, n)$.
2. The ideals of $\mathcal{G}(d, n)$ and $\mathcal{T}(d, n)$ have squarefree Gröbner bases.
3. The normalized volume of the Cayley–Feigin–Fourier–Littelmann–Vinberg polytope CFFLV(d, n) is equal to the coupled cluster degree of the Grassmannian $\mathrm{Gr}(d, n)$.

A result of Evgeny Feigin [39] constructs, for all d and n, a toric degeneration of the graph $\mathcal{G}(d, n)$. Although Feigin's result rests on a different method and does not prove Conjecture 3.4.2 in full, it does prove part (1): the FFLV Khovanskii basis of $\mathrm{Gr}(d, n)$ lifts to $\mathcal{G}(d, n)$. Consequently, part (3) also follows, namely that the CC degree of $\mathrm{Gr}(d, n)$ is equal to the normalized volume of CFFLV(d, n). Thus, in order to prove Conjecture 3.4.2 in full, it remains to establish part (2), namely the existence of squarefree initial ideals. We conclude this chapter with a remark on our computational proofs of the full Conjecture 3.4.2 for the cases $(d, n) = (3, 6), (3, 7), (3, 8), (3, 9), (4, 8)$.

Remark 3.4.3. Our computation in Example 3.4.1 serves as a proof for Conjecture 3.4.2 in the case $(d, n) = (3, 6)$. The same computation in `Macaulay2` terminated successfully for $(d, n) = (3, 7), (3, 8), (3, 9), (4, 8)$. We therefore have a complete computational proof of Conjecture 3.4.2 in these special cases. For the cases $(d, n) = (3, 10)$, $(4, 9)$, we computed the degree of $\mathcal{T}(d, n)$ in `Macaulay2`, so the correctness of the final number assumes the validity of Conjecture 3.4.2 (1) and (3). The CC degrees for $(3, 9), (3, 10), (4, 9)$ were reported in Example 3.1.4.

Khovanskii bases have emerged as an important tool in the recent literature on polynomial system solving [5] and its applications in the physical sciences [6]. Theorems 3.1.1 and 3.1.2 and Conjecture 3.4.2 lay the foundation for a new class of custom-tailored homotopies for numerically solving the CC equations. The extension from CCS and the Grassmannian to other CC approximations and truncation varieties is explored in the next chapter.

In conclusion, we showed that the CC degree of the Grassmannian equals the total degree of its graph. This allowed us to derive an explicit formula for the CC degree for $\mathrm{Gr}(2, n)$. More generally, we were able to associate the CC degree of $\mathrm{Gr}(d, n)$ with the volume of a polytope. In the next chapter we will generalize some of the results obtained here to all truncation varieties. In particular, we will provide a parameterization of V_σ in terms of Laplace polynomials. This not only offers a more algebraic description of the truncation varieties, but also enables us to equate their CC degree with the total degree of a graph.

Chapter 4

Laplace Parameterization of Quantum States

In this chapter we develop truncation varieties as generalizations of the Grassmannian. We introduce Laplace polynomials, a family of polynomials in a ring whose variables correspond to symbolic minors of a matrix. Using these polynomials, we reformulate the exponential parameterization of truncation varieties, see Corollary 4.2.5. Our main results extend the results of Chapter 3, which concerns the Grassmannian, to truncation varieties in general. In Theorem 4.3.8 we construct a new graph parameterization of truncation varieties, using Möbius inversion. In Corollary 4.3.10 we show that the CC degree of a truncation variety coincides with the total degree of the graph of this parameterization. We conclude the chapter by focusing on the chemically relevant CCSD truncation variety.

4.1 Expanding Determinants

Let $\Omega = (\omega_{i,j})$ be an $m \times m$ matrix with entries $\omega_{i,j}$, where $1 \leq i, j \leq m$. We denote by $\omega_{I,J}$ the minor of Ω determined by the rows indexed by I and the columns indexed by J. The determinant of Ω can be found recursively using Laplace expansion. Explicitly, the Laplace expansion along row i gives the following formula for the determinant:

$$\det(\Omega) = \sum_{j=1}^{m} (-1)^{i+j} \omega_{i,j} \omega_{[m]\setminus i,[m]\setminus j}. \tag{4.1}$$

We can obtain a formula for the determinant of Ω purely in terms of its entries, by recursively employing the Laplace expansion on the minors in (4.1). This reveals the following familiar formula for the determinant:

$$\det(\Omega) = \sum_{\rho \in S_m} \operatorname{sign}(\rho) \omega_{1,\rho(1)} \cdots \omega_{m,\rho(m)}. \tag{4.2}$$

Here we sum over all permutations of $[m]$. We call this the Laplace expansion in terms of 1×1 minors, or the 1st order Laplace expansion.

Similarly, for all divisors k of m we can define the kth order Laplace expansion of Ω as an expression of $\det(\Omega)$ in terms of $k \times k$ minors. This is done by generalizing the Laplace expansion and expanding $\det(\Omega)$ along the k rows $I \in \binom{[m]}{k}$. We obtain a cofactor expansion:

$$\det(\Omega) = \sum_{J \in \binom{[m]}{k}} \operatorname{sign}(I)\operatorname{sign}(J)\omega_{I,J}\omega_{[m]\setminus I,[m]\setminus J}. \tag{4.3}$$

Here $\operatorname{sign}(I)$ is the sign of the permutation $[m] \mapsto (I, [m]\setminus I)$. Hence $\operatorname{sign}(I) = (-1)^{\sum_{i\in I} i - \binom{|I|+1}{2}}$ and the sign of the Jth term in (4.3) becomes $(-1)^{\sum_{i\in I} i + \sum_{j\in J} j}$. We can obtain a formula for $\det(\Omega)$ in terms of $k \times k$ minors by recursively applying (4.3) to the non-$k \times k$ minors in the expansion. To write the explicit formula in terms of $k \times k$ minors we have to introduce some combinatorial objects. A *set composition* β of $[m]$ is an ordered tuple $(\beta_1, \ldots, \beta_\ell)$ of disjoint subsets $\beta_i \subseteq [m]$, such that $\sqcup_i \beta_i = [m]$. We say β is k-uniform if all β_i have size k, that is $|\beta_i| = k$ for all i. Notice that a 1-uniform set composition is a permutation. If $m = \ell k$, we denote the set of all k-uniform set compositions of $[m]$ by $\Pi_m^{\mathrm{ord}}(k^\ell)$. By always expanding along the first k rows we obtain an explicit formula in terms of $k \times k$ minors:

$$\det(\Omega) = \sum_{\beta \in \Pi_m^{\mathrm{ord}}(k^\ell)} \operatorname{sign}(\beta)\omega_{[k],\beta_1}\omega_{[2k]\setminus[k],\beta_2}\cdots\omega_{[m]\setminus[m-k],\beta_\ell}. \tag{4.4}$$

Here $\operatorname{sign}(\beta)$ is the sign of the permutation $[m] \mapsto (\beta_1, \ldots, \beta_\ell)$. We call this a kth order Laplace expansion of $\det(\Omega)$. Unlike the 1st order Laplace expansion, it is not a unique expansion of $\det(\Omega)$ in terms of $k \times k$ minors. For any k-uniform set composition α we get a $k \times k$ expansion by recursively expanding along rows α_i. In that case we obtain the formula:

$$\det(\Omega) = \sum_{\beta \in \Pi_m^{\mathrm{ord}}(k^\ell)} \operatorname{sign}(\alpha)\operatorname{sign}(\beta)\omega_{\alpha_1,\beta_1}\cdots\omega_{\alpha_\ell,\beta_\ell}. \tag{4.5}$$

We observe that the formula is invariant under permuting the minors within each term. Hence the order of the tuple $\alpha = (\alpha_1, \ldots, \alpha_\ell)$ is irrelevant, and we may fix the following order: for $i \leq j$ the smallest element of α_i is less than the smallest element of α_j. Therefore α is a k-uniform set partition, and we obtain a unique kth order Laplace expansion for each k-uniform set partition of $[m]$. Let $\overline{[m]}$ be the set $\{\overline{1}, \ldots, \overline{m}\}$ with marked entries. The set partition $\pi = \{\alpha_1 \cup \overline{\beta_1}, \ldots, \alpha_\ell \cup \overline{\beta_\ell}\}$, of $[m] \cup \overline{[m]}$, where $\overline{\beta}_i$ is the set β_i whose elements are marked with $\bar{\cdot}$, is a uniform block permutation, see [79] and Theorem 2.1.5. The sign of the terms in (4.5) is the sign of π, defined in Theorem 2.1.5.

Consider the polynomial ring $\mathbb{C}[\omega] = \mathbb{C}[\omega_{I,J} : I, J \subseteq [m], |I| = |J|]$, whose variables formally represent the minors of a symbolic $m \times m$ matrix $\Omega = (\omega_{i,j})$. We also include the empty minor, determined by $I = J = \varnothing$, and denoted $\omega_{0,0}$. It serves as a homogenizing variable. For a k-uniform set partition α of $[m]$, we define the *kth-order Laplace polynomial* $\mathcal{L}_\alpha(\omega)$ to be the element of $\mathbb{C}[\omega]$ given by the right-hand side of (4.5). In particular, $\mathcal{L}_\alpha(\omega)$ is defined as that formal expression, and is *not* identified with the determinant itself.

Example 4.1.1 (2nd order Laplace expansions)**.** We consider the 4×4 matrix Ω of the form

$$\Omega = \begin{bmatrix} \omega_{1,5} & \omega_{1,6} & \omega_{1,7} & \omega_{1,8} \\ \omega_{2,5} & \omega_{2,6} & \omega_{2,7} & \omega_{2,8} \\ \omega_{3,5} & \omega_{3,6} & \omega_{3,7} & \omega_{3,8} \\ \omega_{4,5} & \omega_{4,6} & \omega_{4,7} & \omega_{4,8} \end{bmatrix}.$$

There are three 2-uniform set partitions of $\{1, 2, 3, 4\}$, namely the following three

$$12|34, \quad 13|24, \quad 14|23. \tag{4.6}$$

There are also six 2-uniform set compositions, found by permuting the blocks in (4.6). The three set partitions correspond to the following three Laplace polynomials in $\mathbb{C}[\omega]$:

$$\begin{aligned}
\mathcal{L}_{12|34}(\omega) &= \omega_{12,56}\omega_{34,78} - \omega_{12,57}\omega_{34,68} + \omega_{12,67}\omega_{34,58} + \omega_{12,58}\omega_{34,67} - \omega_{12,68}\omega_{34,57} + \omega_{12,78}\omega_{34,56}, \\
\mathcal{L}_{13|24}(\omega) &= -\omega_{13,56}\omega_{24,78} + \omega_{13,57}\omega_{24,68} - \omega_{13,67}\omega_{24,58} - \omega_{13,58}\omega_{24,67} + \omega_{13,68}\omega_{24,57} - \omega_{13,78}\omega_{24,56}, \\
\mathcal{L}_{14|23}(\omega) &= \omega_{14,56}\omega_{23,78} - \omega_{14,57}\omega_{23,68} + \omega_{14,67}\omega_{23,58} + \omega_{14,58}\omega_{23,67} - \omega_{14,68}\omega_{23,57} + \omega_{14,78}\omega_{23,56}.
\end{aligned}$$

Each polynomial has six terms. The sum of the three Laplace polynomials therefore has eighteen terms. This sum can be written as a linear combination of monomials indexed by uniform block permutations of shape 2^2. That is,

$$\mathcal{L}_{12|34}(\omega) + \mathcal{L}_{13|24}(\omega) + \mathcal{L}_{14|23}(\omega) = \sum_{\pi \in \mathcal{U}_4(2^2)} \operatorname{sign}(\pi)\omega_{\alpha_1,\beta_1} \cdots \omega_{\alpha_\ell,\beta_\ell}.$$

By identifying the variable $\omega_{I,J}$ with cluster amplitude $t_{I,J}$ we can see that this sum coincides with the truncated master polynomial $\psi_{5678}(t_\sigma)$ for $\sigma = \{2\}$, defined in [33, Section 2.1].

Remark 4.1.2. The Grassmannian $\operatorname{Gr}(m, 2m)$ admits a birational parameterization given by the minors of an $m \times m$ matrix Ω (including the 1×1 minors, i.e., the entries of Ω). In the polynomial ring $\mathbb{C}[\omega]$, its defining ideal $\mathcal{I}(\operatorname{Gr}(m, 2m))$ is precisely the ideal of all polynomial relations among the minors of Ω. It is generated by the Plücker relations. These are quadratic relations among the minors, see Example 1.1.12. The polynomial

$$\omega_{0,0}\,\omega_{12,34} - \omega_{1,3}\,\omega_{2,4} + \omega_{1,4}\,\omega_{2,3}$$

is one such example. Therefore, for a point $\omega \in \operatorname{Gr}(m, 2m)$, all Laplace polynomials evaluate to the same value, namely $\det(\Omega)$. Hence, intersecting any variety defined solely by Laplace polynomials with $\operatorname{Gr}(m, 2m)$ yields the variety defined by $\operatorname{Gr}(m, 2m) \cap V(\det(\Omega))$.

We want to generalize the results of Example 4.1.1, that is describe truncated master polynomials in terms of generalized Laplace polynomials. To do so, we generalize the kth Laplace expansion of $\det(\Omega)$ from k-uniform set partitions to any set partition $\alpha \vdash [m]$. For a set partition α of shape λ we obtain a λ-Laplace expansion of the determinant:

$$\det(\Omega) = \sum_{\beta \in \Pi_m^{\mathrm{ord}}(\lambda)} \operatorname{sign}(\pi)\omega_{\alpha_1,\beta_1} \cdots \omega_{\alpha_\ell,\beta_\ell}. \tag{4.7}$$

Here ℓ is the length of λ and π is the corresponding uniform block permutation

$$\pi = \{\alpha_1 \cup \overline{\beta}_1, \ldots, \alpha_\ell \cup \overline{\beta}_\ell\}.$$

Notice that (4.5) is a special case of (4.7), obtained by setting $\lambda = k^\ell$. The right-hand side of (4.7) is also a polynomial in the polynomial ring $\mathbb{C}[\omega]$. We call it the α-Laplace polynomial and denote it by $\mathcal{L}_\alpha(\omega)$. We can extend the definition of Laplace polynomials to submatrices of Ω. Let $I, J \subseteq [m]$ be index sets with $|I| = |J|$, and let $\Omega_{I,J}$ denote the submatrix of Ω indexed by these sets. For a set partition α of the row set I, we define the *α-Laplace polynomial* $\mathcal{L}_{\alpha,J}(\omega) \in \mathbb{C}[\omega]$ of $\Omega_{I,J}$ as the α-Laplace expansion of the determinant $\det(\Omega_{I,J})$.

Consider the partition lattice Π_m of set partitions of $[m]$, ordered by refinement: $\alpha \leq \beta$ if every block of α is contained in a block of β. When considering set partitions of an arbitrary set I with $|I| = m$, we write $\Pi(I) \cong \Pi_m$. This lattice structure induces a partial order on the Laplace polynomials and reveals a rich combinatorial structure. We illustrate the refinement relations between Laplace polynomials in the following example.

Example 4.1.3. Consider a 3×3 matrix Ω and the set partition refinement $1|2|3 \leq 1|23$. The Laplace polynomial corresponding to the set partition $1|23$ of $\{1, 2, 3\}$ is

$$\mathcal{L}_{1|23}(\omega) = \omega_{1,1}\omega_{23,23} - \omega_{1,2}\omega_{23,13} + \omega_{1,3}\omega_{23,12}.$$

We want to obtain the Laplace polynomial $\mathcal{L}_{1|2|3}(\omega)$ from $\mathcal{L}_{1|23}(\omega)$ by "refining" the variables ω. Precisely, we substitute the variables $\omega_{23,23}$, $\omega_{23,13}$ and $\omega_{23,12}$, which correspond to formal minors, with their corresponding $2|3$-Laplace polynomials. That is, these level 2 variables are replaced by the following 1st order Laplace polynomials:

$$\begin{aligned}
\omega_{23,12} &\mapsto \mathcal{L}_{2|3,12}(\omega) = \omega_{2,1}\omega_{3,2} - \omega_{2,2}\omega_{3,1}, \\
\omega_{23,13} &\mapsto \mathcal{L}_{2|3,13}(\omega) = \omega_{2,1}\omega_{3,3} - \omega_{2,3}\omega_{3,1}, \\
\omega_{23,23} &\mapsto \mathcal{L}_{2|3,23}(\omega) = \omega_{2,2}\omega_{3,3} - \omega_{2,3}\omega_{3,2}.
\end{aligned}$$

Substituting these expressions into $\mathcal{L}_{1|23}(\omega)$ yields the $1|2|3$-Laplace polynomial:

$$\begin{aligned}
\mathcal{L}_{1|2|3}(\omega) &= \omega_{1,1}(\omega_{2,2}\omega_{3,3} - \omega_{2,3}\omega_{3,2}) - \omega_{1,2}(\omega_{2,1}\omega_{3,3} - \omega_{2,3}\omega_{3,1}) + \omega_{1,3}(\omega_{2,1}\omega_{3,2} - \omega_{2,2}\omega_{3,1}) \\
&= \omega_{1,1}\omega_{2,2}\omega_{3,3} - \omega_{1,1}\omega_{2,3}\omega_{3,2} - \omega_{1,2}\omega_{2,1}\omega_{3,3} + \omega_{1,2}\omega_{2,3}\omega_{3,1} + \omega_{1,3}\omega_{2,1}\omega_{3,2} - \omega_{1,3}\omega_{2,2}\omega_{3,1}.
\end{aligned}$$

Hence, refinement in the lattice of Laplace polynomials of the matrix Ω corresponds to expanding some of the variables $\omega_{I,J}$ as minors and replacing them by Laplace polynomials of the corresponding (I, J)-minors of Ω.

We conclude this section with a lemma that formalizes these properties.

Lemma 4.1.4. *Let α be a set partition of $[m]$.*

1. *Let β be a set partition such that $\alpha \leq \beta$ in Π_m. Then*

$$\mathcal{L}_\alpha(\omega) = \mathcal{L}_\beta\big((\mathcal{L}_{\alpha|_I,J}(\omega))_{I,J}\big).$$

Here $\alpha|_I = (\alpha_1 \cap I, \ldots, \alpha_k \cap I)$ denotes the restriction of α to $I \subseteq [m]$, which is a set partition of I. We recall that $\mathcal{L}_\beta$ is a polynomial in variables indexed by pairs (I, J) with $I, J \subseteq [m]$ and $|I| = |J|$.

2. *We take disjoint sets α', α'' such that $\alpha = \alpha' \sqcup \alpha''$. Hence α' and α'' are set partitions of some subsets I and $[m]\backslash I$ of $[m]$. We get*

$$\mathcal{L}_\alpha(\omega) = \sum_{J \in \binom{[m]}{|I|}} \mathrm{sign}(I)\mathrm{sign}(J)\mathcal{L}_{\alpha',J}(\omega)\mathcal{L}_{\alpha'',[m]\backslash J}(\omega).$$

Observe that part (2) of Lemma 4.1.4 is a special case of part (1), obtained by taking set partition $\beta = I \,|\, [m]\backslash I$. The statements of this lemma follow directly from the construction of the Laplace polynomials, and we let Example 4.1.3 serve as a proof.

4.2 Generalizing the Grassmannian

We now transition from a general square matrix Ω to the $d \times (n-d)$ matrix $T = [t_{i,j}]$, whose entries $t_{i,b}$ are the single (level 1) truncated cluster amplitudes in $\mathcal{V}_{\{1\}}$. The rows of T are therefore indexed by $[d]$ and its columns by $[n]\backslash[d]$. The coordinates of the full cluster amplitudes space $\mathcal{V}_d$ represent formal minors of T. More precisely, the cluster amplitude $t_{I,B}$ corresponds formally to the minor of T determined by rows I and columns B. The truncated subspace $\mathcal{V}_\sigma$ consists of those coordinates $t_{I,B}$ for which $|I| \in \sigma \subseteq [d]$.

Accordingly, we consider the polynomial ring $\mathbb{C}[t] = \mathbb{C}[t_{I,B} : I \subseteq [d], B \subseteq [n]\backslash[d], |I| = |B|]$ which is the ring of polynomial functions on $\mathcal{V}_d$. Of special interest is the $d \times n$ matrix

$$[\, I_d \; T \,] = \begin{bmatrix} 1 & 0 & \cdots & 0 & t_{1,d+1} & \cdots & t_{1,n} \\ 0 & 1 & \cdots & 0 & t_{2,d+1} & \cdots & t_{2,n} \\ \vdots & \vdots & \ddots & \vdots & \vdots & \ddots & \vdots \\ 0 & 0 & \cdots & 1 & t_{d,d+1} & \cdots & t_{d,n} \end{bmatrix}. \tag{4.8}$$

This matrix appears in the parameterization of the CCS truncation variety, namely the Grassmannian $\mathrm{Gr}(d, n)$; see Example 4.2.1. The maximal minors of (4.8) are in one-to-one correspondence with the minors of T. More precisely, the maximal minor indexed by a subset $J \subseteq [n]$ equals $(-1)^\tau t_{[d]\backslash J,\, J\backslash[d]}$, where τ denotes the parity of the permutation that sends $[d]$ to $(J, [d] \setminus J)$. Consequently, we assume the λ-Laplace expansion of the maximal minor indexed by J to be the λ-Laplace expansion of the minor $t_{[d]\backslash J, J\backslash[d]}$, up to the sign $(-1)^\tau$.

We recall that the truncation variety V_σ, corresponding to level set $\sigma \subsetneq [d]$, is birationally parameterized by the truncated *exponential map* in (2.6). This is the map

$$\mathcal{V}_\sigma \to \mathcal{H}_d, \quad t_\sigma \mapsto \psi = \exp T(t_\sigma) e_{[d]}. \tag{4.9}$$

Here t_σ denotes the projection of the cluster amplitude $t \in \mathcal{V}_d$ onto $\mathcal{V}_\sigma$.

Example 4.2.1 ($\sigma = \{1\}$)**.** We recall from Theorem 2.2.5 that this parameterization of $V_{\{1\}}$ coincides with the birational Plücker embedding of the Grassmannian described in Remark 1.1.9. In particular, after projectivizing $\mathcal{H}_d$, the map (4.9) induces

$$\mathbb{C}^{d\times(n-d)} \to \mathbb{P}^{\binom{n}{d}-1}, \qquad T = [t_{i,b}] \mapsto \text{all maximal minors of } [\, I_d \; T \,].$$

We note that $\mathbb{P}\mathcal{H}_d \cong \mathbb{P}^{\binom{n}{d}-1}$. The truncated subspace $\mathcal{V}_\sigma$ is generated by the entries of T, and hence $\mathcal{V}_\sigma \cong \mathbb{C}^{d\times(n-d)}$. We may also view the entries $t_{i,b}$ of T as the 1×1 minors of T. The maximal minors of $[\, I_d \; T \,]$ are then obtained via 1st order Laplace expansions.

Example 4.2.2 ($d = 4$, $n = 8$, $\sigma = \{2\}$)**.** We continue Example 4.1.1. The truncation variety $V_{\{2\}}$ is parameterized by 2nd order Laplace polynomials. Explicitly, the truncated exponential parameterization of $V_{\{2\}}$, shown in (4.9), can be written as:

$$\mathbb{C}^{\binom{4}{2}\binom{4}{2}} \longrightarrow \mathbb{C}^{\binom{8}{4}}, \quad \psi_J = \begin{cases} 1 & J = \{1,2,3,4\}, \\ 0 & |J \cap [4]| = 1 \text{ or } 3, \\ (-1)^\tau t_{[4]\setminus J,\, J\setminus[4]} & |J \cap [4]| = 2, \\ \mathcal{L}_{12|34}(t) + \mathcal{L}_{13|24}(t) + \mathcal{L}_{14|23}(t) & J = \{5,6,7,8\}. \end{cases} \tag{4.10}$$

Notice that if J has excitation level 1 or 3, then the contribution from T to the Jth minor of $[\, I_4 \; T \,]$ has size 1 or 3, and therefore admits no 2nd order Laplace expansions. If J has excitation level 2, there is exactly one 2nd order Laplace expansion, namely the signed variable $(-1)^\tau t_{[4]\setminus J,\, J\setminus[4]}$. Hence the map sends ψ_J to the sum of all 2nd order Laplace expansions of the corresponding minor of $[\, I_4 \; T \,]$. Since all nonzero coordinates except the first and the last are variables, the truncated exponential parameterization can be viewed as the graph of the map

$$\mathbb{C}^{36} \to \mathbb{C}^2, \quad \psi_{1234} = 1, \; \psi_{5678} = \mathcal{L}_{12|34}(t) + \mathcal{L}_{13|24}(t) + \mathcal{L}_{14|23}(t). \tag{4.11}$$

that maps the truncated variables t_σ to the sum of the three 2nd order Laplace polynomials.

We present a general result writing the exponential map in terms of Laplace polynomials.

Theorem 4.2.3. *The exponential parameterization can be written in the following way:*

$$\mathcal{V}_d \to \mathcal{H}_d, \quad \psi_J = (-1)^\tau \sum_{\alpha \in \Pi([d]\setminus J)} \mathcal{L}_{\alpha, J\setminus[d]}(t). \tag{4.12}$$

Here τ denotes the parity of $[d] \mapsto (J, [d]\setminus J)$. Hence, under this bijection, the Jth coordinate ψ_J is the sum of all Laplace expansions of the Jth minor of $[\, I_d \; T \,]$.

Proof. Let J be a subset of $[n]$ of size d. Recall that a set partition α of $[d]\setminus J$ and an ordered set partition β of $J\setminus[d]$ of the same shape determine a uniform block permutation $\pi = \{\alpha_1 \cup \beta_1, \ldots, \alpha_\ell \cup \beta_\ell\}$ of J. Hence the sum in (4.12) is the signed linear combination of monomials indexed by uniform block permutations. Thus, by Theorem 2.1.5, the map defined in (4.12) matches the exponential map, proving the statement. □

We use this result to write parameterizations of truncation varieties V_σ in terms of Laplace polynomials. We therefore describe the truncation varieties explicitly as generalizations of the Grassmannian, which is parameterized by 1st order Laplace polynomials. To that end, we define the subposet Π_d^σ of the partition lattice Π_d as the poset of set partitions of $[d]$ with blocks whose sizes are in σ. Note that Π_d^σ is usually not a lattice. These posets of set partitions with restricted block sizes have appeared in the literature. See, for example, [15, 27, 66], where their Möbius functions are studied. When we consider set partitions of a subset $I \subseteq [d]$ of size $|I| = m$ we use the notation $\Pi(I)^\sigma \cong \Pi_m^\sigma$.

Example 4.2.4. Let $d = 4$. We consider the partition lattice Π_4.

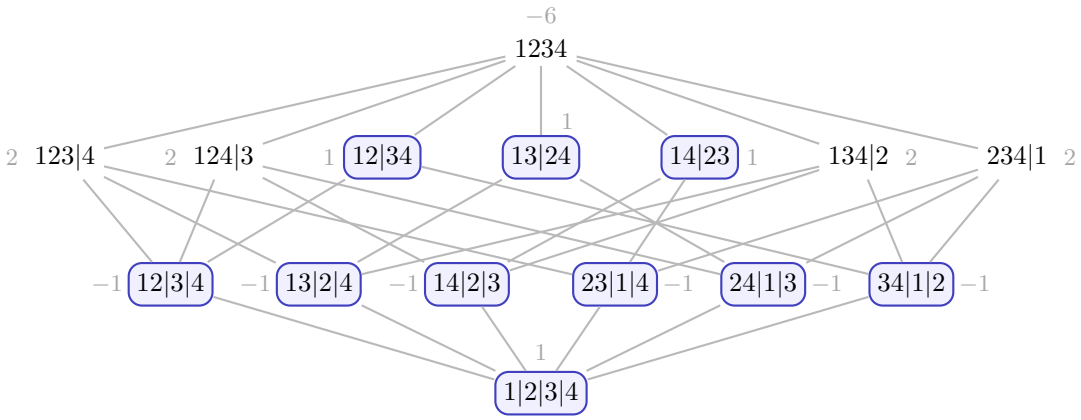

Figure 4.1: The partition lattice Π_4 and its subposet $\Pi_4^{\leq 2}$ whose entries are marked in blue. The number displayed next to each partition α is the Möbius value $\mu(\hat{0}, \alpha)$.

This lattice has a maximum element $\hat{1} = 1234$ and a minimum element $\hat{0} = 1|2|3|4$. The blue circled entries form the subposet $\Pi_4^\sigma \cong \Pi_4^{\leq 2}$ where $\sigma = \{1, 2\}$. We notice that this subposet does not have a unique maximum element and is therefore not a lattice.

Notice that the principal order ideals generated by elements of $\Pi_4^{\leq 2}$ are the same in $\Pi_4^{\leq 2}$ as in the full partition lattice Π_4. Consequently, the Möbius function on $\Pi_4^{\leq 2}$ agrees with the restriction of the Möbius function on Π_4. This is not true for general σ.

Corollary 4.2.5. *The truncated exponential parameterization of the truncation variety V_σ from (4.9) can be written as*

$$\mathcal{V}_\sigma \to \mathcal{H}_d, \quad \psi_J = (-1)^\tau \sum_{\alpha \in \Pi([d]\backslash J)^\sigma} \mathcal{L}_{\alpha, J\backslash[d]}(t). \tag{4.13}$$

Here τ denotes the parity of $[d] \mapsto (J, [d]\backslash J)$.

Usually, the level set σ has one of two forms. Either σ is a singleton $\{k\}$, which yields the kth-order Laplacians. Alternatively, σ is an interval $[\ell]$. In this case, the poset $\Pi([d]\backslash J)^\sigma$ restricts to set partitions whose blocks have size at most ℓ. This poset is denoted by $\Pi([d]\backslash J)^{\leq \ell}$.

4.3 Graphs of Laplace Polynomials

In this section, we relate the CC degree of a truncation variety to a more classical algebraic invariant. Specifically, to the total degree of a graph, as in the case of the Grassmannian in Chapter 3. We begin by stating a generalization of Theorem 3.1.1. To do so, we first introduce some terminology. Let $f : \mathbb{C}^m \to \mathbb{C}^s$ be a polynomial map. We define its *graph map* by

$$\mathbb{C}^m \to \mathbb{C}^{m+s}, \qquad x \mapsto (x, f(x)).$$

Similarly, for a rational map $g : \mathbb{P}^m \dashrightarrow \mathbb{P}^{s-1}$, we define its *graph map* as

$$\mathbb{P}^m \dashrightarrow \mathbb{P}^m \times \mathbb{P}^{s-1}, \qquad x \mapsto (x, g(x)). \tag{4.14}$$

The truncated exponential parameterization of $V_{\{2\}}$, defined in (4.10), provides an example of a graph map. More precisely, it is the graph map of the map (4.11).

The *graph* of a rational map $g\colon \mathbb{P}^m \dashrightarrow \mathbb{P}^{s-1}$, denoted Γ_g, is defined as the closure of the image of the graph map (4.14) of g. It is a variety in the product space $\mathbb{P}^m \times \mathbb{P}^{s-1}$, and it has the same dimension as the variety parameterized by g. The graph of the Grassmannian $\mathcal{G}(d, n)$ in Section 3.1 is a special case of a variety that is a graph. The bidegrees and the total degree of Γ_g are therefore defined in the same way as in Section 3.1.

Remark 4.3.1. The truncation varieties admit birational parameterizations of the form

$$\phi : \mathbb{C}^N \to \mathbb{C}^{\binom{n}{d}}, \quad x \mapsto (1, f(x)), \quad \text{where} \quad f\colon \mathbb{C}^N \to \mathbb{C}^{\binom{n}{d}-1} \text{ is polynomial.}$$

Here $N = \dim(\mathcal{V}_\sigma) = \sum_{k\in\sigma} \binom{d}{k}\binom{n-d}{k}$. We call the map ϕ the *affine representative* of f. See Remark 1.1.8 for a detailed explanation of varieties of this form.

Take a level set $\sigma \subseteq [d]$, and let $\mathcal{H}_\sigma$ denote the image of the projection of $\mathcal{H}_d$ defined by the map $\psi \mapsto \psi_\sigma$. Concretely, the elements of $\mathcal{H}_\sigma$ are vectors ψ_σ consisting of the coordinates ψ_J for which the excitation level $|J \setminus [d]|$ lies in σ. We denote the complementary set of excitation levels by $\sigma^c = [d] \setminus \sigma$. This yields the natural decomposition

$$\mathcal{H}_d \cong \mathbb{C} \times \mathcal{H}_\sigma \times \mathcal{H}_{\sigma^c} \cong \mathbb{C} \times \mathbb{C}^N \times \mathbb{C}^{\binom{n}{d}-N-1},$$

where $N = \dim(\mathcal{V}_\sigma) = \dim(\mathcal{H}_\sigma)$.

Theorem 4.3.2. *Take a level set $\sigma \subseteq [d]$. Assume the truncation variety V_σ is birationally parameterized by a map ϕ which is the graph map of the affine representation*

$$\mathcal{V}_\sigma \to \mathbb{C} \times \mathcal{H}_{\sigma^c}, \quad t_\sigma \mapsto (1, f(t_\sigma)).$$

Now let $\Phi : \mathbb{P}^N \dashrightarrow \mathbb{P}^{\binom{n}{d}-1}$ be the projectivization of ϕ. Then the CC degree of V_σ is the total degree of the graph Γ_Φ of the rational map Φ.

Proof. By hypothesis, V_σ admits a parameterization as the graph map of an affine representative. Consequently, it is parametrized by a map of the form

$$\phi : \mathcal{V}_\sigma \to \mathcal{H}_d, \quad t_\sigma \mapsto \psi = (1, t_\sigma, f(t_\sigma)),$$

where f is a polynomial map $\mathcal{V}_\sigma \to \mathcal{H}_{\sigma^c}$. Projecting onto the σ-coordinates yields $\psi_\sigma = t_\sigma$, and hence the proof is equivalent to the proof of Theorem 3.1.1, using Lemma 3.2.1. □

We view Theorem 4.3.2 as a generalization of Theorem 3.1.1. Notice that here we speak of two graphs. First, we assume the truncation variety can be birationally parameterized by a graph map ϕ. On the other hand, the CC degree of such a truncation variety is the total degree of the graph $\Gamma_\Phi \subseteq \mathbb{P}^N \times \mathbb{P}^{\binom{n}{d}-1}$ of the projectivization Φ. Hence, the truncation variety is itself a graph, and we take its graph to describe its CC degree.

Example 4.3.3 ($d = 4, n = 8, \sigma = \{2\}$)**.** We continue Example 4.2.2. Consider the truncated exponential parameterization of $V_{\{2\}}$, described explicitly in (4.10). It is the graph map of the affine representation (4.11). Hence $V_{\{2\}}$ fulfills the hypothesis of Theorem 4.3.2. We view the projectivization of the truncated exponential map as a rational map

$$\Phi : \mathbb{P}^{\binom{d}{2}\binom{n-d}{2}} \dashrightarrow \mathbb{P}^{\binom{d}{2}\binom{n-d}{2}+\binom{d}{4}\binom{n-d}{4}}.$$

The map Φ parameterizes the projective variety $V_{\{2\}}$. By Theorem 4.3.2 the CC degree of $V_{\{2\}}$ is the total degree of the variety $\Gamma_\Phi \subseteq \mathbb{P}^{36} \times \mathbb{P}^{37}$, i.e. the graph of Φ. By applying the command `multidegree` in `Macaulay2` to our bihomogeneous ideal $\mathcal{I}(\Gamma_\Phi)$, we find that the class of the graph Γ_Φ in the cohomology ring $H^*(\mathbb{P}^{36} \times \mathbb{P}^{37}) = \mathbb{Z}[u, v]/\langle u^{37}, v^{38}\rangle$ is

$$[\Gamma_\Phi] = 2u^{36}v + 2u^{35}v^2 + 2u^{34}v^3 + \cdots + 2u^2v^{35} + 2uv^{36} + v^{37}.$$

Each nonzero coefficient in $[\Gamma_\Phi]$ is 2, except for the coefficient of v^{37}, which is equal to 1. Hence the total degree of Γ_Φ, and therefore the CC degree of $V_{\{2\}}$ is $\mathrm{CCdeg}(V_{\{2\}}) = 36 \cdot 2 + 1 = 73$.

Note that for most level sets σ the truncated exponential parameterization (4.9) is not a graph map. An important exception occurs when the level set σ is a singleton, that is, $\sigma = \{k\}$ for some $k \in [d]$. In this case, the hypothesis of Theorem 4.3.2 is satisfied, and the CC degree equals the degree of the graph of the projectivization of (4.9). In particular, this applies to the CCS truncation variety, namely the Grassmannian; see Chapter 3. It also applies to the CCD truncation variety corresponding to $\sigma = \{2\}$, as illustrated in Example 4.3.3. The CCD case is treated in detail in [33], and the graph map property of the truncation variety $V_{\{2\}}$ is established in [33, Proposition 2.1].

For level sets σ of size greater than one, the truncated exponential parameterization is no longer a graph map. However, these truncation varieties still admit graph parameterizations. Their construction relies on the poset structure of the Laplace polynomials, inherited from the partition lattice. We begin by introducing a bijection that defines new coordinates on $\mathcal{V}_\sigma$.

Remark 4.3.4. We consider the polynomial map

$$\chi_\sigma : \mathcal{V}_\sigma \to \mathcal{V}_\sigma, \qquad x_{I,B} = \sum_{\alpha \in \Pi(I)^\sigma} \mathcal{L}_{\alpha,B}(t), \quad \text{for} \quad I \subseteq [d],\, B \subseteq [n]\backslash[d],\, |I| = |B| \in \sigma.$$

Since $|I| \in \sigma$, the sum contains the term corresponding to the one-block partition $\{I\}$, namely $\mathcal{L}_{I,B}(t) = t_{I,B}$. Thus each coordinate $x_{I,B}$ maps to $t_{I,B}$ plus terms involving coordinates of smaller block size. Consequently, χ_σ is a bijection and defines a change of coordinates on $\mathcal{V}_\sigma$.

The following example illustrates this change of coordinates for CCSD.

Example 4.3.5 (The bijection $\chi_{\{1,2\}}$)**.** In this case $\dim(\mathcal{V}_{\{1,2\}}) = d(n-d) + \binom{d}{2}\binom{n-d}{2}$ and we have coordinates of the form $x_{i,b}$ and $x_{ij,bc}$ where $i, j \in [d]$ and $b, c \in [n]\backslash[d]$. Then

$$\chi_{\{1,2\}} : \mathcal{V}_{\{1,2\}} \to \mathcal{V}_{\{1,2\}}, \quad t \mapsto \begin{cases} x_{i,b} = t_{i,b} \\ x_{ij,bc} = t_{ij,bc} + t_{i,b}t_{j,c} - t_{i,c}t_{j,b}. \end{cases}$$

Before finding the new parameterization, we prove the following technical lemma.

Lemma 4.3.6. *Let α be a set partition in the poset Π_d^σ. We get the following identity:*

$$\mathcal{L}_\alpha \left(\left(\sum_{\gamma \in \Pi(I)^\sigma} \mathcal{L}_{\gamma,B}(t) \right)_{I,B} \right) = \sum_{\beta \leq \alpha} \mathcal{L}_\beta(t).$$

Proof. The Laplace polynomials are squarefree and hence multilinear. Each refinement of α in Π_d^σ is found by partitioning its blocks α_i with set partitions from $\Pi(\alpha_i)^\sigma$. That explains the first equality in the following equation. The second equality follows from part (1) of Lemma 4.1.4:

$$\mathcal{L}_\alpha \left(\left(\sum_{\gamma \in \Pi(I)^\sigma} \mathcal{L}_{\gamma,B}(t) \right)_{I,B} \right) = \sum_{\gamma \leq \alpha} \mathcal{L}_\alpha((\mathcal{L}_{\gamma_I,B}(\omega))_{I,B}) = \sum_{\gamma \leq \alpha} \mathcal{L}_\gamma(t).$$

□

To state the parameterization in the new coordinates, we first need to introduce the *Möbius sums* associated with the poset Π_d^σ. Let μ denote the *Möbius function* of Π_d^σ (see, e.g., [95, Section 3.7]). For $\alpha \in \Pi_d^\sigma$ we define the Möbius sum $\Sigma(\alpha)$ as the following integer

$$\Sigma(\alpha) = \sum_{\gamma \geq \alpha} \mu(\alpha, \gamma).$$

We now illustrate how to compute this integer for a small example.

Example 4.3.7. We consider the partition lattice Π_4 and its subposet $\Pi_4^{\leq 2}$, illustrated in Example 4.2.4. The three partitions of rank 2, namely $12|34$, $13|24$, and $14|23$, are maximal in $\Pi_4^{\leq 2}$. Hence, by definition,

$$\Sigma(12|34) = \Sigma(13|24) = \Sigma(14|23) = \mu(\alpha, \alpha) = 1.$$

The partitions of rank 1 each have only one partition larger than them. Therefore, for example, the Möbius sum of $12|3|4$ is

$$\Sigma(12|3|4) = \mu(12|3|4, 12|3|4) + \mu(12|3|4, 12|34) = 1 - 1 = 0.$$

By the same logic, the Möbius sum of each rank 1 element is 0. Finally, we consider the Möbius sum of the rank 0 element $1|2|3|4$. The Möbius values $\mu(\hat{0}, \alpha)$ are marked in Figure 4.1. We get

$$\Sigma(1|2|3|4) = 1 + 6 \cdot (-1) + 3 \cdot 1 = -2.$$

The following theorem shows that every truncation variety V_σ admits a graph parameterization, with no restriction on the level set σ. It is the main result of this chapter.

Theorem 4.3.8. *The truncation variety V_σ is birationally parameterized by the map*

$$\mathcal{V}_\sigma \to \mathcal{H}_d, \quad \psi_J = (-1)^\tau \sum_{\alpha \in \Pi([d]\backslash J)^\sigma} \Sigma(\alpha) \mathcal{L}_{\alpha, J\backslash[d]}(x), \tag{4.15}$$

where $\Sigma(\alpha)$ is the Möbius sum of α in $\Pi([d]\backslash J)^\sigma$. This map is a graph map.

Proof. We consider the conjugation of χ_σ with (4.15). By Lemma 4.3.6 we get the map

$$\mathcal{V}_\sigma \to \mathcal{H}_d, \quad \psi_J = (-1)^\tau \sum_{\alpha \in \Pi([d]\backslash J)^\sigma} \Sigma(\alpha) \sum_{\gamma \leq \alpha} \mathcal{L}_{\gamma, J\backslash[d]}(t). \tag{4.16}$$

Fix a subset $J \subseteq [n]$, and consider the poset $P = \Pi([d]\backslash J)^\sigma \cup \{\hat{1}\}$, that is, the poset $\Pi([d]\backslash J)^\sigma$ together with a maximum element $\hat{1}$. Our proof uses Möbius inversion. To that end, we define the functions $f, g : P \to \mathbb{C}[t]$ where

$$f(\alpha) = \mathcal{L}_{\alpha, J\backslash[d]}(t), \quad f(\hat{1}) = 0, \quad g(\alpha) = \sum_{\gamma \leq \alpha} f(\gamma) = \sum_{\gamma \leq \alpha} \mathcal{L}_{\gamma, J\backslash[d]}(t).$$

We see that $\mu(\alpha, \hat{1}) = -\sum_{\gamma \geq \alpha} \mu(\alpha, \gamma) = -\Sigma(\alpha)$. Hence by Möbius inversion we get

$$0 = f(\hat{1}) = \sum_{\alpha < \hat{1}} \mu(\alpha, \hat{1}) g(\alpha) + g(\hat{1}) = \sum_{\alpha \in \Pi([d]\backslash J)^\sigma} (-\Sigma(\alpha)) \mathcal{L}_{\alpha, J\backslash[d]}(t) + \sum_{\alpha \in \Pi([d]\backslash J)^\sigma} \mathcal{L}_{\alpha, J\backslash[d]}(t).$$

Note that the truncated exponential map (4.9), which parameterizes V_σ, maps the coordinate ψ_J to $(-1)^\tau g(\hat{1})$. Hence, the conjugated map in (4.16) is exactly the truncated exponential map. Since χ_σ is a bijection, we see that (4.15) also parameterizes V_σ.

Now consider an index set $J \in \binom{[n]}{d}$ with excitation level $|[d]\backslash J|$ in σ. Then $\Pi([d]\backslash J)^\sigma$ has a maximum element $\{[d]\backslash J\}$ and we get the following formulas for the Möbius sum:

$$\Sigma(\{[d]\backslash J\}) = 1 \quad \text{and} \quad \Sigma(\alpha) = 0 \text{ for } \alpha < \{[d]\backslash J\}.$$

Therefore (4.15) maps coordinate ψ_J to signed variable $(-1)^\tau x_{[d]\backslash J, J\backslash[d]}$. This proves that (4.15) is the graph map of the affine representative of the restriction to $\mathcal{H}_{\sigma^c}$. □

This new parameterization provides a graph parameterization for every truncation variety V_σ. Consequently, each truncation variety can be realized as a graph. In particular, we obtain a graph parameterization for the chemically relevant CCSD truncation variety $V_{\{1,2\}}$. This allows us to study the CCSD variety in a manner similar to the analyses of the CCS variety in Chapter 3 and the CCD variety in [33]. We now illustrate a small example:

Example 4.3.9 ($d = 3$, $n = 6$, $\sigma = \{1, 2\}$)**.** We consider the 3×3 matrix

$$X = \begin{bmatrix} x_{1,4} & x_{1,5} & x_{1,6} \\ x_{2,4} & x_{2,5} & x_{2,6} \\ x_{3,4} & x_{3,5} & x_{3,6} \end{bmatrix}.$$

We look at the graph parameterization of $V_{\{1,2\}}$. In this case

$$N = \dim(\mathcal{V}_{\{1,2\}}) = 3(6-3) + \binom{3}{2}\binom{6-3}{2} = 9 + 9 = 18.$$

For an indexing set J of excitation level 1 or 2, the map (4.15) sends ψ_J to the signed variable $(-1)^\tau x_{[d]\backslash J,\, J\backslash[d]}$. The level 3 coordinate ψ_{456} maps to a linear combination of Laplace polynomials of X. Explicitly, (4.15) is the graph map of the affine representative

$$\mathbb{C}^{18} \to \mathbb{C}^2, \qquad \psi_{123} = 1,\ \psi_{456} = \mathcal{L}_{1|23}(x) + \mathcal{L}_{2|13}(x) + \mathcal{L}_{3|12}(x) - 2\mathcal{L}_{1|2|3}(x). \tag{4.17}$$

Here the coefficient -2 is the Möbius sum of $1|2|3$ in $\Pi_3^{\leq 2}$.

We obtain the following immediate corollary of Theorem 4.3.2 and Theorem 4.3.8:

Corollary 4.3.10. *The CC degree of V_σ is the total degree of the graph of the map (4.15).*

We take a deeper look at the Möbius sum over the poset $\Pi(I)^\sigma \cong \Pi_m^\sigma$, where $I \subseteq [d]$ and $|I| = m$. By definition, it is trivial for posets with a maximum element $\hat{1}$. In that case

$$\Sigma(\alpha) = \begin{cases} 1 & \text{if } \alpha = \hat{1} \\ 0 & \text{if } \alpha < \hat{1}. \end{cases}$$

However, Π_m^σ only has a maximum element if $m \in \sigma$. In general we do not have an explicit formula for the Möbius sum of an element α in Π_m^σ. We now focus on the case when $\sigma = [\ell]$ for some $\ell \leq d$. Then Π_m^σ is the poset of set partitions with blocks of size at most ℓ, ordered

by refinement, and denoted $\Pi_m^{\leq \ell}$. We recall that the Möbius function of $\Pi_m^{\leq \ell}$ matches the Möbius function of the partition lattice Π_m. Therefore, in that case

$$\mu(\alpha, \gamma) = (-1)^{|\alpha|-|\gamma|} \prod_{\gamma_i} (s_{\gamma_i} - 1)! \quad \text{so} \quad \Sigma(\alpha) = \sum_{\gamma \geq \alpha} (-1)^{|\alpha|-|\gamma|} \prod_{\gamma_i} (s_{\gamma_i} - 1)!,$$

where s_{γ_i} is the number of blocks of α contained in the block γ_i of γ. We define the *global Möbius sum* of $\Pi_m^{\leq \ell}$ as $\Sigma(m) = \Sigma(\hat{0})$. By [66, Proposition 1.2] the generating function for the global Möbius sum of $\Pi_m^{\leq \ell}$ for $m \in \mathbb{N}$ equals

$$\sum_{k \geq 0} \Sigma(k) \frac{x^k}{k!} = \exp\left(\sum_{k=1}^{\ell} (-1)^{k-1} \frac{x^k}{k} \right).$$

Remark 4.3.11 (Möbius sum of $\Pi_m^{\leq 2}$)**.** Here we assume $\sigma = \{1, 2\}$ and we consider the poset $\Pi_m^{\leq 2}$. The generating function of the global Möbius sum is

$$\sum_{k \geq 0} \Sigma(k) \frac{x^k}{k!} = \exp\left(x - \frac{x^2}{2} \right).$$

This is exactly the generating function for the *Hermite polynomial*, evaluated at $x = 1$, i.e. $\mathrm{He}_k(1)$. These polynomials are well studied and have a nice combinatorial interpretation in terms of involutions of a finite set, see [41, Proposition 1]. By [41, Equation 2] we get the following explicit formula for the global Möbius sum of $\Pi_m^{\leq 2}$:

$$\Sigma(m) = \sum_{k=0}^{\lfloor m/2 \rfloor} (-1)^k \frac{m!}{2^k k!(m-2k)!}.$$

This is also showed in [15, Theorem 5]. This is the signed number of involutions of the set $[m]$. The first values of the sequence of evaluated Hermite polynomials $\mathrm{He}_m(1)$ are

$$1, 1, 0, -2, -2, 6, 16, -20, -132, 28, \ldots, \quad m = 0, 1, 2, 3, 4, 5, 6, 7, 8, 9, \ldots. \tag{4.18}$$

Now let $\alpha \in \Pi_m^{\leq 2}$, and let s denote the number of singleton blocks of α. Since every partition in $\Pi_m^{\leq 2}$ has blocks of size at most 2, the only way to obtain larger partitions is by joining together the singleton blocks of α. Consequently, the principal filter of α (that is, the set of elements $\beta \in \Pi_m^{\leq 2}$ where $\beta \geq \alpha$) is isomorphic to $\Pi_s^{\leq 2}$. In this poset α corresponds to the minimal element, and therefore

$$\Sigma(\alpha) = \Sigma(s) = \mathrm{He}_s(1).$$

This yields an explicit description of the Möbius sums for elements of the poset $\Pi_m^{\leq 2}$, and hence of the coefficients appearing in the parameterization (4.15) of $V_{\{1,2\}}$.

We can now explicitly describe the graph parameterization of the CCSD truncation variety:

Corollary 4.3.12. *The truncation variety $V_{\{1,2\}}$ can be parameterized by the graph map*

$$\mathbb{C}^{d(n-d)+\binom{d}{2}\binom{n-d}{2}} \to \mathcal{H}_{\{1,2\}}, \quad \psi_J = (-1)^\tau \sum_{\alpha \in \Pi([d]\setminus J)^{\leq 2}} \mathrm{He}_{s_\alpha}(1)\mathcal{L}_{\alpha, J\setminus[d]}(x). \tag{4.19}$$

Here s_α denotes the number of singletons in α. The CC degree of $V_{\{1,2\}}$ is the total degree of the graph of this graph map.

We conclude this section with an explicit graph parameterization of a small example of a CCSD truncation variety.

Example 4.3.13 ($d = 4$, $n = 8$, $\sigma = \{1, 2\}$)**.** In this case, the truncation variety $V_{\{1,2\}}$ is parameterized by the graph map

$$\mathbb{C}^{52} \to \mathbb{C}^{70}, \psi_J = \begin{cases} 1 & J = \{1,2,3,4\} \\ (-1)^\tau x_{[4]\setminus J, J\setminus[4]} & |J\setminus[4]| = 1 \text{ or } 2, \\ \mathcal{L}_{ij|k,B}(x) + \mathcal{L}_{ik|j,B}(x) + \mathcal{L}_{jk|i,B}(x) - 2\mathcal{L}_{i|j|k,B}(x) & |J\setminus[4]| = 3, \\ \mathcal{L}_{12|34}(x) + \mathcal{L}_{13|24}(x) + \mathcal{L}_{14|23}(x) - 2\mathcal{L}_{1|2|3|4}(x) & J = \{5,6,7,8\} \end{cases} \tag{4.20}$$

Here, in the case $|J \setminus [4]| = 3$, we set $B = J \setminus [4]$ and write $\{i, j, k\} = [4] \setminus J$ with $i < j < k$. This map differs from the truncated exponential parameterization of $V_{\{1,2\}}$ in Corollary 4.2.5.

When J has excitation level $|J\setminus[4]| = 3$, the coordinate ψ_J is equal to the polynomial in (4.17) up to a relabeling of the indices. Note that the coefficients in front of the Laplace polynomials are entries of the sequence (4.18). The coordinate ψ_{5678} should be given by a linear combination of all 10 Laplace polynomials corresponding to the blue-circled partitions in Figure 4.1. However, since the rank 1 partitions have two singletons, their Möbius sum is equal to $\mathrm{He}_2(1) = 0$; see also Example 4.3.7. Hence those terms do not appear.

In conclusion, we defined the exponential parameterizations of the truncation varieties in terms of Laplace polynomials, offering a more algebraic description of them. With a nonlinear change of coordinates, we were able to reparameterize the truncation varieties with graph maps. This, in turn, allowed us to show that the CC degree equals the total degree of its graph. Although we now shift our focus to numerics, many theoretical questions concerning the truncation varieties and their CC degrees remain open. Among them are the problems of finding a Khovanskii basis for the truncation varieties and understanding symmetries in their defining equations.

Chapter 5

Numerical Exploration

In this chapter we focus on the computational aspects of our algebraic adaptation of coupled cluster theory. We give an elementary introduction to the algebraic computational tools used to *fully* solve the CC equations. The main tools are `parameter homotopy` and `monodromy`, both implemented in the software `HomotopyContinuation.jl` [11]. We describe in detail how we compute the degree and CC degree of truncation varieties. We study the scaling behavior of the CC degree and compare our bounds from Theorem 2.3.2 with previously known bounds. We conclude the chapter with two comprehensive case studies of the CC equations for LiH and H_4 in several symmetries. This chapter is based on Section 5 of [37] and the paper *Exploring Ground and Excited States via Single Reference Coupled-Cluster Theory and Algebraic Geometry* [102], which is joint work with Fabian M. Faulstich. Throughout this chapter we use Julia version 1.9.1 and `HomotopyContinuation.jl` version 2.9.2 [11]. The Python computations were performed using Python 3.8.8 and PySCF 2.0.1 [99]. All computations were carried out on the MPI-MiS computer server using four 18-core Intel Xeon E7-8867 v4 processors at 2.4 GHz (3,072 GB RAM).

5.1 Computational Methods

In this section, we outline the computational procedure employed to compute CC degrees and CC solutions for specific Hamiltonians. We begin by introducing the CC family, a *parametric polynomial family* for the coupled cluster systems in (2.18) corresponding to σ:

$$\mathcal{F}_{\mathbf{CC}}(\sigma) = \left\{ \left[(G - \lambda \cdot I) \exp(T(t)) e_{[d]} \right]_\sigma \;\middle|\; G \in \mathbb{C}^{\binom{n}{d} \times \binom{n}{d}} \right\}. \tag{5.1}$$

The energy $\lambda \in \mathbb{C}$ and cluster amplitudes $t \in \mathcal{V}_\sigma$ are the variables, and the entries of the matrix G are the parameters. This is the set of CC systems truncated at σ, one for each $\binom{n}{d} \times \binom{n}{d}$ matrix G. We will ultimately choose $G = H$ to be a Hamiltonian of interest. We recall from Section 2.3 that generically the CC systems have a finite number of roots.

Theorem 5.1.1 (The Parameter Continuation Theorem)**.** *[10, Theorem 3.18] We denote the number of regular zeros of $F_G \in \mathcal{F}_{\mathbf{CC}}$ by $N(G)$ and set $N = \sup_G N(G)$. The number N*

is finite and there exists a proper algebraic subvariety $\Delta \subsetneq \mathbb{C}^{\binom{n}{d}\times\binom{n}{d}}$*, called the discriminant of* $\mathcal{F}_{\mathbf{CC}}$*, such that* $N(G) = N$ *for all* $G \notin \Delta$*.*

This theorem provides an upper bound on the number of isolated roots of any polynomial system in $\mathcal{F}_{\mathbf{CC}}$. Moreover, this bound is tight and equality is obtained for any polynomial system with parameters outside the discriminant Δ. This bound is the CC degree. Systems on the discriminant Δ might have fewer roots, as well as singular roots and zero sets with extraneous higher-dimensional components. Most physical Hamiltonians, arising from electronic systems, lie on the discriminant, so the number of zeros of the corresponding systems is often significantly fewer than the CC degree. Physical CC equations might also potentially have positive-dimensional solution sets.

The numerical procedure used in this work consists of two steps: First, we solve a general system of equations from the CC family, $\mathcal{F}_{\mathbf{CC}}$, using *monodromy methods*. Second, we use *parameter homotopy* to track the solutions from this solved but generic system of equations to solutions of the CC equations describing a specific chemical system of interest.

We emphasize that, at their core, both methods use a *homotopy* to track new solutions from known solutions [3, 26, 45, 75, 94]. More precisely, for a (piecewise smooth) path $\gamma : [0, 1] \to \mathbb{C}^{\binom{n}{d}\times\binom{n}{d}}$ in the parameter space we define the homotopy

$$H(\lambda, t, \tau) = F_{\gamma(\tau)}(\lambda, t), \quad (\lambda, t) \in \mathbb{C} \times \mathcal{V}_\sigma, \ \tau \in [0, 1]. \tag{5.2}$$

Here $H(\lambda, t, \tau)$ describes the continuous deformation from a start system $G(\lambda, t) = H(\lambda, t, 1)$ to a target system $F(\lambda, t) = H(\lambda, t, 0)$. The individual solution paths of the equation $H(\lambda, t, \tau) = 0$ are then tracked from $G(\lambda, t)$ to $F(\lambda, t)$ as $\tau \to 0$. This is accomplished via an ordinary differential equation, known as the Davidenko differential equation [24, 25],

$$\frac{\partial}{\partial \mathbf{x}} H(\mathbf{x}, \tau) \left(\frac{\mathrm{d}}{\mathrm{d}\tau} \mathbf{x}(\tau) \right) + \frac{\partial}{\partial \tau} H(\mathbf{x}, \tau) = 0, \tag{5.3}$$

initialized by a root $\mathbf{x}$ of the start system, i.e. $G(\mathbf{x}) = 0$, where we set $\mathbf{x} = (\lambda, t) \in \mathbb{C} \times \mathcal{V}_\sigma$.

Monodromy

The monodromy solver is a numerical technique specifically designed for solving generic polynomial systems of equations within a parameterized family, [26, Section 2.1]. We emphasize that the monodromy solver requires the system to be generic, so it is not suitable for solving physical CC equations directly. However, it can be employed to establish a start system $F_G \in \mathcal{F}_{\mathbf{CC}}$ within the CC family, and compute the CC degree. This start system is then used by the parameter homotopy continuation method to solve a (physical) target system of equations. The monodromy method is required only once for a particular system configuration, i.e. the number of electrons d, the number of orbitals n and the level set $\sigma \subsetneq [d]$.

In the monodromy setting, we consider homotopies corresponding to loops in the parameter space. To that end, we define the *fundamental group* of the generic parameter space

$\mathbb{C}^{\binom{n}{d}\times\binom{n}{d}}\backslash\Delta$ based at G, denoted $\pi_1(\mathbb{C}^{\binom{n}{d}\times\binom{n}{d}}\backslash\Delta, G)$, to be the set of all loops in $\mathbb{C}^{\binom{n}{d}\times\binom{n}{d}}\backslash\Delta$ starting (and ending) at matrix G, modulo deformation. We say two loops are equivalent if there exists a continuous deformation of one loop into the other, i.e. we do not cross the discriminant when deforming. See [49, Chapter 1] for the formal definition.

The term monodromy refers to a transformation obtained by transporting a parametric object around a loop in the parameter space. The resulting object may differ from the starting object. This observation forms the basis of the monodromy solver. More precisely, let G be a generic $\binom{n}{d} \times \binom{n}{d}$ matrix and let $\gamma \in \pi_1(\mathbb{C}^{\binom{n}{d}\times\binom{n}{d}}\backslash\Delta, G)$ be a loop in the parameter space based at G, i.e. $\gamma(0) = \gamma(1) = G$. Let $\mathbf{x} \in \mathbb{C} \times \mathcal{V}_\sigma$ be a root of the generic CC system $F_G \in \mathcal{F}_{\mathbf{CC}}$. Denote by $\mathbf{x}(\tau)$ the solution path of the homotopy $H(\lambda, t, \tau) = 0$, starting at $\mathbf{x}(1) = \mathbf{x}$. Since γ is a loop, the target system of H equals the start system. In particular, the endpoint $\mathbf{x}(0)$ is again a root of F_G. However, the endpoint $\mathbf{x}(0)$ need not be equal to the root $\mathbf{x}(1)$. Precisely, let $(\mathbf{x}_1, \ldots, \mathbf{x}_M)$, where $M = \mathrm{CCdeg}(V_\sigma)$, be an ordered list of all the roots of F_G. Then continuation along γ induces a permutation of the roots: $(\mathbf{x}_1(0), \ldots, \mathbf{x}_M(0))$. More generally, the fundamental group *acts* on the solution set of $F_G(\lambda, t) = 0$ by permutation. We therefore obtain a homomorphism

$$\pi_1(\mathbb{C}^{\binom{n}{d}\times\binom{n}{d}}\backslash\Delta, G) \to S_M$$

where S_M is the symmetric group. The image of this map is called the *monodromy group* of F_G.

Example 5.1.2 (A simple monodromy)**.** Consider the parametric polynomial family:

$$\mathcal{F} = \{x^3 - 6\,x^2 + 11\,z\,x - 6 \;\big|\; z \in \mathbb{C}\},$$

with variable $x \in \mathbb{C}$ and parameter $z \in \mathbb{C}$. For $z = 1$, the corresponding polynomial

$$x^3 - 6\,x^2 + 11\,x - 6 = (x-1)(x-2)(x-3)$$

has the roots $x_1 = 1, x_2 = 2, x_3 = 3$. We track the roots along the loop $\gamma : [0,1] \to \mathbb{C}, t \mapsto e^{i2\pi t}$, based at 1, and obtain a permutation $(12)(3)$ of the roots, see Figure 5.1.

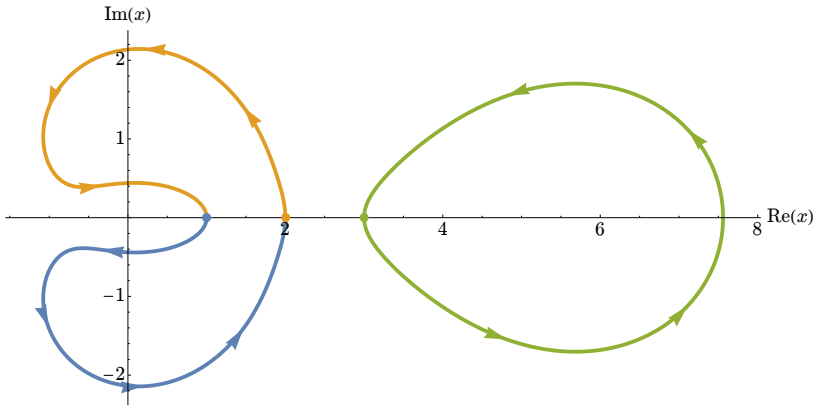

Figure 5.1: The paths of the roots of $x^3 - 6x^2 + 11\gamma(\tau)x - 6$ along $\gamma : [0,1] \to \mathbb{C}, \tau \mapsto e^{i2\pi t}$.

The monodromy solver begins with a single known solution of a system of equations and numerically computes additional solutions by continuing along loops in the parameter space. All solutions of the system can be recovered in this way if and only if the monodromy group is *transitive*, that is, if the solution set consists of a single orbit. Hence, the following well-known theorem provides conditions under which this procedure can recover all solutions.

Theorem 5.1.3. *[48, Exposé V, Theorem 4.1] Let $\mathcal{F}$ be a polynomial family with variables $x \in \mathbb{C}^m$ and parameters $p \in \mathbb{C}^s$, such that generic systems in $\mathcal{F}$ have a finite number of regular zeros. The monodromy group is transitive if and only if the incidence variety*

$$V(\mathcal{F}) = \{(x, p) \in \mathbb{C}^m \times \mathbb{C}^s : F_p(x) = 0\}$$

is irreducible.

We look at the incidence variety of the CC family. It can be written using the implicit formulation of the CC equations found in (2.15),

$$V(\mathcal{F}_{\mathbf{CC}}) = \{((\lambda, \psi), G) : (G\psi)_\sigma = \lambda\psi_\sigma,\ \psi \in V_\sigma\} \subseteq (\mathbb{C} \times V_\sigma) \times \mathbb{C}^{\binom{n}{d}\times\binom{n}{d}}.$$

We recall that the truncation varieties V_σ are irreducible. The defining equations have linear parameters, and so the projection $\pi_1 : V(\mathcal{F}_{\mathbf{CC}}) \to \mathbb{C} \times V_\sigma$ has linear fibers which are nonempty, since $\lambda I \in \pi_1^{-1}(\lambda, \psi)$. Therefore, the incidence variety is also irreducible. Hence, the monodromy groups of coupled cluster systems are transitive and monodromy solvers can be used to find all solutions of generic CC equations, given a single known solution.

If the total number of solutions of the polynomial system of equations is unknown, it is not immediately clear when all solutions have been found. We therefore must specify a stopping criterion. In `HomotopyContinuation.jl`, the default criterion halts the computation after five consecutive loops without finding additional solutions. At that point, we assume that all solutions to the system have been numerically identified.

To use the monodromy solver to find all roots of a generic system in $\mathcal{F}_{\mathbf{CC}}$, one needs a generic instance of the CC equations along with a start solution. Hence, we need a generic matrix G along with a single solution to the corresponding CC equations $F_G = 0$. Often, this pair is found using Newton's method. However, as was mentioned above, the fibers of the projection π_1 are nonempty and linear. Therefore, we can find a generic CC system along with a root by first choosing $(\lambda, t) \in \mathbb{C} \times \mathcal{V}_\sigma$ at random, and then find a matrix G such that (λ, t) is a root of F_G. To do that we only need to solve the linear system

$$[(G - \lambda \cdot I) \exp T(t) e_{[d]}]_\sigma = 0$$

where the unknowns are the entries of matrix G. A generic solution G produces the desired generic CC system F_G with a known root (λ, t).

Parameter Homotopy

Applying the parametric homotopy continuation method to find the solutions of the CC equations corresponding to an electronic system of interest is now straightforward. The goal is to solve

$$F_H(\lambda, t) = [(H - \lambda \cdot I) \exp(T(t)) e_{[d]}]_\sigma = 0$$

for a given Hamiltonian H, arising from a physical electronic system, as in Section 1.2. We note that H may lie on the discriminant Δ. We define a path γ in the parameter space that continuously transforms the generic matrix G into H, such that $\gamma((0,1]) \subseteq \mathbb{C}^{\binom{n}{d}\times\binom{n}{d}} \backslash \Delta$. Hence, only the endpoint $\gamma(0)$ can lie on Δ. This means, γ should not cross the discriminant. Such a path can be chosen generically, since Δ is a proper variety of $\mathbb{C}^{\binom{n}{d}\times\binom{n}{d}}$, and therefore has real codimension at least two and measure zero. Since we have computed all roots of the system F_G using monodromy, the Davidenko differential equation (5.3) allows the tracking of roots from F_G to F_H using e.g. Newton's method. The CC degree therefore serves as a complexity measure, as it equals the number of paths needed to be tracked to fully solve physical CC equations.

As $\tau \to 0$, we may encounter different scenarios when getting close to $\tau = 0$. We illustrate such different scenarios in Figure 5.2.

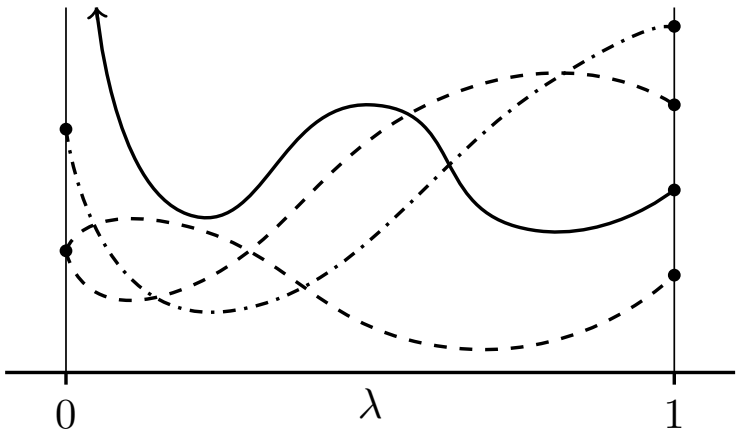

Figure 5.2: Sketch of possible homotopy paths.

First, the tracking might not converge, i.e. the path has no finite limit as $\tau \to 0$ and the solution goes off to infinity. This only happens if the target system F_H lies on the discriminant Δ, and in that case the solution count drops. If the tracking converges, we find either a *non-singular solution* or a *singular solution*. A solution is singular if the Jacobian matrix of F_H is singular (i.e. not invertible), or if the winding number of the solution path is greater than one. A singular solution could indicate that the solution set of $F_H = 0$ has an extraneous component of dimension ≥ 1. It appears that singular solutions can provide highly accurate

approximations to eigenvalues of high multiplicity, see the CCS results for LiH in Section 5.3, and are therefore relevant. When parameter homotopy is implemented in practice, the *endgame* [76] should be employed when τ gets close to 0, to determine the target solutions and their "type".

5.2 Exploring the CC degree

This section covers the state of the art for numerically computing the CC degree along with exploring its scaling and bounds. We use the unlinked formulation (2.18) of the CC equations, as a square system with $\dim(\mathcal{V}_\sigma)+1$ unknowns. Readers familiar with the linked formulations of the CC equations may consult Theorem 2.3.10 for the precise relation. Our new approach outlined in Section 5.1 allows for the solving of systems much larger than those in [36]. This is accomplished by leveraging monodromy techniques.

The starting point of our experiments, for fixed d, n and σ, is the choice of a symmetric matrix H together with a known CC solution. This start pair is constructed in the manner described in Section 5.1. We then use the monodromy solver to find all CC solutions corresponding to H, revealing the CC degree. The degree of V_σ is found in a similar way, by slicing V_σ with an appropriate parametric linear space. Whenever feasible, we use `Macaulay2` [46] to validate the degrees and CC degrees we found numerically. In this manner we found the table entries in Examples 2.2.8, 2.2.9 and 2.3.6. Here is one more case:

Example 5.2.1 ($d = 3, n = 8$)**.** The CC systems for the six varieties for three electrons in eight spin-orbitals are described in Table 5.1.

σ	$\{1\}$	$\{2\}$	$\{3\}$	$\{1,2\}$	$\{1,3\}$	$\{2,3\}$
#variables	16	31	11	46	26	41
$\deg(V_\sigma)$	6 006	1	1	3 894	4 195	1
CC degree	38 610	31	11	145 608	58 214	41
#real	430	31	11	1 376	658	41
solve(sec)	619	8	3	26 757	1 948	7
certify(sec)	7	3	0	41	8	0

Table 5.1: The CC systems for three electrons in eight spin orbitals.

The number of real solutions (listed in row "#real") varies for different choices of real-valued Hamiltonians, unless V_σ is a linear space. The counts 430, 1 376, 658 (in row "#real") are from *one* representative sample run for a random real-valued H. The degree of $V_{\{1,2\}}$ is computed numerically. The runtimes in seconds are for solving and certifying for generic H.

Example 5.2.2. The CC degrees found for various d, n and σ indicate the complexity of fully solving the CC equations. Figure 5.3 concerns d electrons in $n = 2d$ spin-orbitals.

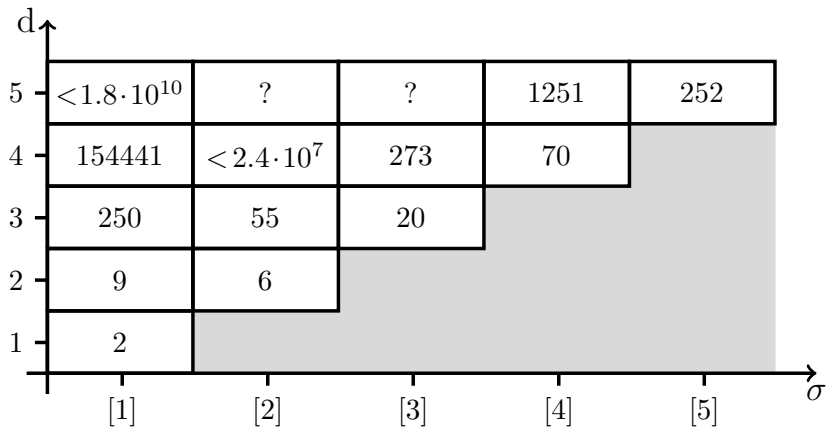

Figure 5.3: CC degrees for different truncation levels with $n = 2d$.

We show CC degrees for rank-complete level sets, i.e. $\sigma = [k]$ for $k = 1, \ldots, d$. For $d = 4$, $\sigma = [2]$ and $d = 5$, $\sigma = [1]$, the upper bound in Theorem 2.3.2 is displayed. The question marks indicate that the degree of V_σ is unknown, and hence the upper bound is not known. A striking observation in Figure 5.3 is the low numbers on the diagonal. This is because CC theory is exact in its untruncated limit, i.e. the number of solutions is the matrix size. For CC at level $[d-1]$, the entries come from Proposition 2.3.7. The left column [1] concerns the Grassmannian $\mathrm{Gr}(d, 2d)$.

Even for larger cases, Theorem 2.3.2 gives a good upper bound on the number of solutions. The key ingredient is the degree of the truncation variety V_σ. This is often easier to compute than $\mathrm{CCdeg}(V_\sigma)$. For computing $\deg(V_\sigma)$, we used a range of techniques. First of all, the degree equals one in the linear cases of Theorem 2.2.10. Second, for the CCS truncation ($\sigma = \{1\}$), the degree of the Grassmannian has an explicit description in (1.7). Third, sometimes we can compute $\deg(V_\sigma)$ symbolically with `Macaulay2` [46]; this requires an explicit description of the ideal of the truncation variety, e.g., as provided in Theorem 2.2.2. Finally, if this all fails, we use numerics. Namely, we intersect V_σ with a generic affine-linear space of dimension $\mathrm{codim}(V_\sigma)$. The number of points in the intersection is the degree of V_σ. Using a parameterization of the affine linear-space, represented by a $\dim(V_\sigma) \times \binom{n}{d}$ matrix L, we may compute the intersection points using the implicit description of V_σ, as a complete intersection cut out by polynomials $x_I(\psi)$. This means, we solve the linear system $L\psi = 0$ joined with the polynomial relations $x_I(\psi) = 0$. We may also take advantage of the fact that the truncated exponential parameterization is injective, and so solving the system $L \exp(T(t_\sigma))e_{[d]} = 0$ reveals the degree of V_σ as well. Since the linear space is chosen to be generic, we may use the monodromy solver in order to compute the degree.

In conclusion, the inequality in Theorem 2.3.2 leads to upper bounds for the number of solutions to the CC equations, even when the equations are too large to be solved completely. It is instructive to compare previously known bounds to those found by our new approach.

Example 5.2.3 (Scaling of the number of solutions)**.** For $d = 2$ we consider the CC equations for singles ($\sigma = \{1\}$) and doubles ($\sigma = \{2\}$) investigating the scaling of the number of CC solutions with respect to n. Figure 5.4 shows different bounds in a log-lin plot.

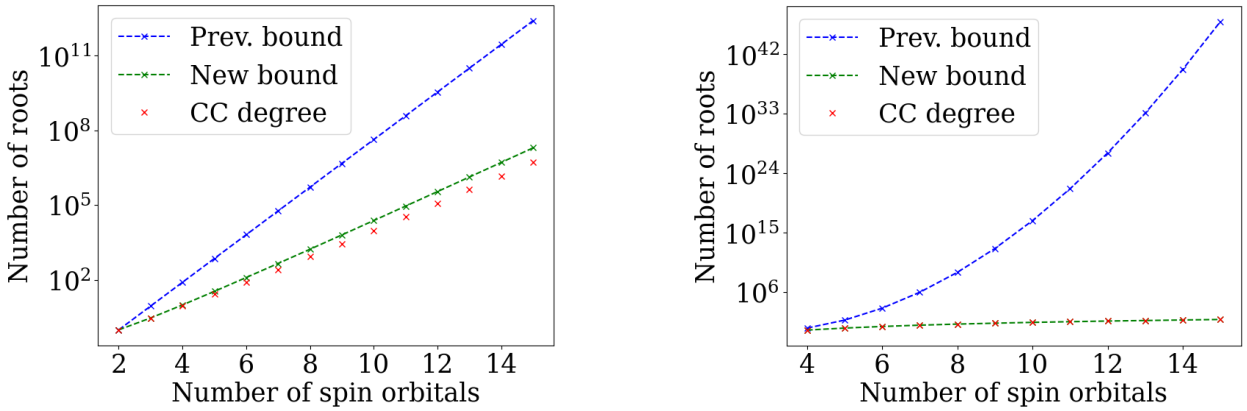

Figure 5.4: Bounds to the number of solutions for CCS (left panel) and CCD (right panel).

The blue curve is the previous bound from [36, Theorem 4.10] and the green curve is our new bound from Theorem 2.3.2. We moreover show the exact number of solutions; for CCD (right panel) this is given in Corollary 2.3.3 and for CCS (left panel), this is given in Theorem 3.1.2. The graphs show that algebraic geometry leads to much improved bounds.

5.3 Lithium Hydride

We investigate the energy spectrum and potential energy curves (PECs) for ground and excited states of lithium hydride (LiH). We compare the eigenspectrum of the respective Hamiltonians, with the CC solutions found for levels CCS, CCD and CCSD. The reported computations use a minimal basis description using the STO-6G basis set and LiH is here considered at half-filling, i.e. four electrons in eight spin orbitals. The construction of the Hamiltonian for LiH in first quantization is described in Example 1.2.6. The one-body and two-body integrals are obtained from the Python-based Simulations of Chemistry Framework (`PySCF`) [98–100].

LiH – Coupled Cluster Singles and Doubles

The CCS truncation variety $V_{\{1\}}$ is the Grassmannian $\mathrm{Gr}(4, 8)$, with $\dim(V_\sigma) = 16$ and $\deg(V_\sigma) = 24\,024$. Its CC degree is $\mathrm{CCdeg}(V_{\{1\}}) = 154\,441$, found by monodromy in 82 minutes. We compare it with the bound in Theorem 2.3.2, which is 408 408. We consider LiH with the bond distance 2.9 bohr, near equilibrium. Tracking all paths using parameter

homotopy yields 3 non-singular real solutions. We also find 110 876 singular solutions, only 418 of which yield real energies. These calculations take 11 minutes and 32 seconds.

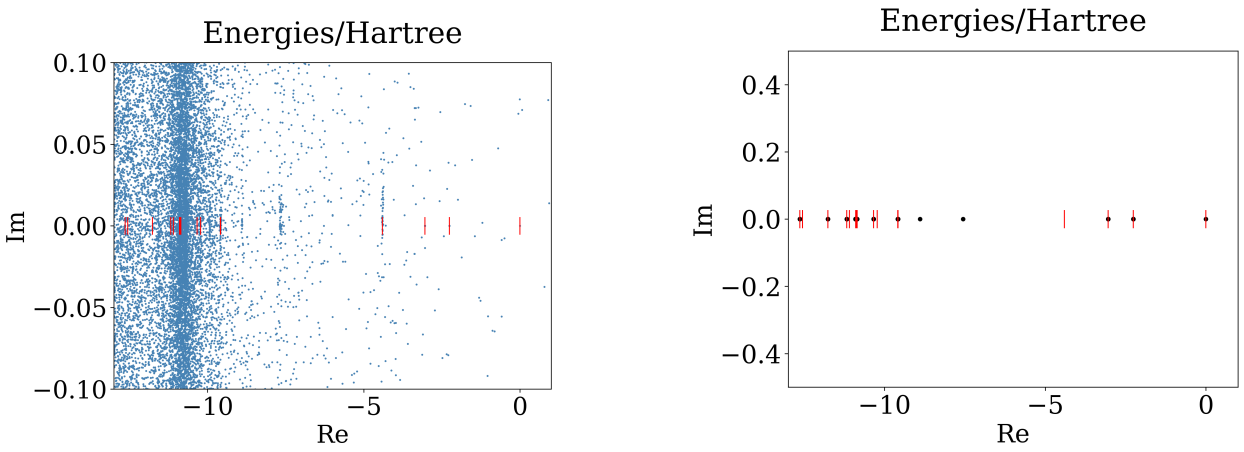

(a) CCS (b) CCS (only real)

Figure 5.5: The eigenvalues from exact diagonalization, shown as red bars, are compared to the energy spectra, shown in black and blue, from CCS.

In Figure 5.5 we compare the exact energies of the system, i.e. the eigenvalues of the Hamiltonian, with the energies obtained from CCS. The energies here are measured in Hartree, the standard atomic unit of energy in quantum chemistry. Since there are so many CC solutions, we also compare the eigenvalues with only the real energies.

LiH – Coupled Cluster Doubles

The CCD truncation variety $V_{\{2\}}$ is a hypersurface of degree $\deg(V_{\{2\}}) = 2$, defined by the inverse master polynomial $\overline{x}_{5678}(\psi)$. Its CC degree is $\mathrm{CCdeg}(V_{\{2\}}) = 73$. We compare it with the upper bound found using Theorem 2.3.2, which is 74. Hence the bound is only off by 1.

We look at the dissociation process of LiH. We consider bond distances ranging from 1.375 to 5.95 bohr. These distances are given in bohr, the standard atomic unit of length in quantum chemistry. The Hamiltonian now depends parametrically on the bond distance, so we obtain a 1-dimensional parametric family of Hamiltonians. The potential energy curves (PECs) are the eigenvalue branches of the parametric Hamiltonian. We solve the CCD equations for a discretized grid on this interval, and compare the CCD energies with the PECs, in Figure 5.6a. We minimize the distance between eigenvalues and CCD energies and extract the PECs of the different states that are well-approximated using CCD, see Figure 5.6b.

We find that 10 PECs are approximated up to $5 \cdot 10^{-2}$ hartree for the entire dissociation process. However, we also note that for various bond distances, more CCD energies approximate exact energies well, see Table 5.2. Investigating the solution spectrum, we observe that the total number of CCD solutions fluctuates along the bond stretching process, see Table 5.2. We find that in this case the CC degree severely overestimates the true number of solutions.

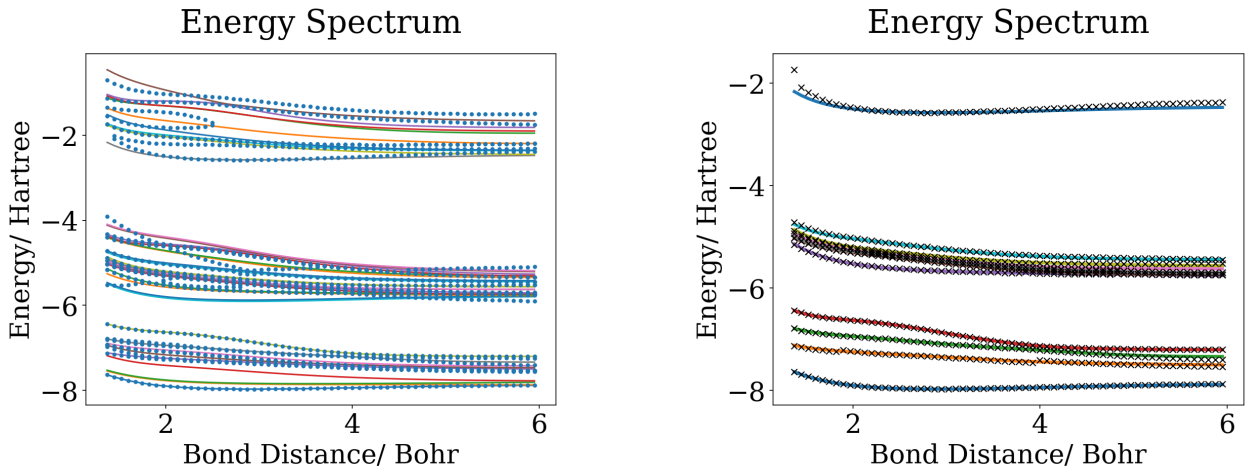

(a) (b)

Figure 5.6: (a) The solid lines describe the exact PECs. The dots correspond to real-valued CCD energies (b) PECs of LiH that can be accurately approximated by CCD energies.

Bond distances	1.375	1.6	1.9	2.2	2.5	3.1	4.0	4.9	5.8
# CCD real	33	40	33	40	34	28	30	33	28
# CCD approx.	22	25	20	23	18	19	17	18	14

Table 5.2: The number of CCD solutions along LiH dissociation for selected bond distances. By "# CCD approx." we denote the energetically relevant CCD solutions.

For the 10 PECs, we moreover compute the overlap between the CCD states and the exact eigenstates, see Figure 5.7. Remarkably, three of the four lowest energy states are well approximated both in terms of energy and states. The highest energy state stands out as well since it is well-approximated near the equilibrium, both in terms of energy as well as the eigenstate. However, as we move from the equilibrium the level of approximation deteriorates.

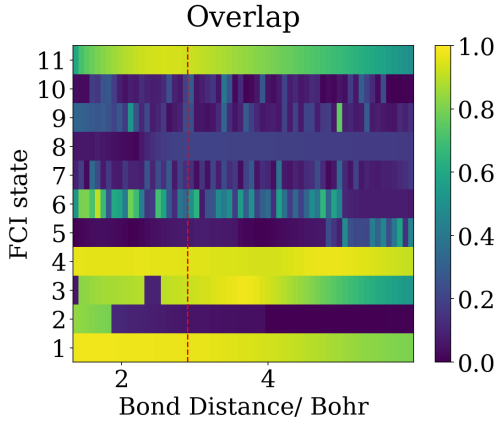

Figure 5.7: Overlaps of the CCD states with the corresponding eigenstate.

Note that poor overlap may be detected when the eigenspace is higher dimensional, that is if the corresponding eigenvalue has multiplicity two or higher. Therefore some of the higher energy states reporting bad overlap might have CCD states that are close to the actual eigenspace – or even within the eigenspace – since we are only reporting overlap with one representative from the eigenspace. A detailed investigation of this is left for future work.

LiH – Coupled Cluster Singles Doubles

We moreover perform CCSD computations on lithium hydride at the bond distance 2.875 bohr – close to the molecule's equilibrium. Recall that the truncation variety $V_{\{1,2\}}$ has dimension $\dim(V_{\{1,2\}}) = 52$ and degree $\deg(V_{\{1,2\}}) = 442\,066$, computed in Example 2.2.9. A monodromy computation revealed the CC degree to be $\approx 16\,952\,996$. The computation was stopped after about 30 days, at which point we were finding about 0 to 10 new solutions per loop. This number is therefore a numerical estimate, and serves as a lower bound for the CC degree. We compare it with the upper bound from Theorem 2.3.2, which is 23 429 498. Computing the solutions to the CCSD equations for LiH with parameter homotopy took about 13 days, yielding 15 954 solutions, 2 170 of which yield real-valued energies, and 1 280 are real-valued solutions. Visualizing all 15 954 CCSD energies shows that the energies tend to cluster around the eigenvalues of the Hamiltonian, see Figure 5.8a. We compare with the exact energy spectrum, and see that only 26 of the CCSD solutions yield energies that are close to an exact energy up to 10^{-3} hartree, see Figure 5.8b.

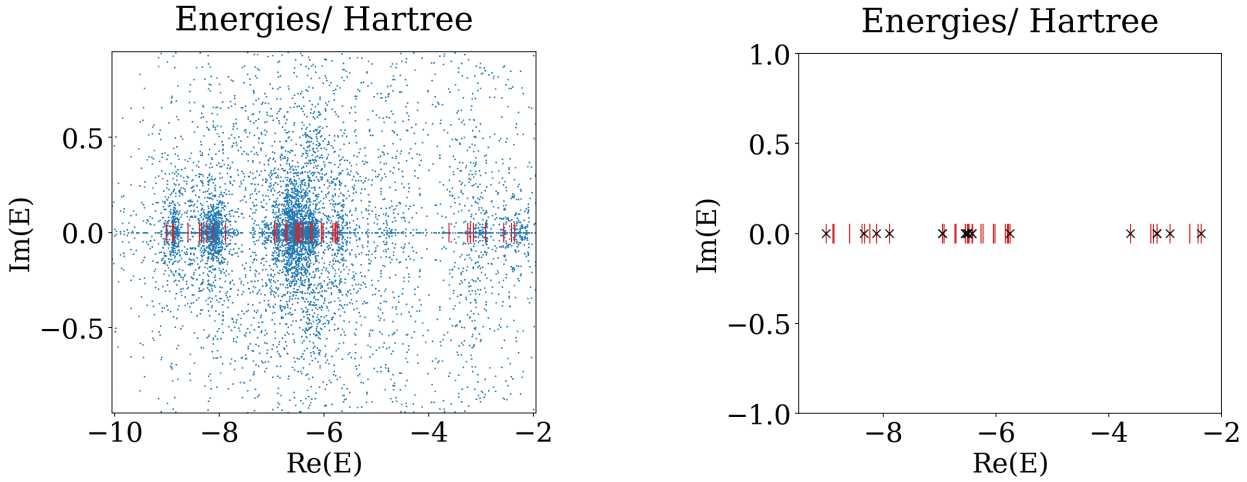

(a) (b)

Figure 5.8: (a) The eigenvalues of the Hamiltonian (red lines) together with all CCSD energies (b) CCSD energies that approximate exact energies up to 10^{-3} hartree.

For all 70 eigenstates, we compute the energetically closest CCSD state together with the overlap with the corresponding states. We find that three of the 26 energetically relevant

CCSD states have good overlaps with the targeted states, so there are at least three CCSD states that are well approximated both in terms of energy and state. Among those well approximated states is the ground state.

5.4 Dissociating Systems of Hydrogen

We now investigate the dissociation of $(H_2)_2$ planar model systems in different geometries [81]. We again consider a minimal basis at half filling, i.e. four electrons in eight spin orbitals.

$(H_2)_2$ dissociation (D_{2h} symmetry)

The bond stretching procedure for $(H_2)_2$ in D_{2h} symmetry is sketched in Figure 5.9. We consider an intra-molecular bond distance of $R = 1.4$ bohr, which corresponds to the equilibrium geometry of H_2; this is kept fixed during the dissociation process. The inter-molecular distance is varied from 1.5 to 4.0 bohr.

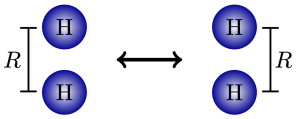

Figure 5.9: Schematic depiction of the dissociation process of $(H_2)_2$ in D_{2h} configuration.

We compare the full eigenspectrum with the CCD solutions and report the PECs that are well-approximated by CCD energies, in Figure 5.10a.

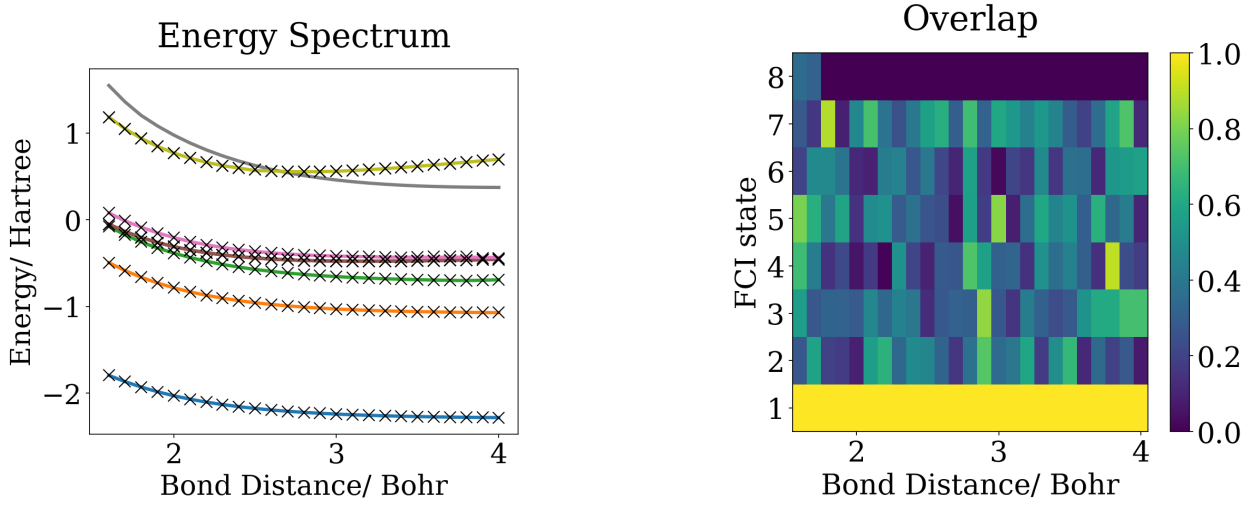

(a) (b)

Figure 5.10: (a) PECs of $(H_2)_2$ in D_{2h} symmetry that are accurately described by CCD energies. (b) Overlap of the CCD states with the corresponding eigenstate.

Here, we observe that eight PECs are well approximated by CCD energies. For these eight eigenstates, we compute the overlap with the corresponding CCD states, see Figure 5.10b. We see that the ground state is well approximated, both in terms of energy as well as the state. The following six states (i.e. states two to seven in Figure 5.10b) have intermediate overlaps with the CCD states; the last state has poor overlap. This illustrates that CC amplitudes could yield good energy approximations while providing poor approximations to the actual eigenstates [86].

In Table 5.3 we report the number of CCD solutions yielding real-valued energies and energetically relevant CCD solutions for selected bond distances. We observe that the number of CCD solutions fluctuates along the bond stretching procedure.

Bond distances	1.6	1.9	2.1	2.5	3.0	3.9
# CCD real	66	45	60	64	55	64
# CCD approx.	32	26	33	32	33	34

Table 5.3: The number of solutions along $(H_2)_2$ dissociation in D_{2h} configuration for selected bond distances. By "# CCD approx." we denote the energetically relevant CCD solutions.

$(H_2)_2$ dissociation ($D_{\infty h}$ symmetry)

We investigate the $(H_2)_2$ dissociation in $D_{\infty h}$ symmetry, see Figure 5.11 for a sketch of the dissociation process. The intra-molecular distance is again fixed at $R = 1.4$ bohr. The inter-molecular distance is varied from 1.5 to 4.0 bohr.

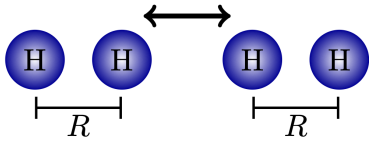

Figure 5.11: Schematic depiction of the dissociation process of $(H_2)_2$ in $D_{\infty h}$ configuration.

We compare the full eigenspectrum with the CCD solutions and identify the PECs that are accurately approximated by CCD, as shown in Figure 5.12a, where four PECs closely match the CCD energies. The overlap of these four CCD states with their respective eigenstates is analyzed in Figure 5.12b. Consistent with observations from the $(H_2)_2$ in D_{2h} configuration, the ground state demonstrates a high degree of accuracy, while the other three states exhibit intermediate to poor overlap with their targeted eigenstates.

Investigating the solution spectrum, we observe that – similar to $(H_2)_2$ in D_{2h} symmetry – the total number of CCD solutions fluctuates along the bond stretching procedure, see Table 5.4. Note that for $(H_2)_2$ in $D_{\infty h}$ symmetry, the total number of CCD solutions is lower than the number of CCD solutions for $(H_2)_2$ in D_{2h} symmetry.

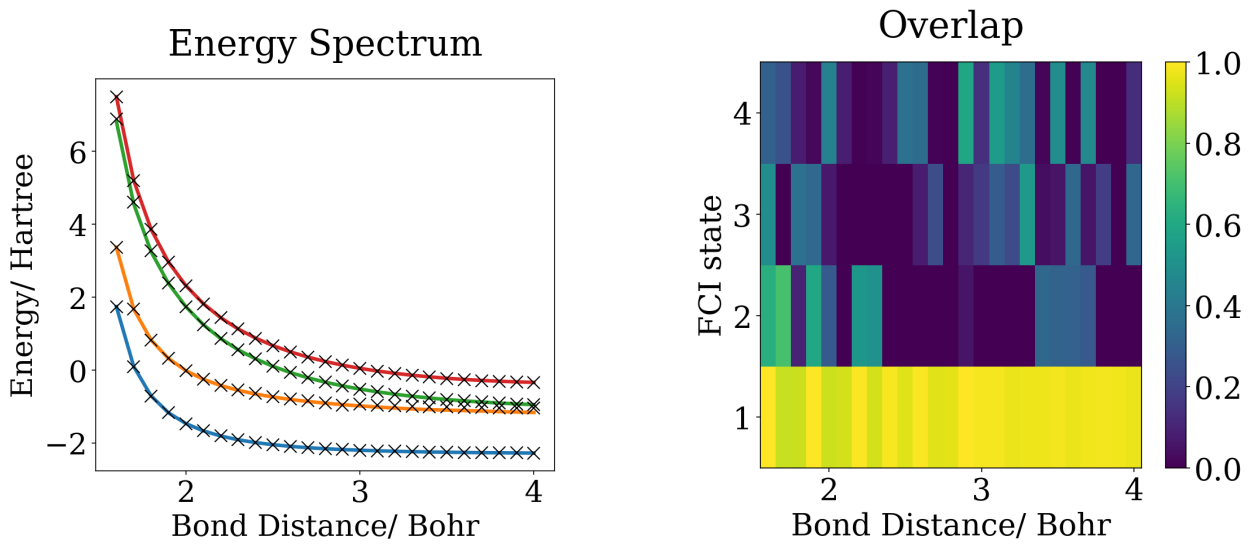

(a) (b)

Figure 5.12: (a) PECs of $(H_2)_2$ in $D_{\infty\mathbf{h}}$ symmetry that are accurately described by CCD energies. (b) Overlap of the CCD states with the corresponding eigenstate.

Bond distances	1.6	1.9	2.1	2.5	3.0	3.9
# CCD real	46	42	40	38	37	35
# CCD approx.	13	19	12	14	16	21

Table 5.4: The number of solutions along $(H_2)_2$ dissociation in $D_{\infty\mathbf{h}}$ configuration for selected bond distances. By "# CCD approx." we denote the energetically relevant CCD solutions.

H_4 distributed on a circle

We proceed by investigating a variant of the H_4 model consisting of four hydrogen atoms symmetrically distributed on a circle of radius $R = \sqrt{2}$ bohr [13, 60, 71], see Figure 5.13.

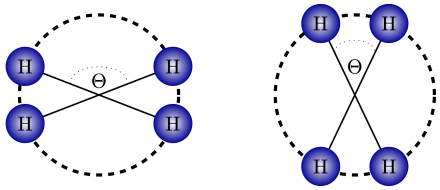

Figure 5.13: Schematic depiction of H_4 undergoing a symmetric disturbance on a circle.

We compare the full eigenspectrum with the CCD solutions and report the PECs that are well-approximated using CCD in Figure 5.14a. Note that it is well-known that for this

system CCD does not perform well in the region close to 90°, due to strong degeneracies [81]. This results in a dramatic reduction of the total number of solutions, we find three solutions at 90° and six solutions at 89°. Since the focus of this work is on the solution spectrum and potentially physically relevant solutions accessible by single-reference CC theory, we focus on cases where single-reference CC theory provides reasonable approximations and therefore excluded these points in Figure 5.14a. Outside of this challenging region, we find PECs that are well approximated by CCD. For these five PECS, we compute the overlap of the eigenstates with the corresponding CCD states, see Figure 5.14b. Consistent with the previous H_4 systems, this model system shows the effect of CCD states accurately resolving excited energies but providing poor overlap to the exact eigenstates. The only state that obtains a good approximation is the ground state.

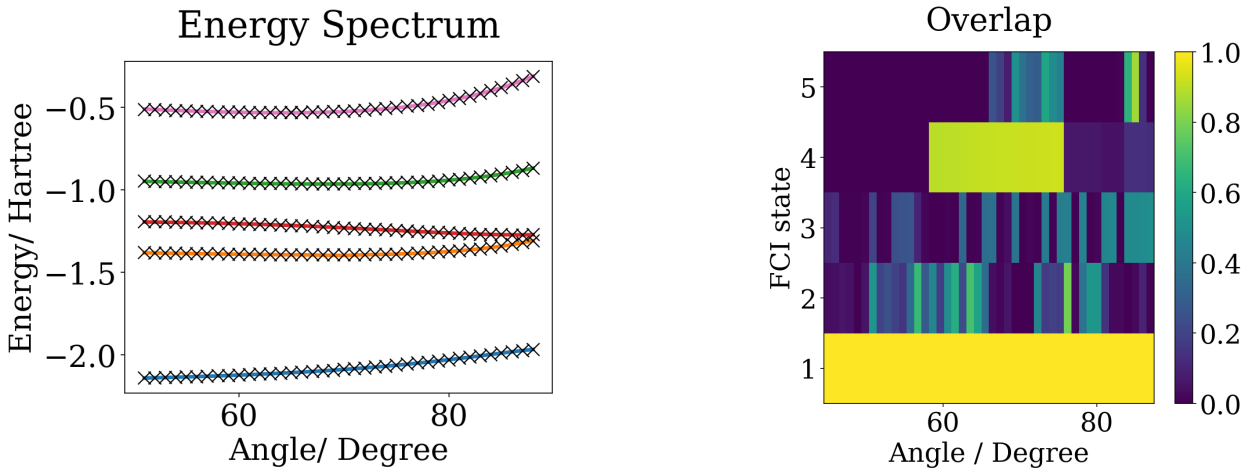

(a) (b)

Figure 5.14: (a) PECs of H_4 symmetrically distributed on a cycle that can be accurately approximated by CCD. (b) Overlap of the CCD states with the corresponding eigenstate.

Similar to $(H_2)_2$ in $D_{\infty h}$ symmetry, we observe that generic counts severely overestimate the number of CCD solutions, though this effect is further amplified for H_4 symmetrically distributed on a circle, see Table 5.5.

Angles in degrees	45	55	65	75	85
# CCD real	35	36	35	36	28
# CCD approx.	18	18	19	21	22

Table 5.5: The number of solutions of H_4 symmetrically distributed on a circle for selected bond distances. By "# CCD approx." we denote the energetically relevant CCD solutions.

We conclude this first part of the thesis with a summary of our contributions and a brief outline of our next steps. In this chapter, we described in detail the methods used to numerically solve the CC equations. An important measure of complexity in solving these systems are their CC degrees. We study the scaling of these degrees, along with a comparison of exact values with our upper bounds, as well as previously known bounds. We finish with an extensive study of two molecules, namely, lithium hydride and H_4. We numerically solve their CC equations for several variants and compare the CC solutions with the exact eigenspectrum. These are, to our knowledge, the first full computations of CC equations of this scale. This hereby concludes our research of the CC equations in first quantization. In the next part of the thesis we focus on a different formulation, known as second quantization. There, operators, such as the Hamiltonian and the cluster operator, are described as elements in a noncommutative algebra called the Fermi–Dirac algebra.

Part II

Second Quantization

Chapter 6

Algebra of Fermionic Operators

In this chapter we develop the second-quantized formalism. In this approach, many-electron systems are described on the full exterior algebra $\mathcal{F} = \wedge\mathbb{R}^n$, known as the fermionic Fock space. Observables are then also expressed in terms of creation and annihilation operators rather than as explicit matrices on $\wedge^d\mathbb{R}^n$. These operators generate the Fermi–Dirac algebra, a Clifford algebra acting on $\mathcal{F}$. We present a noncommutative Gröbner basis for the Fermi–Dirac algebra, which provides an algebraic proof of Wick's theorem, a standard result in quantum chemistry. The Fermi–Dirac algebra is isomorphic to the algebra of endomorphisms of $\mathcal{F}$, explaining why operators acting on electronic systems can be expressed in terms of creation and annihilation operators. This reformulation in second quantization does not change the physical states, but it provides a more convenient algebraic framework: highly structured observables such as the Hamiltonian admit compact and explicit expressions. This is particularly well suited for methods such as CC theory. We conclude the chapter with a detailed study of the Hamiltonian in second quantization, where we show in particular that its one-body part is an additive compound matrix. This chapter is based on Section 2 of my paper *Algebraic Varieties in Second Quantization* [101].

6.1 The Fermi–Dirac algebra

In second quantization, we extend our ambient space from the exterior product $\mathcal{H}_d \cong \wedge^d\mathbb{R}^n$ to the whole exterior algebra,

$$\mathcal{F} \cong \wedge\mathbb{R}^n \cong \bigoplus_{k=0}^{n} \mathcal{H}_k.$$

This space is called the *fermionic Fock space*. It is the exterior algebra of a Hilbert space of wave functions, discretized by molecular orbitals, see Section 1.2. We will also work with its complexification, $\wedge\mathbb{C}^n$, and its projectivization, the space of binary tensors, $\mathbb{P}(\wedge\mathbb{C}^n) \cong \mathbb{P}^{2^n-1}$. Note that here the number of spin orbitals n is fixed, but the number of particles d is not.

The standard basis vector e_p of $\mathbb{R}^n$ corresponds to the pth molecular spin orbital. The basis vectors of $\mathcal{F}$ are denoted by $e_J = e_{j_1} \wedge \cdots \wedge e_{j_k}$ with index sets $J = \{j_1, \ldots, j_k\} \subseteq [n]$.

The size of the set $k = |J|$ can vary from 0 to n. The number of basis vectors is thus 2^n. The basis is ordered by a colexicographic order on the index sets J. That is:

$$\varnothing \leq 1 \leq 2 \leq 12 \leq 3 \leq 13 \leq 23 \leq 123 \leq 4 \leq 14 \leq 24 \leq 124 \leq 34 \leq 134 \leq 234 \leq \cdots .$$

In quantum chemistry, the basis vectors of $\mathcal{F}$ are referred to as *occupation number states*, a term we will also use here. They correspond to a configuration of particles on the molecular orbitals. Recall that Pauli's exclusion principle states that two particles cannot simultaneously occupy the same spin-orbital. Hence, the basis vectors describe every configuration of particles on our electronic system. We say the pth spin orbital is *occupied* in an occupation number state e_J, if $p \in J$; otherwise it is *unoccupied*.

We now extend the terminology from first quantization, working within $\mathcal{H}_d$, to second quantization. The elements of $\mathcal{F}$ are also called *quantum states* and they can be written uniquely as a linear combination of the occupation number states:

$$\psi = \sum_{J \subseteq [n]} \psi_J e_J.$$

As with the quantum states of $\mathcal{H}_d$, the coordinates ψ_I are called Plücker coordinates, highlighting the connection to the Grassmannian and the flag variety. The Plücker coordinate, ψ_J, now corresponds to a minor of an $n \times n$ matrix Θ, taking rows $1, \ldots, k$ and columns $j_1, \ldots, j_k$, where $k = |J|$. These are the Plücker coordinates of the matrix Θ, parameterizing the complete flag spanned by the rows of Θ, [73, Chapter 14.1].

We fix the positive integer d, where $2d \leq n$, as the base number of electrons in the electronic system. As before, we call $e_{[d]}$ the *reference state*. The quantum states can be written in terms of the *configuration interaction coefficients* $c_{I,B}$, where $I \subseteq [d]$ and $B \subseteq [n] \backslash [d]$. The correspondence between the two coordinate systems is:

$$\psi_J = c_{I,B} \quad \text{where} \quad J = ([d] \backslash I) \cup B \quad \text{and} \quad I = [d] \backslash J,\ B = J \backslash [d].$$

The configuration interaction coefficient of the reference state is $c_{0,0}$. The two coordinate sets have the same cardinality, since the number of configuration interaction coefficients is

$$\sum_{m,\ell=0}^{d,n-d} \binom{d}{m} \binom{n-d}{\ell} = \sum_{k=0}^{n} \binom{n}{k} = 2^n.$$

Since we are now working in the exterior algebra, $\mathcal{F} \cong \wedge \mathbb{R}^n$, we can define *exterior and interior products*. For each basis element $e_p \in \mathbb{R}^n$ we define the following endomorphisms:

$$\begin{aligned} a_p^\dagger : \mathcal{F} \to \mathcal{F}, \quad \psi \mapsto e_p \wedge \psi &= \sum_{I \subseteq [n]} \psi_I e_p \wedge e_I \\ a_p : \mathcal{F} \to \mathcal{F}, \quad \psi \mapsto e_p \lrcorner \psi &= \sum_{I \subseteq [n]} \psi_I e_p \lrcorner e_I. \end{aligned} \tag{6.1}$$

Here $\lrcorner$ denotes the dual operation of the wedge product $\wedge$, called the hook product [44, Section 3.6], also defined in (1.18). The operators $a_p^\dagger$ and a_p in (6.1) are called the *creation* and *annihilation operators*, respectively. As the name suggests, the physical meaning of them is to create or annihilate a particle in the pth molecular spin orbital. We can extend them to endomorphisms over $\wedge\mathbb{C}^n$.

Remark 6.1.1 (Jordan–Wigner transformation)**.** We describe the $2^n \times 2^n$ matrix representations of the creation and annihilation operators, using the Jordan–Wigner transformation [57]. For an English reference on the transformation we point the reader to [78]. First, an unoccupied orbital is represented by $\begin{bmatrix}1 & 0\end{bmatrix}^T$, and an occupied orbital by $\begin{bmatrix}0 & 1\end{bmatrix}^T$. An occupation number state e_J can then be represented by a tensor product of the 2-dimensional occupied and unoccupied vectors. For example, the reference state is represented by

$$e_{[d]} \equiv \underbrace{\begin{bmatrix}0\\1\end{bmatrix} \otimes \cdots \otimes \begin{bmatrix}0\\1\end{bmatrix}}_{d \text{ times}} \otimes \underbrace{\begin{bmatrix}1\\0\end{bmatrix} \otimes \cdots \otimes \begin{bmatrix}1\\0\end{bmatrix}}_{n-d \text{ times}}.$$

The creation and annihilation operators can be represented by $2^n \times 2^n$ matrices as follows. Let

$$\sigma_z = \begin{bmatrix}1 & 0\\0 & -1\end{bmatrix}, \quad a = \begin{bmatrix}0 & 1\\0 & 0\end{bmatrix}$$

be the 2×2 *Pauli-z matrix* and *annihilation matrix*. The annihilation matrix, a, turns an occupied orbital into an unoccupied orbital by left matrix multiplication. Its adjoint, $a^\dagger$, is the *creation matrix*, turning unoccupied orbitals into occupied orbitals by left multiplication. The $2^n \times 2^n$ creation and annihilation matrices for the pth orbital are defined as tensor products:

$$a_p^\dagger = \underbrace{\sigma_z \otimes \cdots \otimes \sigma_z}_{p-1 \text{ times}} \otimes a^\dagger \otimes \underbrace{I_2 \otimes \cdots \otimes I_2}_{n-p \text{ times}}, \quad a_p = \underbrace{\sigma_z \otimes \cdots \otimes \sigma_z}_{p-1 \text{ times}} \otimes a \otimes \underbrace{I_2 \otimes \cdots \otimes I_2}_{n-p \text{ times}}.$$

Products of the creation and annihilation operators are defined via composition. These operators therefore generate a subalgebra of $\mathrm{End}(\mathcal{F})$ over $\mathbb{C}$. The defining relations of the creation and annihilation operators are anticommutation relations. Algebras generated by elements subject to such relations are examples of Clifford algebras. We therefore briefly recall the definition. A Clifford algebra associated with a quadratic form q on variables $x_1, \ldots, x_k$ is the quotient of the free associative algebra $\mathbb{C}\langle x_1, \ldots, x_k\rangle$ by the two-sided ideal

$$\langle\, x_i x_j + x_j x_i - q(x_i, x_j)1 \;:\; 1 \le i, j \le k \,\rangle,$$

where 1 is the multiplicative identity. For an in-depth introduction to Clifford algebras and their connection to physics, we refer to Chevalley's book [17].

Proposition 6.1.2. *The creation and annihilation operators span a Clifford algebra on* $\mathbb{C}\langle a_1, \ldots, a_n, a_1^\dagger, \ldots, a_n^\dagger\rangle$*, associated with the quadratic form defined by*

$$Q = \begin{bmatrix}0_n & I_n\\I_n & 0_n\end{bmatrix}.$$

We call this algebra the Fermi–Dirac algebra and denote it by FD_n*.*

Proof. The creation/annihilation operators fulfill the anticommutator relations

$$[a_p^\dagger, a_q^\dagger]_+ = a_p^\dagger a_q^\dagger + a_q^\dagger a_p^\dagger = 0,\ [a_p, a_q]_+ = a_p a_q + a_q a_p = 0,\ [a_p^\dagger, a_q]_+ = a_p^\dagger a_q + a_q a_p^\dagger = \delta_{p,q}, \quad (6.2)$$

where $\delta_{p,q}$ is the Kronecker delta function. This means they span the Fermi–Dirac algebra. □

Corollary 6.1.3. *The creation (annihilation, respectively) operators, span an isotropic vector space of dimension n, with respect to quadratic form Q. Hence, they are nilpotent of order* 1*, i.e. $(a_p^\dagger)^2 = 0$ and $a_p^2 = 0$ for all $p = 1, \ldots, n$.*

Proof. Since Q has zero blocks on the diagonal, we see that $[a_p^\dagger, a_p^\dagger]_+ = 2(a_p^\dagger)^2 = 0$ for all $p = 1, \ldots, n$. Hence the vector space spanned by the creation operators $a_p^\dagger$ is isotropic and $(a_p^\dagger)^2 = 0$. The same holds for the annihilation operators.

□

Remark 6.1.4 (Exterior algebras in the Fermi–Dirac algebra)**.** We look at a subalgebra $\mathcal{V} \subseteq \mathrm{FD}_n$, of the Fermi–Dirac algebra, generated by the n creation and annihilation operators, $a_1, \ldots, a_d, a_{d+1}^\dagger, \ldots, a_n^\dagger$. This is a Clifford algebra associated to a quadratic form, defined by a submatrix of Q, equal to the zero matrix. Hence, $\mathcal{V}$ is isomorphic to the exterior algebra $\wedge\mathbb{C}^n$. A word $\Omega \in \mathcal{V}$ of even length, $\ell(\Omega)$, commutes with any element in $\mathcal{V}$. More specifically, words Ω and Ω' in $\mathcal{V}$ fulfill the following commutator and anticommutator relations

$$[\,\Omega,\, \Omega'\,] = 0,\ \text{if } \ell(\Omega) \text{ or } \ell(\Omega') \text{ is even}, \quad [\,\Omega,\, \Omega'\,]_+ = 0,\ \text{if } \ell(\Omega) \text{ and } \ell(\Omega') \text{ are odd}.$$

Hence, even strings in $\mathcal{V}$ commute with the elements in $\mathcal{V}$. There exist 2^n subalgebras of the Fermi–Dirac algebra isomorphic to $\wedge\mathbb{C}^n$. We construct such a subalgebra by choosing either a creation or annihilation operator for each index $i \in [n]$.

Gröbner bases for commutative ideals were introduced at the end of Section 1.1. We now give the analogous definitions in the noncommutative setting. First we fix the following variable order on the creation and annihilation operators:

$$a_n > a_{n-1} > \cdots > a_1 > a_1^\dagger > a_2^\dagger > \cdots > a_n^\dagger.$$

The monomial orders on polynomial rings do not directly extend to the free associative algebra, and we therefore introduce an appropriate monomial order for our setting. The degree lexicographic order on words in the free associative algebra is defined as follows: a word $w = w_1 \cdots w_\ell$ of degree ℓ is less than word $w' = w_1' \cdots w_p'$ of degree p if $\ell < p$ or $\ell = p$ and at the first position k where the words differ, we have $w_k < w_k'$. For example

$$a_1^\dagger < a_2 < a_2^\dagger a_1^\dagger < a_1^\dagger a_2^\dagger < a_1 a_2^\dagger < a_1 a_2 < a_2 a_1 < a_2^2 < a_1^3 < a_1 a_2^2.$$

The largest term in a polynomial g of the free associative algebra is called the *initial term* of g and it is denoted by $\mathrm{in}(g)$. Let I be a two-sided ideal in $\mathbb{C}\langle a_1, \ldots, a_n, a_1^\dagger, \ldots, a_n^\dagger\rangle$. The *initial ideal* of I, denoted $\mathrm{in}(I)$, is defined as the ideal generated by the initial terms of the

polynomials in I. Explicitly, $\mathrm{in}(I) = \langle\, \mathrm{in}(g) \,:\, g \in I \,\rangle$. A set G is said to be a Gröbner basis of I, if the initial ideal of I is generated by the initial terms of G. That is

$$\mathrm{in}(I) = \langle\, \mathrm{in}(g) \,:\, g \in G \,\rangle.$$

In that case G also generates I. The standard monomials of I are the monomials not contained in the initial ideal $\mathrm{in}(I)$, or equivalently, those not divisible by the leading terms of G. As in the commutative case the standard monomials form a vector space basis for the quotient algebra $\mathbb{C}\langle a_1, \ldots, a_n, a_1^\dagger, \ldots, a_n^\dagger\rangle / I$, see Theorem 1.1.13. For a detailed introduction into noncommutative algebras and their Gröbner bases, we refer to Bergman's foundational paper on the diamond lemma for ring theory, [4], and a paper by Teo Mora on commutative and noncommutative Gröbner bases, [74].

Theorem 6.1.5 (Wick's theorem [106])**.** *The anticommutator relations in (6.2), generating the two-sided ideal that defines the Fermi–Dirac algebra, form a Gröbner basis with respect to the degree lexicographic order.*

Proof. First, we let G be the set of polynomials from (6.2), that is

$$G = \{\underline{a_i a_j} + a_j a_i \,:\, i \geq j\} \cup \{\underline{a_i^\dagger a_j^\dagger} + a_j^\dagger a_i^\dagger \,:\, i \leq j\} \cup \{\underline{a_i a_j^\dagger} + a_j^\dagger a_i - \delta_{ij} \,:\, i, j\}.$$

The initial terms are underlined. We define a *critical pair* of G to be a pair of initial terms $(\mathrm{in}(f), \mathrm{in}(f'))$ of elements f, f' in G such that $\mathrm{in}(f)u = v\mathrm{in}(f')$ for some variables u and v in $\mathbb{C}\langle a_1, \ldots, a_n, a_1^\dagger, \ldots, a_n^\dagger\rangle$. The *S-elements* are the polynomials $fu - vf'$ where $\mathrm{in}(f)$ and $\mathrm{in}(f')$ form a critical pair [74, Section 5.3]. By the diamond lemma for ring theory [4, Theorem 1.2] we only need to check that the S-elements of G have a weak Gröbner representation, see [74, Section 5.3]. First we find the critical pairs of G. They are:

$$\begin{aligned}
&(a_i a_j, a_j a_k) \text{ where } i \geq j \geq k,\ (a_i^\dagger a_j^\dagger, a_j^\dagger a_k^\dagger) \text{ where } i \leq j \leq k,\\
&(a_i a_j, a_j a_k^\dagger) \text{ where } i \geq j,\ (a_i a_j^\dagger, a_j^\dagger a_k^\dagger) \text{ where } j \leq k.
\end{aligned}$$

The S-elements then are

$$\begin{aligned}
&(a_i a_j + a_j a_i)a_k - a_i(a_j a_k + a_k a_j) = a_j a_i a_k - a_i a_k a_j\\
&(a_i^\dagger a_j^\dagger + a_j^\dagger a_i^\dagger)a_k^\dagger - a_i^\dagger(a_j^\dagger a_k^\dagger + a_k^\dagger a_j^\dagger) = a_j^\dagger a_i^\dagger a_k^\dagger - a_i^\dagger a_k^\dagger a_j^\dagger\\
&(a_i a_j + a_j a_i)a_k^\dagger - a_i(a_j a_k^\dagger + a_k^\dagger a_j - \delta_{jk}) = a_j a_i a_k^\dagger - a_i a_k^\dagger a_j + \delta_{jk} a_i\\
&(a_i a_j^\dagger + a_j^\dagger a_i - \delta_{ij})a_k^\dagger - a_i(a_j^\dagger a_k^\dagger + a_k^\dagger a_j^\dagger) = a_j^\dagger a_i a_k^\dagger - a_i a_k^\dagger a_j^\dagger - \delta_{ij} a_k^\dagger.
\end{aligned}$$

One can check that all these polynomials have a weak Gröbner representation. □

The standard monomials of the defining ideal $\langle G\rangle$ are the following monomials

$$a_B^\dagger a_I = a_{b_\ell}^\dagger \cdots a_{b_1}^\dagger a_{i_1} \cdots a_{i_m}.$$

In quantum chemistry these monomials are commonly referred to as normal ordered strings. The standard monomials form a vector space basis of the Fermi–Dirac algebra. Hence, each element in the Fermi–Dirac algebra can be written uniquely in terms of the standard monomials. We call this the *standard representation* of an element.

The free associative algebra $\mathbb{C}\langle a_1, \ldots, a_n, a_1^\dagger, \ldots, a_n^\dagger\rangle$ carries a natural $\mathbb{Z}^2$-grading, given by $\deg(a_p^\dagger) = e_1$ and $\deg(a_p) = e_2$. The ideal $\langle G\rangle$ is not homogeneous, and consequently the Fermi–Dirac algebra does not inherit this $\mathbb{Z}^2$-grading. Although FD_n is no longer graded, the standard monomials are naturally $\mathbb{Z}^2$-graded via the grading of the free algebra. This induces a graded vector space structure on the quotient, though not a graded algebra structure.

Proposition 6.1.6. *There is an isomorphism of* $\mathbb{C}$*-algebras,* $\mathrm{FD}_n \cong \mathrm{End}(\mathcal{F})$.

Proof. Recall that the Fermi–Dirac algebra is a subalgebra of $\mathrm{End}(\mathcal{F})$, so we only need to show the two have the same dimension as vector space over $\mathbb{C}$. There is a standard monomial for each pair of subsets $B \subseteq [n]$ and $I \subseteq [n]$, so the dimension of the Fermi–Dirac algebra as a vector space is $2^{2n} = \dim(\mathrm{End}(\mathcal{F}))$. □

Remark 6.1.7 (Restricting to $\mathcal{H}_d$)**.** The standard monomials of bidegree (m, m), for $0 \leq m \leq n$ preserve the grading of $\mathcal{F}$. Indeed, the subalgebra consisting of all operators that preserve this grading is generated by these standard monomials. It is isomorphic to

$$\mathrm{End}(\mathcal{H}_0) \oplus \mathrm{End}(\mathcal{H}_1) \oplus \cdots \oplus \mathrm{End}(\mathcal{H}_n), \qquad \mathcal{H}_\ell := \wedge^\ell \mathbb{C}^n.$$

We want to find the standard representation of the word $\Omega = \omega_1 \cdots \omega_k$ in the Fermi–Dirac algebra. First, we set I as the index set of the annihilation operators and B as the index set of the creation operators in Ω. Without loss of generality, we assume that $m = |I| \leq |B| = \ell$. We define the *ordered term* of Ω as

$$o(\Omega) = \mathrm{sign}(\Omega) a_B^\dagger a_I$$

where $\mathrm{sign}(\Omega)$ is the sign of the permutation $\Omega \mapsto a_B^\dagger a_I$. This is the standard representation of Ω in the exterior algebra, that is, if all the creation and annihilation operators would anticommute. However, we have relations $a_p^\dagger a_p + a_p a_p^\dagger = 1$ so the operators do not all anticommute. We define the contraction of two operators as

$$\overbrace{\omega\omega'} = \omega\omega' - o(\omega\omega').$$

The contraction is zero unless $\omega = a_p$ and $\omega' = a_p^\dagger$ for some p, then it is 1. The following proposition describes the standard representation of words in the Fermi–Dirac algebra. Specifically, the constant term is important, as it describes elements in the matrix representation.

Proposition 6.1.8. *The word $\Omega = \omega_1 \cdots \omega_k$ in FD_n has the standard representation*

$$\begin{aligned}\Omega \;=\; o(\Omega) &+ \sum_{\substack{i\in I,\, b\in B\\ i<b}} (-1)^{i+b-1} o(\omega_1 \cdots \overbrace{\omega_i \cdots \omega_b} \cdots \omega_k)\\ &+ \sum_{\substack{i<j\in I,\, b\neq c\in B\\ i<b, j<c}} (-1)^{i+j+b+c-2}(-1)^{\#cross} o(\omega_1 \cdots \overbrace{\omega_i \cdots \overbrace{\omega_j \cdots \omega_b} \cdots \omega_c} \cdots \omega_k) + \;\cdots\\ &+ \sum_{\substack{i_1<\cdots<i_m\in I,\\ b_1\neq\cdots\neq b_m\in B,\\ i_1<b_1,\ldots,i_m<b_m}} (-1)^{i_1+b_1+\cdots+i_m+b_m-m}(-1)^{\#cross} o(\overbrace{\omega_{i_1}\omega_{i_2} \cdots \overbrace{\omega_{i_j} \cdots \omega_c}\omega_{b_j} \cdots \omega_{b_1}} \cdots \omega_{b_2})\end{aligned}$$

where #cross denotes the number of crossings between contractions. Each sum corresponds to a fixed number of contractions.

A *complete matching* of the set $[2m]$ is defined to be a set of m pairs (i, j) where $i < j$ and each element in $[2m]$ appears exactly once. We say the element i is the *lefthand endpoint* of pair (i, j) and the element j is the *righthand endpoint*, see [16, Section 1]. The standard representation of Ω sums over all complete matchings of the subsets of $[2m]$ where the lefthand endpoints index annihilation operators and the righthand endpoints index creation operators.

Example 6.1.9 $(a_i a_p^\dagger a_j a_q^\dagger)$**.** We write the word $a_i a_p^\dagger a_j a_q^\dagger$ in standard representation:

$$\begin{aligned}a_i a_p^\dagger a_j a_q^\dagger &= -a_p^\dagger a_q^\dagger a_i a_j + o(\overbrace{a_i a_p^\dagger} a_j a_q^\dagger) + o(\overbrace{a_i a_p^\dagger a_j a_q^\dagger}) + o(a_i a_p^\dagger \overbrace{a_j a_q^\dagger}) + \overbrace{a_i a_p^\dagger} \overbrace{a_j a_q^\dagger}\\ &= -a_p^\dagger a_q^\dagger a_i a_j - \delta_{ip} a_q^\dagger a_j + \delta_{iq} a_p^\dagger a_j - \delta_{jq} a_p^\dagger a_i + \delta_{ip}\delta_{jq}.\end{aligned}$$

Remark 6.1.10. The standard representation of a word Ω in the Fermi–Dirac algebra has a constant term only if there is an equal number of annihilation operators and creation operators, that is $|I| = |B| = m$. In that case, the parity of the first sign of the constant term in Proposition 6.1.8 is

$$i_1 + b_1 + \cdots + i_m + b_m - m = \sum_{i=1}^{2m} i - m = \frac{(2m+1)2m}{2} - m = 2m^2.$$

The constant term of the standard representation of Ω is then equal to

$$\sum (-1)^{\#\mathrm{cross}} \overbrace{\omega_{i_1}\omega_{i_2} \cdots \overbrace{\omega_{i_j} \cdots \omega_{b_j}} \cdots \omega_{b_1}} \cdots \omega_{b_2}$$

where we sum over all complete matchings of $[2m]$ where the lefthand endpoints are annihilation operators and the righthand endpoints are creation operators. We note that a fully contracted word Ω, is a product of δ-functions. Therefore only complete matchings of the form $\{\, (a_p, a_p^\dagger) \,:\, p \,\}$ produce a nonzero contraction. Such a matching exists only if the annihilation index set I equals the creation index set B.

Remark 6.1.11. The matrix representation of the word Ω in FD_n is explicitly $(e_I^\dagger \Omega e_J)_{I,J\subseteq[n]}$. We notice that the occupation number state e_I can be written as $e_I = a_{i_1}^\dagger \cdots a_{i_m}^\dagger 1$. Hence the entries of this matrix are the following evaluations

$$e_I^\dagger \Omega e_J = 1^\dagger a_{i_m} \cdots a_{i_1} \Omega a_{j_1}^\dagger \cdots a_{j_\ell}^\dagger 1.$$

For every standard monomial $a_B^\dagger a_I$ we get $1^\dagger a_B^\dagger a_I 1 = 0$. Hence, we see that the entries of the matrix are constant terms of standard representations:

$$e_I^\dagger \Omega e_J = \text{constant term of standard rep. of } a_{i_m} \cdots a_{i_1} \Omega a_{j_1}^\dagger \cdots a_{j_\ell}^\dagger.$$

By Remark 6.1.10, the constant term is given by the sum over all complete matchings of the form $\{(a_p, a_p^\dagger)\}$, with each matching contributing a sign $(-1)^{\#\text{cross}}$. If no complete matching exists, the constant term is zero.

Electronic operators such as the Hamiltonian and the cluster operator — introduced in the following sections — are elements of the Fermi–Dirac algebra. By employing Remark 6.1.11, the coupled cluster equations, seen in Section 7.4, can be derived through straightforward combinatorial manipulations. In contrast, the first-quantized operators are represented by $\binom{n}{d} \times \binom{n}{d}$ matrices. Then, deriving approximation schemes like the coupled cluster equations requires prohibitively large matrix multiplications. This highlights the advantage of the second-quantized formalism, where corollaries of Wick's theorem enable efficient derivations. This framework for CC theory was first established in the foundational 1966 paper [18].

6.2 The Hamiltonian Operator

An *observable* in quantum chemistry refers to a physical quantity that can be measured and is represented mathematically by a self-adjoint (Hermitian) operator on the space of quantum states. A central observable is the electronic Hamiltonian. In the real setting considered here, self-adjointness reduces to symmetry. When extending scalars to $\mathbb{C}$ for algebraic-geometric purposes, we retain this symmetry condition and do not impose conjugate-linearity; thus, operators are treated as symmetric rather than Hermitian, see Remark 1.2.7.

Representing the Hamiltonian as an operator on the Hilbert space $\mathcal{H}_d \cong \wedge^d \mathbb{R}^n$, as is illustrated in Remark 1.2.5, is commonly referred to as *first quantization*. While conceptually straightforward, the resulting operators act on a high-dimensional space and quickly become difficult to manipulate. An equivalent and more flexible formulation is obtained by working in the fermionic Fock space and expressing observables as polynomials in the creation and annihilation operators, i.e. *second quantization* [42]; see also the subsection in Section 1.2 with the same name. This approach is justified by Proposition 6.1.6, stating that the Fermi–Dirac algebra is isomorphic to the algebra of endomorphisms of $\mathcal{F}$.

The electronic Hamiltonian is defined as the following element in the Fermi–Dirac algebra:

$$H = \sum_{p,q=1}^{n} h_{p,q}\, a_p^\dagger a_q + \frac{1}{2} \sum_{p,q,r,s=1}^{n} v_{p,q,r,s}\, a_p^\dagger a_r^\dagger a_s a_q. \tag{6.3}$$

The first sum is called the *one body operator*, and the second sum the *two body operator*. The coefficients $h_{p,q}$ form a symmetric $n\times n$ matrix h, and the coefficients $v_{p,q,r,s}$ form an $n\times n\times n\times n$ tensor v, which is pairwise symmetric in the first two indices, last two indices, and invariant under interchange of these two pairs. Hence, $h \in \mathrm{Sym}^2(\mathbb{C}^n)$ and $v \in \mathrm{Sym}^2(\mathrm{Sym}^2(\mathbb{C}^n))$.

Consider an electronic system with a basis $\{\xi_1, \ldots, \xi_n\}$ of molecular orbitals, as described in Section 1.2. The entries of the coefficient tensors h and v can be evaluated using PySCF [99]:

$$h_{p,q} = -\int_X \xi_p(\mathbf{x}) \left(\frac{\Delta}{2} + \sum_j \frac{Z_j}{|\mathbf{r} - R_j|} \right) \xi_q(\mathbf{x}) d\mathbf{x}, \;\; v_{p,q,r,s} = \int_{X\times X} \frac{\xi_p(\mathbf{x})\xi_q(\mathbf{x})\xi_r(\mathbf{x}')\xi_s(\mathbf{x}')}{|\mathbf{r} - \mathbf{r}'|} d\mathbf{x} d\mathbf{x}'. \tag{6.4}$$

Here $X = \mathbb{R}^3 \times \{\uparrow, \downarrow\}$ and $\mathbf{x} = (\mathbf{r}, s)$, where $\mathbf{r}$ denotes the spatial position of an electron and s its spin. The constant Z_j is the charge of the jth nucleus and $R_j \in \mathbb{R}^3$ its position. The above integrals satisfy exactly the symmetry relations stated for h and v; in fact, these symmetry properties arise directly from the structure of the integrals. A generic Hamiltonian is then an operator of the form (6.3) whose coefficients are taken to be generic elements in $\mathrm{Sym}^2(\mathbb{C}^n)$ and $\mathrm{Sym}^2(\mathrm{Sym}^2(\mathbb{C}^n))$ respectively.

Remark 6.2.1 (Skew-symmetrization)**.** We recall that the creation operators pairwise anticommute, and the same holds for the annihilation operators. In particular,

$$a_p^\dagger a_r^\dagger a_s a_q = -a_r^\dagger a_p^\dagger a_s a_q = -a_p^\dagger a_r^\dagger a_q a_s = a_r^\dagger a_p^\dagger a_q a_s.$$

We therefore skew-symmetrize the tensor v in the index pairs (p, r) and (q, s). We define a new $n \times n \times n \times n$ tensor w by setting

$$w_{pr,qs} = v_{p,q,r,s} - v_{r,q,p,s} - v_{p,s,r,q} + v_{r,s,p,q} = 2v_{p,q,r,s} - 2v_{r,q,p,s},$$

where the last equality follows from the symmetries of v. Note that when passing from v to w, we change the order of the indices from (p, q, r, s) to (p, r, q, s). The tensor w is pairwise skew-symmetric in the first two indices and in the last two indices. Furthermore, the symmetries of v give rise to an additional symmetry $w_{pr,qs} = w_{qs,pr}$ of w. Hence $w \in \mathrm{Sym}^2(\wedge^2\mathbb{C}^n)$, which captures all symmetry properties of w. We can now rewrite the Hamiltonian in terms of w:

$$H = \sum_{p,q=1}^{n} h_{p,q}\, a_p^\dagger a_q + \sum_{\substack{1\le p<r\le n \\ 1\le q<s\le n}} w_{pr,qs}\, a_p^\dagger a_r^\dagger a_s a_q.$$

The Hamiltonian is the sum of two homogeneous operators of bidegree $(1, 1)$ and $(2, 2)$, respectively. In particular, it preserves the grading of $\mathcal{F}$ and therefore, by Remark 6.1.7, restricts to an endomorphism of $\mathcal{H}_d$.

Example 6.2.2 $(d = 2, n = 4)$**.** We look at the matrix representation of H restricted to the second exterior power $\wedge^2\mathbb{C}^4 \cong \mathbb{C}^6$. The one body part has the form

$$\begin{bmatrix} h_{11}+h_{22} & h_{23} & h_{24} & -h_{13} & -h_{14} & 0 \\ h_{23} & h_{11}+h_{33} & h_{34} & h_{12} & 0 & -h_{14} \\ h_{24} & h_{34} & h_{11}+h_{44} & 0 & h_{12} & h_{13} \\ -h_{13} & h_{12} & 0 & h_{22}+h_{33} & h_{34} & -h_{24} \\ -h_{14} & 0 & h_{12} & h_{34} & h_{22}+h_{44} & h_{23} \\ 0 & -h_{14} & h_{13} & -h_{24} & h_{23} & h_{33}+h_{44} \end{bmatrix}.$$

This is an additive compound matrix of the 4×4 symmetric matrix h. We look at the matrix representation of the two body operator:

$$\begin{bmatrix} w_{12,12} & w_{12,13} & w_{12,14} & w_{12,23} & w_{12,24} & w_{12,34} \\ w_{12,13} & w_{13,13} & w_{13,14} & w_{13,23} & w_{13,24} & w_{13,34} \\ w_{12,14} & w_{13,14} & w_{14,14} & w_{14,23} & w_{14,24} & w_{14,34} \\ w_{12,23} & w_{13,23} & w_{14,23} & w_{23,23} & w_{23,24} & w_{23,34} \\ w_{12,24} & w_{13,24} & w_{14,24} & w_{23,24} & w_{24,24} & w_{24,34} \\ w_{12,34} & w_{13,34} & w_{14,34} & w_{23,34} & w_{24,34} & w_{34,34} \end{bmatrix}.$$

This is a generic symmetric matrix of size 6×6 and it is the $(pr|qs)$ flattening of the tensor w.

We define the *kth additive compound operator* $A^{(k)}$ of a linear operator $A : \mathbb{C}^n \to \mathbb{C}^n$ as the unique derivation on the exterior space $\wedge^k\mathbb{C}^n$ given by:

$$A^{(k)}(v_1 \wedge \cdots \wedge v_k) = \sum_{i=1}^{k} v_1 \wedge \cdots \wedge Av_i \wedge \cdots \wedge v_k.$$

This operator represents the induced Lie algebra representation of $\mathfrak{gl}_n(\mathbb{C})$ on $\wedge^k\mathbb{C}^n$, obtained by differentiating the natural Lie group action of $\mathrm{GL}_n(\mathbb{C})$. The corresponding $\binom{n}{k} \times \binom{n}{k}$ matrix is called the *kth additive compound matrix* of the $n \times n$ matrix A.

Let $\lambda_1, \ldots, \lambda_n$ be the eigenvalues of A. It follows directly from the multi-linearity of the wedge product that the eigenvalues of $A^{(k)}$ are the sums $\lambda_{i_1} + \cdots + \lambda_{i_k}$, where $I \in \binom{[n]}{k}$. Moreover, if the corresponding eigenvectors $w_{i_1}, \ldots, w_{i_k}$ of A are linearly independent, then the corresponding eigenvectors of $A^{(k)}$ are given by the k-fold wedge products $w_{i_1} \wedge \cdots \wedge w_{i_k}$. If A is diagonalizable, these wedge products account for all eigenvectors of $A^{(k)}$. Since such eigenvectors are decomposable tensors, they correspond to points on the Grassmannian $\mathrm{Gr}(k, n)$ via the Plücker embedding. See e.g. [90, Lemma 3.3].

Proposition 6.2.3. *The one body operator of H restricted to $\mathcal{H}_d$ is represented by the dth additive compound matrix of the $n \times n$ symmetric matrix h.*

Proof. We see that the action of the one body operator on a basis vector e_I is:

$$\sum_{p,q=1}^{n} h_{p,q}\, a_p^\dagger a_q e_I = \sum_{\substack{1 \le p \le n \\ q \in I}} h_{p,q}\, a_p^\dagger a_q e_I = \sum_{k=1}^{d} e_{i_1} \wedge \cdots \wedge he_{i_k} \wedge \cdots \wedge e_{i_d} = h^{(d)} e_I,$$

proving our claim. □

The matrix representation of the one body operator over the full Fock space then becomes a direct sum of additive compound matrices, $h^{(0)} \oplus h^{(1)} \oplus \cdots \oplus h^{(n)}$.

Remark 6.2.4. In practice, the coefficient matrix h is real and symmetric and therefore it is diagonalizable. The eigenvalues and eigenvectors of the $\binom{n}{d} \times \binom{n}{d}$ one-body matrix $h^{(d)}$ can thus be determined directly from the eigenspectrum of the $n \times n$ matrix h. This substantially reduces the complexity of computing eigenstates of one-body operators.

The eigenvectors of physical one-body operators are therefore *separable states*, that is, rank-one tensors. Under the Plücker embedding, they lie on the Grassmannian $\mathrm{Gr}(d, n)$. In contrast, most physically relevant ground states are *entangled* (tensors of rank > 1). This is precisely because the inclusion of the two-body term in H changes the structure of the problem. The Hamiltonian is no longer an additive compound operator, and its eigenvectors are no longer constrained to the Grassmannian; in particular, they need not be separable. Determining the eigenspectrum of H then becomes exponentially more difficult in n. This is illustrated in Example 6.2.2, where the two-body operator is represented by a generic symmetric matrix and so the eigenvalue problem cannot be reduced. Approximating such states is a central problem in quantum chemistry and forms the focus of this work.

In this chapter we focused on the Fermi–Dirac algebra, a Clifford algebra of linear operators acting on the Fock space. We described a noncommutative Gröbner basis for this algebra, and with that, we were able to provide an explicit standard representation of its elements, as well as their matrix representation. Moreover, this enabled us to show that the Fermi–Dirac algebra is isomorphic to the space of endomorphisms on the Fock space. Hence, every operator acting on quantum states can be represented within the Fermi–Dirac algebra. This is known as second quantization. We conclude the chapter by describing the Hamiltonian in second quantized form. In the next chapter we shift our focus back to the CC equations. We reformulate them in second quantized form, which allows us to expand to electronic systems with varying number of electrons, i.e. ionization. This reveals many new truncation varieties, such as the flag variety and the spinor variety.

Chapter 7

Fock Space Coupled Cluster Theory

In this chapter we formulate the coupled cluster equations in the second-quantized formalism. In many ways, this chapter parallels Chapter 2, where the equations were developed in the first-quantized setting. By extending to the full exterior algebra (the fermionic Fock space), we move beyond fixed-electron systems (fixed–N) and allow for processes such as ionization and electron attachment. This more general formulation also naturally encompasses well-known approximation schemes such as Fock space coupled cluster (FSCC) and equation of motion coupled cluster (EOM-CC). We introduce the Fock space truncation varieties, which generalize the truncation varieties defined in Section 2.2. This reveals well-known varieties, such as the flag and spinor varieties. Moreover, we classify all cases in which the coupled cluster degree coincides with the degree of the graph of the exponential parameterization, see also Section 4.3. The most notable examples include the singleton truncation varieties (such as those arising in CCD) and the Schubert-like truncation varieties, including the Grassmannian, the flag variety, and the spinor variety. This chapter is based on [101].

7.1 Exponential Parameterization

This section generalizes Section 2.1 from first quantization to second quantization. There we defined a parameterization of the quantum states, called the exponential parameterization, writing them as a column of the exponential matrix of a $\binom{n}{d} \times \binom{n}{d}$ matrix $T(t)$. We assumed the particle number was fixed, a convention denoted by fixed–N, and worked within the dth grading of the Fock space, $\mathcal{H}_d \cong \wedge^d \mathbb{R}^n$. By extending to the whole Fock space we are able to describe the exponential parameterization explicitly using an element of the Fermi–Dirac algebra. Now we do not make the assumption that the number of particles is conserved. Indeed, this framework also captures cases of ionization and electron attachment. Our goal is to build a general algebraic framework for coupled cluster theory encapsulating fixed–N coupled cluster as well as Fock space coupled cluster (FSCC) [30, 58, 65] and equations of motion coupled cluster (EOM-CC) [93], as can be seen in Remark 7.2.1 and Theorem 7.2.9. See Table 1.1 for classification of the common CC variants.

We consider the subalgebra $\mathcal{V}$ of the Fermi–Dirac algebra, defined in Remark 6.1.4. It is isomorphic to the exterior algebra, i.e. $\mathcal{V} \cong \wedge\mathbb{C}^n$. As a vector space it is generated by the standard monomials $a_B^\dagger a_I$, where $I \subseteq [d]$ and $B \subseteq [n]\backslash[d]$. Its coordinate vectors are denoted by $t = (t_{I,B})$, and they are called *cluster amplitudes*. We present a canonical isomorphism between the complex Fock space $\mathcal{F} \cong \wedge\mathbb{C}^n$ and the subalgebra $\mathcal{V}$ of the Fermi–Dirac algebra:

Proposition 7.1.1. *The following map is a vector space isomorphism*

$$\Phi : \mathcal{V} \to \mathcal{F}, \quad T \mapsto Te_{[d]}.$$

The isomorphism above gives rise to alternative coordinate vectors $x = (x_J)$ of $\mathcal{V}$ obtained from $t_{I,B}$ by the correspondence $J = ([d]\backslash I) \cup B$. It also gives rise to the alternative coordinates $c = (c_{I,B})$ of the Fock space $\mathcal{F}$, defined in Section 6.1.

The algebra $\mathcal{V}$ is defined as a quotient of the free associative algebra by a homogeneous ideal and therefore it inherits the $\mathbb{Z}^2$-grading on the free algebra, defined in Section 6.1. This gives rise to a $\mathbb{Z}^2$-grading on the exterior algebra, called the *excitation grading*. Specifically, we define the *annihilation level* a and *creation level* c of a standard basis vector e_J as

$$a(e_J) = a(J) = |[d]\backslash J| \quad \text{and} \quad c(e_J) = c(J) = |J\backslash[d]|.$$

The pair $(a(e_J), c(e_J))$ is called the *excitation level* of e_J. Tautologically, for a standard basis monomial $a_B^\dagger a_I$ of $\mathcal{V}$, these levels are simply given by $|I|$ and $|B|$. This is an alternative grading to the canonical *particle number grading* of the exterior algebra, which assigns a total degree of $|J|$ to the basis element e_J.

A *cluster operator* $T(t)$ is an element of $\mathcal{V}$ with a zero constant coefficient, i.e. $t_{0,0} = 0$. In symbols:

$$T(t) = \sum_{\substack{I\subseteq[d],\, B\subseteq[n]\backslash[d] \\ |I|+|B|>0}} t_{I,B} a_{b_\ell}^\dagger \cdots a_{b_1}^\dagger a_{i_1} \ldots a_{i_m} = \sum_{\substack{I\subseteq[d],\, B\subseteq[n]\backslash[d] \\ |I|+|B|>0}} t_{I,B} a_B^\dagger a_I.$$

The matrix representation of $T(t)$ is called the *cluster matrix*. Since $T(t) \in \mathcal{V}$ has a zero constant term, each term of $T(t)$ has at least one operator $a_p^\dagger$ where $p \in [n]\backslash[d]$ or a_p where $p \in [d]$. Therefore by the pigeonhole principle the cluster matrix $T(t)$ is nilpotent of order n, i.e. $T(t)^{n+1} = 0$. We can therefore define the matrix exponential of $T(t)$ as a finite sum

$$\exp(T(t)) = \sum_{k=0}^{n} \frac{1}{k!} T(t)^k.$$

See Section 2.1 and [36, Section 3] for a more detailed overview of $T(t)$ and its properties. We define the *exponential parameterization* as the following map

$$\mathcal{V} \to \mathcal{F}, \;\; t \mapsto \psi = \exp(T(t))e_{[d]}. \tag{7.1}$$

The transformation (7.1) gives a formula for the quantum states ψ in terms of the cluster amplitudes t. To be precise, each of the 2^n coordinates ψ_J is a polynomial $\psi_J(t)$ in the 2^n unknowns $t_{I,B}$. In the definition (7.1), we assumed that $t_{0,0} = 0$ and $\psi_{[d]} = 1$. Geometrically, this means that we work in affine spaces $\mathcal{V}'$ and $\mathcal{F}'$, both of which are identified with $\mathbb{C}^{2^n-1}$. Later, we extend (7.1) to a birational automorphism of the projective space $\mathbb{P}^{2^n-1}$. The reference coordinates $x_{[d]} = t_{0,0}$ and $\psi_{[d]} = c_{0,0}$ will then serve as homogenizing variables.

Example 7.1.2 ($d = 2$, $n = 4$)**.** We look at the case when we have four spin orbitals and two base particles. The cluster matrix is the 16×16 matrix of the form:

$$T(t) = \begin{bmatrix}
0 & t_{1,0} & t_{2,0} & t_{12,0} & 0 & 0 & 0 & 0 & 0 & 0 & 0 & 0 & 0 & 0 & 0 & 0 \\
0 & 0 & 0 & -t_{2,0} & 0 & 0 & 0 & 0 & 0 & 0 & 0 & 0 & 0 & 0 & 0 & 0 \\
0 & 0 & 0 & t_{1,0} & 0 & 0 & 0 & 0 & 0 & 0 & 0 & 0 & 0 & 0 & 0 & 0 \\
0 & 0 & 0 & 0 & 0 & 0 & 0 & 0 & 0 & 0 & 0 & 0 & 0 & 0 & 0 & 0 \\
t_{0,3} & t_{1,3} & t_{2,3} & t_{12,3} & 0 & t_{1,0} & t_{2,0} & t_{12,0} & 0 & 0 & 0 & 0 & 0 & 0 & 0 & 0 \\
0 & -t_{0,3} & 0 & t_{2,3} & 0 & 0 & 0 & -t_{2,0} & 0 & 0 & 0 & 0 & 0 & 0 & 0 & 0 \\
0 & 0 & -t_{0,3} & -t_{1,3} & 0 & 0 & 0 & t_{1,0} & 0 & 0 & 0 & 0 & 0 & 0 & 0 & 0 \\
0 & 0 & 0 & t_{0,3} & 0 & 0 & 0 & 0 & 0 & 0 & 0 & 0 & 0 & 0 & 0 & 0 \\
t_{0,4} & t_{1,4} & t_{2,4} & t_{12,4} & 0 & 0 & 0 & 0 & 0 & t_{1,0} & t_{2,0} & t_{12,0} & 0 & 0 & 0 & 0 \\
0 & -t_{0,4} & 0 & t_{2,4} & 0 & 0 & 0 & 0 & 0 & 0 & 0 & -t_{2,0} & 0 & 0 & 0 & 0 \\
0 & 0 & -t_{0,4} & -t_{1,4} & 0 & 0 & 0 & 0 & 0 & 0 & 0 & t_{1,0} & 0 & 0 & 0 & 0 \\
0 & 0 & 0 & t_{0,4} & 0 & 0 & 0 & 0 & 0 & 0 & 0 & 0 & 0 & 0 & 0 & 0 \\
t_{0,34} & t_{1,34} & t_{2,34} & t_{12,34} & -t_{0,4} & -t_{1,4} & -t_{2,4} & -t_{12,4} & t_{0,3} & t_{1,3} & t_{2,3} & t_{12,3} & 0 & t_{1,0} & t_{2,0} & t_{12,0} \\
0 & t_{0,34} & 0 & -t_{2,34} & 0 & t_{0,4} & 0 & -t_{2,4} & 0 & -t_{0,3} & 0 & t_{2,3} & 0 & 0 & 0 & -t_{2,0} \\
0 & 0 & t_{0,34} & t_{1,34} & 0 & 0 & t_{0,4} & t_{1,4} & 0 & 0 & -t_{0,3} & -t_{1,3} & 0 & 0 & 0 & t_{1,0} \\
0 & 0 & 0 & t_{0,34} & 0 & 0 & 0 & -t_{0,4} & 0 & 0 & 0 & t_{0,3} & 0 & 0 & 0 & 0
\end{bmatrix}.$$

The level zero variable $t_{0,0}$ does not appear and the level four variable $t_{12,34}$ only appears once. The matrix is not lower triangular, unlike the cluster matrices defined in Section 2.1. However, it is nilpotent of order 3, so $T(t)^3 = 0$. The fourth column of the exponential matrix is of the form

$$\psi = \exp(T(t))e_{12} = \begin{bmatrix}
t_{12,0} \\
-t_{2,0} \\
t_{1,0} \\
1 \\
t_{0,3}t_{12,0} - t_{2,0}t_{1,3} + t_{1,0}t_{2,3} + t_{12,3} \\
t_{2,3} \\
-t_{1,3} \\
t_{0,3} \\
t_{0,4}t_{12,0} - t_{2,0}t_{1,4} + t_{1,0}t_{2,4} + t_{12,4} \\
t_{2,4} \\
-t_{1,4} \\
t_{0,4} \\
t_{12,0}t_{0,34} - t_{1,4}t_{2,3} + t_{1,3}t_{2,4} + t_{12,34} \\
-t_{2,0}t_{0,34} + t_{0,4}t_{2,3} - t_{0,3}t_{2,4} - t_{2,34} \\
t_{1,0}t_{0,34} - t_{0,4}t_{1,3} + t_{0,3}t_{1,4} + t_{1,34} \\
t_{0,34}
\end{bmatrix}.$$

Proposition 7.1.3. *The exponential parameterization is bijective and has a polynomial inverse.*

Proof. First we notice that at level zero we have $\psi_{[d]} = 1$ and at level one we have $t_{j,0} = \pm\psi_{[d]\setminus\{j\}}$ and $t_{0,b} = \pm\psi_{[d]\cup\{b\}}$. If ψ_J has level r then we can write ψ_J as $\pm t_{I,B}$, where $I = [d]\setminus J$ and $B = J\setminus[d]$, plus a polynomial in variables t of level $< r$. Each of these lower level t's can now be replaced with a polynomial in ψ, by the induction hypothesis. This yields a representation for $t_{I,B}$ as $\pm\psi_J$ plus a polynomial in lower level ψ-coordinates. □

The polynomials $\psi_{[2d]\setminus[d]}$ are called the *master polynomials*. For example, when $d = 3$ and $n = 6$, we have the following master polynomial $\psi_{456}(t)$:

$$\begin{aligned}
&t_{23,0}t_{0,56}t_{1,4} - t_{23,0}t_{0,46}t_{1,5} + t_{23,0}t_{0,45}t_{1,6} - t_{13,0}t_{0,56}t_{2,4} + t_{13,0}t_{0,46}t_{2,5} - t_{13,0}t_{0,45}t_{2,6}\\
&+t_{12,0}t_{0,56}t_{3,4} - t_{1,6}t_{2,5}t_{3,4} + t_{1,5}t_{2,6}t_{3,4} - t_{12,0}t_{0,46}t_{3,5} + t_{1,6}t_{2,4}t_{3,5} - t_{1,4}t_{2,6}t_{3,5}\\
&+t_{12,0}t_{0,45}t_{3,6} - t_{1,5}t_{2,4}t_{3,6} + t_{1,4}t_{2,5}t_{3,6} + t_{0,56}t_{123,4} - t_{0,46}t_{123,5} + t_{0,45}t_{123,6}\\
&+t_{23,0}t_{1,456} - t_{13,0}t_{2,456} + t_{12,0}t_{3,456} + t_{3,6}t_{12,45} - t_{3,5}t_{12,46} + t_{3,4}t_{12,56}\\
&-t_{2,6}t_{13,45} + t_{2,5}t_{13,46} - t_{2,4}t_{13,56} + t_{1,6}t_{23,45} - t_{1,5}t_{23,46} + t_{1,4}t_{23,56} + t_{123,456}.
\end{aligned}$$

It has 31 terms. We compare them to the 16 terms of the master polynomial from Example 2.1.3. All the terms of the master polynomial in first quantization do appear in the master polynomial above. However, in second quantization we have extra terms, such as $t_{23,0}t_{0,56}t_{1,4}$, which have variables indexed by sets I and B where $|I| \neq |B|$. Recall that the monomials in the master polynomials in first quantization are indexed by uniform block permutations of $[2d]$, see Theorem 2.1.5. The variables t in the master polynomials above are also indexed by subsets of $[2d]$, that is, for $K \subseteq [2d]$ we have variable $t_{K\cap[d],K\setminus[d]}$. In particular, the monomials of the master polynomial in second quantization are indexed by set partitions of $[2d]$.

The other polynomials $\psi_I(t)$ in the exponential parameterization are relabelings of the master polynomials, see e.g. Example 7.1.2 where all the entries of the exponential map are relabelings of the two master polynomials $\psi_2(t) = t_{1,2}$ and $\psi_{34}(t) = t_{12,0}t_{0,34} - t_{1,4}t_{2,3} + t_{1,3}t_{2,4} + t_{12,34}$. The variables t in $\psi_I(t)$ are indexed by subsets of the symmetric difference $I \oplus [d]$, and the monomials are indexed by set partitions of $I \oplus [d]$. In particular, if $|I \oplus [d]| = 2k$ is even, $\psi_I(t)$ is a relabeling of master polynomial $\psi_{[2k]\setminus[k]}(t)$. If $|I \oplus [d]| = 2k - 1$ is odd, we add a formal element $\varnothing$ to the index set, and the polynomial $\psi_I(t)$ is also a relabeling of the master polynomial $\psi_{[2k]\setminus[k]}(t)$. We illustrate this with an example:

Example 7.1.4 ($n = 5$, $d = 2$)**.** There are $2^5 = 32$ polynomials $\psi_I(t)$. Polynomials like

$$\begin{aligned}
&\psi_{35}(t) = t_{12,0}t_{0,35} - t_{1,5}t_{2,3} + t_{1,3}t_{2,5} + t_{12,35}, \quad \psi_{1345}(t) = t_{0,45}t_{2,3} - t_{0,35}t_{2,4} + t_{0,34}t_{2,5} + t_{2,345},\\
&\psi_{45}(t) = t_{12,0}t_{0,45} - t_{1,5}t_{2,4} + t_{1,4}t_{2,5} + t_{12,45}, \quad \psi_{2345}(t) = t_{0,45}t_{1,3} - t_{0,35}t_{1,4} + t_{0,34}t_{1,5} + t_{1,345}
\end{aligned}$$

are relabelings of the master polynomial $\psi_{34}(t) = t_{12,0}t_{0,34} - t_{1,4}t_{2,3} + t_{1,3}t_{2,4} + t_{12,34}$. The following polynomials are also relabelings of $\psi_{34}(t)$, but a formal element is added to the index set $I \oplus \{1, 2\}$ to obtain a one-to-one correspondence with $\{1, 2, 3, 4\}$:

$$\begin{aligned}
&\psi_5(t) = t_{12,0}t_{0,5} - t_{1,5}t_{2,0} + t_{1,0}t_{2,5} + t_{12,5}, \quad \psi_{235}(t) = t_{1,0}t_{0,35} - t_{0,5}t_{1,3} + t_{0,3}t_{1,5} + t_{1,35},\\
&\psi_{12345}(t) = t_{0,34}t_{0,5} - t_{0,35}t_{0,4} + t_{0,45}t_{0,3} + t_{0,345}.
\end{aligned}$$

The indexing sets here are $\{\varnothing, 1, 2, 5\}$, $\{\varnothing, 1, 3, 5\}$ and $\{\varnothing, 3, 4, 5\}$ respectively. The formal element $\varnothing$ is not shown when writing out the polynomials. The polynomial $\psi_{345}(t)$ has 31 terms and it is a relabeling of the master polynomial $\psi_{456}(t)$.

The number of terms in the master polynomials can be found in *The On-Line Encyclopedia of Integer Sequences*. Namely, it is the sequence

$$1, 4, 31, 379, 6\,556, 150\,349, 4\,373\,461 \quad \text{for} \quad d = 1, 2, 3, 4, 5, 6, 7 \qquad \text{(A005046)}$$

This is the number of even set partitions of $[2d]$. We recall that an *even set partition* of a set $[2d]$ is a set partition $\pi = \{\pi_1, \ldots, \pi_k\}$ of $[2d]$ into blocks of even cardinality, that is each block π_i has even length $|\pi_i|$. We can identify the monomials that appear in the polynomials $\psi_I(t)$ with such partitions. To that end, write the monomial corresponding to set partition π as

$$t_\pi = t_{\pi_1 \cap [d], \pi_1 \setminus [d]} \cdots t_{\pi_k \cap [d], \pi_k \setminus [d]} \quad \text{or} \quad x_\pi = x_{\pi_1 \oplus [d]} \cdots x_{\pi_k \oplus [d]}.$$

Theorem 7.1.5. *The master polynomials $\psi_{[2d]\setminus[d]}(t)$ are linear combinations of the monomials t_π, where π is an even partition of $[2d]$. More specifically, we get*

$$\psi_{[2d]\setminus[d]}(t) = \sum_{\substack{\pi \vdash [2d] \\ \pi \text{ even}}} \operatorname{sign}(\pi) t_\pi,$$

where the sign of π is the product of the signs of the following two permutations

$$[d] \mapsto (\pi_1 \cap [d], \ldots, \pi_k \cap [d]), \quad [2d]\setminus[d] \mapsto (\pi_1 \setminus [d], \ldots, \pi_k \setminus [d]).$$

Proof. By Remark 6.1.11 we can write

$$\begin{aligned}\psi_{[2d]\setminus[d]}(t) &= e^\dagger_{[2d]\setminus[d]} \exp(T(t)) e_{[d]} \\ &= \sum_{k=1}^{d} \frac{1}{k!} \sum_{\substack{I_i \subseteq [d], \\ B_i \subseteq [2d]\setminus[d]}} t_{I_1, B_1} \cdots t_{I_k, B_k} 1^\dagger a_{2d} \cdots a_{d+1} a^\dagger_{B_1} a_{I_1} \cdots a^\dagger_{B_k} a_{I_k} a^\dagger_1 \cdots a^\dagger_d 1.\end{aligned}$$

By Remark 6.1.10, only those ordered collections, $((I_i, B_i))_{i=1}^k$, contribute for which the blocks $I_i \sqcup B_i$ are pairwise disjoint and satisfy $\bigsqcup_{i=1}^k (I_i \sqcup B_i) = [2d]$. Thus each contributing term corresponds to an ordered set partition of $[2d]$.

Fix an unordered set partition $\pi = \{I_1 \sqcup B_1, \ldots, I_k \sqcup B_k\}$. In the above sum, all $k!$ orderings of its blocks appear. Since the creation and annihilation operators anti-commute, permuting two blocks changes the corresponding operator product by a sign. Hence, the contributions arising from the different orderings of π are either all equal or cancel pairwise. By Remark 6.1.4, cancellation occurs precisely when π contains at least two blocks of odd cardinality. In that case the total contribution vanishes. If all blocks of π have even cardinality, then all $k!$ orderings produce the same term. The factor $1/k!$ in the exponential expansion

therefore cancels the factor $k!$ and π contributes exactly once. Consequently, the sum reduces to a sum over even set partitions $\pi \vdash [2d]$:

$$\psi_{[2d]\setminus[d]}(t) = \sum_{\substack{\pi \vdash [2d] \\ \pi \text{ even}}} t_\pi 1^\dagger a_{2d} \cdots a_{d+1} a^\dagger_{B_1} a_{I_1} \cdots a^\dagger_{B_k} a_{I_k} a^\dagger_1 \cdots a^\dagger_d 1.$$

The number of crossings in $a_{2d} \cdots a_{d+1} a^\dagger_{B_1} a_{I_1} \cdots a^\dagger_{B_k} a_{I_k} a^\dagger_1 \cdots a^\dagger_d$ is the sum of the number of inversions of the two permutations defined in the statement of the theorem. □

As a direct result, we see that the degree of the polynomial $\psi_I(t)$ depends only on the symmetric difference $I \oplus [d]$. That is $\deg \psi_I(t) = \lceil \frac{1}{2} |I \oplus [d]| \rceil$.

The exponential parameterization is a nonlinear bijection and its inverse is also defined by polynomials. Just as for the polynomials $\psi_I(t)$ in the forward map, each inverse polynomial $t_{I,B}(\psi) = x_J(\psi)$ is a relabeling of an inverse master polynomial $x_{[2k]\setminus[k]}(\psi)$, where $|J \oplus [d]| = 2k, 2k-1$. We use the coordinates $c_{I,B}$ instead of ψ_J and write monomials in c corresponding to set partitions $\pi = \{\pi_1, \ldots, \pi_k\}$ as we do for t. Then for each even set partition ρ we get

$$(-1)^\nu \operatorname{sign}(\rho) c_\rho = \sum_{\pi \le \rho} \operatorname{sign}(\pi) t_\pi,$$

where $\nu = \binom{d}{2} - \sum_{r=1}^k \binom{|\rho_r \cap [d]|}{2}$. An analogous identification can be found in the proof of Theorem 2.1.5, where the sign ν appears as well. The Möbius function for even set partitions of $[2d]$ is $\mu(\pi) = (-1)^{k-1}(k-1)!$, where $\pi = \{\pi_1, \ldots, \pi_k\}$. With Möbius inversion we get

$$x_{[2d]\setminus[d]}(c) = \sum_{\substack{\pi \vdash [2d] \\ \pi \text{ even}}} (-1)^{\nu+k-1} (k-1)! \operatorname{sign}(\pi) c_\pi.$$

This proof is analogous to the proof of Theorem 2.1.5.

7.2 Fock Space Truncation Varieties

We define the *truncation grid*

$$\mathcal{G} = \{(m, \ell) \ : \ 0 \le m \le d \quad \text{and} \quad 0 \le \ell \le n - d\} \setminus \{(0,0)\}$$

enumerating feasible excitation levels. The corresponding construct in first quantization is the diagonal of the truncation grid or the set $[d] \cong \{(m,m) : 1 \le m \le d\}$. For a proper subset $\sigma \subsetneq \mathcal{G}$, called the *level set*, we define a subspace $\mathcal{V}_\sigma$ of $\mathcal{V}$ spanned by occupation number states e_J with excitation level in σ. Explicitly we set

$$\mathcal{V}_\sigma = \operatorname{span}\{\, e_J \ : J \subseteq [n] \ \text{ and } \ (a(e_J), c(e_J)) \ \in \ \sigma \,\}.$$

The projection of cluster amplitudes $t \in \mathcal{V}$ onto $\mathcal{V}_\sigma$ is denoted t_σ. As a variety in the projectivization of $\mathcal{V}$, $\mathbb{P}(\mathcal{V}) \cong \mathbb{P}^{2^n-1}$, the subspace $\mathcal{V}_\sigma$ is the vanishing set of the linear ideal

$$\langle\, x_J : J \subseteq [n] \text{ and } (a(J), c(J)) \in \mathcal{G}\backslash\sigma \,\rangle \subseteq \mathbb{C}[x_J : J \subseteq [n]].$$

We look at the restriction of the exponential map to the subspace $\mathcal{V}_\sigma$:

$$\mathcal{V}_\sigma \to \mathcal{F}, \quad t_\sigma \mapsto \psi = \exp(T(t_\sigma))e_{[d]}.$$

It is injective and maps $\mathcal{V}_\sigma$ into the Fock space $\mathcal{F}$, which further maps to the projective space $\mathbb{P}(\mathcal{F}) \cong \mathbb{P}^{2^n-1}$, see Remark 1.1.8. The *Fock space truncation variety* V_σ is defined as the closure of the image of $\mathcal{V}_\sigma$ under this map to $\mathbb{P}^{2^n-1}$. The varieties live in the projective space of binary tensors. Since the exponential map is injective, the dimension of the truncation variety is equal to the dimension of the subspace $\mathcal{V}_\sigma$. In symbols:

$$\dim(V_\sigma) = \dim(\mathcal{V}_\sigma) = |\{J : (a(J), c(J)) \in \sigma\}| = \sum_{(m,\ell)\in\sigma} \binom{d}{m}\binom{n-d}{\ell}.$$

In the case when the level set σ is a subset of the diagonal of the truncation grid, i.e. $\sigma = \{(k,k) : k\} \subseteq [d]$, we obtain the truncation varieties from Section 2.2, embedded into the projective space of binary tensors $\mathbb{P}^{2^n-1}$. Those truncation varieties contain quantum states of electronic systems with a fixed number of electrons. When we relax the particle-number conservation we work with truncation varieties corresponding to level sets not lying on the diagonal. The truncation varieties defined in this Section extend the truncation varieties defined in Section 2.2 from fixed-N CC to broader approximation schemes.

Remark 7.2.1. In Fock-space coupled cluster (FSCC) theory, one allows for ionization and electron attachment. Consider ionization and the approximation schemes FSCCS, FSCCD, and FSCCSD. In these cases we work with quantum states lying on the truncation varieties corresponding to level sets $\sigma = \{(1,0),(1,1)\}, \{(2,1),(2,2)\}, \{(1,0),(2,1),(1,1),(2,2)\}$, respectively. When electron attachment is considered, the quantum states lie on the truncation varieties corresponding to level sets $\sigma = \{(0,1),(1,1)\}, \{(1,2),(2,2)\}, \{(0,1),(1,2),(1,1),(2,2)\}$. See Table 1.1 for the classification of the common CC variants in the different formulations.

Example 7.2.2 ($d = 2$, $n = 4$)**.** The truncation grid is the set

$$\mathcal{G} = \{(0,1),(0,2),(1,0),(1,1),(1,2),(2,0),(2,1),(2,2)\}.$$

This is a set of size 8. Therefore, we have $2^8 - 2 = 254$ choices of non-empty proper level sets $\sigma \subsetneq \mathcal{G}$. Hence, there are 254 truncation varieties in $\mathbb{P}^{15}$ for 2 base electrons in 4 orbitals. The truncation varieties corresponding to $\sigma = \{(1,1)\}, \{(2,2)\}, \{(1,1),(2,2)\}$ are respectively isomorphic to the truncation varieties $V_{\{1\}}, V_{\{2\}}$ and $V_{\{1,2\}}$ defined in Section 2.2, embedded into $\mathbb{P}^{15}$. We do not obtain 254 distinct varieties since some of the truncation varieties are isomorphic. For example, the truncation variety corresponding to $\{(0,1),(1,1)\}$ is isomorphic

to the truncation variety corresponding to $\{(1,0),(1,1)\}$, see Theorem 7.2.3. We also note that 119 of the 254 truncation varieties are linear subspaces, see upcoming Theorem 7.2.5. Also, 74 truncation varieties fulfill the hypothesis of Theorem 7.4.1 and their CC degree is the degree of the graph of the exponential map.

For d base electrons and n orbitals, the truncation grid $\mathcal{G}$ has cardinality $(d+1)(n-d+1)-1 = dn+n-d^2$. The number of truncation varieties V_σ is $2^{dn+n-d^2}-2$. Some of these varieties are isomorphic. With that being said, we present an isomorphism between truncation varieties, known as the particle-hole formalism:

Proposition 7.2.3. *Fix a subset $\sigma \subsetneq \mathcal{G}$ and let $n \geq 2d$. There is a linear isomorphism between the truncation varieties V_σ for (d,n) and $V_{\overline{\sigma}}$ for $(n-d,n)$, where $\overline{\sigma} = \{(\ell,m) : (m,\ell) \in \sigma\}$.*

Proof. This isomorphism is obtained through the following relabeling of Plücker coordinates:

$$J \mapsto J' = \{n+1-j : j \notin J\}.$$

This is the same relabeling used in an analogous isomorphism in Proposition 2.2.7. □

Let $\overline{x}_J(\psi)$ denote the homogenization of $x_J(\psi)$ using homogenizing variable $\psi_{[d]}$.

Theorem 7.2.4. *The homogeneous prime ideal of the truncation variety $V_\sigma \subseteq \mathbb{P}^{2^n-1}$ is the following saturation, which is analogous to Theorem 2.2.2:*

$$I(V_\sigma) \;=\; \langle\, \overline{x}_J(\psi) \;:\; (a(J),c(J)) \in \mathcal{G}\backslash\sigma \,\rangle : \langle\, \psi_{[d]} \,\rangle^\infty.$$

In particular, the ideal of the restriction of V_σ to the affine chart $\mathbb{C}^{2^n-1} = \{\psi_{[d]} = 1\}$ of projective space $\mathbb{P}^{2^n-1}$ is the complete intersection

$$I(V_\sigma) + \langle\, \psi_{[d]} - 1 \,\rangle = \langle\, x_J(\psi) \;:\; (a(J),c(J)) \in \mathcal{G}\backslash\sigma \,\rangle.$$

The proof of the theorem stated here above is analogous to the proof of Theorem 2.2.2 and is therefore omitted here.

For the sake of the next theorem, we define a partial order $\preceq$ on the truncation grid $\mathcal{G}$. We say excitation level (m,ℓ) is less than or equal to excitation level (k,p), $(m,\ell) \preceq (k,p)$ if the creation and annihilation levels fulfill $m \leq k$, $\ell \leq p$ respectively, and either $m+\ell$ is even or $k+p$ is odd. One can check that this is in fact a partial order. The level sets σ and $\mathcal{G}\backslash\sigma$ can be defined as posets with the same partial order $\preceq$. We say $\sigma \subseteq \mathcal{G}$ is *closed under addition with respect to partial order* $\preceq$ if for $(m,\ell),(k,p) \in \sigma$, where $(m,\ell),(k,p) \preceq (m+k,\ell+p) \in \mathcal{G}$, then $(m+k,\ell+p) \in \sigma$. The following result generalizes Theorem 2.2.10, where we assume particle-number conservation. Then σ is a totally ordered set in a totally ordered truncation grid $[d]$. We emphasize that the truncation grid should not be confused with the posets introduced in [23]. In that setting, a partial order is defined on the indexing sets $I \in \binom{[n]}{d}$, whereas here we define a partial order on the excitation levels of the indexing set $I \subseteq [n]$.

Theorem 7.2.5. *The variety V_σ is linear if and only if σ is closed under addition with respect to the partial order defined above. In other words, V_σ is linear if and only if for all $(m,\ell),(k,p) \in \sigma$ such that either $m+\ell$ or $k+p$ is even, then either*

$$(m,\ell)+(k,p) \notin \mathcal{G} \quad \text{or} \quad (m,\ell)+(k,p) \in \sigma.$$

Proof. We identify V_σ with its restriction to the affine chart $\mathcal{F}' = \mathbb{C}^{2^n-1}$. We assume that σ is closed under addition with respect to $\preceq$. We first prove by induction that $\psi_I = 0$ for all $I \subseteq [n]$ whose creation and annihilation level is in $\mathcal{G}\backslash\sigma$.

Since σ is closed under addition with respect to $\preceq$, the minimal elements of $\mathcal{G}\backslash\sigma$ are a subset of the minimal elements of $\mathcal{G}$. The minimal elements of $\mathcal{G}$ are $(0,1),(1,0),(2,0),(0,2)$ and $(1,1)$. These are also all pairs with total level ≤ 2. We take a set J of creation and annihilation level (m,ℓ) that is minimal in $\mathcal{G}\backslash\sigma$. Then $x_J(\psi) = \psi_J = 0$, since $|J \oplus [d]| \leq 2$.

Now consider a set K with creation and annihilation level $(m,\ell) \in \mathcal{G}\backslash\sigma$. Then

$$x_K(\psi) = \sum_{\substack{\pi \vdash K \oplus [d] \\ \pi \text{ even}}} \pm\psi_\pi = \pm\psi_K + \sum_j a_j \psi_{K_1^{(j)}} \cdots \psi_{K_{r_j}^{(j)}} = 0$$

where $a_j \in \mathbb{Z}^*$ and $K_s^{(j)} = \pi_s^{(j)} \oplus [d]$ such that $\pi^{(j)} = \{\pi_1^{(j)}, \ldots, \pi_{r_j}^{(j)}\}$ forms an even set partition of $K \oplus [d]$. We let $(m_s^{(j)}, \ell_s^{(j)})$ be the excitation levels of the sets $K_s^{(j)}$, and notice that $\sum_{s=1}^{r_j} (m_s^{(j)}, \ell_s^{(j)}) = (m,\ell)$ for each j. If K has an odd level then $(m_s^{(j)}, \ell_s^{(j)}) \preceq (m,\ell)$ for all s and j. If K has an even level, then all the $(m_s^{(j)}, \ell_s^{(j)})$ have an even level, so $(m_s^{(j)}, \ell_s^{(j)}) \preceq (m,\ell)$ as well. Since σ is closed under addition with respect to $\preceq$, there must be one pair $(m_s^{(j)}, \ell_s^{(j)}) \in \mathcal{G}\backslash\sigma$ for each j. Thus by induction there is some s for each j such that $\psi_{K_s^{(j)}} = 0$ and hence $0 = x_K(\psi) = \psi_K$. The defining equations of the truncation variety are therefore linear of the form $\psi_K = 0$ where $K \in \mathcal{G}\backslash\sigma$.

We now assume σ is not closed under addition with respect to $\preceq$. We take a minimal $(m,\ell) \in \mathcal{G}\backslash\sigma$, such that there are some $(i,r),(j,s) \in \sigma$ where $(i,r),(j,s) \preceq (m,\ell)$ in $\mathcal{G}$ and $(m,\ell) = (i,r)+(j,s)$. Consider a polynomial $x_K(\psi)$ vanishing on V_σ where K has excitation level (m,ℓ). Fix any degree-compatible monomial order. The initial monomial of $x_K(\psi)$ has degree > 1, and we write

$$\text{in}(x_K(\psi)) = \psi_{K_1} \cdots \psi_{K_r}, \qquad \text{where } r \geq 2.$$

Assume some element in the initial ideal of $\mathcal{I}(V_\sigma)$ divides $\text{in}(x_K(\psi))$. This element must divide a monomial of some generator $x_J(\psi)$, where $(a(J), c(J)) \in \mathcal{G}\backslash\sigma$. Without loss of generality we may pick the divisor to be a monomial of $x_J(\psi)$. We also see that $(a(J), c(J)) \preceq (m,\ell)$, so by the same argument as above we get $x_J(\psi) = \psi_J$. We also obtain the relation $\psi_J = 0$ and thus $\psi_J \nmid \text{in}(x_K(\psi))$, a contradiction. Hence $\text{in}(x_K(\psi))$ is a minimal generator for the initial ideal of $\mathcal{I}(V_\sigma)$. This cannot be an initial ideal for a linear variety, and therefore V_σ itself is not linear. □

Example 7.2.6 ($d = 3$, $n = 6$)**.** There are $2^{15} - 2 = 32\,766$ truncation varieties in $\mathbb{P}^{63}$. Among those, 4 790 are linear by Theorem 7.2.5 and 2 186 fulfill the hypothesis of Theorem 7.4.1. We look at a few chosen cases of non-linear truncation varieties:

- $\sigma = \{(1,0),(2,0)\}$:
  This is a hypersurface of the subspace generated by basis vectors e_J where $J \subseteq [3]$. Its defining equation is the homogeneous inverse coordinate $\overline{x}_\varnothing(\psi)$.

- $\sigma = \{(1,0),(2,0),(1,1),(0,1),(0,2)\}$:
  Its ideal is generated by 364 quadrics. It has dimension 21 and degree 33 592.

- $\sigma = \{(1,0),(2,1),(1,1),(2,2)\}$:
  Its ideal is generated by 7 quadrics and the 30 coordinates indexed by sets of size $0, 1, 4, 5$ or 6. It has dimension 30 and degree 43, see Example 7.5.3.

- $\sigma = \{(1,0),(1,1),(0,1)\}$:
  This is the partial flag variety $\mathcal{F}\ell(2,3,4,6)$. It has dimension 15 and degree 4 550. It is the zero set of 281 quadrics and the 14 coordinates indexed by sets of size $0, 1, 5$ or 6.

- $\sigma = \{(2,0),(1,1),(0,2)\}$:
  This is the spinor variety S_+ for a 12 dimensional space. It has dimension 15 and degree 286. It is the zero set of 66 quadrics and the 32 coordinates indexed by even sets.

When extending from the exterior power $\mathcal{H}_d$ to the full Fock space $\mathcal{F}$, we allow the number of particles in the electronic system to vary. In this broader setting, we encounter several well-known algebraic varieties, such as the flag variety and the spinor variety, which will be examined in detail in the next section. Beyond these classical examples, the framework developed here naturally gives rise to many new and intriguing varieties, whose study is of independent mathematical interest, regardless of their origins in quantum chemistry.

Remark 7.2.7. The linear span of a truncation variety $V_\sigma \subseteq \mathcal{F}$ is the vector space generated by its elements, that is, the smallest linear subspace of $\mathcal{F}$ containing V_σ. In general, this span can be a proper subspace of $\mathcal{F}$. For instance, the truncation varieties considered in Section 2.2 are contained in the dth graded component $\mathcal{H}_d \subseteq \mathcal{F}$.

It is natural to ask which graded subspaces of $\mathcal{F}$ contain a given truncation variety V_σ. In particular, it is of interest to find the smallest subspaces that are direct sums of homogeneous components $\mathcal{H}_k \cong \wedge^k\mathbb{C}^n$. If such a graded subspace is written as $\bigoplus_{k\in S}\mathcal{H}_k$, then the index set $S \subseteq \{0,\dots,n\}$ describes the possible particle numbers of quantum states in V_σ. In Example 7.2.6, the corresponding supports are $S = \{0,1,2,3\}, \{1,2,3,4,5,6\}, \{2,3\}, \{2,3,4\}, \{1,3,5\}$, for the respective level sets.

Returning to the motivating context, it is natural to ask which of the Fock space truncation varieties are most relevant for practical applications in quantum chemistry.

Remark 7.2.8 (EOM-CC for ionization and electron attachment)**.** In addition to FSCC, the equation-of-motion coupled cluster method (EOM-CC) also addresses ionized electronic systems and electron attachment, see [93, Chapter 13.4]. There the *ionization operator* is introduced. It is defined as the following operator:

$$T(t_\iota) = \sum_{\substack{I\subseteq[d],\, B\subseteq[n]\setminus[d]\\ |I|=|B|+1}} t_{I,B} a^\dagger_{b_m}\cdots a^\dagger_{b_1} a_{i_1}\ldots a_{i_{m+1}} = \sum_{\substack{I\subseteq[d],\, B\subseteq[n]\setminus[d]\\ |I|=|B|+1}} t_{I,B} a^\dagger_B a_I$$

where $\iota = \{(k+1,k) : 0 \le k \le d-1\}$, is the subdiagonal of the truncation grid. This operator is an element of the Fermi–Dirac algebra. The ionized quantum states are then parameterized by the following exponential map

$$\mathcal{V}_\iota \times \mathcal{V}_{[d]} \to \wedge^{d-1}\mathbb{C}^n, \quad (t_\iota, t_{[d]}) \mapsto \psi = T(t_\iota)\exp T(t_{[d]})e_{[d]}. \tag{7.2}$$

Here $[d] = \{(k,k) : 1 \le k \le d\}$ is the diagonal of the truncation grid. We truncate the ionized quantum states using subsets of the subdiagonal ι and the diagonal $[d]$ and restricting the exponential map (7.2) accordingly. The projectivization of the closure of the image of this restriction is a variety of $\mathbb{P}(\wedge^{d-1}\mathbb{C}^n) \cong \mathbb{P}^{\binom{n}{d-1}-1}$. In most applications, we fix a positive integer k and truncate with subsets $\{(i+1,i) : 0 \le i \le k\} \subseteq \iota$ and $[k] \subseteq [d]$. Electron attachment is treated dually using the particle-hole formalism. We define the *electron attachment operator* as $T(t_\epsilon)$ where $\epsilon = \bar{\iota} = \{(k,k+1) : 0 \le k \le d-1\}$ is the super diagonal.

At first glance, the varieties in Remark 7.2.8 arising from EOM-CC appear incompatible with our construction of truncation varieties. The following theorem, however, demonstrates how these two frameworks are related.

Theorem 7.2.9. *Let $\tau \subseteq \iota$ be a subset on the subdiagonal and $\sigma \subseteq [d]$ a subset on the diagonal of the truncation grid. The variety of truncated ionized EOM-CC quantum states, parameterized by the restriction of (7.2) to $\mathcal{V}_\tau \times \mathcal{V}_\sigma$, is equal to the restriction of the truncation variety $V_{\tau\cup\sigma}$ to $\mathbb{P}(\wedge^{d-1}\mathbb{C}^n)$. A dual statement holds for electron attachment.*

Proof. The truncation variety $V_{\tau\cup\sigma}$ is parameterized by the following restriction of the exponential map

$$\mathcal{V}_{\tau\cup\sigma} \to \mathcal{F}, \quad t_{\tau\cup\sigma} \mapsto \psi = \exp\left(T(t_\tau) + T(t_\sigma)\right)e_{[d]}.$$

The operator $T(t_\sigma)$ is a linear combination of words of even length. Hence, by Remark 6.1.4, the operators $T(t_\sigma)$ and $T(t_\tau)$ commute. Thus we can factor the exponential operator:

$$\exp\left(T(t_\tau) + T(t_\sigma)\right) = \exp T(t_\tau)\exp T(t_\sigma).$$

Moreover, the operator $T(t_\tau)$ is a linear combination of monomials of odd degree so, by Remark 6.1.4, $T(t_\tau)$ is nilpotent of order 1. We can write $\exp T(t_\tau) = 1 + T(t_\tau)$. We rewrite the restricted exponential map:

$$\mathcal{V}_{\tau\cup\sigma} \to \mathcal{F}, \quad t_{\tau\cup\sigma} \mapsto \psi = \exp T(t_\sigma)e_{[d]} + T(t_\tau)\exp T(t_\sigma)e_{[d]}.$$

The first summand of the parameterization is an element in the dth exterior power $\wedge^d\mathbb{C}^n$ and the second summand is an element of $\wedge^{d-1}\mathbb{C}^n$. This proves our statement. □

7.3 Flag Varieties and Spinor Varieties

We define a *flag* $F_\bullet$ in $\mathbb{C}^n$ to be a sequence of subspaces increasing with respect to inclusion, that is:

$$F_\bullet : \{0\} = F_0 \subsetneq F_1 \subsetneq \cdots \subsetneq F_k = \mathbb{C}^n.$$

We say a flag is *complete* if $d_i = \dim(F_i) = i$ for all $0 \leq i \leq k$; otherwise, it is called a *partial* flag. The *partial flag variety* $\mathcal{F}l(d_1, \ldots, d_k, n) \subseteq \mathbb{P}(\wedge\mathbb{C}^n) \cong \mathbb{P}^{2^n-1}$ is the set of all flags in $\mathbb{C}^n$ with dimensions $d_1 \leq d_2 \leq \cdots \leq d_k$.

We recall that a d dimensional subspace of $\mathbb{C}^n$ can be parametrized by the maximal minors of a $d \times n$ matrix Θ with entries in $\mathbb{C}$. The matrix Θ has full rank and since row reduction does not change the row span of Θ we may assume that $\Theta = [I_d \,|\, M]$, where M is a $d \times (n-d)$ matrix. Similarly, for a flag $F_\bullet$ we look at a full rank $d_k \times n$ matrix $\Theta = [I_{d_k \times d_1} | M]$ where the first d_i rows of Θ span F_i. The flag $F_\bullet$ can then be parametrized by the maximal minors of the first d_i rows of Θ for each i. We refer to Ezra Miller's and Bernd Sturmfels' book [73, Section 14.1] for a more detailed introduction to flag varieties.

Remark 7.3.1. We describe an alternative parameterization of the flag variety $\mathcal{F}l(d-1, d, d+1, n)$. We look at the $(d+1) \times (n+1)$ matrix

$$\Theta = \begin{bmatrix} 1 & 0 & \cdots & 0 & \theta_{1,d+1} & \cdots & \theta_{1,n} & \theta_{1,n+1} \\ 0 & 1 & \cdots & 0 & \theta_{2,d+1} & \cdots & \theta_{2,n} & \theta_{2,n+1} \\ \vdots & \vdots & \ddots & \vdots & \vdots & \ddots & \vdots & \vdots \\ 0 & 0 & \cdots & 1 & \theta_{d,d+1} & \cdots & \theta_{d,n} & \theta_{d,n+1} \\ 0 & 0 & \cdots & 0 & \theta_{d+1,d+1} & \cdots & \theta_{d+1,n} & 0 \end{bmatrix}.$$

The first d rows of Θ span a d dimensional subspace E of $\mathbb{C}^{n+1}$. The intersection of E with the orthogonal space $(e_{n+1})^\perp \cong \mathbb{C}^n$ is generically isomorphic to a $d-1$ dimensional subspace of $\mathbb{C}^n$, which we will denote by F_{d-1}. We now look at the submatrix $\tilde{\Theta}$ of Θ taking only the first n columns. Its row span is a subspace F_{d+1} of $\mathbb{C}^n$, which is generically of dimension $d+1$. Also, the first d rows of $\tilde{\Theta}$ span a d dimensional subspace $F_d \subseteq F_{d+1}$. Therefore, we have obtained a partial flag

$$F_{d-1} \subseteq F_d \subseteq F_{d+1} \subseteq \mathbb{C}^n.$$

This flag is parametrized by the $d \times d$ minors of the first d rows of Θ and the $(d+1) \times (d+1)$ minors of the first n columns of Θ. These minors define a birational parameterization of the partial flag variety $\mathcal{F}l(d-1, d, d+1, n)$.

The partial flag variety $\mathcal{F}l(d-1, d, d+1, n)$ appears as a truncation variety. Before stating the general theorem, we first illustrate this in an example.

Example 7.3.2. Let $d = 2$, $n = 4$ and $\sigma = \{(1,1), (0,1), (1,0)\}$. The cluster matrix $T(t_\sigma)$ is a 16×16 matrix, nilpotent of order 2. The truncation variety has dimension

$$\dim(V_\sigma) = \binom{2}{1} + \binom{2}{1} + \binom{2}{1} \cdot \binom{2}{1} = 8$$

and degree $\deg(V_\sigma) = 12$. The coordinates of the parameterization are

$$\psi_\varnothing = 0,\ \psi_1 = -t_{2,0},\ \psi_2 = t_{1,0},\ \psi_{12} = 1,\ \psi_3 = -t_{2,0}t_{1,3} + t_{1,0}t_{2,3},\ \psi_{13} = t_{2,3},$$
$$\psi_{23} = -t_{1,3},\ \psi_{123} = t_{0,3},\ \psi_4 = -t_{2,0}t_{1,4} + t_{1,0}t_{2,4},\ \psi_{14} = t_{2,4},\ \psi_{24} = -t_{1,4},$$
$$\psi_{124} = t_{0,4},\ \psi_{34} = -t_{1,4}t_{2,3} + t_{1,3}t_{2,4},\ \psi_{134} = -t_{2,4}t_{0,3} + t_{2,3}t_{0,4},$$
$$\psi_{234} = t_{1,4}t_{0,3} - t_{1,3}t_{0,4},\ \psi_{1234} = 0.$$

These are the 2×2 minors of the first two rows; and the 3×3 minors of the last four columns of the 3×5 matrix

$$M = \begin{bmatrix} 0 & 0 & 0 & t_{0,3} & t_{0,4} \\ t_{1,0} & 1 & 0 & t_{1,3} & t_{1,4} \\ t_{2,0} & 0 & 1 & t_{2,3} & t_{2,4} \end{bmatrix}.$$

Here the rows are indexed by $(0, 1, 2)$ and columns are indexed by $(0, 1, 2, 3, 4)$. By Remark 7.3.1 we see that this is a parameterization of the partial flag variety $\mathcal{F}l(1, 2, 3, 4)$.

Theorem 7.3.3. *When $\sigma = \{(1, 1), (0, 1), (1, 0)\}$, the truncation variety V_σ is the flag variety $\mathcal{F}l(d - 1, d, d + 1, n)$.*

Proof. We recall that the truncated cluster operator $T(t_\sigma)$ is an element of the Fermi–Dirac algebra of the form

$$T(t_\sigma) = T(t_{(1,0)}) + T(t_{(1,1)}) + T(t_{(0,1)}) = \sum_{1 \le i \le d} t_{i,0} a_i + \sum_{1 \le i \le d < b \le n} t_{i,b} a_b^\dagger a_i + \sum_{d < b \le n} t_{0,b} a_b^\dagger.$$

From Remark 6.1.4 we see that the operator $T(t_{(1,1)})$ commutes with the sum $T(t_{(1,0)}) + T(t_{(0,1)})$. Additionally, the sum is nilpotent of order 2. Therefore, the truncation variety V_σ is parameterized by the map $\mathcal{V}_\sigma \to \mathcal{F}$ where

$$t_\sigma \mapsto \exp T(t_{(1,1)}) e_{[d]} + T(t_{(0,1)}) \exp T(t_{(1,1)}) e_{[d]} + T(t_{(1,0)}) \exp T(t_{(1,1)}) e_{[d]}.$$

The first summand $\exp T(t_{(1,1)}) e_{[d]}$ is an element of the dth exterior power $\wedge^d \mathbb{C}^n$ and by Theorem 2.2.5 it parameterizes the Grassmannian $\mathrm{Gr}(d, n)$ in its Plücker embedding. We get that $\exp T(t_{(1,1)}) e_{[d]} = t_1 \wedge \cdots \wedge t_d$ where $t_i = (I + T(t_{(1,1)})) e_i$. The second summand is an element in the $(d + 1)$st exterior power $\wedge^{d+1} \mathbb{C}^n$ and

$$T(t_{(0,1)}) \exp T(t_{(1,1)}) e_{[d]} = T(t_{(0,1)}) t_1 \wedge \cdots \wedge t_d = t_{(0,1)} \wedge t_1 \wedge \cdots \wedge t_d.$$

Here we set $t_{(0,1)} = T(t_{(0,1)})1$. Finally we note that the third summand is an element in the $(d - 1)$st exterior power $\wedge^{d-1} \mathbb{C}^n$. Dually, we get that

$$T(t_{(1,0)}) \exp T(t_{(1,1)}) e_{[d]} = T(t_{(1,0)}) t_1 \wedge \cdots \wedge t_d = t_{(1,0)} \lrcorner\, t_1 \wedge \cdots \wedge t_d.$$

Here we set $t_{(1,0)} = T(t_{(1,0)})^\dagger 1$. The coordinates of this element in $\wedge^{d-1}\mathbb{C}^n$ turn out to be $d \times d$ minors of a matrix

$$T = \begin{bmatrix} 0 & 0 & 0 & \cdots & 0 & t_{0,d+1} & \cdots & t_{0,n} \\ t_{1,0} & 1 & 0 & \cdots & 0 & t_{1,d+1} & \cdots & t_{1,n} \\ t_{2,0} & 0 & 1 & \cdots & 0 & t_{2,d+1} & \cdots & t_{2,n} \\ \vdots & \vdots & \vdots & \ddots & \vdots & \vdots & \ddots & \vdots \\ t_{d,0} & 0 & 0 & \cdots & 1 & t_{d,d+1} & \cdots & t_{d,n} \end{bmatrix}.$$

The rows of the matrix T are indexed by $(0, 1, 2, \ldots, d)$ and the columns are indexed by $(0, 1, 2, \ldots, n)$. In fact, the coordinates of the whole parameterization are minors of T. A coordinate indexed by J, where $|J| = d + 1$, is equal to the maximal minor of T taking columns J. A coordinate indexed by J where $|J| = d$ is equal to the minor of T taking the last d rows and columns J. If $|J| = d - 1$ we do as before by adding the 0th column. By Remark 7.3.1 this is a parameterization of $\mathcal{F}l(d-1, d, d+1, n)$. □

Theorem 7.3.3 is analogous to Thouless' theorem and Theorem 2.2.5 for ionization and electron attachment. We explain the connection to EOM-CC in the following remark.

Remark 7.3.4 (Flag varieties in EOM-CC)**.** We notice that when $\sigma = \{(1, 1), (1, 0)\}$ the truncation variety V_σ is the flag variety $\mathcal{F}\ell(d-1, d, n)$. From Theorem 7.2.9 we see that the truncated EOM-CC ionized quantum states live in the Grassmannian

$$\mathrm{Gr}(d-1, n) = \mathcal{F}\ell(d-1, d, n) \cap \mathbb{P}(\wedge^{d-1}\mathbb{C}^n).$$

Dually the truncated EOM-CC electron attachment quantum states are elements in the Grassmannian $\mathrm{Gr}(d+1, n)$.

In the title of this section, we also name spinor varieties; and for the rest of the section, we will study them and show how they appear in our construction. Let $V = E \oplus F$ be a $2n$-dimensional vector space, where E and F are maximal isotropic subspaces with respect to some non-degenerate quadratic form q. Since V is even dimensional, an isotropic subspace is *maximal* if and only if it is n-dimensional. The variety of maximal isotropic subspaces in V splits into two isomorphic components denoted S_- and S_+. Without loss of generality, we can assume that $E \in S_+$. Two maximal isotropic subspaces are in the same irreducible component if the dimension of their intersection has the same parity as n. The *spinor variety* for V is defined to be the irreducible component S_+. Its dimension is $\dim(S_+) = \binom{n}{2}$ and its degree is the number of shifted standard Young tableaux of shape $(n, n-1, \ldots, 1)$ [54]. See Manivel's paper [70, Section 2] for a more detailed discussion on spinor varieties.

Remark 7.3.5 (Parameterizing S_+)**.** We choose a basis $\{e_1, \ldots, e_n, f_1, \ldots, f_n\}$ for V, such that the e_i's form a basis for E and the f_i's form a basis for F. We look at an $n \times 2n$ matrix $M = [\, I_n \,|\, U \,]$ where U is some $n \times n$ skew-symmetric matrix. The matrix M is written over

the basis described above. One can check that the rows of M span an n-dimensional isotropic subspace E_U. We also get that

$$\dim(E \cap E_U) = n - \operatorname{rank}(U).$$

Since U is skew-symmetric, its rank is an even number, and so the parity of the dimension of the intersection is the same as n. Hence $E_U \in S_+$. The subspace E_U can be parametrized by the Pfaffians of U. For a generic skew-symmetric matrix U the subspace E_U is a generic maximal isotropic subspace in S_+, so the map

$$\mathbb{P}^{\binom{n}{2}-1} \dashrightarrow \mathbb{P}^{2^{n-1}}, \quad U \mapsto \text{ } 2k \times 2k \text{ Pfaffians of } U \text{ for all } 1 \leq k \leq n/2$$

defines a birational parameterization of S_+.

Example 7.3.6. We set $d = 2$, $n = 4$ and level set $\sigma = \{(1,1),(0,2),(2,0)\}$. The variety V_σ is parametrized by the even Plücker coordinates

$$\begin{aligned}&\psi_\varnothing = t_{12,0},\ \psi_{12} = 1,\ \psi_{13} = t_{2,3},\ \psi_{23} = -t_{1,3},\ \psi_{14} = t_{2,4},\\ &\psi_{24} = -t_{1,4},\ \psi_{34} = -t_{1,4}t_{2,3} + t_{1,3}t_{2,4} + t_{12,0}t_{0,34},\ \psi_{1234} = t_{0,34}.\end{aligned}$$

These are the Pfaffians of a skew-symmetric matrix

$$\begin{bmatrix} 0 & -t_{12,0} & -t_{1,3} & -t_{1,4} \\ t_{12,0} & 0 & t_{2,3} & t_{2,4} \\ t_{1,3} & -t_{2,3} & 0 & -t_{0,34} \\ t_{1,4} & -t_{2,4} & t_{0,34} & 0 \end{bmatrix}.$$

Coordinate ψ_I is equal to the Pfaffian whose rows and columns come from the symmetric difference $I \oplus [d]$. This is a parameterization of the spinor variety for the vector space $\mathbb{C}^8$. It has dimension

$$\dim(V_\sigma) = \binom{2}{2} + \binom{2}{2} + \binom{2}{1} \cdot \binom{2}{1} = 6$$

and degree $\deg(V_\sigma) = 2$. It is defined by a single quadric, the homogeneous inverse master polynomial

$$\overline{x}_{34}(\psi) = \psi_{23}\psi_{14} - \psi_{13}\psi_{24} + \psi_{12}\psi_{34} - \psi_\varnothing\psi_{1234}$$

and the odd Plücker coordinates $\psi_1, \psi_2, \psi_3, \psi_4, \psi_{123}, \psi_{124}, \psi_{134}, \psi_{234}$.

Theorem 7.3.7. *The truncation variety for $\sigma = \{(1,1),(0,2),(2,0)\}$ is the spinor variety of the $2n$-dimensional vector space $\mathbb{C}^{2n}$.*

Proof. Look at the n-dimensional vector space $F = \operatorname{span}\{a_1, \ldots a_d, a_{d+1}^\dagger, \ldots, a_n^\dagger\}$. The basis vectors generate the subalgebra $\mathcal{V} \cong \wedge\mathbb{C}^n$ of the Fermi–Dirac algebra, defined in Remark 6.1.4. The truncated cluster operator is an element in the second exterior power of F:

$$T(t_\sigma) = \sum_{1 \leq i < j \leq d} t_{ij,0} a_i a_j + \sum_{1 \leq i \leq d < b \leq n} t_{i,b} a_b^\dagger a_i + \sum_{d < b < c \leq n} t_{0,bc} a_c^\dagger a_b^\dagger \in \wedge^2 F.$$

The set $\{(-1)^{i-1}a_i : 1 \leq i \leq d\} \cup \{(-1)^d a_b^\dagger : d < b \leq n\}$ also forms a basis for F. We rewrite the operator $T(t_\sigma)$ in terms of this basis:

$$\sum_{1\leq i<j\leq d}(-1)^{i+j}t_{ij,0}(-1)^{i-1+j-1}a_ia_j + \sum_{1\leq i\leq d<b\leq n}(-1)^{i+d}t_{i,b}(-1)^{i-1+d}a_ia_b^\dagger - \sum_{d<b<c\leq n}t_{0,bc}(-1)^{2d}a_b^\dagger a_c^\dagger.$$

We set T as the $n \times n$ skew-symmetric matrix corresponding to $T(t_\sigma)$ with respect to the signed basis of F. The exponential of $T(t_\sigma)$ is the operator

$$\exp(T(t_\sigma)) = \sum_{k=0}^{d}\frac{1}{k!}T(t_\sigma)^{\wedge k} = \sum_{\substack{I\subseteq[n]\\|I|=2k}}(-1)^{\ell d+\sum_{i\in[d]\cap I}(i-1)}\operatorname{Pf}(T_I)a_{i_1}\cdots a_{i_\ell}a_{i_{\ell+1}}^\dagger\cdots a_{i_{2k}}^\dagger,$$

where $\operatorname{Pf}(T_I)$ is the Pfaffian of T using columns and rows from I. For a compatible definition of the Pfaffian see [62, Section 2.7.4.]. The exponential map is then

$$\begin{aligned}\exp\left(T(t_\sigma)\right)e_{[d]} &= \sum_{\substack{I\subseteq[n]\\ I \text{ even}}}(-1)^{\ell d+\sum_{i\in[d]\cap I}(i-1)}\operatorname{Pf}(T_I)a_{i_1}\cdots a_{i_\ell}a_{i_{\ell+1}}^\dagger\cdots a_{i_{2k}}^\dagger a_1^\dagger\cdots a_d^\dagger 1\\ &= \sum_{\substack{I\subseteq[n]\\ I \text{ even}}}\operatorname{Pf}(T_I)e_{[d]\oplus I}.\end{aligned}$$

The reason we introduced the signed basis for F is to cancel out the signs appearing when multiplying the exponential operator $\exp\left(T(t_\sigma)\right)$ with the reference state $e_{[d]}$. We now see that the truncation variety is parametrized by the Pfaffians of a skew-symmetric matrix T. This is a parameterization of the spinor variety for vector space $\mathbb{C}^{2n}$. □

We notice the truncation variety $V_{\{(2,0),(1,1),(0,2)\}} \cong S_+$ does not depend on the number d of base electrons. It only depends on the number n of spin orbitals.

7.4 The Coupled Cluster Equations

We recall the electronic Schrödinger equation from (1.13), now set in second quantization:

$$H\psi = \lambda\psi, \quad \psi \in \mathcal{F}.$$

Here the Hamiltonian H is a $2^n \times 2^n$ symmetric matrix associated with an electronic system of interest, see Section 6.2. The solutions to the Schrödinger equation describe the stable states of our system; the eigenvalues λ are the energies and the eigenvectors ψ describe the wave functions representing the probability amplitude of finding an electron at a particular location. The lowest eigenvalue and the corresponding eigenvector describe the *ground state*, which is the most stable arrangement of electrons in the system. The higher energy solutions

are called *excited states* and they require energy input, such as from heat, electricity or light, to be observed. Hence, all solutions of the equation can be of interest.

For large n, solving the Schrödinger equation is infeasible. *Coupled cluster theory* describes a hierarchy of approximation schemes for finding the solutions of the Schrödinger equation. There we restrict the quantum states ψ to the truncation varieties introduced in Section 7.2. We will now describe the construction of the coupled cluster equations for a given truncation.

With that being said, let σ be a proper subset of the truncation grid $\mathcal{G}$. We define ψ_σ to be the projection of vector $\psi \in \mathcal{F}$ to coordinates with excitation level in σ. This is the projection of quantum states in $\mathcal{F}$ onto the subspace

$$\mathcal{F}_\sigma = \operatorname{span}\{e_J : J \subseteq [n] \text{ and } (a(J), c(J)) \in \sigma \cup \{(0,0)\}\} \subseteq \mathcal{F}.$$

The *unlinked coupled cluster (CC) equations* truncated at level set σ are obtained in the same manner as the CC equations in (2.15). Explicitly,

$$(H\psi)_\sigma = \lambda\psi_\sigma, \quad \psi \in V_\sigma. \tag{7.3}$$

As with first quantization, two variants of the coupled cluster equations are commonly used in the theory, the linked and unlinked CC equations. See Section 1.2, (2.20) for the definition of the linked CC equations. By Theorem 2.3.10 the two formulations agree in all cases that appear in the computational chemistry literature, including CCS, CCD, CCSD and CCSDT [36]. As was mentioned in Section 2.3 the unlinked equations are more elegant from an algebraic point of view and its algebraic degree is lower, explaining our choice. The coupled cluster equations for systems with a fixed number of electrons correspond to choosing level sets σ along the diagonal of the truncation grid. These cases are covered in detail in Section 2.3. In the spirit of this Chapter, this section extends the coupled cluster framework to the full Fock space, thereby allowing both ionization and electron attachment.

The dimension of the truncation variety V_σ is equal to the number of constraints imposed by the equations in (7.3). Hence, the number of solutions to the CC equations is finite for a generic matrix H. We call this number the *CC degree* of truncation variety V_σ, denoted $\operatorname{CCdeg}(V_\sigma)$. By Theorem 2.3.2 we obtain an upper bound:

$$\operatorname{CCdeg}(V_\sigma) \leq (\dim(V_\sigma) + 1)\deg(V_\sigma). \tag{7.4}$$

By Corollary 2.3.3 this bound is tight when V_σ is linear. In that case the CC equations are eigenvalue equations for the submatrix $H_{\sigma,\sigma}$ and $\operatorname{CCdeg}(V_\sigma) = \dim(V_\sigma) + 1$. So if H is a real symmetric matrix and the truncation variety is linear then all solutions are real.

In Theorem 3.1.1, we show that the CC degree of the Grassmannian is the total degree of the graph of the truncated exponential map $\mathcal{V}_{\{1\}} \to \mathcal{F}$. In Section 4.3 we generalize these results to all the truncation varieties from Section 2.2. In particular in Theorem 4.3.2 we show that the if the truncation variety V_σ can be parameterized by a graph map, then its CC degree is the total degree of the graph of that parameterization.

We want to extend this to the Fock space truncation varieties and, in particular, to determine which of them already admit the truncated exponential map as a graph parameterization. To that end, we say a pair (m, ℓ) has a partition $\{(m_1, \ell_1), \cdots, (m_k, \ell_k)\}$ over the level set $\sigma \subsetneq \mathcal{G}$ if

$$(m, \ell) = \sum_{i=1}^{k} (m_i, \ell_i)$$

and $(m_i, \ell_i) \in \sigma$ for all $1 \leq i \leq k$. We call k the length of the partition. We say that this partition is even if at most one of the parts (m_i, ℓ_i) has an odd level $m_i + \ell_i$. If the element (m, ℓ) has an even level, then a set partition is even if and only if all of the parts have an even level. If the element (m, ℓ) has an odd level, then a set partition is even if and only if exactly one part has an odd level.

Theorem 7.4.1. *Let $\sigma \subseteq \mathcal{G}$ be a level set such that no element in σ has an even partition over σ of length > 1. The CC degree of the truncation variety V_σ is the total degree of the graph of the map*

$$\mathcal{V}_\sigma \to \mathcal{F}, \quad t \mapsto \psi = \exp\left(T_\sigma(t)\right) e_{[d]}. \tag{7.5}$$

Proof. We look at the projection ψ_σ of ψ onto $\mathcal{F}_\sigma$. Take set J with excitation level $(a(J), c(J))$ in σ. By Theorem 7.1.5 the exponential parameterization maps ψ_J to a signed sum of monomials $t_\pi = t_{\pi_1 \cap [d], \pi_1 \setminus [d]} \cdots t_{\pi_k \cap [d], \pi_k \setminus [d]}$, where π is an even set partition of $[d] \oplus J$. In the truncated parameterization (7.5), we set $t_{I,B} = 0$ if $(|I|, |B|) \notin \sigma$. Hence, we only need to sum over monomials t_π such that $(a(\pi_i), c(\pi_i)) \in \sigma$ for all i. We note that at most one of the levels $(a(\pi_i), c(\pi_i))$ is odd and $(a(J), c(J)) = \sum_i (a(\pi_i), c(\pi_i))$. Assuming the hypothesis of the theorem the only even partition of (m, ℓ) over σ is the trivial one $\{(m, \ell)\}$ of length 1. Hence the monomials t_π vanish for all even set partitions π except the trivial partition $\{[d] \oplus J\}$. Thus $\psi_J = \pm t_{[d] \setminus J, J \setminus [d]}$. Now we use the same argument as in the proof of Theorem 4.3.2 to show that the CC degree is the total degree of the graph of (7.5). □

In particular, the CC degree of the flag variety $\mathcal{F}l(d-1, d, d+1, n)$ is the total degree of the graph of the parameterization defined in Remark 7.3.1. Also the CC degree of the spinor variety S_+ is the total degree of the graph of the map

$$\mathbb{P}^{\binom{n}{2}-1} \dashrightarrow \mathbb{P}^{2^{n-1}-1}, \quad \text{skew sym. } T \mapsto \mathrm{Pf}(T_I) \text{ for all even } I \subseteq [n],$$

mapping skew-symmetric matrix T to its sub-Pfaffians. The degrees of the flag variety and the spinor variety can be computed using Schubert calculus. This naturally raises the question of whether Schubert calculus can also be used to determine the total degrees of their graphs, and thereby explain the fifth row of Tables 7.1 and 7.2. In Chapter 3 and in [39, 40], toric degenerations are used to find the total degrees of the graphs of birational parameterizations of the Grassmannian and the flag variety. A similar approach might reveal the CC degree of the flag variety and the spinor variety. We leave this question open and instead present, in the following section, a numerical study of the CC degrees of flag and spinor varieties.

Currently, we do not have a graph parameterization of every Fock space truncation variety, as we do for the truncation varieties defined in Section 2.2; see Theorem 4.3.8. Whether such parameterizations exist, and how they should be defined, remains a subject for future research.

7.5 Numerical Solutions

The truncation variety V_σ is parametrized by the restriction of the exponential map in (7.1) to the subspace $\mathcal{V}_\sigma$:

$$\mathcal{V}_\sigma \to \mathcal{F}, \quad t_\sigma \mapsto \psi = \exp(T(t_\sigma))e_{[d]}.$$

This map is birational and hence its fibers are zero dimensional and of degree one. Therefore we can rewrite the coupled cluster equations like (2.18). That is:

$$((H - \lambda I)\exp(T(t_\sigma))e_{[d]})_\sigma = 0. \tag{7.6}$$

This is a square polynomial equation of size $\dim(V_\sigma)+1$ with polynomials in variables (λ, t_σ) of degree $\leq d+1$. The above formulation works well for numerically solving the CC equations. In our computations we use `HomotopyContinuation.jl` [11]. For a detailed introduction into numerical homotopy methods and how they can be used to both solve generic and special CC equations, see Section 5.1. Throughout this section, we use Julia version 1.11.4 and `HomotopyContinuation.jl` version 2.9.2. Computations were done on the MPI-MiS computer server using four 18-Core Intel Xeon E7-8867 v4 at 2.4 GHz (3072 GB RAM). Symbolic calculations are done in the `Macaulay2` software system [46] on a MacBook Pro with 16 cores and an Apple M4 Max chip.

Example 7.5.1 (CC degrees of flag varieties)**.** We look at the truncation variety $V_{\{(1,0),(1,1),(0,1)\}} \cong \mathcal{F}\ell(d-1, d, d+1, n)$ when $d = 2, 3$ and $n = 4, 5, 6, 7, 8$.

Table 7.1: CC systems corresponding to the flag varieties.

(d, n)	(2,4)	(2,5)	(2,6)	(3,6)	(2,7)	(3,7)
dim	8	11	14	15	17	19
degree	12	110	1 274	4 550	17 136	271 320
mingens	[2, 10]	[7, 50]	[23, 175]	[14, 281]	[65, 490]	[37, 1148]
CCdeg	74	713	8 499	30 070	116 602	1 821 528
# real	18	51	151	332	503	3 262
solve (sec)	1	6	174	712	14 638	398 022
certify (sec)	0	0	2	4	24	329

The dimension of V_σ is $d(n-d)+n$. The degree and the minimal generators of V_σ are calculated using `Macaulay2` [46]. The fourth row labeled "mingens" gives us the number of minimal generators of degree 1 and 2. The linear generators are the variables indexed

by sets J where $|J| < d-1$ or $|J| > d+1$. We note that the flag variety $\mathcal{F}\ell(d-1, d, d+1, n)$ is cut out by quadrics, so we do not have any higher-degree generators. The CC degrees are calculated by solving (7.6) for a generic matrix, using the `monodromy` function in `HomotopyContinuation.jl` [11]. The row "# real" lists the number of real solutions to the CC equations for one generic real Hamiltonian. The number of real solutions might vary, and the number listed is only from one case.

Another truncation variety of interest is the spinor variety, S_+ of $\mathbb{C}^{2n}$. From Theorem 7.3.7 we see that the spinor variety, as a truncation variety, only depends on the number of orbitals n but not on the number of electrons d.

Example 7.5.2 (CC degrees of spinor varieties)**.** We look at the truncation variety $V_{\{(2,0),(1,1),(0,2)\}} \cong S_+$, isomorphic to the spinor variety of $\mathbb{C}^{2n}$, when $n = 4, 5, 6, 7$.

Table 7.2: CC systems corresponding to the spinor variety.

n	4	5	6	7
dim	6	10	15	21
degree	2	12	286	33 592
mingens	[8, 1]	[16, 10]	[32, 66]	[64, 364]
CCdeg	13	98	2 572	318 118
# real	5	10	70	904
solve (sec)	0	1	32	60 504
certify (sec)	0	0	1	55

The dimension of V_σ is $\binom{n}{2}$. The linear generators of the truncation variety are the variables indexed by the odd set $J \subseteq [n]$. We note that the spinor variety is cut out by quadrics so we only have minimal generators of degree 1 and 2.

Similar tables can be given for the truncation varieties corresponding to FSCCD and FSCCSD. Recall that here FSCC stands for Fock space coupled cluster; see Remark 7.2.1 and Table 1.1 for the explicit definition of these CC variants. The computation of the CC degree for these variants become infeasible quickly as can be seen in this final example.

Example 7.5.3. We look at FSCCSD for ionized electronic systems with d base electrons in n orbitals. Our level set is of the form $\sigma = \{(1,0), (2,1), (1,1), (2,2)\}$. The corresponding truncation variety has dimension

$$\dim(V_\sigma) = d + d(n-d) + \binom{d}{2}(n-d) + \binom{d}{2}\binom{n-d}{2}.$$

By Theorem 7.2.5 the truncation variety V_σ is linear when $d = 2$. We now focus on the case when $d = 3$. The dimension of V_σ is

$$30, 45, 63, 84, 108, 135, 165, \ldots \quad \text{for } n = 6, 7, 8, 9, 10, 11, 12, \ldots .$$

Solving square polynomial systems of these sizes is hard, even numerically. Using `Homotopy Continuation.jl` we are able to compute the CC degree of V_σ when $n = 6, 7$. In these cases V_σ has degrees $43, 3\,894$, respectively. Thus (7.4) provides us with the upper bounds of $31 \cdot 43 = 1\,333$ and $46 \cdot 3894 = 179\,124$. Computations using `monodromy` show that the actual CC degrees for $d = 3$ and $n = 6, 7$ are

$$\mathrm{CCdeg}(V_\sigma) = 1\,195, 145\,608.$$

We conclude this second part of the thesis with a short summary of our contributions. In this chapter we reformulated the CC equations in second quantization. Additionally, we expanded beyond fixed-electron systems, allowing for ionization and electron attachment. This revealed flag varieties and spinor varieties as truncation varieties. We offered an extensive study of these varieties, in particular, their exponential parameterizations and CC degrees. We classified all truncation varieties for which the CC degree is the total degree of graph of their exponential parameterization. Among those are the flag varieties and spinor varieties, and future research directions include studying these degrees through the lens of intersection theory or Khovanskii bases. Another direction would be to explore graph parameterizations of all Fock space truncation varieties, similar as in Chapter 4. In the next part of the thesis we will focus on incorporating electronic spin into our formulations.

Part III

Spin-Adapted Formalism

Chapter 8

Representations of SU(2)

In this chapter we develop the mathematical framework for spin adaptation in coupled cluster theory. The spin operators give rise to an SU(2)–action on the state space $\mathcal{H}_d$. Since the electronic Hamiltonian commutes with these operators, it preserves the total spin of the quantum state. Consequently, one typically restricts to the spin singlet sector, that is, the SU(2)–invariant subspace. We study the derived $\mathfrak{su}(2)$–action on both the state space $\mathcal{H}_d$ and the Fermi–Dirac algebra. Viewing these spaces as $\mathfrak{su}(2)$–representations, we decompose them into irreducible components using the representation theory of $\mathfrak{sl}_2(\mathbb{C})$, the complexification of $\mathfrak{su}(2)$. We introduce the *excitation ring*, an Artinian commutative ring defined by cubic relations. Its dimension is given by the Narayana numbers, which refine the Catalan numbers. Our main result establishes an isomorphism between the excitation ring and the SU(2)–invariant state space. Finally, we construct a combinatorial bijection between Dyck paths enumerated by the Narayana numbers and the basis vectors of the invariant state space via the RSK correspondence. This yields an algebraic and combinatorial description of the SU(2)–invariant subspace through the excitation ring. This chapter is based on the paper *Plane Partitions and Spin Adapted Quantum States* [87], joint work with Abigail Price and Ada Stelzer, and on Sections 2–4 of *Algebraic Geometry for Spin-Adapted Coupled Cluster Theory* [38], joint work with Fabian M. Faulstich.

8.1 The Spin-Adapted Electronic Structure Problem

We recall from Section 1.2 that the *electronic Schrödinger equation* describing d electrons in the electromagnetic field generated by d_{nuc} fixed nuclei is the eigenvalue problem

$$\mathscr{H}\,\psi(\mathbf{x}_1, \mathbf{x}_2, \ldots, \mathbf{x}_d) = \lambda\,\psi(\mathbf{x}_1, \mathbf{x}_2, \ldots, \mathbf{x}_d), \tag{8.1}$$

where the unknown *wave function* $\psi(\mathbf{x}_1, \mathbf{x}_2, \ldots, \mathbf{x}_d)$ fully characterizes a physical system [92]. Here $\mathbf{x}_i = (\mathbf{r}_i, s_i) \in \mathbb{R}^3 \times \{\uparrow, \downarrow\} = X$ denotes the spatial coordinate $\mathbf{r}_i$ and spin coordinate s_i

of the ith electron. In atomic units, the electronic Hamiltonian $\mathscr{H}$ is the differential operator

$$\mathscr{H} := -\frac{1}{2}\sum_{i=1}^{d}\Delta_{\mathbf{r}_i} - \sum_{i=1}^{d}\sum_{j=1}^{d_{\text{nuc}}}\frac{Z_j}{|\mathbf{r}_i - \mathbf{R}_j|} + \sum_{1\le i<j\le d}\frac{1}{|\mathbf{r}_i - \mathbf{r}_j|}. \tag{8.2}$$

Electrons possess an intrinsic angular momentum called *spin* [89]. In the non-relativistic Born–Oppenheimer model considered here, spin does not appear explicitly in the Hamiltonian operator in (8.2). However, it enters the *state space* and the admissibility condition (Pauli principle) in the following way: The physical d-electron wave function is a map

$$\psi : X^d \to \mathbb{C}, \quad (\mathbf{r}, s) \mapsto \psi(\mathbf{r}, s),$$

i.e. it depends on spatial coordinates $\mathbf{r} = (\mathbf{r}_1, \ldots, \mathbf{r}_d)$ and spin labels $s = (s_1, \ldots, s_d)$. Pauli's exclusion principle [82] states that admissible states are skew-symmetric under exchange of variables. In particular, two electrons with equal spin cannot occupy the same position.

Since the Hamiltonian does not explicitly depend on the electronic spin, we can discretize it with respect to a product basis. To that end, we introduce an orthonormal set of spatial basis functions (orbitals) $\{\varphi_p\}_{p=1}^m \subseteq L^2(\mathbb{R}^3)$, found using Hartree–Fock theory; see Example 1.2.4. Each spatial orbital gives rise to two spin-orbitals

$$\phi_{p\uparrow}(\mathbf{r}, s) := \varphi_p(\mathbf{r})\,\delta_{s,\uparrow}, \qquad \phi_{p\downarrow}(\mathbf{r}, s) := \varphi_p(\mathbf{r})\,\delta_{s,\downarrow}.$$

The spin orbitals span the one-particle space $\mathcal{H} \cong \mathbb{C}^m \otimes \mathcal{H}_{\text{spin}}$, where $\mathcal{H}_{\text{spin}} \cong \mathbb{C}^2$ is the *spin space* with orthonormal basis $\{e_\uparrow, e_\downarrow\}$ (spin up/down). Here $\dim(\mathcal{H}) = n = 2m$. We compare this basis with the molecular spin-orbital basis introduced in Section 1.2. In the present basis, for each $i \in [m]$, the two spin orbitals $\phi_{i\uparrow}$ and $\phi_{i\downarrow}$ have the same spatial part and differ only in their spin component. A general molecular spin orbital basis $\{\xi_i\}_{i\in[n]}$, such as those considered in Section 1.2, need not have this property. Note, however, that the explicit molecular spin-orbital basis for LiH constructed in Example 1.2.4 does. There, Hartree-Fock is applied before imposing spin. This is done when one wishes to preserve spin symmetry, as we do in this chapter.

The Galerkin space of skew-symmetric d-electron functions is given by $\mathcal{H}_d \cong \wedge^d\mathcal{H}$, spanned by the canonical skew-symmetric product basis, i.e., the d-electron Slater determinants.

Second Quantization and Fermi–Dirac Algebra

We provide a short overview of second quantization for spin–adaptation. Subsequently, we use the explicit basis $e_\downarrow = -e_2$, $e_\uparrow = e_1$ for $\mathcal{H}_{\text{spin}}$, where e_1 and e_2 form the standard basis of $\mathbb{C}^2$. We denote the standard basis vectors of $\mathbb{C}^m$ by e_p with $p \in [m]$. For notational convenience, we define $[\![m]\!] := [m] \times \{\downarrow, \uparrow\}$, with $n = 2m$ elements. Hence, a basis of $\mathcal{H}$ is given by $e_{p\alpha} := e_p \otimes e_\alpha$, $(p, \alpha) \in [\![m]\!]$. The associated fermionic Fock space is the exterior algebra

$$\mathcal{F} \cong \bigwedge \mathcal{H} = \bigoplus_{\ell=0}^{n} \bigwedge^{\ell} \mathcal{H},$$

with canonical exterior basis vectors $e_I := \wedge_{(p,\alpha)\in I} e_{p\alpha}$ indexed by sets $I \subseteq [\![m]\!]$.

For each basis element $e_{p\alpha} \in \mathcal{H}$ we define the creation and annihilation operators as the following exterior and interior products on $\mathcal{F}$:

$$a^\dagger_{p\alpha} : \mathcal{F} \to \mathcal{F},\ \psi \mapsto e_{p\alpha} \wedge \psi \quad \text{and} \quad a_{p\alpha} : \mathcal{F} \to \mathcal{F},\ \psi \mapsto e_{p\alpha} \lrcorner\, \psi.$$

Here, $\lrcorner$ is the dual operation to the wedge product $\wedge$, see Section 6.1 for further explanation. These operators satisfy the following anticommutation relations:

$$a^\dagger_{p\alpha} a^\dagger_{q\beta} + a^\dagger_{q\beta} a^\dagger_{p\alpha} = 0, \quad a_{p\alpha} a_{q\beta} + a_{q\beta} a_{p\alpha} = 0, \quad a^\dagger_{p\alpha} a_{q\beta} + a_{q\beta} a^\dagger_{p\alpha} = \delta_{p,q}\delta_{\alpha,\beta},$$

Note that these relations implement Pauli's exclusion principle at the operator level, since $(a^\dagger_{p\alpha})^2 = 0$. Therefore, the creation and annihilation operators generate the Fermi–Dirac algebra FD_{2m}, defined in Section 6.1.

We can then discretize the Hamiltonian over $\mathcal{F}$ [51, 89], i.e.,

$$H = \sum_{\substack{1\le p,q\le m,\\ \sigma\in\{\uparrow,\downarrow\}}} h_{pq}\, a^\dagger_{p\sigma} a_{q\sigma} + \tfrac{1}{2} \sum_{1\le p,q,r,s\le m} \sum_{\sigma,\tau\in\{\uparrow,\downarrow\}} v_{pqrs}\, a^\dagger_{p\sigma} a^\dagger_{r\tau} a_{s\tau} a_{q\sigma}, \tag{8.3}$$

where h_{pq} and v_{pqrs} are one- and two-electron integrals over spatial orbitals,

$$h_{pq} := \int \varphi_p^*(\mathbf{r}) \left(-\frac{1}{2}\Delta - \sum_j \frac{Z_j}{\|\mathbf{r} - \mathbf{R}_j\|} \right) \varphi_q(\mathbf{r})\, d\mathbf{r},$$
$$v_{pqrs} := \iint \varphi_p^*(\mathbf{r}_1)\varphi_q(\mathbf{r}_1) \frac{1}{\|\mathbf{r}_1 - \mathbf{r}_2\|} \varphi_r(\mathbf{r}_2)^*\varphi_s(\mathbf{r}_2)\, d\mathbf{r}_1\, d\mathbf{r}_2.$$

Note that here the integrals are taken over the spatial orbitals, whereas in Example 1.2.6 and (6.4) they are taken over the spin orbitals. This is possible because the spin orbitals $\phi_{p\uparrow}$ and $\phi_{p\downarrow}$ have the same spatial part and differ only in their spin component, so the value of the integral is unchanged. Since the monomials in H contain equal numbers of creation and annihilation operators, H conserves particle number and may be restricted to an endomorphism of the dth exterior power $\mathcal{H}_d$.

Subsequently, we assume particle–number conservation and restrict attention to the subalgebra defined in Remark 6.1.7. It is generated by standard monomials $a^\dagger_B a_I$ of bidegree (ℓ, ℓ) for $1 \le \ell \le m$, which we here refer to as having *excitation level* ℓ. Hence, we may restrict our operators to endomorphisms of the dth exterior power $\mathcal{H}_d \cong \wedge^d\mathcal{H}$.

8.2 Representations of the State Space

The electronic spin can be viewed as a two-dimensional internal degree of freedom of each electron [84, 89], see the final part of Section 1.2. In the non-relativistic Born–Oppenheimer setting (i.e., in the absence of spin–orbit and magnetic-field terms), the Hamiltonian H is

SU(2)-invariant (i.e., spin-rotationally invariant) and hence commutes with the total-spin operators S^2 and S_z (see below), so that the Hilbert space decomposes into spin sectors (e.g., singlets, triplets, etc.) [84]. For spin-$\frac{1}{2}$ the relevant symmetry group is not SO(3) itself but its double cover SU(2), whose defining representation acts on the spin space $\mathcal{H}_{\text{spin}} \cong \mathbb{C}^2$ [84, 89, 104]. To exploit this symmetry in many-electron computations, we study the induced SU(2)-action on the skewsymmetric d-electron space and, equivalently, on the operator algebra in second quantization. This provides a precise algebraic notion of spin invariance and allows us to isolate, in particular, the singlet sector used in spin-adapted formulations [80]. The argument uses two standard facts. First, differentiation induces a one-to-one correspondence between finite-dimensional representations of SU(2) and finite-dimensional representations of $\mathfrak{su}(2)$. Indeed, since SU(2) is simply connected, every finite-dimensional $\mathfrak{su}(2)$–representation integrates to SU(2). Second, complex representations of $\mathfrak{su}(2)$ are in one-to-one correspondence with representations of $\mathfrak{sl}_2(\mathbb{C})$ via complexification, since $\mathfrak{su}(2) \otimes_{\mathbb{R}} \mathbb{C} \cong \mathfrak{sl}_2(\mathbb{C})$.

Spin of a Single Electron

Recall that the Lie algebra $\mathfrak{su}(2)$ consists of traceless skew-Hermitian 2×2 matrices,

$$\mathfrak{su}(2) = \{A \in \mathbb{C}^{2\times 2} : \; A^* = -A, \; \operatorname{tr}(A) = 0\}.$$

The three 2×2 matrices $(\frac{i}{2}\sigma_x, \frac{i}{2}\sigma_y, \frac{i}{2}\sigma_z)$, where $\sigma_x, \sigma_y, \sigma_z$ are the Pauli matrices [83],

$$\sigma_x = \begin{bmatrix} 0 & 1 \\ 1 & 0 \end{bmatrix}, \quad \sigma_y = \begin{bmatrix} 0 & -i \\ i & 0 \end{bmatrix}, \quad \sigma_z = \begin{bmatrix} 1 & 0 \\ 0 & -1 \end{bmatrix},$$

form a basis for $\mathfrak{su}(2)$. Similarly, it is common to work with the associated Hermitian operators, i.e., $S_x = \frac{1}{2}\sigma_x$, $S_y = \frac{1}{2}\sigma_y$, and $S_z = \frac{1}{2}\sigma_z$, noting that $-iS_x, -iS_y, -iS_z \in \mathfrak{su}(2)$ and that spin rotations are given by $\exp(-i\,\theta_x S_x - i\,\theta_y S_y - i\,\theta_z S_z) \in \mathrm{SU}(2)$. For our purposes, it is convenient to work with the associated spin ladder operators, i.e.,

$$S_+ = S_x + iS_y = \frac{1}{2}(\sigma_x + i\sigma_y), \qquad S_- = S_x - iS_y = \frac{1}{2}(\sigma_x - i\sigma_y), \qquad S_z = \frac{1}{2}\sigma_z.$$

Here, S_z is diagonal in the $\{\uparrow, \downarrow\}$ basis and hence directly encodes the spin projection, while S_+ and S_- act as raising and lowering operators, i.e., flipping "$\downarrow \mapsto \uparrow$" and "$\uparrow \mapsto \downarrow$", respectively. Note that $S_\pm$ are not elements of $\mathfrak{su}(2)$ but lie in its complexification $\mathfrak{sl}_2(\mathbb{C})$. For the rest of the chapter we will work over this complexification. A central operator for the discussion of spin symmetry is the *total–spin operator*, which is the following element, *not in* $\mathfrak{sl}_2(\mathbb{C})$,

$$S^2 := S_x^2 + S_y^2 + S_z^2 = S_z^2 + \tfrac{1}{2}\big(S_+S_- + S_-S_+\big).$$

Remark 8.2.1. The finite-dimensional irreducible representations of SU(2) are parametrized by non-negative half-integers: for each $j \in \frac{1}{2}\mathbb{Z}_{\geq 0}$ there is an irreducible representation $V_j \cong \mathrm{Sym}^{2j}(\mathbb{C}^2)$, see [43, Section 11.1]. The space $\mathrm{Sym}^{2j}(\mathbb{C}^2)$ can be realized as the space

of homogeneous polynomials in two variables x, y of degree $2j$. It has the monomial basis $\{x^{2j-i}y^i \mid 0 \leq i \leq 2j\}$, and hence $\dim V_j = 2j+1$. The SU(2)–action on V_j is the induced action on homogeneous polynomials coming from left multiplication of the variable vector.

The irreducible representation of SU(2) on $V_{\frac{1}{2}} \cong \mathbb{C}^2$ is called the spin-$\frac{1}{2}$ representation. Differentiation and complexification yields the corresponding representation of the Lie algebra $\mathfrak{sl}_2(\mathbb{C})$, commonly referred to as the fundamental representation.

Remark 8.2.2 (Lie algebra actions)**.** Let G be a connected and simply connected Lie group and $\mathfrak{g}$ be its corresponding Lie algebra. The derivative of a G-action $\Psi : G \to GL(V)$ on a vector space V is a $\mathfrak{g}$-action $\Psi' : \mathfrak{g} \to \mathrm{End}(V)$ on V. Derivatives preserve the algebraic properties of the G-action – the $\mathfrak{g}$-representations and G-representations are in one-to-one correspondence, see [43, Section 8.1, Exercise 8.10]. In particular (and most importantly for our purposes), their trivial representations agree, i.e., the subspace of V invariant under the G-action is equal to the subspace of V that vanishes under the $\mathfrak{g}$-action. Since Lie algebra actions are simpler than Lie group actions (for example, the Lie algebra $\mathfrak{g}$ does not preserve the topological properties of G), we use Lie algebra actions to study G-invariant spaces.

We define an $\mathfrak{sl}_2(\mathbb{C})$–action on the spin space $\mathcal{H}_{\text{spin}} \cong V_{\frac{1}{2}}$ by describing the action of the generators on the basis vectors,

$$\begin{aligned} S_+(e_\downarrow) &= -e_\uparrow & S_-(e_\downarrow) &= 0 & S_z(e_\downarrow) &= -\frac{1}{2}e_\downarrow \\ S_+(e_\uparrow) &= 0 & S_-(e_\uparrow) &= -e_\downarrow & S_z(e_\uparrow) &= \frac{1}{2}e_\uparrow. \end{aligned}$$

See equations (3.10)–(3.12) in [104, Section 3.2]. In the explicit basis $e_\downarrow = -e_2$, $e_\uparrow = e_1$ this action coincides with left multiplication: $g \in \mathfrak{sl}_2(\mathbb{C})$ acts on $\mathcal{H}_{\text{spin}}$ by $v \mapsto gv$.

We can extend this action to an $\mathfrak{sl}_2(\mathbb{C})$–action on the one-particle space $\mathcal{H}$ by acting only on the spin factor, i.e., $g(e_{p\alpha}) = e_p \otimes ge_\alpha$ for $g \in \mathfrak{sl}_2(\mathbb{C})$. Equivalently, in the basis $\{e_{p\alpha}\}_{(p,\alpha)\in[\![m]\!]}$ the action is represented by an $n \times n$ matrix:

$$g_m := I_m \otimes g \in \mathbb{C}^{(2m)\times(2m)} \cong \mathbb{C}^{n\times n}.$$

Note that this representation is reducible.

Spin of d-Electron States and Spin-Singlet d-Electron States

We further induce the $\mathfrak{sl}_2(\mathbb{C})$–action onto the space $\mathcal{H}_d$ of d-particle states, canonically via

$$g(e_I) := \sum_{r=1}^{d} e_{i_1\alpha_1} \wedge \cdots \wedge g(e_{i_r\alpha_r}) \wedge \cdots \wedge e_{i_d\alpha_d}. \tag{8.4}$$

In the exterior basis $\{e_I : I \in \binom{[\![m]\!]}{d}\}$ of $\mathcal{H}_d$, the action is represented by an $\binom{n}{d} \times \binom{n}{d}$ matrix acting by left multiplication on the coordinate vectors:

$$g^{(d)} := \sum_{k=1}^{d} \underbrace{I_{\mathcal{H}} \wedge \cdots \wedge I_{\mathcal{H}}}_{k-1 \text{ times}} \wedge g_m \wedge \underbrace{I_{\mathcal{H}} \wedge \cdots \wedge I_{\mathcal{H}}}_{d-k \text{ times}} \in \mathrm{End}(\mathcal{H}_d). \tag{8.5}$$

The space of *total-spin singlet states* (or simply *spin singlets*) $\mathcal{H}_d^{\mathrm{SU}(2)}$ is defined by the quantum states that are invariant under the natural SU(2)-action on the spin factor, or equivalently, the quantum states that are mapped to zero by the derived $\mathfrak{sl}_2(\mathbb{C})$–action (cf. (8.4)). We can describe this SU(2)-invariant subspace explicitly by

$$\mathcal{H}_d^{\mathrm{SU}(2)} := \{\psi \in \mathcal{H}_d \ : \ S_z^{(d)}\psi = S_+^{(d)}\psi = S_-^{(d)}\psi = 0\}. \tag{8.6}$$

Alternatively, we define the space of spin singlets as the eigenspace of S^2 with eigenvalue 0:

$$\mathcal{H}_d^{\mathrm{SU}(2)} = \{\psi \in \mathcal{H}_d \ : \ \left(S^{(d)}\right)^2 \psi = 0\}. \tag{8.7}$$

The two definitions of $\mathcal{H}_d^{\mathrm{SU}(2)}$ are equivalent. First, we see by the definition of $\left(S^{(d)}\right)^2$ that (8.6) implies (8.7). For the inverse, recall that $S_x^{(d)}$, $S_y^{(d)}$, and $S_z^{(d)}$ are self-adjoint and therefore

$$\begin{aligned}\langle \psi, \left(S^{(d)}\right)^2 \psi\rangle &= \langle \psi, \left(S_x^{(d)}\right)^2 \psi\rangle + \langle \psi, \left(S_y^{(d)}\right)^2 \psi\rangle + \langle \psi, \left(S_z^{(d)}\right)^2 \psi\rangle \\ &= \|S_x^{(d)}\psi\|^2 + \|S_y^{(d)}\psi\|^2 + \|S_z^{(d)}\psi\|^2 \geq 0.\end{aligned}$$

Hence, $\psi \in \ker(\left(S^{(d)}\right)^2)$ implies $S_x^{(d)}\psi = S_y^{(d)}\psi = S_z^{(d)}\psi = 0$ and consequently $S_\pm^{(d)}\psi = 0$.

More generally, the total-spin operator $\left(S^{(d)}\right)^2$ is the Casimir operator of the induced $\mathfrak{sl}_2(\mathbb{C})$–action [47]. Consequently, it acts on $\mathcal{H}_d$ by multiplication of a scalar. In particular, we define the spin-s sector as the subspace of $\mathcal{H}_d$ with quantum states ψ such that

$$\left(S^{(d)}\right)^2 \psi = s(s+1)\,\psi.$$

For $s = 0, \frac{1}{2}, 1, \frac{3}{2}, \ldots$, these spaces are referred to as the spin singlet, doublet, triplet, quartet, and higher spin sectors, respectively. For example, the spin triplet sector is the eigenspace of $\left(S^{(d)}\right)^2$ corresponding to eigenvalue 2. This yields a canonical decomposition of $\mathcal{H}_d$ into irreducible spin sectors. The electronic Hamiltonian is SU(2)–invariant and hence it commutes with $\left(S^{(d)}\right)^2$, and therefore preserves the decomposition. Computations are thus typically carried out within a fixed sector – in this thesis, the spin singlet sector $\mathcal{H}_d^{\mathrm{SU}(2)}$.

From a representation-theoretic viewpoint, the singlet sector corresponds to the trivial representation V_0 of SU(2), which is 1-dimensional and consists of SU(2)–invariant vectors (equivalently, vectors annihilated by the derived $\mathfrak{sl}_2(\mathbb{C})$–action). The space $\mathcal{H}_d$ is completely reducible as an SU(2)–module. Hence it decomposes into irreducibles with multiplicities,

$$\mathcal{H}_d \cong \bigoplus_{j \in \frac{1}{2}\mathbb{Z}_{\geq 0}} V_j^{\oplus c_j},$$

where V_j denotes the jth irreducible SU(2)–representation, defined in Remark 8.2.1. In this decomposition, the spin singlet sector is exactly the $j = 0$ isotypic component,

$$\mathcal{H}_d^{\mathrm{SU}(2)} \cong V_0^{\oplus c_0} \cong \mathbb{C}^{c_0}.$$

Equivalently, the spin-s sectors are isomorphic to the s isotypic components $V_s^{\oplus c_s}$ [47].

Remark 8.2.3. In quantum chemistry, "spin-restricted" refers to a constraint at the one-particle (orbital) level, e.g., in spin-restricted Hartree–Fock theory, the $\uparrow$ and $\downarrow$ electrons share the same spatial orbitals. In particular, spin-restricted is primarily a statement about the reference and orbital parameterization, not about the symmetry content of a correlated ansatz. By contrast, *spin-adapted* (i.e., SU(2)-adapted) refers to the *many-electron* level: the wavefunction (or equivalently the operator ansatz acting on a reference) is constructed to transform in a fixed irreducible SU(2)–representation. Thus, "restricted" and "adapted" address different levels of theory (i.e., orbitals vs. many-body symmetry) and are logically independent. A restricted reference does not by itself enforce SU(2) adaptation of a correlation ansatz, whereas SU(2) adaptation explicitly restricts the state to a chosen spin sector.

Remark 8.2.4. We note that $\mathcal{H}_d^{\mathrm{SU}(2)} \neq \{0\}$ only when d is even, e.g., $d = 2k$. An exterior basis vector $e_{I\uparrow} \wedge e_{J\downarrow} = e_{i_1\uparrow} \wedge \cdots \wedge e_{i_p\uparrow} \wedge e_{j_1\downarrow} \wedge \cdots \wedge e_{j_q\downarrow}$ of $\mathcal{H}_d$ (with $|I| + |J| = d$) is an eigenvector of $S_z^{(d)}$. Here, each spin-up ("$\uparrow$") contributes additively $+\frac{1}{2}$ to the eigenvalue and each spin-down ("$\downarrow$") contributes additively $-\frac{1}{2}$. Explicitly,

$$S_z^{(d)}\big(e_{I\uparrow} \wedge e_{J\downarrow}\big) = \sum_{\ell \in I \cup J} e_{i_1\uparrow} \wedge \cdots \wedge S_z^{(d)} e_{\ell\alpha} \wedge \cdots \wedge e_{j_q\downarrow} = \frac{1}{2}\big(|I| - |J|\big)\, e_{I\uparrow} \wedge e_{J\downarrow}.$$

If $\psi \in \mathcal{H}_d^{\mathrm{SU}(2)}$, then in particular $S_z^{(d)}\psi = 0$, so ψ can have support only on basis vectors with $|I| = |J|$. This enforces $d = |I| + |J| = 2|J|$ to be even. Therefore $\ker(S_z^{(d)}) = \{0\}$ for odd d, and since $\mathcal{H}_d^{\mathrm{SU}(2)} \subseteq \ker(S_z^{(d)})$, this implies $\mathcal{H}_d^{\mathrm{SU}(2)} = \{0\}$ whenever d is odd. We will therefore from now on assume $d = 2k$.

Remark 8.2.5 (Proper embeddings of $\mathcal{H}_d^{\mathrm{SU}(2)}$)**.** Note that the condition $S_z\psi = 0$ alone selects the sector $\ker(S_z) \supseteq \mathcal{H}_d^{\mathrm{SU}(2)}$, isomorphic to $\wedge^k\mathbb{C}^m \otimes \wedge^k\mathbb{C}^m$ via $e_{I\uparrow} \wedge e_{J\downarrow} \mapsto e_I \otimes e_J$. Since $\ker(S_z)$ generally contains contributions from higher-spin irreducibles, we obtain a proper embedding

$$\mathcal{H}_d^{\mathrm{SU}(2)} \subsetneq \ker(S_z) \cong \wedge^k\mathbb{C}^m \otimes \wedge^k\mathbb{C}^m.$$

In particular, the conditions $S_\pm\psi = 0$ enforce the spin–up and spin–down orbitals to be isomorphic. Therefore, we instead consider the symmetric power $\mathrm{Sym}^2(\wedge^k\mathbb{C}^m)$, which has dimension $\binom{\binom{m}{k}+1}{2}$. This space is isomorphic to the subspace of $\mathcal{H}_d$ generated by

$$e_{J\uparrow} \wedge e_{J\downarrow}, \qquad e_{J\uparrow} \wedge e_{K\downarrow} + (-1)^{|J\setminus K|} e_{K\uparrow} \wedge e_{J\downarrow},$$

where $J < K \in \binom{[m]}{k}$ are distinct subsets of size k. This symmetry, however, still does not enforce SU(2)-invariance: the above generators need not vanish under the action of $S_\pm$. For example, when $k = 2$, consider the vector

$$\psi = e_{1\uparrow} \wedge e_{2\uparrow} \wedge e_{3\downarrow} \wedge e_{4\downarrow} + e_{1\downarrow} \wedge e_{2\downarrow} \wedge e_{3\uparrow} \wedge e_{4\uparrow}.$$

Here, $\psi \in \mathrm{Sym}^2(\wedge^k \mathbb{C}^m)$, but $S_+\psi \neq 0$. Hence $\mathcal{H}_d^{\mathrm{SU}(2)}$ is also a proper subspace of $\mathrm{Sym}^2(\wedge^k \mathbb{C}^m)$ and determining the invariant space itself requires more refined tools. Nonetheless, the proper embedding of the invariant space $\mathcal{H}_d^{\mathrm{SU}(2)}$ into $\mathrm{Sym}^2(\wedge^k \mathbb{C}^m)$ will be useful in Section 9.2, as the larger space exhibits a simpler structure than the invariant space itself.

We analyze the irreducible decomposition of the SU(2)–representation $\mathcal{H}_d$ using characters. Recall that the *character* of a finite-dimensional complex representation V of SU(2) is the class function

$$\chi_V : \mathrm{SU}(2) \to \mathbb{C} \; ; \; g \mapsto \mathrm{Tr}\big(g\big|_V\big) \, .$$

Here, $g|_V$ denotes the endomorphism $V \to V$ defined by a 2×2 matrix $g \in \mathrm{SU}(2)$, and $\mathrm{Tr}\big(g\big|_V\big)$ is the trace of the corresponding matrix of size $\dim(V)$. The character χ_V is constant on conjugacy classes [72, Chapter 10]. Since every $U \in \mathrm{SU}(2)$ is unitary (hence normal), it is conjugate in SU(2) to an element of the maximal torus

$$\mathbb{T} := \big\{ \mathrm{diag}(z, z^{-1}) \;\; : \;\; |z| = 1 \big\} \cong S^1.$$

Ergo, characters of SU(2) are determined by their restriction to $\mathbb{T}$. It is therefore convenient to write $\chi_V(z) \;:=\; \chi_V(\mathrm{diag}(z, z^{-1}))$, so that χ_V is a Laurent polynomial with finite support. Moreover, since $t \in \mathbb{T}$ is conjugate with t^{-1}, the Weyl symmetry $\chi_V(z) = \chi_V(z^{-1})$ holds.

The irreducible representations of SU(2) are indexed by $j \in \frac{1}{2}\mathbb{Z}_{\geq 0}$ and may be realized as $V_j \cong \mathrm{Sym}^{2j}(\mathbb{C}^2)$. The action of $t = \mathrm{diag}(z, z^{-1}) \in \mathbb{T}$ on $\mathrm{Sym}^{2j}(\mathbb{C}^2)$ is diagonal in the standard monomial basis, with eigenvalues $z^{2j}, z^{2j-2}, \ldots, z^{-2j}$. Hence, the irreducible character is

$$\chi_j(z) = \mathrm{Tr}\left(t\big|_{V_j}\right) = \sum_{i=0}^{2j} z^{2j-2i} = z^{2j} + z^{2j-2} + \cdots + z^{-2j}. \tag{8.8}$$

In particular, $\chi_{1/2}(z) = z + z^{-1}$. These characters are linearly independent and, by [43, Proposition 2.1], an irreducible decomposition $V \cong \bigoplus_j V_j^{\oplus c_j}$ implies the character identity

$$\chi_V(z) = \sum_j c_j \, \chi_j(z),$$

and vice versa. Thus the multiplicities c_j (and in particular $c_0 = \dim(\mathcal{H}_d^{\mathrm{SU}(2)})$) can be recovered by decomposing χ_V in the basis $\{\chi_j\}_j$ of irreducible characters.

Lemma 8.2.6. *The character of the representation $\mathcal{H}_d$ of* SU(2) *is the Laurent polynomial*

$$\chi_{\mathcal{H}_d}(z) = \sum_{i=0}^{d} \binom{m}{i}\binom{m}{d-i} z^{\,d-2i}. \tag{8.9}$$

If $d = 2k$ then $\mathcal{H}_d$ decomposes into a sum of integer irreducible representations V_j where $0 \le j \le k$, with multiplicity

$$c_j = \binom{m}{k-j}\binom{m}{k+j} - \binom{m}{k-j-1}\binom{m}{k+j+1}. \tag{8.10}$$

If $d = 2k+1$ then $\mathcal{H}_d$ decomposes into a sum of half-integer irreducible representations $V_{j+\frac{1}{2}}$ where $0 \le j \le k$ with multiplicity

$$c_{j+\frac{1}{2}} = \binom{m}{k-j}\binom{m}{k+j+1} - \binom{m}{k-j-1}\binom{m}{k+j+2}. \tag{8.11}$$

Proof. Note that on the one-particle space $\mathcal{H} \cong \mathbb{C}^m \otimes \mathbb{C}^2$, the element $\mathrm{diag}(z, z^{-1}) \in \mathbb{T}$ acts by the endomorphism described by the $n \times n$ diagonal matrix

$$g_n(z) = \mathrm{diag}(z, z^{-1}, z, z^{-1}, \dots, z, z^{-1}).$$

Hence, the character of $\mathcal{H}_d = \wedge^d \mathcal{H}$ is the trace of the dth exterior power of $g_n(z)$. Its diagonal entries are the principal $d \times d$ minors of $g_n(z)$, each obtained by selecting d diagonal entries of $g_n(z)$. Choosing i entries equal to z^{-1} and $d-i$ entries equal to z yields the monomial $z^{d-i}(z^{-1})^i = z^{d-2i}$, and the number of such choices is $\binom{m}{i}\binom{m}{d-i}$, proving (8.9).

We now decompose $\chi_{\mathcal{H}_d}$ into the irreducible characters from (8.8). We first assume $d = 2k$, and without loss of generality, we may assume $2k \le m$. We determine the multiplicities recursively by matching the highest power of z. Write

$$\chi_{\mathcal{H}_d}(z) = \sum_{j \in \mathbb{Z}} a_j\, z^{2j}, \qquad a_j = \binom{m}{k-j}\binom{m}{k+j}, \qquad a_{-j} = a_j.$$

We use the convention $\binom{m}{r} = 0$ for $r \notin \{0, \dots, m\}$. In particular, $a_j = 0$ for $j > k$, so the highest power occurring in $\chi_{\mathcal{H}_d}(z)$ is z^{2k}. Its coefficient is a_k, so we set $c_k := a_k$ and consider

$$\chi^{(1)}(z) := \chi_{\mathcal{H}_d}(z) - c_k \chi_k(z).$$

Since $\chi_{\mathcal{H}_d}$ is invariant under $z \mapsto z^{-1}$ and has nonnegative integer coefficients, the same holds for $\chi^{(1)}$. Moreover, the terms z^{2k} and z^{-2k} are removed, and the remaining highest term is $z^{2(k-1)}$ with coefficient c_{k-1}. Continuing downward, we find that the coefficient of z^{2j} in $\chi_{\mathcal{H}_d}(z)$ is $\sum_{\ell \ge j} c_\ell$, so the multiplicities satisfy

$$c_j = a_j - a_{j+1} = \binom{m}{k-j}\binom{m}{k+j} - \binom{m}{k-j-1}\binom{m}{k+j+1},$$

proving (8.10). Now, let $d = 2k+1$. The character formula (8.9) becomes

$$\chi_{\mathcal{H}_{2k+1}}(z) = \sum_{j\in\mathbb{Z}} \binom{m}{k-j}\binom{m}{k+1+j} z^{2j+1},$$

hence $\chi_{\mathcal{H}_{2k+1}}(z)$ is a Laurent polynomial with only odd exponents. Therefore, in the decomposition of $\mathcal{H}_{2k+1}$ into irreducibles, only half-integer representations can occur. We determine the coefficients $c_{j+\frac{1}{2}}$ by the same triangular elimination as in the even case, matching the highest powers of z successively. This gives the formula in (8.11). □

Theorem 8.2.7. *For $d = 2k$ electrons in $n = 2m$ spin orbitals, the dimension of the spin singlet sector $\mathcal{H}_d^{\mathrm{SU}(2)} \subsetneq \mathcal{H}_d$ is given by*

$$\dim\big(\mathcal{H}_d^{\mathrm{SU}(2)}\big) = N(m+1, k+1),$$

where $N(m+1,k+1)$ is a Narayana number (see `A001263`*).*

Proof. This is a direct consequence of Lemma 8.2.6 since

$$\dim\big(\mathcal{H}_d^{\mathrm{SU}(2)}\big) = c_0 = \binom{m}{k}^2 - \binom{m}{k-1}\binom{m}{k+1} = \frac{1}{m+1}\binom{m+1}{k+1}\binom{m+1}{k} = N(m+1,k+1).$$

□

Remark 8.2.8. The Narayana numbers form a triangle of positive integers for $0 \le k \le m$ and refine the Catalan numbers via

$$\sum_{r=0}^{m} N(m+1, r+1) = C_{m+1}. \tag{8.12}$$

The Catalan number C_{m+1} counts Dyck paths from $(0,0)$ to $(2m+2,0)$, while the Narayana number $N(m+1,k+1)$ counts Dyck paths with exactly $k+1$ peaks (equivalently, k valleys).

Example 8.2.9 ($2k = d = 4$, $2m = n = 8$)**.** We consider 4 electrons in 4 spatial orbitals. Then $\mathcal{H}_4 \cong \wedge^4\mathbb{C}^8$ has dimension $\dim(\mathcal{H}_4) = \binom{8}{4} = 70$ and Theorem 8.2.7 yields

$$\dim\big(\mathcal{H}_4^{\mathrm{SU}(2)}\big) = N(5,3) = 20.$$

The invariant space $\mathcal{H}_4^{\mathrm{SU}(2)}$ is the intersection of the kernels of the three 70×70 matrices $S_z^{(d)}, S_+^{(d)}, S_-^{(d)}$ and it is generated by the following 20 vectors:

$$e_{1\uparrow,1\downarrow,2\uparrow,2\downarrow},\ e_{1\uparrow,1\downarrow,2\downarrow,3\uparrow} - e_{1\uparrow,1\downarrow,2\uparrow,3\downarrow},\ e_{1\downarrow,2\uparrow,2\downarrow,3\uparrow} - e_{1\uparrow,2\uparrow,2\downarrow,3\downarrow},\ e_{1\uparrow,1\downarrow,3\uparrow,3\downarrow},$$
$$e_{1\downarrow,2\uparrow,3\uparrow,3\downarrow} - e_{1\uparrow,2\downarrow,3\uparrow,3\downarrow},\ e_{2\uparrow,2\downarrow,3\uparrow,3\downarrow},\ e_{1\uparrow,1\downarrow,2\downarrow,4\uparrow} - e_{1\uparrow,1\downarrow,2\uparrow,4\downarrow},\ e_{1\downarrow,2\uparrow,2\downarrow,4\uparrow} - e_{1\uparrow,2\uparrow,2\downarrow,4\downarrow},$$
$$e_{1\uparrow,1\downarrow,3\downarrow,4\uparrow} - e_{1\uparrow,1\downarrow,3\uparrow,4\downarrow},\ e_{1\downarrow,2\uparrow,3\downarrow,4\uparrow} - e_{1\uparrow,2\downarrow,3\downarrow,4\uparrow} - e_{1\downarrow,2\uparrow,3\uparrow,4\downarrow} + e_{1\uparrow,2\downarrow,3\uparrow,4\downarrow},$$
$$e_{2\uparrow,2\downarrow,3\downarrow,4\uparrow} - e_{2\uparrow,2\downarrow,3\uparrow,4\downarrow},\ e_{1\downarrow,2\downarrow,3\uparrow,4\uparrow} - e_{1\uparrow,2\downarrow,3\downarrow,4\uparrow} - e_{1\downarrow,2\uparrow,3\uparrow,4\downarrow} + e_{1\uparrow,2\uparrow,3\downarrow,4\downarrow},$$
$$e_{1\downarrow,3\uparrow,3\downarrow,4\uparrow} - e_{1\uparrow,3\uparrow,3\downarrow,4\downarrow},\ e_{2\downarrow,3\uparrow,3\downarrow,4\uparrow} - e_{2\uparrow,3\uparrow,3\downarrow,4\downarrow},\ e_{1\uparrow,1\downarrow,4\uparrow,4\downarrow},\ e_{1\downarrow,2\uparrow,4\uparrow,4\downarrow} - e_{1\uparrow,2\downarrow,4\uparrow,4\downarrow},$$
$$e_{2\uparrow,2\downarrow,4\uparrow,4\downarrow},\ e_{1\downarrow,3\uparrow,4\uparrow,4\downarrow} - e_{1\uparrow,3\downarrow,4\uparrow,4\downarrow},\ e_{2\downarrow,3\uparrow,4\uparrow,4\downarrow} - e_{2\uparrow,3\downarrow,4\uparrow,4\downarrow},\ e_{3\uparrow,3\downarrow,4\uparrow,4\downarrow}.$$

Spin of Fock States and Spin-Singlet Fock States

We now pass from the d-electron sector to the full fermionic Fock space i.e., the direct sum of all particle-number sectors (see Section 8.1). The induced $\mathfrak{sl}_2(\mathbb{C})$–action preserves each exterior power $\mathcal{H}_\ell = \wedge^\ell \mathcal{H}$ and, in the canonical exterior basis, the action of element $g \in \mathfrak{sl}_2(\mathbb{C})$ is represented by the block diagonal matrix

$$\hat{g} = g^{(0)} \oplus g^{(1)} \oplus \cdots \oplus g^{(2m)}, \tag{8.13}$$

where $g^{(\ell)}$ is defined in (8.5). We can now define the subspace $\mathcal{F}^{\mathrm{SU}(2)} \subsetneq \mathcal{F}$ of total-spin singlet states as the direct sum of the spin singlet sectors of all the exterior powers, i.e.,

$$\mathcal{F} = \bigoplus_{\ell=0}^{2m} \mathcal{H}_\ell, \quad \text{and} \quad \mathcal{F}^{\mathrm{SU}(2)} = \bigoplus_{\ell=0}^{2m} \mathcal{H}_\ell^{\mathrm{SU}(2)} = \bigoplus_{k=0}^{m} \mathcal{H}_{2k}^{\mathrm{SU}(2)}.$$

Since $\mathcal{H}_\ell^{\mathrm{SU}(2)} = \{0\}$ for odd ℓ, while $\dim(\mathcal{H}_{2k}^{\mathrm{SU}(2)}) = N(m+1, k+1)$ for $0 \leq k \leq m$, the identity in (8.12) yields

$$\dim\big(\mathcal{F}^{\mathrm{SU}(2)}\big) = \sum_{k=0}^{m} N(m+1, k+1) = C_{m+1}.$$

We recall from Proposition 6.1.6 that $\mathrm{FD}_{2m} \cong \mathrm{End}(\mathcal{F}) \cong \mathcal{F} \otimes \mathcal{F}^\dagger$. Hence, we can write elements of FD_{2m} as

$$\Omega = \sum_{I,J \subseteq [\![m]\!]} a_{I,J}\, e_I \otimes e_J^\dagger.$$

Therefore, we can canonically induce an $\mathfrak{sl}_2(\mathbb{C})$–action on $\mathrm{End}(\mathcal{F})$, via the action on $\mathcal{F}$ and the canonical action on its conjugate $\mathcal{F}^\dagger$. This yields the following action for $\mathfrak{sl}_2(\mathbb{C})$,

$$g(\Omega) = \sum_{I,J \subseteq [\![m]\!]} a_{I,J}\, g(e_I) \otimes e_J^\dagger - \sum_{I,J \subseteq [\![m]\!]} a_{I,J}\, e_I \otimes g(e_J^\dagger) = \hat{g}\Omega - \Omega\hat{g} = [\hat{g}, \Omega]. \tag{8.14}$$

Here $\hat{g}$ is the $2^{2m} \times 2^{2m}$ matrix defined in (8.13). Note that $\hat{g}$ is an endomorphism of $\mathcal{F}$ and thus it is an element in the Fermi–Dirac algebra. The Fermi–Dirac representation of the generators $S_\pm$ and S_z of $\mathfrak{sl}_2(\mathbb{C})$ is

$$\hat{S}_+ = -\sum_{k=1}^{m} a_{k\uparrow}^\dagger a_{k\downarrow}, \quad \hat{S}_- = -\sum_{k=1}^{m} a_{k\downarrow}^\dagger a_{k\uparrow}, \quad \hat{S}_z = \frac{1}{2}\sum_{k=1}^{m} (a_{k\uparrow}^\dagger a_{k\uparrow} - a_{k\downarrow}^\dagger a_{k\downarrow}). \tag{8.15}$$

Note that the elements in the Fermi–Dirac algebra, FD_{2m}, that vanish under the $\mathfrak{sl}_2(\mathbb{C})$–action defined in (8.14) are precisely those that commute with $\hat{S}_\pm$ and $\hat{S}_z$.

The next two sections introduce a commutative ring called the excitation ring. Although this ring will later be connected to our quantum-chemical constructions, the sections can also be read quite independently of the rest of the chapter, since the ring is also of interest from a purely combinatorial commutative algebra perspective. In Section 8.5, we will return to the chemistry and show that this ring is isomorphic to the SU(2)-invariant subalgebra of the Fermi–Dirac algebra.

8.3 The Excitation Ring

Consider the indeterminate $k \times (m-k)$ matrix $X = (x_{i,j})$. We write $\mathbb{C}[X]$ for the polynomial ring generated by the $k(m-k)$ variables $x_{i,j}$, where $1 \leq i \leq k$ and $1 \leq j \leq m-k$. We consider the lexicographic term order (that is $x_{i,j} > x_{i',j'}$ if $i < i'$ or if $i = i'$ and $j < j'$). Let $I_{m,k} \subseteq \mathbb{C}[X]$ be the homogeneous ideal generated by the following $\binom{k+2}{3}\binom{m-k+2}{3}$ cubics:

$$f^{a,b,c}_{p,q,r} = \sum_{\rho \in S_{\{a,b,c\}}} x_{p,\rho(a)} x_{q,\rho(b)} x_{r,\rho(c)}, \qquad \text{where } p \leq q \leq r \text{ and } a \leq b \leq c. \tag{8.16}$$

Here, $S_{\{a,b,c\}}$ denotes the set of permutations of the 3-element multiset $\{a,b,c\}$. Each cubic $f^{a,b,c}_{p,q,r}$ has $1, 2, 3$ or 6 distinct terms, with positive integer coefficients summing to 6. For example, all monomial generators are of the form $f^{a,b,c}_{p,p,p} = 6x_{p,a}x_{p,b}x_{p,c}$ or $f^{a,a,a}_{p,q,r} = 6x_{p,a}x_{q,a}x_{r,a}$.

Example 8.3.1. Let $m = 4$ and $k = 2$. The ideal $I_{4,2}$ is generated by 16 cubics of the form (8.16). There are 12 monomial generators in this case:

$$6x^3_{1,1},\ 6x^3_{1,2},\ 6x^3_{2,1},\ 6x^3_{2,2},$$
$$6x^2_{1,1}x_{1,2},\ 6x_{1,1}x^2_{1,2},\ 6x^2_{2,1}x_{2,2},\ 6x_{2,1}x^2_{2,2},\ 6x^2_{1,1}x_{2,1},\ 6x_{1,1}x^2_{2,1},\ 6x^2_{1,2}x_{2,2},\ 6x_{1,2}x^2_{2,2}.$$

There are also 4 binomial generators, presented here with their leading terms underlined:

$$f^{1,1,2}_{1,1,2} = \underline{2x^2_{1,1}x_{2,2}} + 4x_{1,1}x_{1,2}x_{2,1}, \quad f^{1,2,2}_{1,2,2} = \underline{2x_{1,1}x^2_{2,2}} + 4x_{1,2}x_{2,1}x_{2,2},$$
$$f^{1,2,2}_{1,1,2} = \underline{4x_{1,1}x_{1,2}x_{2,2}} + 2x^2_{1,2}x_{2,1}, \quad f^{1,1,2}_{1,2,2} = \underline{4x_{1,1}x_{2,1}x_{2,2}} + 2x_{1,2}x^2_{2,1}.$$

The quotient $\mathbb{C}[X]/I_{4,2}$ has Krull dimension 0 and degree 20.

The ideal $I_{m,k}$ has previously appeared in the literature on combinatorial commutative algebra and representation theory as the ideal of 3×3 *generalized permanents*, see [12, Example 11.8.5]. We call the quotient ring $S_{m,k} := \mathbb{C}[X]/I_{m,k}$, the *excitation ring*. The name originates from its connection to quantum chemistry – in Corollary 8.5.4 we show that $S_{m,k}$ is isomorphic to the SU(2)–invariant subalgebra of FD_{2m}. It is an Artinian ring, and therefore a vector space. Its degree matches its vector space dimension, which is formulated here:

Theorem 8.3.2. *The excitation ring $S_{m,k}$ is a vector space of dimension*

$$\dim_{\mathbb{C}}(S_{m,k}) = \frac{1}{m+1}\binom{m+1}{k+1}\binom{m+1}{k} = N(m+1, k+1).$$

The proof of Theorem 8.3.2 is combinatorial. We show that the defining generators of $I_{m,k}$ form a Gröbner basis. We thereby obtain a vector space basis consisting of the *standard monomials* for $S_{m,k}$, indexed by certain nonnegative integer matrices. Section 8.4 enumerates this basis by constructing a bijection between the standard monomials and Dyck paths

of length $2m+2$ with exactly k valleys, which are enumerated by the *Narayana number* $N(m+1,k+1) = \frac{1}{m+1}\binom{m+1}{k+1}\binom{m+1}{k}$. Theorem 8.3.2 follows immediately from this enumeration.

In Section 8.5, we explain the relevance of the excitation ring $S_{m,k}$ in our study of spin-adapted electronic systems. We identify $S_{m,k}$ as the SU(2)-invariant ring of the Fermi–Dirac algebra and describe a noncommutative parameterization of $S_{m,k}$ in terms of the *creation and annihilation operators*. The proof of Theorem 8.3.2 provides an explicit model for the space of spin adapted quantum states via the combinatorics of plane partitions, enabling future study of this space using algebro-geometric methods.

We now describe a vector space basis for the excitation ring $S_{m,k}$. This is accomplished using the theory of *Gröbner bases*; see Section 1.1 for an introduction. In particular, this theory provides an algorithmic construction of a vector space basis of *standard monomials* for any quotient $\mathbb{C}[X]/I$, see Theorem 1.1.13. In what follows, we will index monomials in $\mathbb{C}[X]$ by their exponent vectors, written as $k \times (m-k)$ nonnegative integer matrices.

Proposition 8.3.3. *The ideal generators (8.16) of $I_{m,k} \subseteq \mathbb{C}[X]$ form a Gröbner basis with respect to the lexicographic monomial order.*

Proof. By Buchberger's criterion [21, Theorem 2.9.3], it suffices to show that the S-polynomial of any pair (f,g) of generators for $I_{m,k}$ reduces to 0. If the leading monomials of f and g are co-prime, then their S-polynomial reduces to 0 by [21, Proposition 2.9.4]. If they are not co-prime, then f and g only use variables from a 5×5 submatrix of X. Thus f and g are generators of $I_{10,5}$, up to relabeling of the variables in X. Direct computation with `Macaulay2`, [46], verifies that the generators of $I_{10,5}$ form a Gröbner basis, completing the proof. □

Let $M \in \mathsf{Mat}_{a,b}(\mathbb{Z}_{\geq 0})$ be an $a \times b$ nonnegative integer matrix. A *weak diagonal* of M is a sequence of nonzero entries of M in matrix positions $(i_1,j_1),\ldots,(i_r,j_r)$, such that $i_1 \leq \cdots \leq i_r$ and $j_1 \leq \cdots \leq j_r$. The *width* of M, denoted $\mathsf{width}(M)$, is the maximum sum of entries $\sum M_{i,j}$ along a weak diagonal of M.

Corollary 8.3.4. *The standard monomial basis of $S_{m,k}$ is indexed by the set*

$$\{M \in \mathsf{Mat}_{k,m-k}(\mathbb{Z}_{\geq 0}) \,:\, \mathsf{width}(M) \leq 2\}.$$

Proof. Proposition 8.3.3 shows that the defining generators (8.16) of $I_{m,k}$ form a Gröbner basis. By definition, the standard monomial basis of $S_{m,k}$ then consists of monomials not divisible by the leading terms of these generators [21, Proposition 5.3.4]. Write monomials as products $x_{i_1,j_1}\cdots x_{i_r,j_r}$ in lexicographic order, i.e., so that $i_1 \leq i_2 \leq \cdots \leq i_r$ and $j_p \leq j_{p+1}$ whenever $i_p = i_{p+1}$. The leading terms of (8.16) are exactly the degree-3 monomials $x_{i_1,j_1}x_{i_2,j_2}x_{i_3,j_3}$ such that $j_1 \leq j_2 \leq j_3$. Thus the standard monomial basis consists of monomials $x_{i_1,j_1}\cdots x_{i_r,j_r}$ such that the sequence $j_1,\ldots,j_r$ contains no triple ascent, i.e., there are no indices $a<b<c$ with $j_a \leq j_b \leq j_c$. The exponent vectors of these monomials are exactly the $k \times (m-k)$ nonnegative integer matrices of width at most 2, as desired. □

Example 8.3.5. Let $m = 4$ and $k = 2$. The ring $S_{4,2}$ has 20 standard monomials. Since the ideal generators are of degree three, we can see that all 15 monomials of degree at most two in $\mathbb{C}[X]$ are standard monomials for $S_{4,2}$. Of these, $10 = \binom{4+1}{2}$ are monomials of degree two, while the others are the four variables $x_{i,j}$ and the constant 1. The 10 monomials of degree two correspond to the following matrices in $\mathsf{Mat}_{2,2}(\mathbb{Z}_{\geq 0})$:

$$\begin{bmatrix}2&0\\0&0\end{bmatrix}, \begin{bmatrix}0&2\\0&0\end{bmatrix}, \begin{bmatrix}0&0\\2&0\end{bmatrix}, \begin{bmatrix}0&0\\0&2\end{bmatrix}, \begin{bmatrix}1&1\\0&0\end{bmatrix}, \begin{bmatrix}1&0\\1&0\end{bmatrix}, \begin{bmatrix}1&0\\0&1\end{bmatrix}, \begin{bmatrix}0&1\\1&0\end{bmatrix}, \begin{bmatrix}0&1\\0&1\end{bmatrix}, \begin{bmatrix}0&0\\1&1\end{bmatrix}.$$

There are four standard monomials of degree three: $x_{1,1}x_{1,2}x_{2,1}$, $x_{1,2}^2x_{2,1}$, $x_{1,2}x_{2,1}^2$ and $x_{1,2}x_{2,1}x_{2,2}$. They correspond respectively to the matrices

$$\begin{bmatrix}1&1\\1&0\end{bmatrix}, \begin{bmatrix}0&2\\1&0\end{bmatrix}, \begin{bmatrix}0&1\\2&0\end{bmatrix}, \begin{bmatrix}0&1\\1&1\end{bmatrix}.$$

The only standard monomial of degree four is $x_{1,2}^2x_{2,1}^2$, which corresponds to

$$\begin{bmatrix}0&2\\2&0\end{bmatrix}.$$

In order to prove Theorem 8.3.2, it remains to enumerate our standard monomial basis for $S_{m,k}$. We carry this out combinatorially in the next section.

8.4 RSK and Plane Partitions

To enumerate the basis for $S_{m,k}$ from Corollary 8.3.4, we map the standard monomials to a well-studied set of *plane partitions* by applying a version of the *Robinson–Schensted–Knuth correspondence* (RSK). We briefly recount the necessary notation and results. A *semistandard Young tableau* of partition *shape* λ and *content* n is a filling of the Young diagram of λ with numbers in $[n]$ (with repetitions allowed), such that the entries are weakly increasing from left to right along rows and strictly increasing down columns from top to bottom. The set of all semistandard Young tableaux with shape λ and content n is denoted $\mathsf{SSYT}(\lambda, n)$.

Example 8.4.1. Let $\lambda = (4, 2, 1)$. The filling

1	1	2	4
2	3		
5			

is a semistandard Young tableau of shape λ and content c for any $c \geq 5$.

The *Robinson–Schensted–Knuth correspondence* is a classical bijection between nonnegative integer matrices and pairs of semistandard Young tableaux of the same shape. Before stating it, we first recall that the *conjugate* of a partition λ, denoted λ', is the partition whose Young diagram is obtained by transposing the rows and columns of the Young diagram of λ. The *length* $\ell(\lambda)$ of λ is the number of rows in its Young diagram.

Theorem 8.4.2 (RSK, [96, Theorem 7.11.5], [91, Theorem 1 and Section II]). *For all nonnegative integers a, b and c there exists a bijection*

$$\{M \in \mathsf{Mat}_{a,b}(\mathbb{Z}_{\geq 0}) \,:\, \mathsf{width}(M) \leq c\} \overset{RSK}{\longleftrightarrow} \bigsqcup_{\ell(\lambda') \leq c} (\mathsf{SSYT}(\lambda, a) \times \mathsf{SSYT}(\lambda, b)) \,.$$

Theorem 8.4.2 is the usual statement of the RSK bijection. However, the correspondence can be recast as a bijection between nonnegative integer matrices and *plane partitions*. This is the interpretation we use for our enumeration. We follow Hopkins' exposition in [55] to state this alternative version of RSK. It relies on plane partitions: An $a \times b \times c$ *plane partition* is an $a \times b$ nonnegative integer matrix whose entries are bounded above by c and are weakly decreasing along rows and columns. The set of all such objects is denoted by $\mathcal{B}(a, b, c)$.

Example 8.4.3. The matrix $\begin{bmatrix} 5 & 4 & 3 & 1 \\ 3 & 2 & 2 & 1 \\ 3 & 2 & 1 & 0 \\ 2 & 1 & 1 & 0 \end{bmatrix}$ is a $4 \times 4 \times c$ plane partition for any $c \geq 5$.

Theorem 8.4.4 ([55, pg. 3]). *For all $a, b, c \in \mathbb{Z}_{\geq 0}$, there is a bijection*

$$\bigsqcup_{\ell(\lambda') \leq c} (SSYT(\lambda, a) \times SSYT(\lambda, b)) \leftrightarrow \mathcal{B}(a, b, c).$$

The following example illustrates the bijection between pairs of semistandard Young tableaux and plane partitions, which proves Theorem 8.4.4. Before proceeding, we recall some standard matrix terminology. Let $A = (a_{i,j})$ be an $n \times n$ matrix. For any integer k such that $-(n-1) \leq k \leq n-1$, we define the *kth diagonal* of A to be the finite sequence of entries $(a_{i,j})$ satisfying the index relation $j - i = k$. The case $k = 0$ yields the main diagonal of A. For $k > 0$, the sequence lies in the upper triangular part of the matrix and is called the *kth superdiagonal*. Conversely, for $k < 0$, the sequence resides in the lower triangular part of the matrix and is referred to as the *$|k|$th subdiagonal*.

Example 8.4.5. Consider the pair of tableaux $(P, Q) = \left(\begin{array}{|c|c|c|c|c|} \hline 1 & 1 & 2 & 4 & 4 \\ \hline 2 & 3 \\ \cline{1-2} 3 \\ \cline{1-1} \end{array} \,, \begin{array}{|c|c|c|c|c|} \hline 1 & 2 & 2 & 3 & 4 \\ \hline 2 & 3 \\ \cline{1-2} 4 \\ \cline{1-1} \end{array} \right)$, both with entries in $\{1, 2, 3, 4\}$. The P tableau corresponds to the following nested chain of partition shapes, where the ith member consists of only those boxes filled with numbers $\leq i$:

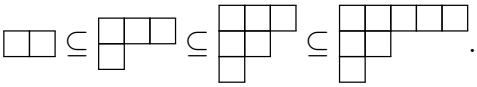

The Q tableau corresponds to the chain

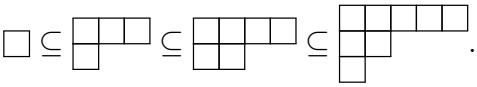

The corresponding plane partition is constructed by mapping these chains of integer partitions directly onto the diagonals of a 4×4 matrix. Specifically, for each $1 \leq i \leq 4$, the ith integer

partition in the chain for P forms the $(4-i)$th subdiagonal, while the ith integer partition in the chain for Q forms the $(4-i)$th superdiagonal. Notice that both sequences naturally terminate at the maximum shape $(5,2,1)$. We obtain the following plane partition:

$$\begin{bmatrix} 5 & 4 & 3 & 1 \\ 3 & 2 & 2 & 1 \\ 3 & 2 & 1 & 0 \\ 2 & 1 & 1 & 0 \end{bmatrix}.$$

The largest entry of this plane partition is 5 precisely because P and Q have 5 columns.

Remark 8.4.6. There is a direct bijection between nonnegative integer matrices and plane partitions which does not require first passing through semistandard Young tableaux. For details, we direct the reader to Hopkins' exposition in [55].

The following enumeration for $\mathcal{B}(a,b,c)$ is classical, deriving from MacMahon's generating series for plane partitions [67]. See, e.g., [96, Equation (7.109)] for a modern statement:

$$|\mathcal{B}(a,b,c)| = \prod_{i=1}^{c} \frac{\binom{a+b+i-1}{a+i-1}\binom{a+b+i-1}{b+i-1}}{\binom{a+b+i-1}{a}\binom{b+i-1}{b}}. \tag{8.17}$$

This formula suffices to prove Theorem 8.3.2.

Proof of Theorem 8.3.2. We wish to show that the excitation ring $S_{m,k}$ has vector space dimension $N(m+1,k+1) = \frac{1}{m+1}\binom{m+1}{k+1}\binom{m+1}{k}$. By Corollary 8.3.4, it suffices to show that

$$|\{M \in \mathsf{Mat}_{k,m-k}(\mathbb{Z}_{\geq 0}) \,:\, \mathsf{width}(M) \leq 2\}| = N(m+1,k+1).$$

Chaining together the bijections from Theorems 8.4.2 and 8.4.4 shows that

$$|\{M \in \mathsf{Mat}_{k,m-k}(\mathbb{Z}_{\geq 0}) \,:\, \mathsf{width}(M) \leq 2\}| = |\mathcal{B}(k,m-k,2)|.$$

The enumeration in (8.17) then proves that $|\mathcal{B}(k,m-k,2)| = N(m+1,k+1)$, as desired. □

The remainder of this section presents another bijection, combinatorially explaining the appearance of the Narayana numbers $N(m+1,k+1)$ in Theorem 8.3.2. We recall the standard combinatorial interpretation for these numbers. A *Dyck word* of length $2n$ is a string w of n "u" symbols and n "d" symbols that is *ballot*, meaning that every initial substring of w contains at least as many u's as d's. A *valley* in w is a du-substring. Let $\mathcal{D}(n,r)$ denote the set of Dyck words of length $2n$ with exactly $r-1$ valleys. The term "valley" originates from the visual interpretation of Dyck words as walks in the first quadrant from $(0,0)$ to $(2n,0)$, consisting of "up" moves $(i,j) \to (i+1,j+1)$ and "down" moves $(i,j) \to (i+1,j-1)$. See Figure 8.1 for an example.

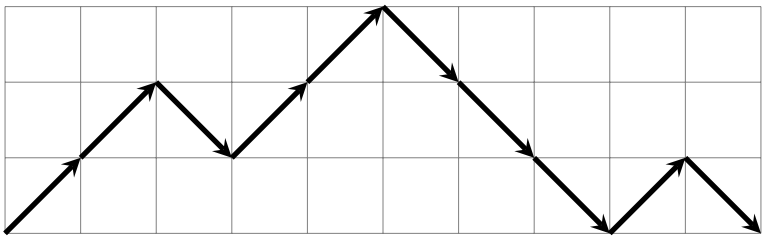

Figure 8.1: The element $w = uuduudddud$ of $\mathcal{D}(5,3)$.

The Narayana number $N(n,r)$ classically arises as the cardinality of $\mathcal{D}(n,r)$, see e.g. [85, Section 2.4.2]. They define a refinement of the Catalan numbers C_n, which count the number of Dyck words of length $2n$ with any number of valleys. By definition,

$$\sum_{r=1}^{n} N(n,r) = \frac{1}{n+1}\binom{2n}{n} = C_n.$$

In order to give an explicit bijection between $\mathcal{B}(k,m-k,2)$ and $\mathcal{D}(m+1,k+1)$, we introduce some additional terminology. A letter in a Dyck word w is *central* if it is not the first or last letter of w, and it is not part of a valley of w. Let $\mathsf{up}_i(w)$ and $\mathsf{down}_i(w)$ respectively denote the number of central u's and d's occurring before the ith valley of w. If i exceeds the number of valleys in w, $\mathsf{up}_i(w)$ and $\mathsf{down}_i(w)$ are defined to count the total number of central u's and d's in w.

Theorem 8.4.7. *The map $\mathcal{D}(m+1,k+1) \to \mathcal{B}(k,m-k,2)$ sending $w \mapsto B^w$, where*

$$B^w_{ij} = \begin{cases} 2 & \text{if } \mathsf{down}_{k+1-i}(w) \geq j, \\ 1 & \text{if } \mathsf{down}_{k+1-i}(w) < j \text{ and } \mathsf{up}_{k+1-i}(w) \geq j, \\ 0 & \text{if } \mathsf{up}_{k+1-i}(w) < j, \end{cases}$$

is a well-defined bijection.

The following example demonstrates the bijection of Theorem 8.4.7.

Example 8.4.8. Let $m = 4$ and $k = 2$, and consider the Dyck word $w = uuduudddud$ illustrated in Figure 8.2 (central paths are highlighted in blue). We can compute that

$$\mathsf{up}_1(w) = 1,\ \mathsf{up}_2(w) = 2,\ \mathsf{down}_1(w) = 0,\ \mathsf{down}_2(w) = 2.$$

The corresponding plane partition B^w is $\left[\begin{smallmatrix} 2 & 2 \\ 1 & 0 \end{smallmatrix}\right]$. For instance, $B^w_{21} = 1$ since $\mathsf{down}_{3-2}(w) = \mathsf{down}_1(w) = 0 < 1$ and $\mathsf{up}_{3-2}(w) = \mathsf{up}_1(w) = 1 \geq 1$.

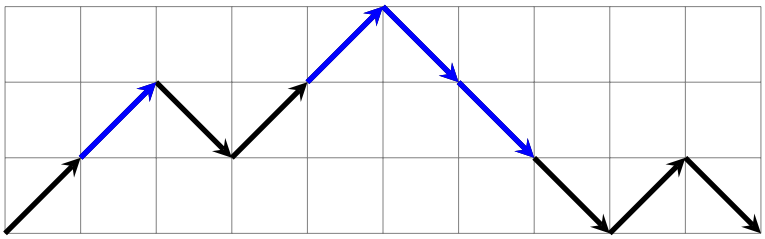

Figure 8.2: The central paths of $w = u\mathbf{u}du\mathbf{udd}dud \in \mathcal{D}(5,3)$ in blue.

8.5 Commutative Algebra to Quantum Chemistry

In this section, we explain the significance of Theorem 8.3.2 in quantum chemistry. Our goal is to give an explicit combinatorial model (i.e., an explicit vector space basis) for the space of spin adapted quantum states $\mathcal{H}_d^{\mathrm{SU}(2)}$.

Coupled cluster theory is commonly formulated in the molecular orbital (particle–hole) picture [18]. Accordingly, we focus on the subalgebra of FD_{2m} generated by the occupied annihilators $a_{i\alpha}$, $i \in [k]$, and the virtual creators $a_{b\alpha}^\dagger$, $b \in [m]\backslash[k]$ (with $\alpha \in \{\uparrow,\downarrow\}$). These generators mutually anticommute, so this subalgebra is an exterior algebra. In symbols,

$$\mathbb{C}\langle a_{1\downarrow}, a_{1\uparrow}, \ldots, a_{k\downarrow}, a_{k\uparrow}, a_{k+1,\downarrow}^\dagger, a_{k+1,\uparrow}^\dagger, \ldots, a_{m\downarrow}^\dagger, a_{m\uparrow}^\dagger\rangle/\langle G\rangle \;\cong\; \wedge\mathbb{C}^{2m},$$

where G denotes the set of relations in (6.2). This is the subalgebra defined in Remark 6.1.4. Since the electronic Hamiltonian conserves particle number, we further restrict to the particle–number preserving subalgebra, denoted $\mathcal{V}_d$, generated by the excitation words $a_{b\alpha}^\dagger a_{i\beta}$ of bidegree $(1,1)$, where $i \in [k]$, $b \in [m]\backslash[k]$, and $\alpha, \beta \in \{\uparrow,\downarrow\}$. Therefore $\mathcal{V}_d$ is also a subalgebra of the particle–number preserving algebra $\mathcal{V}$ defined in Remark 6.1.7. Since these generators are words of total degree two in $\wedge\mathbb{C}^{2m}$, the induced product on $\mathcal{V}_d$ is commutative, and hence $\mathcal{V}_d$ is a commutative ring. It is also a graded ring, graded by the excitation levels. Hence $\mathcal{V}_d = \bigoplus_{\ell=0}^d \mathcal{V}_d^{(\ell)}$, where the ℓth grading $\mathcal{V}_d^{(\ell)}$ is the vector space generated by words with excitation level ℓ (bidegree (ℓ,ℓ) monomials):

$$a_{b_1,\alpha_1}^\dagger a_{i_1\beta_1} \cdots a_{b_\ell,\alpha_\ell}^\dagger a_{i_\ell,\beta_\ell} = a_{b_\ell,\alpha_\ell}^\dagger \cdots a_{b_1,\alpha_1}^\dagger a_{i_1\beta_1} \cdots a_{i_\ell\beta_\ell}.$$

By Pauli's exclusion principle ($a_p^{\dagger 2} = 0$) it follows that $\mathcal{V}_d^{(d+1)} = \{0\}$. That is, the elements of $\mathcal{V}_d$ are nilpotent of order at most d. Elements in $\mathcal{V}_d$ can thus be written as sums of graded elements: $T = T_0 + T_1 + T_2 + \cdots + T_d$ where

$$T_\ell = \sum_{\substack{I\subseteq[\![k]\!],B\subseteq[\![m]\!]\backslash[\![k]\!]\\ |I|=|B|=\ell}} t_{I,B} a_{b_\ell,\alpha_\ell}^\dagger \cdots a_{b_1,\alpha_1}^\dagger a_{i_1\beta_1} \cdots a_{i_\ell\beta_\ell} = \sum_{\substack{I\subseteq[\![k]\!],B\subseteq[\![m]\!]\backslash[\![k]\!]\\ |I|=|B|=\ell}} t_{I,B} a_B^\dagger a_I \;\in\; \mathcal{V}_d^{(\ell)}.$$

The coordinates $t_{I,B} \in \mathbb{C}$ of $\mathcal{V}_d$ are called *cluster amplitudes*, see also Section 7.1. Note that the indexing sets $[\![m]\!]$ and $[\![k]\!]$ are of size $n = 2m$ and $d = 2k$ respectively and hence the combinatorial identity $\sum_{\ell=0}^d \binom{d}{\ell}\binom{n-d}{\ell} = \binom{n}{d}$ reveals that $\mathcal{V}_d \cong \mathbb{C}^{\binom{n}{d}}$ as a vector space.

The ring $\mathcal{V}_{2k}$ inherits the $\mathfrak{sl}_2(\mathbb{C})$–action of the Fermi–Dirac algebra FD_{2m}. That is $g(T) = [\hat{g}, T]$ for $g \in \mathfrak{sl}_2(\mathbb{C})$ and $T \in \mathcal{V}_{2k}$. Indeed it is isomorphic to $\mathcal{H}_{2k}$ as an SU(2)–module.

Proposition 8.5.1. *With the induced $\mathfrak{sl}_2(\mathbb{C})$–actions on $\mathcal{H}_{2k} \subseteq \mathcal{F}$ and on $\mathcal{V}_{2k}$, the map*

$$\Phi : \mathcal{V}_{2k} \to \mathcal{H}_{2k}, \quad T \mapsto T e_{[\![k]\!]}.$$

is an isomorphism of $\mathfrak{sl}_2(\mathbb{C})$–modules.

Proof. The Jth coordinate of $\Phi(T)$ is of the form $(-1)^\sigma t_{I,B}$, where $I = [\![k]\!] \backslash J$, $B = J \backslash [\![k]\!]$ and σ is the parity of the permutation $[\![k]\!] \mapsto (I, [\![k]\!] \backslash I)$. This is true since $a_B^\dagger a_I \, e_{[\![k]\!]} = (-1)^\sigma e_J$. This proves Φ is a bijection. The reference state $e_{[\![k]\!]}$ is a spin singlet state, i.e. $e_{[\![k]\!]} \in \mathcal{H}_{2k}^{\mathrm{SU}(2)}$. Therefore, for any $T \in \mathcal{V}_{2k}$ and any $g \in \mathfrak{sl}_2(\mathbb{C})$ we get that

$$\Phi(g \cdot T) = \Phi([\hat{g}, T]) = [\hat{g}, T] \, e_{[\![k]\!]} = \hat{g} \, T e_{[\![k]\!]} - T \, \hat{g} \, e_{[\![k]\!]} = \hat{g} \, \Phi(T) = g \cdot \Phi(T).$$

Hence Φ is $\mathfrak{sl}_2(\mathbb{C})$–equivariant, and therefore an isomorphism of $\mathfrak{sl}_2(\mathbb{C})$–modules. □

The isomorphism above also induces a grading on $\mathcal{H}_{2k}$: We say a basis vector e_J of $\mathcal{H}_{2k}$ has degree/excitation level $|J \backslash [\![k]\!]|$, and we denote the ℓth grading of $\mathcal{H}_{2k}$ by $\mathcal{H}_{2k}^{(\ell)}$. As a consequence of Proposition 8.5.1, we can study the irreducible decomposition of $\mathcal{H}_d$ via the irreducible decomposition of $\mathcal{V}_d$. In particular:

Corollary 8.5.2. *The map Φ restricts to the invariant spaces of $\mathcal{V}_{2k}$ and $\mathcal{H}_{2k}$. Therefore*

$$\mathcal{H}_{2k}^{\mathrm{SU}(2)} \cong \mathcal{V}_{2k}^{\mathrm{SU}(2)}.$$

A vector space basis for $\mathcal{V}_{2k}^{\mathrm{SU}(2)}$ will serve as our desired model for $\mathcal{H}_{2k}^{\mathrm{SU}(2)}$. We can construct a homogeneous basis for $\mathcal{V}_{2k}^{\mathrm{SU}(2)}$, since the generators in (8.15) are homogeneous, and hence the $\mathfrak{sl}_2(\mathbb{C})$–action preserves excitation levels. In particular, each basis element lives in a graded component $\mathcal{V}_{2k}^{(\ell)}$ for some $1 \leq \ell \leq d$. We start with the simplest generators of $\mathcal{V}_{2k}^{\mathrm{SU}(2)}$, namely those of excitation level 1. The *excitation operators* are the homogeneous elements of bidegree $(1,1)$ given by:

$$X_{i,b} = a_{b\uparrow}^\dagger a_{i\uparrow} + a_{b\downarrow}^\dagger a_{i\downarrow}, \qquad 1 \leq i \leq k < b \leq m.$$

They are linearly independent and commute with $\hat{S}_\pm$ and $\hat{S}_z$ and are therefore generators of $\mathcal{V}_{2k}^{\mathrm{SU}(2)}$. Hence, every polynomial in variables $X_{i,b}$ also commutes with $\hat{S}_\pm$ and $\hat{S}_z$ and the excitation operators generate a subring of $\mathcal{V}_{2k}^{\mathrm{SU}(2)}$. In particular, this is the *excitation ring*:

Theorem 8.5.3. *The excitation operators $X_{i,b}$ parameterize the excitation ring $S_{m,k}$.*

Proof. Let R be the ring generated by *excitation operators* $X_{i,b}$, where $1 \leq i \leq k < b \leq m$. We notice that R is a subring of the ring Z generated by the fixed spin level-one words $x_{i,b,\alpha} := a^\dagger_{b\alpha} a_{i\alpha}$ where $1 \leq i \leq k < b \leq m$ and $\alpha \in \{\downarrow, \uparrow\}$. Note Z is a proper subring of $\mathcal{V}_{2k}$, since we restrict to products with a fixed spin. The ring Z has $2k(m-k)$ variables and can implicitly be described as

$$Z \cong \mathbb{C}[x_{1,k+1,\downarrow}, x_{1,k+1,\uparrow}, \ldots, x_{k,m,\downarrow}, x_{k,m,\uparrow}] \Big/ \langle x_{i,a,\alpha} x_{j,b,\alpha} + x_{j,a,\alpha} x_{i,b,\alpha} \rangle.$$

The ring R is isomorphic to the subring of Z generated by the $k(m-k)$ linear combinations $x_{i,b} := x_{i,b,\uparrow} + x_{i,b,\downarrow} = X_{i,b}$, where $1 \leq i \leq k < b \leq m$. They fulfill exactly the degree-three relations (8.16) and therefore generate $S_{m,k}$. □

The following direct corollary of Theorems 8.3.2 and 8.5.3 is a main result of the chapter. It identifies $S_{m,k}$ with $\mathcal{V}_{2k}^{\mathrm{SU}(2)}$ and therefore describes an explicit vector space basis for $\mathcal{V}_{2k}^{\mathrm{SU}(2)}$, giving the desired combinatorial model for $\mathcal{H}_{2k}^{\mathrm{SU}(2)}$.

Corollary 8.5.4. *The excitation ring $S_{m,k}$ is isomorphic to the invariant ring of $\mathcal{V}_{2k}$. The basis vectors of $\mathcal{V}_{2k}^{\mathrm{SU}(2)}$ are in one-to-one correspondence with $k \times (m-k) \times 2$ plane partitions.*

Proof. By Theorem 8.5.3 the excitation ring is isomorphic to a subring of $\mathcal{V}_{2k}^{\mathrm{SU}(2)}$. By Theorem 8.3.2, Theorem 8.2.7 and Proposition 8.5.1, we have

$$\dim \mathcal{V}_{2k}^{\mathrm{SU}(2)} = \dim \mathcal{H}_{2k}^{\mathrm{SU}(2)} = N(m+1, k+1) = \dim S_{m,k}.$$

The claim $S_{m,k} \cong \mathcal{V}_{2k}^{\mathrm{SU}(2)}$ follows. The second claim follows by applying the RSK bijections of Theorems 8.4.2 and 8.4.4 to the standard monomial basis for $S_{m,k}$ from Corollary 8.3.4. □

Remark 8.5.5 (Explicit generators of the invariance space)**.** The standard monomials of $S_{m,k}$ indexed by plane partitions form the desired homogeneous basis for $\mathcal{V}_{2k}^{\mathrm{SU}(2)}$. We look at the degree 2 component of $S_{m,k}$, i.e., the space $S_{m,k}^{(2)}$ of homogeneous polynomials in $S_{m,k}$ of degree 2. There are no linear relations among the $\binom{km-k^2+1}{2}$ degree two monomials. Therefore they are standard monomials of $S_{m,k}$ and form a basis for $S_{m,k}^{(2)}$. Together with the unit 1 and the degree one generators $x_{i,b}$, they yield a basis for the subspace of $\mathcal{V}_{2k}^{\mathrm{SU}(2)}$ consisting of elements of degree at most 2. Now consider the degree 3 component $S_{m,k}^{(3)}$. There are linear relations among the degree three monomials in $x_{i,b}$, namely the generators in (8.16). Consequently, an explicit description of the standard monomials and hence the basis elements of excitation level ≥ 3 requires plane partitions. Since we focus on the CCD and CCSD formalisms, for which only invariants up to degree two are required, we do not pursue these higher-degree invariants further.

We conclude this chapter by exhibiting a symmetry commonly appearing in quantum chemistry. This symmetry appears at every level of our reasoning, from quantum chemistry through algebra, and into combinatorics.

Remark 8.5.6 (Particle-hole symmetry)**.** For any m, k with $k \leq m$, the excitation rings $S_{m,k}$ and $S_{m,m-k}$ have the same dimension, since

$$\begin{aligned} N(m+1,k+1) &= \frac{1}{m+1}\binom{m+1}{k+1}\binom{m+1}{k} \\ &= \frac{1}{m+1}\binom{m+1}{m-k}\binom{m+1}{m+1-k} \\ &= N(m+1,m-k+1). \end{aligned}$$

In quantum chemistry there exists a classical bijection between $\mathcal{H}_{2k}^{\mathrm{SU}(2)}$ and $\mathcal{H}_{2m-2k}^{\mathrm{SU}(2)}$ known as the *particle-hole symmetry*. It is defined by the map $e_{J\uparrow} \wedge e_{K\downarrow} \mapsto e_{[m]\setminus J\uparrow} \wedge e_{[m]\setminus K\downarrow}$, sending quantum states to their duals. Since $S_{m,k}$ is isomorphic to the invariant space $\mathcal{H}_{2k}^{\mathrm{SU}(2)}$ the map lifts to a bijection between the standard monomials of $S_{m,k}$ and $S_{m,m-k}$. Similarly, the map $\mathsf{Mat}_{k,m-k}(\mathbb{Z}_{\geq 0}) \to \mathsf{Mat}_{m-k,k}(\mathbb{Z}_{\geq 0})$ sending each matrix M to its transpose M^T restricts to a bijection between the standard monomials of $S_{m,k}$ and those of $S_{m,m-k}$. The plane partition B' corresponding to M^T under the RSK correspondence of Theorem 8.4.4 is the transpose of the plane partition B corresponding to M. One can check that all three bijections are equal. We are not aware of a similarly nice bijection between $\mathcal{D}(m+1,k+1)$ and $\mathcal{D}(m+1,m-k+1)$.

In this chapter, we described an SU(2)-action on the space of quantum states, making the state space an SU(2)-representation. This allowed us to decompose it into irreducible components. Of particular interest is the SU(2)-invariant component, whose dimension is governed by the Narayana numbers. We showed this space is isomorphic to the excitation ring, an Artinian commutative ring defined by an ideal generated by cubics. We found a Gröbner basis for this ideal, and described a bijection between its standard monomials and Dyck paths with a fixed number of valleys. This yields an explicit basis of the SU(2)-invariant space through these Dyck paths. This space plays a central role in the next chapter, where we formulate the spin-adapted CC equations by restricting to quantum states in this exact SU(2)-invariant state space.

Chapter 9

Spin-Adapted Coupled Cluster Theory

In this chapter, we derive the spin-adapted coupled cluster equations. To this end we restrict the truncation varieties to their SU(2)–invariant subvarieties. This reveals new algebraic structures, such as the Veronese square of the Grassmannian, which serves as the analogue of the Grassmannian in first quantization and of the flag variety in second quantization. Imposing spin symmetry significantly reduces the dimension of the state space and improves both the efficiency and the numerical stability of coupled cluster calculations. This is illustrated in Section 9.3, where the scaling of the restricted CC degree is compared with the general CC degree. We also exploit this reduction to fully solve the spin-adapted CC equations for the all-orbital lithium hydride molecule (LiH) and for water (H_2O). To our knowledge, these are the largest electronic systems for which the entire CC solution set has been explicitly computed. This chapter is based on [38].

9.1 Spin-Adapted Truncation Varieties

The (spin-free) electronic Hamiltonian in (8.3) is SU(2)-invariant, see end of Section 1.2. This follows since it commutes with the generators of the induced $\mathfrak{sl}_2(\mathbb{C})$–action on the Fock space. In symbols,

$$[H, \hat{S}_+] = [H, \hat{S}_-] = [H, \hat{S}_z] = 0.$$

Here $\hat{S}_\pm$ and $\hat{S}_z$ are the $2^n \times 2^n$ matrices representing the Lie algebra generators $S_\pm$ and S_z, described in (8.15). Consequently, H commutes with the Casimir operator $\hat{S}^2$, and preserves the decomposition of the Hilbert space into SU(2)-isotypic components. The *spin-singlet Schrödinger equation* can therefore be defined as the eigenvalue problem for SU(2)-invariant quantum states,

$$H\psi = \lambda\psi, \qquad \psi \in \mathcal{H}_d^{\mathrm{SU}(2)}. \tag{9.1}$$

We recall that coupled cluster theory employs the ansatz $\psi = e^T e_{[\![k]\!]}$ where *the cluster operator* $T \in \mathrm{End}(\mathcal{F})$ is the new unknown variable and $e_{[\![k]\!]} \in \mathcal{F}$ is the reference state [18, 20]. In particular, here we choose the reference state as a closed-shell spin-restricted state (as is done in restricted Hartree–Fock theory).

Remark 9.1.1. The *closed-shell spin-restricted reference state*

$$\phi_0 = e_{[\![k]\!]} = e_{1\downarrow} \wedge e_{1\uparrow} \wedge \cdots \wedge e_{k\downarrow} \wedge e_{k\uparrow}$$

is a singlet state, i.e. it lies in the spin singlet sector $\mathcal{H}_d^{\mathrm{SU}(2)}$. This can be seen by observing that it is annihilated by the generators $\hat{S}_\pm$ and $\hat{S}_z$. Note that the S_z–action vanishes by Remark 8.2.4. Moreover, the raising operator $\hat{S}_+$ acts by replacing a $\downarrow$-spin electron in a given orbital by an $\uparrow$-spin electron in the same orbital. The reference state is a closed shell state, meaning that for each occupied spatial orbital $i \in [k]$, both spin orbitals $e_{i\downarrow}$ and $e_{i\uparrow}$ occur. Thus it follows by Pauli's exclusion principle that $\hat{S}_+ e_{[\![k]\!]} = 0$. The same holds for $\hat{S}_-$.

Since the reference state $e_{[\![k]\!]}$ is a singlet, the physically relevant correlated Ansätze may be taken entirely within the singlet sector. In other words, we can formulate the coupled cluster equations within the SU(2)–invariant space of $\mathcal{H}_d$. We now describe the construction.

For $1 \leq \ell \leq d$ we define the *ℓth truncated cluster operator* T_ℓ to be a general element in the ℓth grading of $\mathcal{V}_d^{\mathrm{SU}(2)}$. We can write the truncated cluster operators T_1 and T_2 explicitly:

$$T_1 = \sum_{(i,b)} t_{i,b} X_{i,b}, \quad T_2 = \sum_{(i,b)\leq(j,c)} t_{ij,bc} X_{i,b} X_{j,c}, \quad \text{where } t_{i,b}, t_{ij,bc} \in \mathbb{C}. \tag{9.2}$$

Here the pairs $(i,b) \in [k] \times ([m]\backslash[k])$ are ordered lexicographically, and the condition $(i,b) \leq (j,c)$ avoids double counting of quadratic monomials. We then define the *cluster operator* T as the sum of the truncated cluster operators, that is $T = T_1 + T_2 + \cdots + T_d$. We notice that T is a general element in the invariant space $\mathcal{V}_d^{\mathrm{SU}(2)}$ with a zero constant term. We denote the space of cluster operators as

$$\mathcal{V}_d^{\mathrm{SU}(2)'} = \bigoplus_{\ell=1}^{d} \mathcal{V}_{d\,(\ell)}^{\mathrm{SU}(2)}, \quad \text{with} \quad \mathcal{V}_{d\,(\ell)}^{\mathrm{SU}(2)} := \mathcal{V}^{\mathrm{SU}(2)} \cap \mathcal{V}_d^{(\ell)}.$$

This is the space of SU(2)–invariant operators in $\mathcal{V}_d$ with a zero constant term. Equivalently this is the space of nilpotent operators in $\mathcal{V}_d^{\mathrm{SU}(2)}$, that is those T such that $T^{d+1} = 0$.

Proposition 9.1.2. *The spin-singlet exponential map*

$$\mathcal{V}_{2k}^{\mathrm{SU}(2)'} \to \mathcal{H}_{2k}^{\mathrm{SU}(2)}, \qquad T \mapsto \exp(T)\, e_{[\![k]\!]}, \tag{9.3}$$

is an injective polynomial map. Its image coincides with the subspace

$$\{\psi \in \mathcal{H}_{2k}^{\mathrm{SU}(2)} \ : \ e_{[\![k]\!]}^T \psi = 1\} \subsetneq \mathcal{H}_{2k}^{\mathrm{SU}(2)}$$

and the corresponding restriction is a bijection with a polynomial inverse.

Proof. Take a cluster operator $T \in \mathcal{V}_{2k}^{\mathrm{SU}(2)'}$. We recall that T is nilpotent and therefore $\exp(T)e_{[\![k]\!]}$ has polynomial entries. The operator $\exp(T)$ also commutes with the generators $\hat{S}_\pm$ and $\hat{S}_z$ so $\exp(T)e_{[\![k]\!]} \in \mathcal{H}_{2k}^{\mathrm{SU}(2)}$ and the map is well defined and polynomial. Since T is nilpotent, the diagonal entries of $\exp(T)$ are 1 and so $e_{[\![k]\!]}^T \exp(T)e_{[\![k]\!]} = 1$. The bijectivity and the existence of a polynomial inverse follow from the same excitation-level induction as in Proposition 2.1.4, applied within the invariant subspaces. □

Fix a *level set* $\sigma \subseteq [d]$, specifying the allowed excitation levels. For instance, when employing CCS, CCD or CCSD, we set $\sigma = \{1\}, \{2\}, \{1,2\}$, respectively, see also Table 1.1. Let $\mathcal{V}_\sigma^{\mathrm{SU}(2)}$ denote the subspace of $\mathcal{V}_d^{\mathrm{SU}(2)}$ consisting of operators whose excitation level lies in σ. Explicitly:

$$\mathcal{V}_\sigma^{\mathrm{SU}(2)} := \bigoplus_{\ell \in \sigma} \mathcal{V}_{d\,(\ell)}^{\mathrm{SU}(2)} \subseteq \mathcal{V}_d^{\mathrm{SU}(2)'}.$$

The restriction of the spin-singlet exponential map, defined in Proposition 9.1.2, to this subspace is injective. We may further compose it with the projective embedding

$$\mathcal{H}_{2k}^{\mathrm{SU}(2)} \hookrightarrow \mathbb{P}\mathcal{H}_{2k}^{\mathrm{SU}(2)} \cong \mathbb{P}^{N(m+1,k+1)-1}.$$

We define the *spin-singlet truncation variety* $V_\sigma^{\mathrm{SU}(2)} \subseteq \mathbb{P}\mathcal{H}_{2k}^{\mathrm{SU}(2)}$ to be the Zariski closure of the image of $\mathcal{V}_\sigma^{\mathrm{SU}(2)}$ under this composed map. This is analogous to the definition of the truncation varieties in Section 2.2 and Section 7.2, and to Remark 1.1.8. The spin-singlet truncation varieties are therefore parameterized by restrictions of the spin-singlet exponential map. In this chapter we focus on CCS, CCD and CCSD, where the elements of the subspaces $\mathcal{V}_\sigma^{\mathrm{SU}(2)}$ are the truncated cluster operators T_1, T_2 and $T_1 + T_2$ in (9.2). The corresponding truncation varieties are then parameterized by vectors:

$$\psi = \exp(T_1)e_{[\![k]\!]}, \qquad \psi = \exp(T_2)e_{[\![k]\!]}, \qquad \psi = \exp(T_1 + T_2)e_{[\![k]\!]}.$$

Example 9.1.3 (CCS for $m = 4$, $k = 2$)**.** The CCS cluster operator is of the form

$$T_1 = t_{1,3}X_{1,3} + t_{2,3}X_{2,3} + t_{1,4}X_{1,4} + t_{2,4}X_{2,4}.$$

We recall from Theorem 2.2.5 that the (spin-orbital) CCS truncation variety is the Grassmannian $\mathrm{Gr}(4,8) \subseteq \mathbb{P}^{69}$ in its Plücker embedding. To relate this to the spin-singlet truncation variety, we compose the spin-singlet CCS exponential map with the natural inclusion $\mathcal{H}_4^{\mathrm{SU}(2)} \hookrightarrow \mathcal{H}_4 \cong \mathbb{C}^{70}$. This yields a parameterization $\mathbb{C}^4 \to \mathbb{P}\mathcal{H}_4 \cong \mathbb{P}^{69}$ of $V_{\{1\}}^{\mathrm{SU}(2)}$ in the cluster amplitudes $(t_{1,3}, t_{2,3}, t_{1,4}, t_{2,4})$, given by the maximal minors of the 4×8 matrix

$$\begin{bmatrix} 1 & 0 & 0 & 0 & t_{1,3} & 0 & t_{1,4} & 0 \\ 0 & 1 & 0 & 0 & 0 & t_{1,3} & 0 & t_{1,4} \\ 0 & 0 & 1 & 0 & t_{2,3} & 0 & t_{2,4} & 0 \\ 0 & 0 & 0 & 1 & 0 & t_{2,3} & 0 & t_{2,4} \end{bmatrix}. \tag{9.4}$$

Here the rows are indexed by $[\![2]\!]$ and the columns by $[\![4]\!]$. We further project the image onto the 20 dimensional subspace $\mathbb{P}\operatorname{Sym}^2(\wedge^2\mathbb{C}^4)$ described in Remark 8.2.5. The resulting map is the quadratic Veronese embedding ν_2 of the Plücker embedding of $\operatorname{Gr}(2,4) \subseteq \mathbb{P}^5$. More precisely, on the standard affine chart $p_{12} = 1$, the Plücker coordinates are

$$(p_{12}, p_{13}, p_{23}, p_{14}, p_{24}, p_{34}) = \big(1,\ t_{2,3},\ -t_{1,3},\ t_{2,4},\ -t_{1,4},\ t_{1,3}t_{2,4} - t_{2,3}t_{1,4}\big).$$

Composing with ν_2 gives all degree two monomials in the Plücker coordinates. Consequently, the spin-singlet truncation variety embedded into $\mathbb{P}\operatorname{Sym}^2(\wedge^2\mathbb{C}^4)$ is the Veronese square of the Grassmannian:

$$V_{\{1\}}^{\mathrm{SU}(2)} = \nu_2(\operatorname{Gr}(2,4)) \subseteq \mathbb{P}\operatorname{Sym}^2(\wedge^2\mathbb{C}^4).$$

In particular, $V_{\{1\}}^{\mathrm{SU}(2)}$ has dimension 4 and degree 32. Notice that the ambient singlet space $\mathcal{H}_4^{\mathrm{SU}(2)}$ has projective dimension 19, whereas $\operatorname{Sym}^2(\wedge^2\mathbb{C}^4)$ has projective dimension 20. The difference is accounted for by the Plücker relation

$$p_{12}p_{34} - p_{13}p_{24} + p_{23}p_{14} = 0,$$

which becomes a *linear* relation among the Veronese coordinates. We can therefore project onto $\mathbb{P}\mathcal{H}_4^{\mathrm{SU}(2)}$ and embed the truncation variety $\nu_2(\operatorname{Gr}(2,4))$ into the invariant space.

This example generalizes to arbitrary m and k:

Theorem 9.1.4. *The singlet CCS truncation variety is isomorphic to the Veronese square of the Grassmannian, specifically* $V_{\{1\}}^{\mathrm{SU}(2)} \cong \nu_2\big(\operatorname{Gr}(k,m)\big)$. *In particular,*

$$\dim V_{\{1\}}^{\mathrm{SU}(2)} = k(m-k), \quad \text{and} \quad \deg V_{\{1\}}^{\mathrm{SU}(2)} = 2^{k(m-k)} \deg\big(\operatorname{Gr}(k,m)\big).$$

Proof. Recall that the Plücker embedding parameterizes the Grassmannian $\operatorname{Gr}(k,m)$ by the maximal minors of a $k \times m$ matrix $m(t) = \begin{bmatrix} I_k & t \end{bmatrix}$. Here $t = (t_{i,b})_{1 \le i \le k < b \le m}$ is a $k \times (m-k)$ matrix with the CCS cluster amplitudes as entries. We denote the *Plücker coordinates* by $p_I(t) = \det(m(t)_I)$ where $I \subseteq [m]$ and $|I| = k$.

We consider the composition of the spin-singlet exponential map with the natural inclusion $\mathcal{H}_d^{\mathrm{SU}(2)} \hookrightarrow \mathcal{H}_d \cong \mathbb{C}^{\binom{n}{d}}$. Its coordinates are the maximal minors of a $d \times n$ matrix $M(t)$, analogous to (9.4). The columns of this matrix are indexed by the spin orbitals, i.e., $[\![m]\!]$, and the rows by the occupied spin orbitals, i.e., $[\![k]\!]$. Row and column permutation such that spin-up orbitals precede spin-down orbitals yields a block-diagonalization of $M(t)$, i.e.

$$M'(t) = \begin{bmatrix} m(t) & 0_{k,m} \\ 0_{k,m} & m(t) \end{bmatrix}.$$

The maximal minors of $M'(t)$ can be computed using $k \times k$ Laplace expansion, see Section 4.1. First, we note that a $2k \times 2k$ minor of $M'(t)$ is nonzero only if it selects exactly k columns from the spin-down block and k columns from the spin-up block. Now for $I, J \in \binom{[m]}{k}$ we get

$$\det\big(M'(t)_{\{I\downarrow\} \cup \{J\uparrow\}}\big) = \det\big(m(t)_I\big)\, \det\big(m(t)_J\big) = p_I(t)\, p_J(t).$$

These are the coordinates of the composed map. We have now embedded the spin-singlet truncation variety into the full space of quantum states, and want to project down again to the space of SU(2)–invariants. To that end, we embed the image into the space $\mathbb{P}\operatorname{Sym}^2(\wedge^k\mathbb{C}^m)$ — as is described in Remark 8.2.5. We obtain the Veronese embedding of $\operatorname{Gr}(k,m)$:

$$\mathbb{C}^{k\times(m-k)} \to \mathbb{P}^{\binom{m}{k}-1} \to \mathbb{P}\operatorname{Sym}^2(\wedge^k\mathbb{C}^m), \quad t \mapsto (p_I(t)p_J(t))_{I\le J\in\binom{[m]}{k}}.$$

By Proposition 9.1.2 the spin-singlet exponential parameterization maps into the invariant space $\mathcal{H}_{2k}^{\mathrm{SU}(2)}$, so we can further embed the Veronese square of the Grassmannian into $\mathbb{P}\mathcal{H}_{2k}^{\mathrm{SU}(2)}$. Note that there are linear relations among the coordinates, namely, the Plücker relations — quadratic equations in the $p_I(t)$ that cut out the Grassmannian. There are exactly

$$\dim(\operatorname{Sym}^2(\wedge^k\mathbb{C}^m)) - \dim(\mathcal{H}_{2k}^{\mathrm{SU}(2)}) = \binom{\binom{m}{k}+1}{2} - N(m+1,k+1).$$

Plücker relations minimally generating the Grassmannian. The projection of the Veronese square into $\mathbb{P}\mathcal{H}_{2k}^{\mathrm{SU}(2)}$ is therefore also an embedding of $\nu_2(\operatorname{Gr}(k,m))$. □

The Grassmannian of lines in m-dimensional space is a projective space, namely $\operatorname{Gr}(1,m) \cong \mathbb{P}^{m-1}$, and therefore linear. The CCS spin-singlet truncation varieties corresponding to one electron pair, $k=1$, are therefore the *2nd Veronese varieties*, $V_{\{1\}}^{\mathrm{SU}(2)} \cong \nu_2(\mathbb{P}^{m-1})$.

9.2 The Spin-Adapted Coupled Cluster Equations

The truncation varieties are used to approximate the solutions of the Schrödinger equation (9.1). We fix a level set σ and consider quantum states on the spin-singlet truncation variety $V_\sigma^{\mathrm{SU}(2)}$. In general, none of the quantum states on $V_\sigma^{\mathrm{SU}(2)}$ will be eigenvectors of the Hamiltonian. We then relax the constraints of the eigenvalue problem and define the *spin-adapted coupled cluster equations*:

$$(H\psi)_\sigma = \lambda\psi_\sigma, \quad \psi \in V_\sigma^{\mathrm{SU}(2)}. \tag{9.5}$$

Here ψ_σ denotes the projection of the quantum state ψ onto coordinates ψ_J with excitation level $|J\backslash[\![k]\!]| \in \sigma$. Hence, $(\cdot)_\sigma$ defines a projection from $\mathcal{H}_{2k}$ onto the graded subspace $\oplus_{\ell\in\sigma}\mathcal{H}_{2k}^{(\ell)}$. The most common spin-adapted CC approximations correspond to the level sets $\sigma=\{1\}$, $\sigma=\{2\}$, and $\sigma=\{1,2\}$. In the quantum chemistry literature, these are referred to as RCCS, RCCD, and RCCSD, respectively. See also Table 1.1, which lists common CC variants in both the chemistry and mathematical notation.

The Hamiltonian H, defined in (8.3), is an endomorphism of $\mathcal{H}_d^{\mathrm{SU}(2)}$. As such it has an $N(m+1,k+1)\times N(m+1,k+1)$ matrix representation. We say it is *generic* if the parameters h_{pq} and v_{pqrs} are generic. For generic Hamiltonians, the number of solutions to the CC equations in (9.5) is finite and fixed. We call this number the *coupled cluster*

degree of the truncation variety $V_\sigma^{\mathrm{SU}(2)}$ and denote it by $\mathrm{CCdeg}(V_\sigma^{\mathrm{SU}(2)})$. By the parameter continuation theorem, i.e. Theorem 5.1.1, the CC degree serves as an upper bound to the number of solutions of (9.5) for any Hamiltonian operator H of the form (8.3). Note that we define the CC degree using generic two-body operators (8.3), rather than generic $N(m+1,k+1) \times N(m+1,k+1)$ matrices H. This choice reflects the natural algebraic structure of the Hamiltonian. Moreover, it leads to sharper bounds for the number of solutions of physical CC equations. Analogous definitions of the CC degree for two-body operators can be given for the spin-generalized CC equations in Sections 2.3 and 7.4. However, numerical experiments indicate that the resulting reduction in root count is low.

Computing the CC degree of a truncation variety is generally difficult, as it requires solving the CC equations for a generic Hamiltonian H. Nevertheless, one can obtain an upper bound in terms of invariants of $V_\sigma^{\mathrm{SU}(2)}$:

Proposition 9.2.1. *The coupled cluster degree of $V_\sigma^{\mathrm{SU}(2)}$ fulfills the following inequality:*

$$\mathrm{CCdeg}(V_\sigma^{\mathrm{SU}(2)}) \leq (\dim(V_\sigma^{\mathrm{SU}(2)}) + 1)\, \deg(V_\sigma^{\mathrm{SU}(2)}).$$

The proof of this proposition is omitted as it is analogous to the proof of Theorem 2.3.2. The dimension of a truncation variety can easily be computed by counting basis vectors with excitation level in σ. For example, the CCS and CCD spin-singlet truncation varieties have dimensions

$$\dim(V_{\{1\}}^{\mathrm{SU}(2)}) = k(m-k), \quad \dim(V_{\{2\}}^{\mathrm{SU}(2)}) = \binom{k(m-k)+1}{2},$$

respectively, and the dimension of the CCSD truncation variety is their sum. Finding an explicit formula for the degree of a truncation variety is more challenging. In the CCS case, an explicit formula was obtained in Theorem 9.1.4. By contrast, for CCD and CCSD no such formula is known, and the degree for specific values of k and m must be determined numerically. In some cases, we can obtain explicit formulas for the CC degree itself, such as:

Theorem 9.2.2. *Let $k = 1$. The CC degree of the 2nd Veronese variety $V_{\{1\}}^{\mathrm{SU}(2)} \cong \nu_2(\mathbb{P}^{m-1})$ is*

$$\mathrm{CCdeg}(\nu_2(\mathbb{P}^{m-1})) = 2^m - 1.$$

The CC and ED degrees of the Veronese variety coincide; see [10, Section 12.2].

Proof. Here $k = 1$ and so the dimension of the invariant space simplifies to

$$\dim(\mathcal{H}_{2k}^{\mathrm{SU}(2)}) = N(m+1,2) = \binom{m+1}{2}.$$

Remark 8.2.5 implies that, in this case, $\mathcal{H}_2^{\mathrm{SU}(2)} \cong \mathrm{Sym}^2(\mathbb{C}^m)$, so the basis vectors of $\mathcal{H}_2^{\mathrm{SU}(2)}$ are $e_{i\downarrow,i\uparrow}$ and $e_{i\downarrow,j\uparrow} + e_{i\uparrow,j\downarrow}$. They are indexed by subsets in $[m]$ of size one and two. Also,

the Veronese square $x^{\otimes 2} \in \nu_2(\mathbb{P}^{m-1})$ of $x \in \mathbb{P}^{m-1}$ projects onto x under truncation, that is $(x^{\otimes 2})_{\{1\}} = x$. We can therefore rewrite the CC equations as

$$H_{\{1\}} x^{\otimes 2} = \lambda x, \qquad x \in \mathbb{P}^{m-1}, \tag{9.6}$$

where $H_{\{1\}}$ is an $m \times \binom{m+1}{2}$ submatrix of the generic Hamiltonian H, with only the rows indexed by singletons in $[m]$. Note that since $k = 1$, the generic Hamiltonian is a generic matrix, i.e. the structure (8.3) imposes no constraints on the $\binom{m+1}{2} \times \binom{m+1}{2}$ matrix H. We can therefore construct a generic $m \times m \times m$ symmetric tensor η such that $H_{\{1\}}$ has entries $H_{i,j\ell} = \eta_{i,j,\ell}$. The tensor η uniquely corresponds to a homogeneous polynomial of degree three, given by $F_\eta = \langle \eta, x^{\otimes 3} \rangle$, and its gradient satisfies $\nabla F_\eta = H_{\{1\}} x^{\otimes 2}$. The CC equations in (9.6) are therefore precisely the fixed-point equations of ∇F_η. Equivalently, they are the eigenpair equations for the symmetric tensor η, see [10, Equation 12.13]. Also see [72, Section 9.1] for the definition of eigenpairs of tensors as fixed-points of a gradient map. Since H and η are generic tensors the CC degree is $2^m - 1$, by [10, Theorem 12.17]. □

In (9.5) we formulate the unlinked coupled cluster equations in an algebraic way. This might be unintuitive for readers that are experienced in electronic structure theory. Nonetheless this formulation is important to prove results such as Proposition 9.2.1. However, this presentation is not optimal for explicitly solving the CC equations. Since the restriction of the exponential map to $\mathcal{V}_\sigma$ is injective, we can write the unlinked coupled cluster equations in the following way:

$$((H - \lambda \cdot I_{\mathcal{F}}) \exp(T_\sigma) e_{[\![k]\!]})_\sigma = 0.$$

This is a square polynomial system of size $\dim(V_\sigma^{\mathrm{SU}(2)}) + 1$, whose variables are the energy λ and the cluster amplitudes $t_{I,B}$ with excitation level $|I| \in \sigma$. We compare this with the elements of the CC family in (5.1). Using this formulation, we can solve the CC equations with `HomotopyContinuation.jl` [11]. For an in-depth description of how we solve the CC equations, see Section 5.1.

We close this section with a short remark on Löwdin's symmetry dilemma:

Remark 9.2.3. Although the Hamiltonian is SU(2)-invariant and its exact eigenstates can be chosen as simultaneous eigenstates of $\hat{S}^2$ and $\hat{S}_z$, approximate ansätze may face a trade-off commonly referred to as *Löwdin's symmetry dilemma*. At the mean-field level, enforcing spin symmetry (e.g. restricted Hartree–Fock) yields a spin-pure reference but may give qualitatively poor energies in regimes of strong (static) correlation (for instance, along bond dissociation), because a single symmetry-adapted determinant cannot represent near-degeneracy effects. Allowing symmetry breaking (e.g. unrestricted Hartree–Fock) often lowers the energy and captures part of the static correlation, but produces *spin-contaminated* states that do not lie in $\mathcal{H}_d^{\mathrm{SU}(2)}$. The same tension can propagate to correlated methods built on a mean-field reference. In *restricted* coupled cluster theory we deliberately formulate the equations on the SU(2)–invariant sector, see (9.1), so that the CC state is spin-adapted by construction; however, this restriction can necessitate higher excitation rank to recover correlation effects

that a broken-symmetry reference may mimic at lower rank. Alternative strategies include symmetry restoration (spin projection) applied to broken-symmetry references, which aims to combine the energetic flexibility of symmetry breaking with a final spin-pure wavefunction.

9.3 Numerical Simulations

A practical algebraic measure of computational complexity in CC theory is the *number of isolated solutions* (counted with multiplicity) for a generic instance of the CC equations, i.e., the *CC degree*, see Chapter 5. In homotopy-based solvers, the CC degree directly controls the number of solution paths that need to be tracked, and is therefore a reliable proxy for runtime and memory. The central numerical message of this section is that imposing SU(2)–spin adaptation reduces the CC degree by orders of magnitude, making exhaustive solution and continuation computations feasible in regimes where the spin-generalized formulation becomes intractable. The simulations presented here were performed using the software packages `HomotopyContinuation.jl` [11] and `PySCF` [98–100]. All computations were done on the MPI-MiS computer server, using four 18-Core Intel Xeon E7-8867 v4 at 2.4 GHz (3072 GB RAM).

Scaling of Generic Spin Restricted Systems

We begin by comparing the number of roots of the spin restricted coupled cluster equations (RCC) with the number of roots of the spin generalized coupled cluster equations (GCC) from Section 2.3. See Table 1.1 to refresh on these naming conventions. For $k = 1$ (and $d = 2$) we investigate how the CC degree scales with the number of spin orbitals n, both for the CC equations for singles ($\sigma = \{1\}$) and for doubles ($\sigma = \{2\}$), similar to Example 5.2.3.

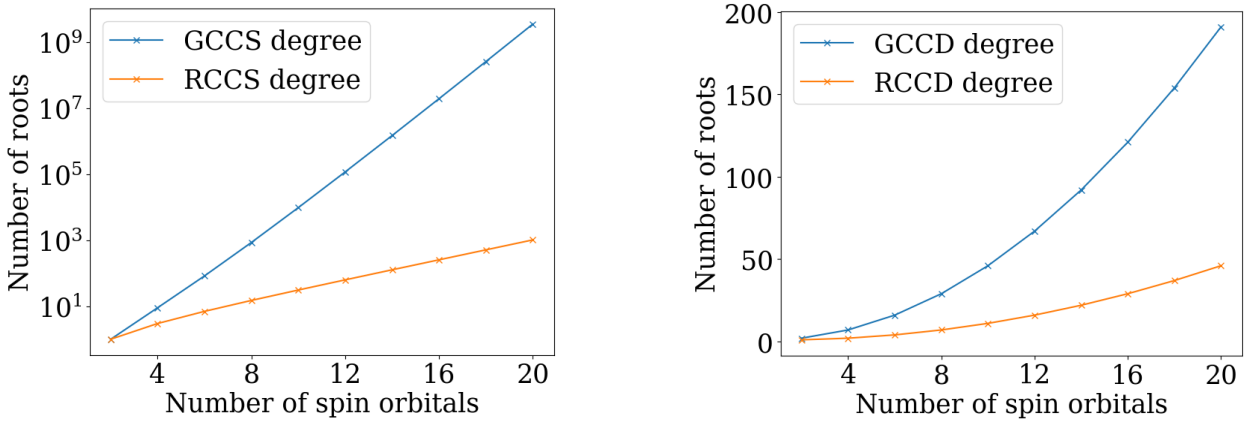

Figure 9.1: Comparison of the number of roots between spin restricted and spin generalized CC equations for CCS (left) and CCD (right) at $k = 1$. The reduction in degree translates into a corresponding reduction in the number of solution paths that must be tracked.

The blue curve shows the spin-generalized CC degree (see Theorem 3.1.2 and Corollary 2.3.3 for CCS and CCD, respectively), while the orange curve shows the corresponding spin-adapted CC degree. Figure 9.1 quantifies the reduction in generic solution complexity obtained by imposing SU(2)–invariance. For $k = 1$ and CCS, the spin-generalized degree grows to $\sim 10^9$ at 20 spin orbitals, whereas the spin-adapted degree is only $\sim 10^3$, corresponding to a reduction of roughly six orders of magnitude in the number of isolated solutions (and hence in the number of continuation paths in homotopy-based solvers). For CCD, the degrees are smaller but the same trend persists: at 20 spin orbitals the degree decreases from about 190 (generalized) to about 45 (restricted), a reduction by a factor of ≈ 4. These data indicate that spin adaptation yields a substantial algorithmic simplification of the CC polynomial systems already in the minimal-electron setting, motivating its use in the numerical studies below.

Indeed, we observe that the effect becomes numerically pronounced and computationally observable already for systems as small as four electrons. We compare CCD degrees for the spin-adapted (RCCD) and spin-generalized (GCCD) formalisms when $d = 4$ (two electron pairs, $k = 2$) and the number of spin-orbitals is $n = 8, 9, 10, 11, 12$. The spin-generalized CCD degrees are taken from Section 2.3 where available, and for larger n we report the best available upper bounds from [33]. The resulting degrees are summarized in Table 9.1.

n	8	9	10	11	12
RCCD	20	–	998	–	$\sim 1.19 \cdot 10^7$
GCCD	72	1 823	2 523 135	$\leq 3.2 \cdot 10^{11}$	$\leq 1.18 \cdot 10^{23}$

Table 9.1: RCCD and GCCD degrees for four electrons ($d = 4$). For $n = 11, 12$ the GCCD entries are upper bounds. The collapse in degree under spin adaptation directly reflects a collapse in the number of solution branches.

Two features are noteworthy. First, even at modest size ($n = 10$), the degree collapses from 2 523 135 in GCCD to 998 in RCCD, a reduction by more than three orders of magnitude. Second, the available bounds indicate that the gap continues to widen rapidly as n grows, underscoring that spin adaptation is not a cosmetic symmetry constraint but a decisive computational simplification. We now illustrate how the incorporation of spin-adaptation pushes the boundaries of algebraic computations for chemical systems.

Lithium Hydride

Lithium hydride (LiH) has served as a small yet "chemically realistic" benchmark system for our algebraic computations, see for example Sections 1.2 and 5.3. In a minimal-basis (STO-6G) description, LiH is modeled with four electrons (two electron pairs) in six spatial orbitals, i.e., twelve spin orbitals. The minimal spatial basis is given by the atomic orbitals

$$\mathrm{H}\,1s, \quad \mathrm{Li}\,1s, \quad \mathrm{Li}\,2s, \quad \mathrm{Li}\,2p_x, \quad \mathrm{Li}\,2p_y, \quad \mathrm{Li}\,2p_z.$$

We compute the molecular orbitals for LiH at bond length $R = 2.85$, using spin-restricted Hartree–Fock; see Example 1.2.4. The molecular orbitals are eigenvectors of a $m \times m$ matrix F, called the *Fock matrix* [103, Section 3.4]. The corresponding eigenvalues are

$$(-2.38524385,\ -0.29351662,\ 0.07939386,\ 0.16259687,\ 0.16259687,\ 0.57210126).$$

These are called the molecular-orbital energies. For LiH, the lowest molecular orbital has much lower energy than all the others. This suggests that it plays a different role from the remaining orbitals and contributes little to the correlation effects relevant for bonding. It is therefore common to approximate the model by keeping this lowest orbital fixed. This is the so-called frozen-core approximation. We do not do this here. Instead, we simplify the model in a different way, by splitting the orbitals into two classes determined by their relation to the bond axis; we explain this decomposition below.

LiH Dissociation in a σ-Active Space

We choose the Li–H bond axis as the z-axis of the coordinate frame; that is, both nuclei lie on the z-axis. In this setting, the one-particle space $\mathcal{H}$ decomposes as

$$\mathcal{H} \cong \mathcal{H}^{(\sigma)} \oplus \mathcal{H}^{(\pi)}.$$

The subspace $\mathcal{H}^{(\sigma)}$ contains the orbitals aligned with the bond axis and thus describes σ-bonding. Here, σ-bonding means bonding arising from orbital overlap along the bond axis (z-axis). On the other hand, the subspace $\mathcal{H}^{(\pi)}$ contains the orbitals perpendicular to the bond axis and corresponds to π-bonding. Here, π-bonding means bonding arising from orbital overlap perpendicular to the bond axis. Explicitly, the subspace $\mathcal{H}^{(\sigma)}$ is the four-dimensional space spanned by the atomic orbitals H $1s$, Li $1s$, Li $2s$, and Li $2p_z$. We refer to it as the *σ-active space*. The subspace $\mathcal{H}^{(\pi)}$ is spanned by the two remaining atomic orbitals Li $2p_x$ and Li $2p_y$, which are perpendicular to the bond axis.

Accordingly, the molecular-orbital coefficient matrix can be arranged in block diagonal form. We obtain the molecular-orbital coefficient matrix C from a spin-restricted Hartree–Fock calculation [103, Section 3.4] using PySCF [99, 100]:

$$C = \left[\begin{array}{ccc|cc|c} 0.994 & -0.165 & -0.198 & 0 & 0 & 0.074 \\ 0.023 & 0.438 & 0.799 & 0 & 0 & -0.747 \\ \hline 0 & 0 & 0 & 0.398 & 0.917 & 0 \\ 0 & 0 & 0 & 0.917 & -0.398 & 0 \\ \hline -0.006 & 0.349 & -0.617 & 0 & 0 & -1.004 \\ 0.005 & 0.551 & -0.124 & 0 & 0 & 1.231 \end{array}\right].$$

Here, two molecular orbitals are supported entirely on the basis functions $\{\text{Li}\,2p_x, \text{Li}\,2p_y\}$ and have zero coefficients on the remaining atomic orbitals. Hence C can indeed be written in block diagonal form with a 4×4 σ-block and a 2×2 π-block. Also, compare this MO

coefficient matrix with the 4×4 MO coefficient matrix computed in Example 1.2.4; note that there we had already removed the $2p_x$ and $2p_y$ orbitals.

Since the orbitals in $\mathcal{H}^{(\sigma)}$ are the ones aligned with the bond axis and relevant for the Li–H bond, we restrict our simulations to the σ-active space $\mathcal{H}^{(\sigma)}$. This leads to a reduced model with two electron pairs and four spatial orbitals, i.e. $d = 2k = 4$ and $n = 2m = 8$. This is exactly the model for LiH used in our computations in Example 1.2.4 and Section 5.3. Note that if the molecule is no longer aligned along the z-axis during the reaction, then this separation is no longer exact, and the σ- and π-subspaces may start to interact. For the active-space viewpoint underlying this reduction, see [88, Chapter 9].

We investigate the root structure for RCCSD while dissociating LiH over bond lengths from 1 to 3 bohr. The spin-singlet CC degree in this case is

$$\mathrm{CCdeg}(V_{\{1,2\}}^{\mathrm{SU}(2)}) = 620$$

as opposed to the spin-generalized CC degree reported in Section 5.3:

$$\mathrm{CCdeg}(V_{\{1,2\}}) \approx 16\,952\,996.$$

We discretize the interval $[1, 3]$ using an equidistant grid with 50 points and compute between 618 and 620 RCCSD solutions per grid point. For comparison, diagonalizing the corresponding Hamiltonian (i.e., a 20×20 real-valued symmetric matrix) yields 20 distinct eigenvalues.

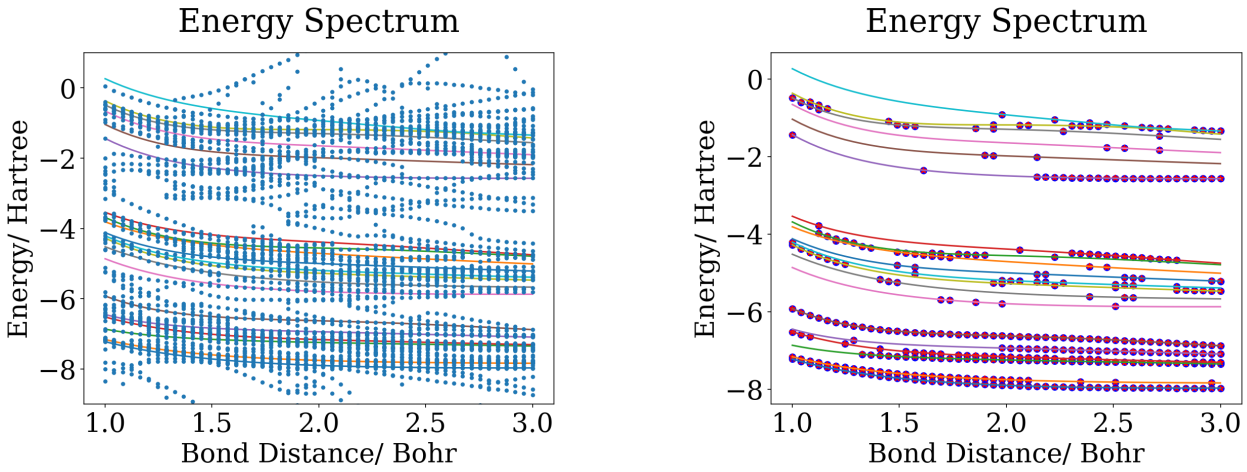

(a) (b)

Figure 9.2: LiH dissociation in a minimal basis ($k = 2$, $m = 4$): comparison of RCCSD energy branches with the exact eigenvalue curves. (a) All RCCSD energy branches compared to the exact spectrum. (b) RCCSD energies lying near an eigenvalue (i.e. physically relevant).

Figure 9.2a shows all RCCSD energy branches together with the exact eigenvalue curves, while Figure 9.2b highlights only those RCCSD energies that lie close to an eigenvalue, i.e., within an energy difference of less than 10^{-3}.

All-electron LiH calculations

In our previous algebro-computational investigations, all-orbital simulations for LiH were out of computational reach due to the sheer size of the CC polynomial system and the corresponding solution count. As reported in Section 2.3, the corresponding CCD and CCSD systems consist of 168 and 200 equations, respectively — well beyond the practical limits of current algebraic numerical solvers. Moreover, the number of homotopy paths that would need to be tracked vastly exceeds the approximately 1.7×10^7 paths tracked in Sections 5.3 and 5.4, where the CCSD calculations for LiH in 8 spin orbitals took over 30 days. In the present setting, however, imposing spin adaptation reduces the effective algebraic complexity sufficiently to make a RCCD solution-landscape computation feasible for the all-orbital system. We now present these computations for LiH with $k = 2$ electron pairs in $m = 6$ spatial orbitals, at bond distance $R = 2.85$ bohr.

For a generic RCCD system with $k = 2$ electron pairs in $m = 6$ spatial orbitals, the monodromy solver required 21 days to recover the complete solution set, revealing the RCCD degree as

$$\mathrm{CCdeg}(V_{\{2\}}^{\mathrm{SU}(2)}) \approx 11\,920\,113. \tag{9.7}$$

Recall that an upper bound for the same system in GCCD is 10^{23}, see Table 9.1. Once the generic solutions were obtained, a parameter homotopy tracked them to the LiH instances in 3 days and 48 minutes. This computation produced 67 909 solutions, of which 552 are non-singular and 106 are real. In Figure 9.3a we compare the full RCCD energy spectrum with the 71 distinct eigenvalues of the symmetric 105×105 Hamiltonian matrix.

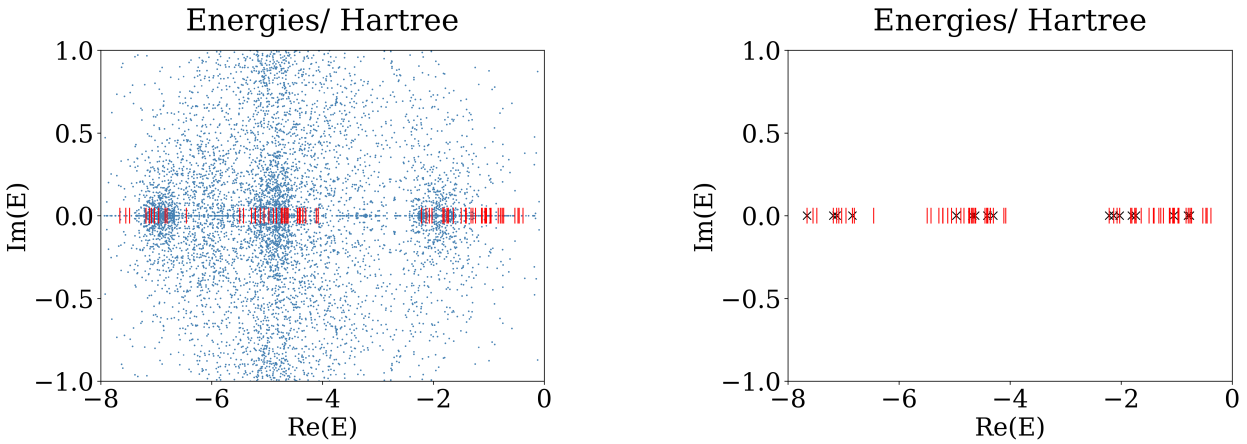

(a) (b)

Figure 9.3: LiH dissociation in a full basis ($k = 2$, $m = 6$): comparison of RCCD energies with the exact eigenvalues. (a) All RCCD energies compared to the exact spectrum. (b) RCCD energies lying near an eigenvalue (physically relevant).

In Figure 9.3b we highlight only those RCCD energies that lie within a 10^{-3} radius of an

eigenvalue. In total, this provides (to our knowledge) the first all-electron LiH computation in which the *entire* RCCD solution set is explicitly resolved.

The resulting all-electron picture reinforces two qualitative observations already present in the σ-active-space study. First, there are multiple physically relevant RCCD energies close to exact eigenvalues. Second, the RCCD polynomial system admits additional, non-physical branches whose energies do not correspond to any eigenvalue of the Hamiltonian and may even fall below the exact ground-state energy. Such "overcorrelated" solutions are consistent with the non-variational character of coupled cluster theory, but here they appear as a *structural* feature of the RCCD algebraic solution set rather than a numerical accident. Their systematic presence in the all-electron calculation emphasizes the value of global solution methods (monodromy/parameter homotopy) for characterizing the full CC landscape and motivates *a posteriori* diagnostics for identifying the physically meaningful roots among many mathematically valid ones [2, 34, 56, 77].

Water

Water (H_2O) in a minimal basis set has ten electrons (five electron pairs) in seven spatial orbitals, and hence in 14 spin orbitals. The minimal spatial basis is given by the atomic orbitals

$$\mathrm{H}\,1s, \quad \mathrm{H}\,1s, \quad \mathrm{O}\,1s, \quad \mathrm{O}\,2s, \quad \mathrm{O}\,2p_x, \quad \mathrm{O}\,2p_y, \quad \mathrm{O}\,2p_z.$$

We perform the spin-restricted Hartree–Fock calculations as we did with LiH at the beginning of this section and obtain a molecular orbital basis. The corresponding molecular-orbital energies are

$$(-20.5043,\ -1.2759,\ -0.6209,\ -0.4593,\ -0.3975,\ 0.5970,\ 0.7299).$$

One of the molecular orbitals lies much lower in energy than all the others, i.e. the lowest orbital is separated from the remaining orbitals by a large energy gap, $\Delta\varepsilon \approx 19.23\,\text{hartree} \approx 523\,\text{eV}$. This suggests that the lowest molecular orbital is an inner core orbital, that is, an orbital close to the nucleus that contributes little to bonding or low-energy excitations. In the frozen-core approximation, such an orbital is kept fixed and doubly occupied by one spin-up and one spin-down electron. The remaining orbitals are then taken to describe the chemically active part of the system, and the computations are carried out only in this reduced space.

To verify this, we measure how strongly the molecular orbitals are concentrated on the oxygen $1s$ atomic orbital. We take this to be the core orbital, since it is the innermost atomic orbital of the heaviest atom in the molecule and is therefore the natural candidate for a tightly bound core state. With the above ordering of the atomic orbitals, the oxygen $1s$ orbital is the third basis function. Thus, for molecular orbital i, we define the quantity

$$w_{\mathrm{O\,1s}}^{(i)} = C_{3i}(SC)_{3i}.$$

Here C is the molecular-orbital coefficient matrix, and S is the atomic-orbital overlap matrix. This measures the contribution (weight) of the oxygen $1s$ atomic orbital to molecular orbital

i. Since the atomic-orbital basis is not orthonormal (see Remark 1.2.5) this quantity is not simply C_{3i}^2; the overlap matrix S is needed to account for overlaps between AO basis functions. We find for the lowest molecular orbital, which has the lowest MO energy, that the contribution of O $1s$ is

$$w_{\mathrm{O}\,1\mathrm{s}}^{(1)} = 0.996559.$$

Since this value is very close to 1, the lowest molecular orbital is almost entirely supported on oxygen $1s$. We therefore keep this orbital fixed and doubly occupied, and perform the remaining calculations only for $k = 4$ electron pairs in $m = 6$ spatial orbitals. This is called the frozen-core approximation.

We solved a generic instance of the RCCD equations for $k = 4$ and $m = 6$ using a monodromy solver. After running the solver for 6 days and 15 hours, we obtained 11 920 154 solutions. By particle-hole symmetry, the corresponding RCCD degree coincides with that for $k = 2$ and $m = 6$. Comparing this count with the approximate CC degree reported in (9.7), we find a discrepancy of 41 solutions. We attribute this discrepancy to numerical error and assume that both monodromy computations failed to detect some solutions. In Section 5.1, we describe the stopping criteria used in monodromy computations and explain why, by their very nature, such methods make it difficult to verify solution completeness. Consequently, the computed solution counts provide numerical approximations to the CC degree that are always lower bounds. With high probability these lower bounds are exact or at least very close to the true value. Once the generic solutions were obtained, a parameter homotopy tracked them to the H_2O instances in 13 hours, finding 10 628 368 solutions, of which 603 are singular and 7 396 are real.

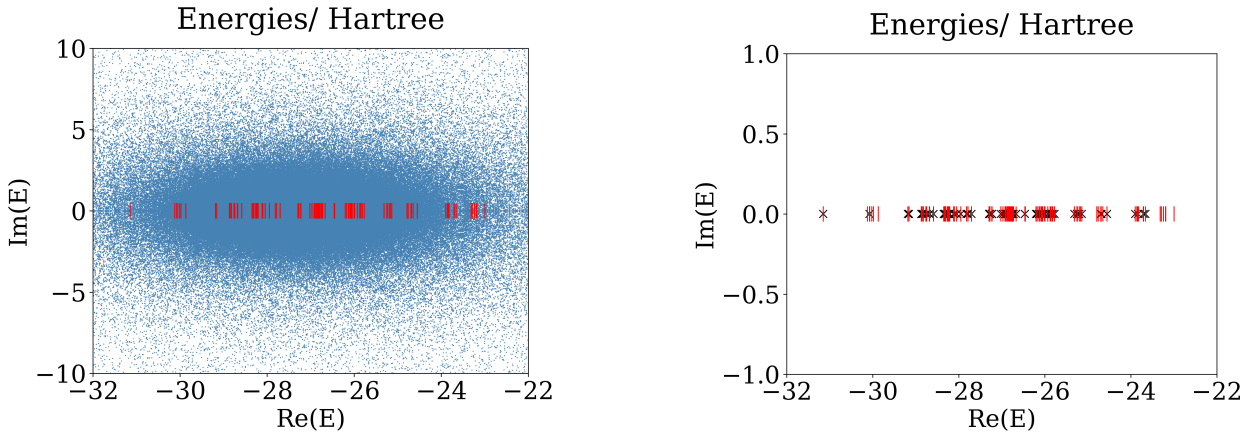

(a) (b)

Figure 9.4: H_2O dissociation in a minimal basis ($k = 4$, $m = 6$): comparison of RCCD energies with the exact eigenvalues. (a) All RCCD energies compared to the exact spectrum. (b) RCCD energies lying near an eigenvalue (physically relevant).

In Figure 9.4a we compare the full energy spectrum with the 105 distinct eigenvalues of the nonsingular Hamiltonian matrix. In Figure 9.4b we highlight only those RCCD energies that lie within a 10^{-3} radius of an eigenvalue.

The full RCCD energy spectrum for H_2O appears as a cloud surrounding the exact eigenvalues, becoming denser toward the center of the spectrum. Consequently, some solution energies may lie close to an eigenvalue for purely statistical reasons, rather than being physically significant. This indicates that further investigation into the numerical stability of the computed roots is needed. This lies beyond the scope of the thesis and is left for future work.

We conclude this chapter, and therefore this thesis, with a summary of our contributions and future directions. In this chapter, we formulated the spin-adapted coupled cluster equations. This entailed restricting the truncation varieties defined in Section 2.2 to the SU(2)-invariant state space, revealing, for example, the Veronese square of the Grassmannian. This restriction lowers the dimensions of the truncation varieties and, correspondingly, their CC degrees. This reduction in complexity makes it possible to study the full CC solution spectrum for larger systems than was previously possible. We illustrate this for lithium hydride (without orbital reduction) and water.

In this thesis, we used nonlinear algebraic methods to tackle a central problem in quantum chemistry, namely, solving the Schrödinger equation. In particular, we built an algebraic geometric framework for coupled cluster theory, using a great deal of combinatorics and representation theory as well. This process revealed many well-known varieties, such as the Grassmannian, flag varieties, spinor varieties and the Veronese varieties. With these algebraic tools in hand, we were able to resolve the full CC solution spectrum for the water molecule, a physically relevant system that serves as a fundamental benchmark in quantum chemistry. That, to our knowledge, has not been achieved before. Beyond the results obtained here, several directions remain open. This includes a deeper study of the different truncation varieties, their CC degrees and projective defining equations. Another direction would involve understanding the special structure of the Hamiltonian, and how this structure impacts its eigenvectors. In particular, we would want to understand whether these eigenvectors lie close to, or even on, a truncation variety. This would qualify the accuracy of the CC method.

Bibliography

[1] Federico Ardila, Thomas Bliem, and Dido Salazar. "Gelfand–Tsetlin polytopes and Feigin–Fourier–Littelmann–Vinberg polytopes as marked poset polytopes". *Journal of Combinatorial Theory, Series A* 118.8 (2011), 2454–2462.

[2] Rodney J. Bartlett, Young Choon Park, Nicholas P. Bauman, Ann Melnichuk, et al. "Index of multi-determinantal and multi-reference character in coupled-cluster theory". *The Journal of Chemical Physics* 153.23 (2020), 234103.

[3] Daniel J. Bates, Paul Breiding, Tianran Chen, Jonathan D. Hauenstein, Anton Leykin, and Frank Sottile. "Numerical nonlinear algebra" (2024). arXiv: 2302.08585.

[4] George M. Bergman. "The diamond lemma for ring theory". *Advances in Mathematics* 29.2 (1978), 178–218.

[5] Barbara Betti, Marta Panizzut, and Simon Telen. "Solving equations using Khovanskii bases". *Journal of Symbolic Computation* 126 (2025), 102340.

[6] Viktoriia Borovik, Paul Breiding, Javier del Pino, Mateusz Michałek, and Oded Zilberberg. "Khovanskii bases for semimixed systems of polynomial equations – a case of approximating stationary nonlinear Newtonian dynamics". *Journal de Mathématiques Pures et Appliquées* 182 (2024), 195–222.

[7] Viktoriia Borovik, Timothy Duff, and Elima Shehu. "SAGBI and Gröbner bases detection" (2024). arXiv: 2404.16796.

[8] Viktoriia Borovik, Bernd Sturmfels, and Svala Sverrisdóttir. "Coupled cluster degree of the Grassmannian". *Journal of Symbolic Computation* 128 (2025), 102396.

[9] Lara Bossinger. "A survey on toric degenerations of projective varieties" (2024). Proceedings of the Nottingham Algebraic Geometry Seminar. arXiv: 2301.02545.

[10] Paul Breiding, Kathlén Kohn, and Bernd Sturmfels. *Metric Algebraic Geometry*. Vol. 53. Oberwolfach Seminars. Springer, 2024.

[11] Paul Breiding and Sascha Timme. "HomotopyContinuation.jl: a package for homotopy continuation in Julia". *Math Software - ICMS 2018*. Springer, 2018, 458–465.

[12] Winfried Bruns, Aldo Conca, Claudiu Raicu, and Matteo Varbaro. *Determinants, Gröbner Bases and Cohomology*. Springer Monographs in Mathematics. Springer, 2022.

[13] Ireneusz W. Bulik, Thomas M. Henderson, and Gustavo E. Scuseria. "Can single-reference coupled cluster theory describe static correlation?" *Journal of Chemical Theory and Computation* 11.7 (2015), 3171–3179.

[14] Michael Burr, Oliver Clarke, Timothy Duff, Jackson Leaman, Nathan Nichols, and Elise Walker. "SubalgebraBases in Macaulay2". *Journal of Software for Algebra and Geometry* 14 (2024), 97–109.

[15] Jhon B. Caicedo, István Mező, and José L. Ramírez. "Partition lattice with limited block sizes". *Graphs and Combinatorics* 38.146 (2022).

[16] William Chen, Eva Deng, Rosena Du, Richard Stanley, and Catherine Yan. "Crossings and nestings of matchings and partitions". *Transactions of the American Mathematical Society* 359.4 (2007), 1555–1575.

[17] Claude Chevalley. *The Algebraic Theory of Spinors and Clifford Algebras*. Vol. 2. Collected Works of Claude Chevalley. Springer, 1997.

[18] Jiří Čížek. "On the correlation problem in atomic and molecular systems. Calculation of wavefunction components in Ursell-type expansion using quantum-field theoretical methods". *The Journal of Chemical Physics* 45.11 (1966), 4256–4266.

[19] Oliver Clarke and Fatemeh Mohammadi. "Toric degenerations of Grassmannians and Schubert varieties from matching field tableaux". *Journal of Algebra* 559.3 (2020), 646–678.

[20] Fritz Coester. "Bound states of a many-particle system". *Nuclear Physics* 7 (1958), 421–424.

[21] David Cox, John Little, and Donal O'Shea. *Ideals, Varieties, and Algorithms*. 4th ed. Undergraduate Texts in Mathematics. Springer, 2015.

[22] David A. Cox, John Little, and Donal O'Shea. *Using Algebraic Geometry*. 2nd ed. Springer, 2005.

[23] Mihály A. Csirik and Andre Laestadius. "Coupled cluster theory revisited – part I: discretization". *ESAIM: Mathematical Modelling and Numerical Analysis* 57 (2023), 645–670.

[24] D. F. Davidenko. "On a new method of numerical solution of systems of nonlinear equations". *Proceedings of the USSR Academy of Sciences*. Vol. 88. 4. 1953, 601–602.

[25] D. F. Davidenko. "On the approximate solution of systems of nonlinear equations". *Ukrainian Mathematical Journal* 5.2 (1953), 196–206.

[26] Timothy Duff, Cvetelina Hill, Anders Jensen, Kisun Lee, Anton Leykin, and Jeff Sommars. "Solving polynomial systems via homotopy continuation and monodromy". *IMA Journal of Numerical Analysis* 39.3 (2019), 1421–1446.

[27] Richard Ehrenborg and Margaret A. Readdy. "The Möbius function of partitions with restricted block sizes". *Advances in Applied Mathematics* 39.3 (2007), 283–292.

[28] David Eisenbud. *Commutative Algebra with a View Toward Algebraic Geometry*. Vol. 150. Graduate Texts in Mathematics. Springer, 1995.

[29] David Eisenbud and Joe Harris. *3264 and All That: A Second Course in Algebraic Geometry*. Cambridge University Press, 2016.

[30] Ephraim Eliav, Anastasia Borschevsky, Andréi Zaitsevskii, Alexander Oleynichenko, and Uzi Kaldor. "Relativistic Fock-space coupled cluster method: theory and recent applications". In: *Reference Module in Chemistry, Molecular Sciences and Chemical Engineering*. Ed. by Jan Reedijk. Elsevier Reference Collection in Chemistry, Molecular Sciences and Chemical Engineering. Elsevier, 2021.

[31] Xin Fang, Evgeny Feigin, Ghislain Fourier, and Igor Makhlin. "Weighted PBW degenerations and tropical flag varieties". *Communications in Contemporary Mathematics* 21.1 (2019), 1850016.

[32] Fabian M. Faulstich. "Recent mathematical advances in coupled cluster theory". *International Journal of Quantum Chemistry* 124.13 (2024), e27437.

[33] Fabian M. Faulstich, Vincenzo Galgano, Elke Neuhaus, and Irem Portakal. "On the coupled cluster doubles truncation variety of four electrons" (2026). arXiv: 2602.16580.

[34] Fabian M. Faulstich, Håkon E. Kristiansen, Mihály A. Csirik, Simen Kvaal, Thomas Bondo Pedersen, and Andre Laestadius. "S-diagnostic – an a posteriori error assessment for single-reference coupled-cluster methods". *The Journal of Physical Chemistry A* 127.43 (2023), 9106–9120.

[35] Fabian M. Faulstich and Andre Laestadius. "Homotopy continuation methods for coupled cluster theory in quantum chemistry". *Molecular Physics* (2023).

[36] Fabian M. Faulstich and Mathias Oster. "Coupled cluster theory: towards an algebraic geometry formulation". *SIAM Journal on Applied Algebra and Geometry* 8.1 (2024), 138–188.

[37] Fabian M. Faulstich, Bernd Sturmfels, and Svala Sverrisdóttir. "Algebraic varieties in quantum chemistry". *Foundations of Computational Mathematics* 25 (2025), 1167–1198.

[38] Fabian M. Faulstich and Svala Sverrisdóttir. "Algebraic geometry for spin-adapted coupled cluster theory" (2026). arXiv: 2601.16646.

[39] Evgeny Feigin. "Birational maps to Grassmannians, representations and poset polytopes". *Algebras and Representation Theory* 27 (2024), 1981–1999.

[40] Evgeny Feigin. "Birational maps, PBW degenerate flags and poset polytopes". *Journal of Algebra* 674.8 (2025), 235–256.

[41] Dominique Foata and Adriano M. Garsia. "A combinatorial approach to the Mehler formulas for Hermite polynomials". In: *Relations between Combinatorics and Other Parts of Mathematics*. Ed. by Dijen K. Ray-Chaudhuri. Vol. 34. Proceedings of Symposia in Pure Mathematics. American Mathematical Society, 1979, 163–179.

[42] Vladimir Fock. "Konfigurationsraum und zweite Quantelung". *Zeitschrift für Physik* 75 (1932), 622–647.

[43] William Fulton and Joe Harris. *Representation Theory: A First Course*. Vol. 129. Graduate Texts in Mathematics. Springer, 2004.

[44] Jean Gallier and Jocelyn Quaintance. *Differential Geometry and Lie Groups: A Second Course*. Vol. 13. Geometry and Computing. Springer, 2020.

[45] Camilo B Garcia and Willard I. Zangwill. "Finding all solutions to polynomial systems and other systems of equations". *Mathematical Programming* 16 (1979), 159–176.

[46] Daniel R. Grayson and Michael E. Stillman. *Macaulay2, a software system for research in algebraic geometry*. Available at http://www2.macaulay2.com.

[47] Walter Greiner and Berndt Müller. *Quantum Mechanics: Symmetries*. Springer, 1994.

[48] Alexander Grothendieck. *Revêtements Étales et Groupe Fondamental (SGA 1): Séminaire de Géométrie Algébrique du Bois Marie 1960–61*. Vol. 3. Documents Mathématiques. Société Mathématique de France, 2003.

[49] Allen Hatcher. *Algebraic Topology*. Cambridge University Press, 2002.

[50] Trygve Helgaker and Poul Jørgensen. "Analytical calculation of geometrical derivatives in molecular electronic structure theory". *Advances in Quantum Chemistry* 19 (1988), 183–245.

[51] Trygve Helgaker, Poul Jørgensen, and Jeppe Olsen. *Molecular Electronic-Structure Theory*. John Wiley & Sons, 2000.

[52] Takayuki Hibi and Nan Li. "Chain polytopes and algebras with straightening laws". *Acta Mathematica Vietnamica* 40 (2015), 447–452.

[53] Nicholas J. Higham. *Functions of Matrices: Theory and Computation*. SIAM, 2008.

[54] Howard Hiller. "Combinatorics and intersections of Schubert varieties". *Commentarii Mathematici Helvetici* 57 (1982), 41–59.

[55] Sam Hopkins. "RSK via local transformations" (2025). arXiv: 2510.22082.

[56] Curtis L. Janssen and Ida M. B. Nielsen. "New diagnostics for coupled-cluster and Møller–Plesset perturbation theory". *Chemical Physics Letters* 290.4-6 (1998), 423–430.

[57] Pascual Jordan and Eugene Wigner. "Über das Paulische Äquivalenzverbot". *Zeitschrift für Physik* 47 (1928), 631–651.

[58] Uzi Kaldor. "The Fock space coupled cluster method: theory and application". *Theoretica Chimica Acta* 80 (1991), 427–439.

[59] Kiumars Kaveh and Christopher Manon. "Khovanskii bases, higher rank valuations, and tropical geometry". *SIAM Journal on Applied Algebra and Geometry* 3.2 (2019), 292–336.

[60] Fábris Kossoski, Antoine Marie, Anthony Scemama, Michel Caffarel, and Pierre-François Loos. "Excited states from state-specific orbital-optimized pair coupled cluster". *Journal of Chemical Theory and Computation* 17.8 (2021), 4756–4768.

[61] Karol Kowalski and Piotr Piecuch. "Complete set of solutions of multireference coupled-cluster equations: the state-universal formalism". *Physical Review A* 61 (2000), 052506.

[62] Joseph M. Landsberg. *Tensors: Geometry and Applications*. Vol. 128. Graduate Studies in Mathematics. American Mathematical Society, 2012.

[63] Susi Lehtola, Frank Blockhuys, and Christian Van Alsenoy. "An overview of self-consistent field calculations within finite basis sets". *Molecules* 25.5 (2020), 1218.

[64] Lin Lin and Jianfeng Lu. *A Mathematical Introduction to Electronic Structure Theory*. SIAM, 2019.

[65] Ingvar Lindgren and Debashis Mukherjee. "On the connectivity criteria in the open-shell coupled-cluster theory". *Physics Reports* 151.2 (1987), 93–127.

[66] Svante Linusson. "Partitions with restricted block sizes, Möbius functions, and the k-of-each problem". *SIAM Journal on Discrete Mathematics* 10.1 (1997), 18–29.

[67] Percy A. MacMahon. *Combinatory Analysis*. Vol. I and II. Dover, 2004.

[68] Igor Makhlin. "Gröbner fans of Hibi ideals, generalized Hibi ideals and flag varieties". *Journal of Combinatorial Theory, Series A* 185 (2022), 105541.

[69] Igor Makhlin. "Chain-order polytopes: toric degenerations, Young tableaux and monomial bases". *Algebraic Combinatorics* 7.5 (2024), 1525–1550.

[70] Laurent Manivel. "On spinor varieties and their secants". *SIGMA* 5 (2009), 078.

[71] Antoine Marie, Fábris Kossoski, and Pierre-François Loos. "Variational coupled cluster for ground and excited states". *The Journal of Chemical Physics* 155.10 (2021), 104105.

[72] Mateusz Michałek and Bernd Sturmfels. *Invitation to Nonlinear Algebra*. Vol. 211. Graduate Studies in Mathematics. American Mathematical Society, 2021.

[73] Ezra Miller and Bernd Sturmfels. *Combinatorial Commutative Algebra*. Vol. 227. Graduate Texts in Mathematics. Springer, 2005.

[74] Teo Mora. "An introduction to commutative and noncommutative Gröbner bases". *Theoretical Computer Science* 134.1 (1994), 131–173.

[75] Alexander P. Morgan. *Solving Polynomial Systems Using Continuation for Engineering and Scientific Problems*. SIAM, 2009.

[76] Alexander P. Morgan, Andrew J. Sommese, and Charles W. Wampler. "Computing singular solutions to polynomial systems". *Advances in Applied Mathematics* 13.3 (1992), 305–327.

[77] Ida M. B. Nielsen and Curtis L. Janssen. "Double-substitution-based diagnostics for coupled-cluster and Møller–Plesset perturbation theory". *Chemical Physics Letters* 310.5–6 (1999), 568–576.

[78] Michael A. Nielsen. *The fermionic canonical commutation relations and the Jordan–Wigner transform*. Lecture notes, University of Queensland. https://futureofmatter.com/assets/fermions_and_jordan_wigner.pdf. 2005.

[79] Rosa Orellana, Franco Saliola, Anne Schilling, and Mike Zabrocki. "Plethysm and the algebra of uniform block permutations". *Algebraic Combinatorics* 5 (2022), 1165–1203.

[80] Joseph Paldus, Jiří Čížek, and Isaiah Shavitt. "Correlation problems in atomic and molecular systems. IV. extended coupled-pair many-electron theory and its application to the BH3 molecule". *Physical Review A* 5 (1972), 50.

[81] Joseph Paldus, Piotr Piecuch, Laura Pylypow, and Bogumił Jeziorski. "Application of Hilbert-space coupled-cluster theory to simple (H2)2 model systems: planar models". *Physical Review A* 47 (1993), 2738.

[82] Wolfgang Pauli. "Über den Zusammenhang des Abschlusses der Elektronengruppen im Atom mit der Komplexstruktur der Spektren". *Zeitschrift für Physik* 31.1 (1925), 765–783.

[83] Wolfgang Pauli. "Zur Quantenmechanik des magnetischen Elektrons". *Zeitschrift für Physik* 43.9 (1927), 601–623.

[84] Ruben Pauncz. *Spin Eigenfunctions: Construction and Use*. Plenum Press, 1979.

[85] T. Kyle Petersen. *Eulerian Numbers*. Birkhäuser, 2015.

[86] Piotr Piecuch and Karol Kowalski. "In search of the relationship between multiple solutions characterizing coupled-cluster theories". In: *Computational Chemistry: Reviews of Current Trends*. Ed. by Jerzy Leszczynski. World Scientific, 2000, 1–104.

[87] Abigail Price, Ada Stelzer, and Svala Sverrisdóttir. "Plane partitions and spin adapted quantum states" (2026). arXiv: 2601.06295.

[88] Björn O. Roos, Roland Lindh, Per Åke Malmqvist, Valera Veryazov, and Per-Olof Widmark. *Multiconfigurational Quantum Chemistry*. John Wiley & Sons, 2016.

[89] J. J. Sakurai and Jim Napolitano. *Modern Quantum Mechanics*. 3rd ed. Cambridge University Press, 2021.

[90] Raman Sanyal, Frank Sottile, and Bernd Sturmfels. "Orbitopes". *Mathematika* 57.2 (2011), 275–314.

[91] Craig Schensted. "Longest increasing and decreasing subsequences". *Canadian Journal of Mathematics* 13 (1961), 179–191.

[92] Erwin Schrödinger. "An undulatory theory of the mechanics of atoms and molecules". *Physical Review* 28 (1926), 1049.

[93] Isaiah Shavitt and Rodney J. Bartlett. *Many-Body Methods in Chemistry and Physics: MBPT and Coupled-Cluster Theory*. Cambridge University Press, 2009.

[94] Andrew J. Sommese and Charles W. Wampler. *The Numerical Solution of Systems of Polynomials Arising in Engineering and Science*. World Scientific, 2005.

[95] Richard P. Stanley. *Enumerative Combinatorics, Volume 1*. 2nd ed. Cambridge University Press, 1997.

[96] Richard P. Stanley. *Enumerative Combinatorics, Volume 2*. Cambridge University Press, 1999.

[97] Bernd Sturmfels. *Gröbner Bases and Convex Polytopes*. Vol. 8. University Lecture Series. American Mathematical Society, 1996.

[98] Qiming Sun. "Libcint: an efficient general integral library for Gaussian basis functions". *Journal of Computational Chemistry* 36.22 (2015), 1664–1671.

[99] Qiming Sun, Timothy C. Berkelbach, Nick S. Blunt, George H. Booth, et al. "PySCF: the Python-based simulations of chemistry framework". *WIREs Computational Molecular Science* 8.1 (2018), e1340.

[100] Qiming Sun, Xing Zhang, Samragni Banerjee, Peng Bao, et al. "Recent developments in the PySCF program package". *The Journal of Chemical Physics* 153.2 (2020), 024109.

[101] Svala Sverrisdóttir. "Algebraic varieties in second quantization" (2025). arXiv: 2505.17276.

[102] Svala Sverrisdóttir and Fabian M. Faulstich. "Exploring ground and excited states via single reference coupled-cluster theory and algebraic geometry". *Journal of Chemical Theory and Computation* 20.19 (2024), 8517–8528.

[103] Attila Szabo and Neil S. Ostlund. *Modern Quantum Chemistry: Introduction to Advanced Electronic Structure Theory*. Dover Publications, 1989.

[104] Leon A. Takhtajan. *Quantum Mechanics for Mathematicians*. Vol. 95. Graduate Studies in Mathematics. American Mathematical Society, 2008.

[105] Bartel L. Van der Waerden. "On varieties in multiple-projective spaces". *Indagationes Mathematicae* 81.1 (1978), 303–312.

[106] Gian-Carlo Wick. "The evaluation of the collision matrix". *Physical Review* 80 (1950), 268–272.